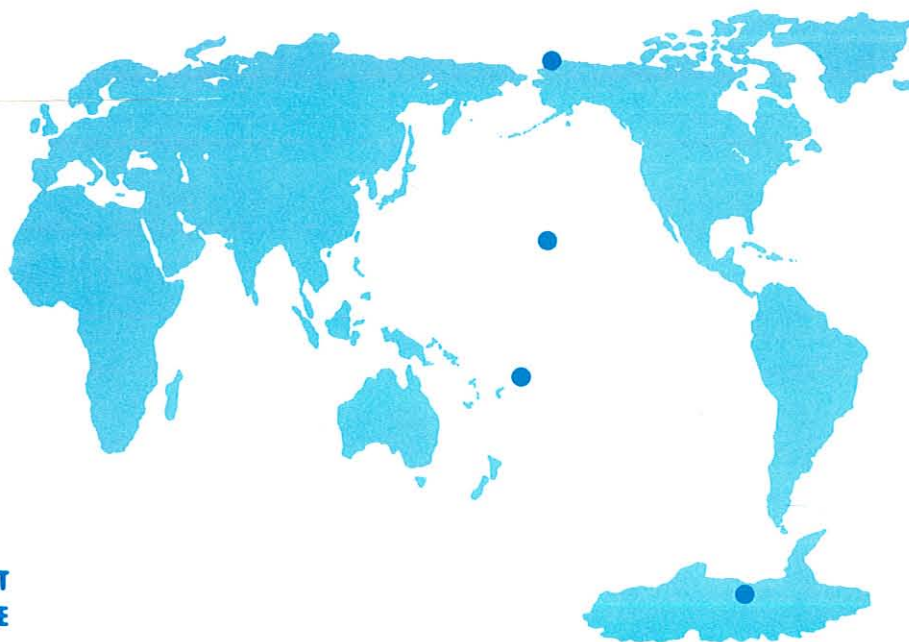


# *Geophysical Monitoring for Climatic Change*

*No. 14*

## **Summary Report 1985**



**U.S. DEPARTMENT  
OF COMMERCE**

**NATIONAL  
OCEANIC AND  
ATMOSPHERIC  
ADMINISTRATION**

**ENVIRONMENTAL  
RESEARCH  
LABORATORIES**





# Geophysical Monitoring for Climatic Change No. 14

## Summary Report 1985

Russell C. Schnell, Editor  
Rita M. Rosson, Assistant Editor

Air Resources Laboratory  
Geophysical Monitoring for Climatic Change

Boulder, Colorado

December 1986

### **U.S. DEPARTMENT OF COMMERCE**

Malcolm Baldrige, Secretary

National Oceanic and Atmospheric Administration  
Anthony J. Calio, Administrator

Environmental Research Laboratories  
Vernon E. Derr, Director

## NOTICE

Mention of a commercial company or product does not constitute an endorsement by NOAA Environmental Research Laboratories. Use for publicity or advertising purposes of information from this publication concerning proprietary products or the tests of such products is not authorized.

For sale by the National Technical Information Service, 5285 Port Royal Road  
Springfield, VA 22161

# CONTENTS

Page

GMCC STAFF.....	vii
GMCC STATION INFORMATION.....	x
1. SUMMARY.....	1
2. OBSERVATORY REPORTS.....	3
2.1 Mauna Loa.....	3
2.2 Barrow.....	10
2.3 Samoa.....	13
2.4 South Pole.....	16
3. AEROSOLS AND RADIATION MONITORING GROUP.....	21
3.1 Continuing Programs.....	21
3.2 Special Projects.....	35
3.3 References.....	36
4. CARBON DIOXIDE GROUP.....	37
4.1 Continuing Programs.....	37
4.2 Special Projects.....	44
4.3 References.....	46
5. TRACE GASES GROUP.....	47
5.1 Continuing Programs.....	47
5.2 References.....	60
6. ACQUISITION AND DATA MANAGEMENT GROUP.....	61
6.1 Continuing Programs.....	61
6.2 Special Projects.....	68
6.3 References.....	72
7. AIR QUALITY GROUP.....	73
7.1 Continuing Programs.....	73
7.2 Special Projects.....	85
7.3 References.....	90

8.	DIRECTORS OFFICE.....	92
8.1	Continuing Programs.....	92
	Impact of Alkaline Aerosols on Precipitation Chemistry.....	92
	Precipitation Chemistry.....	95
	(R. S. Artz)	
8.2	Arctic Gas and Aerosol Sampling Program.....	98
	Arctic Haze Above the Barrow Baseline Station.....	98
	(R. C. Schnell)	
8.3	Cooperative Programs.....	103
	Monitoring for Sulfur Dioxide and Total Suspended Particulate at Mauna Loa Observatory.....	103
	(Henry Yee, Wilfred Ching, and Richard Sasaki)	
	The Global Precipitation Chemistry Project.....	105
	(W. C. Keene, J. N. Galloway, G. E. Likens, and J. M. Miller)	
	$\delta^{13}C$ In Atmospheric Carbon Dioxide.....	108
	(Irving Friedman, Jim Gleason, and Augusta Warden)	
	Following the Trail of Antarctic Winds.....	111
	(Eugene J. Mroz, Mohammed Alei, John H. Cappis, Paul R. Guthals, Allen S. Mason, and Donald J. Rokop)	
	Some Results from UVB Measurements at Mauna Loa and Rockville, MD.....	114
	(Bernard Goldberg)	
	Logistic and Other Models for the Trends of Nitrous Oxide.....	117
	(M. A. K. Khalil and R. A. Rasmussen)	
	Atmospheric Submicron Particle Collection at the SPO.....	121
	(R. E. Witkowski, W. A. Cassidy, and G. W. Penney)	
	Washout Ratios of Nitrate, Non-Sea-Salt Sulfate, and Seasalt on Virginia Key, Florida and American Samoa.....	124
	(Dennis L. Savoie, Joseph M. Prospero, and Ruby T. Nees)	
	Seasonal Variations of $^{210}Pb$ and $^7Be$ at Mauna Loa and Barrow.....	127
	(Richard Larsen and Herbert Feely)	
	Radioactivity at Barrow and Mauna Loa Following the Chernobyl Accident.....	130
	(Richard Larsen and Z. Russell Juzdan)	
	Experimental Sampling of Atmospheric Methane.....	133
	(Lester Machta, Kirby Hanson, and Monte Poindexter)	
9.	INTERNATIONAL ACTIVITIES.....	134
10.	PUBLICATIONS AND PRESENTATIONS BY GMCC STAFF.....	137
11.	ACRONYMS .....	144



Mauna Loa Observatory after the construction of the lava diversion embankments in 1985. (U.S.G.S. photo by J. P. Lockwood.)



GMCC Staff, 1985

Director's Office

James Peterson, Director  
Bernard Mendonca, Deputy Directory  
Jeanne Kelsey, Secretary  
Roland Christofferson, CIRES  
Edwin Flowers, CIRES  
Dale Gillette, Physical Scientist  
Paul David Herrera, CO-OP  
Lori Neff, Scientific Data Clerk  
Everett C. Nickerson, Meteorologist  
Rita Rosson, Clerk-Typist  
Russell Schnell, CIRES  
L. Paul Steele, CIRES  
Paul Stockton, Physical Science Aid  
Delois Roberson, CO-OP  
Thomas Watson, Physical Science Aid  
David Wuertz, CO-OP

Acquisition and Data Management Group

Gary Herbert, Chief  
Karen Ciocchetti, Secretary  
Sandra Furney, Secretary  
Richard Clark, Computer Programmer  
Richard Cook, Physical Science Aid  
Teresa Davenport, Physical Science Aid  
Joyce Harris, Computer Specialist  
Troy Higgins, Jr. Fellow  
Steve Roughton, Computer Assistant  
Kenneth Thaut, Electronic Technician

Aerosols and Radiation Monitoring Group

John DeLuisi, Chief  
Karen Ciocchetti, Secretary  
James Baumhover, Electronic Technician  
Barry Bodhaine, Meteorologist  
Fernando Congeduti, -Guest Scientist  
Ellsworth Dutton, Meteorologist  
Jeffrey Guerrieri, Engineering Technician  
Rudy Haas, Mathematician  
Gerard Jennings, NRC  
David Longenecker, CIRES  
David Massey, Physical Science Aid  
Hong Minh, Engineering Technician  
Linda Mitchell, CIRES  
Kevin Moore, Physical Science Aid  
Donald Nelson, Meteorologist  
Tony Puig, Physical Science Aid  
Timothy Quakenbush, Physical Science Aid  
Patrick Reddy, CIRES  
Traci Simms, Physical Science Aid  
Lois Stearns, Meteorologist

#### Air Quality Group

Joseph Boatman, Chief  
Sandra Furney, Secretary  
Mark Cichy, CO-OP  
Laureen Gunter, Meteorologist  
Helmut Horvath, CIRES  
Menachem Luria, NRC, Post Doctorate  
Herman Sievering, Guest Worker  
Karen Stamminger, Physical Science Aid  
Slavko Cvencek, Physical Science Aid  
Charles VanValin, Research Chemist  
Dennis Wellman, Engineer  
Stan Wilkinson, Meteorologist

#### Carbon Dioxide Group

Pieter Tans, CIRES  
Lee Prendergast, Secretary  
Rita Brown, Secretary  
Dana Fleming, Secretary  
Brian Anderson, Physical Science Aid  
Craig Averman, CO-OP  
Teresa Bals, CO-OP  
David Bontrager, Physical Science Aid  
Thomas Conway, Research Chemist  
Ellen DeMoney, CIRES  
Duane Kitzis, CIRES  
Bradley Halter, Meteorologist  
Kenneth Masarie, CIRES  
John Parker, CO-OP  
Kirk Thoning, CIRES  
Lee Waterman, Chemist

#### Monitoring Trace Gases Group

Walter Komhyr, Chief  
Lee Prendergast, Secretary  
Rita Brown, Secretary  
Dana Fleming, Secretary  
Sean Coleman, Physical Science Aid  
Egan, Keith, CIRES  
Robert Evans, CIRES  
Mark Fish, Physical Science Aid  
Paul Franchois, CIRES  
Robert Grass, Physicist  
Gloria Koenig, Computer Programmer  
Kent Leonard, CIRES  
Samuel Oltmans, Physicist  
Frank Polacek, III, Meteorological Technician  
Gregory M. Siedelberg, CIRES  
Thayne Thompson, Physicist  
Ronald Thorne, Engineering Technician  
Thomas Stewart, Physical Science Aid  
Glenn Weiler, Physical Science Aid

Barrow Observatory

Daniel Endres, Station Chief  
Steve Ryan, Station Chief  
James Wendell, Electronic Technician

Mauna Loa Observatory

Elmer Robinson, Director  
Judith Pereira, Secretary  
Arne Austring, Physical Scientist  
John Chin, Physicist  
Thomas DeFoor, Electronic Engineer  
Thomas Garcia, Meteorological Technician  
Dorothy Johnson, Physical Science Aid  
Barbara Kerecman, Data Clerk  
Darryl Kuniyuki, NOAA Jr. Fellow  
Stephen Lent, Physical Science Aid  
Mamoru Shibata, Electronic Technician  
Alan Yoshinaga, Chemist

Samoa Observatory

Steve Ryan, Station Chief  
Donald Nelson, Station Chief  
Roger Williams, Electronic Technician  
Meridith E. Wilson, Electronic Technician  
Efaraima Peau, W. G. Laborer

South Pole Observatory

James Waddell, NOAA Corps, Station Chief  
Mark Mihalic, Electronic Technician  
Clifford Wilson, NOAA Corps, Station Chief  
Bradley Halter, Electronic Technician

GMCC Station Information

	Barrow (BRW)	Mauna Loa (MLO)	Samoa (SMO)	South Pole (SPO)
Name:	Barrow (BRW)	Mauna Loa (MLO)	Samoa (SMO)	South Pole (SPO)
Latitude:	71.3233	19.533	-14.2522	-90.000
Longitude:	156.6067	155.578	170.5628	0.000
Elevation:	0 km	3.4 km	0 km	2.8 km
Time Zone:	GMT -9	GMT -10	GMT -11	GMT +12
Office Hours:	8:00am-5:00pm	8:00am-5:00pm	8:00am-5:00pm	8:00am-5:00pm
Telephone -				
Office hours:	(907) 852-6500	(808) 961-3788	011-(684) 622-7455	Relayed through
After hours:	(907) 852-6500	(808) 961-3788	011-(684) 699-9953	GMCC Boulder
Postal Address:	Officer in Charge NOAA/ERL/ARL/GMCC Pouch 8888 Barrow, AL 99723	US Dept. of Commerce NOAA - Mauna Loa Observatory P.O. Box 275 Hilo, HI 96720	US Dept. of Commerce NOAA - GMCC Samoa Observatory P.O. Box 2568 Pago Pago, American Samoa 96799	Officer in Charge, GMCC Program Box 400 USARP C/O NAVSUPFORANTARCTICA FPO San Francisco, CA 96692 ATTN: South Pole #S-257 S. Kuester
Freight Address:		US Dept. of Commerce NOAA - Mauna Loa Observatory 154 Waiianuenu Ave. Hilo, HI 96720		

# GEOPHYSICAL MONITORING FOR CLIMATIC CHANGE

NO. 14

SUMMARY REPORT 1985

## 1. SUMMARY

At MLO, the major facilities change was construction of lava diversion embankments. The diversion system, which hopefully will never be tested, was designed to divert a flowing lava stream around the observatory. Upgrade of the lidar system continued. It detected an enhanced stratospheric aerosol layer late in the year, presumably the result of the November eruption of Nevada del Ruiz in Columbia. A new solar radiation program was begun cooperatively with the University of Arizona. The program goal is to study 22-year variability in solar constant as measurable at ground level.

At BRW, the long-term problem of availability of reliable electrical power was solved with an agreement with the USAF DEW line facility to supply power to the observatory. A major cost savings was achieved by arranging for annual shipment of gas tanks by barge rather than regular shipments by air. LBL discontinued their long-running cooperative aerosol measurements when the project leader took a position in a private company.

At SMO, our long-term Station Chief and Electronic Technician took new NOAA jobs in Boulder, resulting in a completely new station staff. The photovoltaic system performed well, providing uninterrupted power to several projects. The ALE/OGC cooperative halocarbon monitoring project was improved with the installation of upgraded gas chromatographs.

At SPO, the new crew modified the CAF floor plans. The remodeling was done to improve efficiency of operations, sampling intake lines, and reliability of power. Drifting snow around CAF continued; plans have been drafted to raise CAF next year. There were few changes in NOAA and cooperative scientific programs during the year.

The ongoing GMCC core measurement programs continued. These programs include measurements of  $\text{CO}_2$  from the flask network and observatories, total column ozone, ozone vertical distribution by ECC sonde and Umkehr technique, surface ozone, stratospheric water vapor by balloon soundings at Boulder, CFC-11 and -12 and  $\text{N}_2\text{O}$  from flask samples, stratospheric aerosols at MLO using lidar, aerosol light scattering and CN concentration, direct and diffuse solar radiation, meteorological variables, and chemistry of precipitation.

In the Aerosols and Radiation Group, the observatory CN records, all at least 10 years long, show no significant long-term trends. A first assessment was completed of upward- and downward-directed solar and longwave radiation measurements at Barrow. The MLO concurrent Umkehr ozone and lidar aerosol profiles following the El Chichon eruption were used to confirm theoretical aerosol corrections to long-term Umkehr measurements. Administratively, the ARL Solar Radiation Facility was transferred to the ARM Group. The facility maintains U.S. radiometric standards and calibrates instruments for the NOAA solar network.

The Carbon Dioxide Group continued in situ CO<sub>2</sub> measurements at the observatories and flask analyses of CO<sub>2</sub> and CH<sub>4</sub> at 26 sites. The mean global CO<sub>2</sub> 1985 increase was about 1.2 ppm. A report by Komhyr et al. (1985) gives a complete history and comprehensive analysis of the CO<sub>2</sub> flask sampling network through 1982. The 1985 methane global growth rate averaged about 0.9%. Sampling of CO<sub>2</sub> in the air and ocean surface water during a May-July oceanographic cruise showed equatorial pCO<sub>2</sub> values as high as 500 ppm.

The Trace Gases Group continued the Dobson total ozone measurement record at 14 sites and its international calibration work. The South Pole record shows large October-November decreases, particularly during the 1980's, now referred to as the Antarctic Ozone Hole. The NESDIS SBUV/2 program continued with ozone profiles by Umkehr at five sites and by ECC sonde at three sites. The 12-year surface ozone measurements at BRW and MLO show long-term, significant increases. Regular balloon soundings of stratospheric water vapor continued. We continued to take flask samples at the observatories for CFC-11, CFC-12, and N<sub>2</sub>O. As part of RITS, a gas chromatographic system was designed and purchased for in situ, continuous measurements at the observatories of these species.

The Acquisition and Data Management Group reported the meteorological data from the observatories. The annual distribution of wind direction was near normal, but wind speeds were significantly greater (than normal) at SMO and slightly greater at SPO. The new data acquisition systems installed during 1984 are more reliable than their predecessors. The air mass trajectory program was improved with the capability for computations over Southern Hemisphere polar regions, which was tested via comparison to South Pole measurements of sea salt ambient aerosol. Numerous trajectories were computed for NOAA researchers and affiliates at universities and other agencies.

An administrative change transferred the ARL Air Quality Division to GMCC as the Air Quality Group. Projects undertaken by the Group included: contribution of natural sulfur emissions from the Gulf of Mexico to the North American total sulfur budget; computer simulation of the natural sulfur cycle in the marine boundary layer; mechanism by which aerosols are released to the atmosphere by evaporating clouds; the role of thunderstorm convective processes in the vertical transport of air pollutants; participation in WATOX to determine the flux of anthropogenic emissions from the eastern edge of the North American continent; installation and improvement of scientific instruments on the NOAA King Air aircraft; deposition of sulfur particles during high wind-speed conditions; and Grand Canyon wind flow patterns when visibility is reduced during controlled forest burning periods.

Within the Director's Office, research is continuing on the effects of natural sources of alkaline materials (wind-blown soil aerosol, and road dust) on precipitation chemistry precipitation and on chemical analyses of precipitation samples collected at the observatories and a six-site network in Hawaii. Many data analyses from AGASP flights during 1983 were published. Planning for AGASP-II during March-April 1986 was well underway. Many scientists from universities and other institutions used the observatories for cooperative research. This report includes summaries from several projects.

## 2. OBSERVATORY REPORTS

### 2.1 Mauna Loa

#### FACILITIES

The MLO research and monitoring program was carried out through the year without major disruptions in the core observations. The CAMS units performed well, and essentially complete data recovery was achieved.

A major construction program was carried out at the end of the year when the long-planned lava diversion embankments were constructed. The design of the diversion system was developed by USGS Hawaiian Volcanoes Observatory. The embankments, upslope from MLO, were bulldozed from the on-site lava and designed so that a flowing lava stream would be diverted around the MLO site. Lava embankments were used successfully during a 1983 eruption of Mt. Etna in Sicily to divert a lava flow and protect several facilities (Lockwood and Romano, 1985).

The ozonesonde program, begun in December 1984 with NOAA NESDIS support, was continued on approximately a weekly schedule through the year using the NWS radiosonde facility at Hilo airport.

Lidar observations continued on a weekly schedule, sky conditions permitting. In November and December a characteristic stratospheric volcanic cloud signal was detected, which apparently was due to the 13 November 1985 eruption of Nevada del Ruiz in Columbia. The upgrade of the MLO lidar with EPA grant support continued throughout the year.

The Pu'u O'o vent of Kilauea volcano erupted periodically, on an almost regular 27-day schedule, throughout the year. There was no impact, generally, on MLO operations or data, although occasionally an outgassing Kilauea plume drifted past the Observatory.

In August IAMAP held a 2-week-long meeting in Honolulu. MLO staff attended and participated in the meeting. Visitors in August totaled more than 90, mainly IAMAP attendees, including many foreign scientists, and an IAMAP-organized tour.

An emergency, break-glass-to-use telephone has been installed at MLO for public use in case of emergencies on the mountain.

#### PROGRAMS

The principal programs conducted at MLO during the year are listed in table 1. Those instruments recorded continuously by the CAMS are indicated by \*. Brief comments on some of the individual programs follow.

Table 1.--Summary of sampling programs at MLO in 1985

Program	Instrument	Sampling Frequency	Remarks
<u>Gases</u>			
CO <sub>2</sub>	URAS-2T infrared analyzer*	Continuous	MLO
	3-L glass flasks	1 pair wk <sup>-1</sup>	MLO and Kumukahi (seacoast)
CO <sub>2</sub> and CH <sub>4</sub>	0.5-L glass flasks, p <sup>3</sup>	1 pair wk <sup>-1</sup>	MLO and Kumukahi
	0.5-L glass flasks, through analyzer	1 pair wk <sup>-1</sup>	MLO
Surface ozone	5-L evacuated glass flasks	1 pair wk <sup>-1</sup>	MLO and Kumukahi
Total ozone	Gas chromatograph	Continuous	MLO
Ozone profile	Dasibi ozone meter*	Continuous	MLO
CFC-11, CFC-12, and N <sub>2</sub> O	Dobson spectrophotometer no. 76	3 day <sup>-1</sup>	Weekdays
	Dobson spectrophotometer no. 76	2 day <sup>-1</sup>	Umkehr
	Balloonborne ECC sonde	1 wk <sup>-1</sup>	From Hilo Airport
	300-mL stainless steel flasks	1 pair wk <sup>-1</sup>	MLO
<u>Aerosols</u>			
Condensation Nuclei	Pollak CNC	Discrete	Weekdays
Optical properties	G.E. CNC*	Continuous	
	Four-wavelength nephelometer*	Continuous	450, 550, 700, 850 nm
Stratospheric aerosols	Lidar	Discrete	694.3 nm; average 1 profile wk <sup>-1</sup>
<u>Solar Radiation</u>			
Global irradiance	Eppley pyranometers (3) with Q, OG1, and RG8 filters*	Continuous	Weekdays
Direct irradiance	Eppley pyrhemometers (2) with Q filter*	Continuous	Weekdays
	Eppley pyrhemometer with Q, OG1, RG2, and RG8 filters	3 day <sup>-1</sup>	Weekdays
Diffuse irradiance	Eppley/Kendall active cavity radiometer	Discrete	Weekdays
	Eppley pyranometer with shading disk and Q filter*	Continuous	
Turbidity	J-series 1982 sunphotometers	3-day <sup>-1</sup>	380, 500, 778, 862 nm; narrowband
	PMOD three-wavelength sunphotometer*	Continuous	380, 500, 778 nm; narrowband
<u>Meteorology</u>			
Air Temperature	Thermistor (aspirated)*	Continuous	2-m height
Dewpoint temperature	Max.-min. thermometers	1 day <sup>-1</sup>	Standard shelter
	Hygrothermograph	Continuous	MLO and Kulani Mauka
Relative humidity	Dewpoint hygrometer*	Continuous	2-m height
Pressure	Hygrothermograph	Continuous	MLO and Kulani Mauka (8300 ft)
	Capacitance transducer*	Continuous	
Wind (speed and direction)	Microbarograph	Continuous	
	Mercurial barometer	1 day <sup>-1</sup>	
Precipitation	Bendix Aerovane*	Continuous	6-m height
	Rain gauge, 8-in	1 day <sup>-1</sup>	
Total precipitable water	Rain gauge, 8-in	1 wk <sup>-1</sup>	Kulani Mauka
	Rain gauge, weighing bucket	Continuous	Weekly chart record
	Rain gauge, tipping bucket*†	Continuous	Program began Oct.
	Foskett infrared hygrometer*	Continuous	
	HAO infrared hygrometer*	Continuous	
<u>Precipitation Chemistry</u>			
pH	pH meter - Hilo lab.	Weekly	Rainwater collections, 5 sites
Conductivity	Conductivity bridge - Hilo lab.	Weekly	Rainwater collections, 5 sites
Chemical components	Ion chromatograph - Hilo lab.	Weekly	Rainwater collections, 5 sites
<u>Cooperative Programs</u>			
CO <sub>2</sub> (SIO)	Infrared analyzer (Applied Physics)	Continuous	
CO <sub>2</sub> , <sup>13</sup> C, N <sub>2</sub> O (SIO)	5-L evacuated glass flasks	1 pair wk <sup>-1</sup>	MLO and Kumukahi
Surface SO <sub>2</sub> (EPA)	Chemical bubbler system	Every 12 days	24-h (0000-2400) sample
CO <sub>2</sub> , CO, CH <sub>4</sub> , <sup>13</sup> C/ <sup>12</sup> C (CSIRO)	Pressurized glass flask sample	1 mo <sup>-1</sup>	MLO
CO <sub>2</sub> , CH <sub>4</sub> and other trace gases (NCAR)	Evacuated stainless steel flasks	1 pair wk <sup>-1</sup>	MLO and Kumukahi
HNO <sub>3</sub> and HCl vapor (Colorado College)	Special sampling system	4 periods yr <sup>-1</sup>	

Table 1.-- Summary of sampling programs at MLO in 1985--Continued

Programs	Instrument	Sampling frequency	Remarks
<u>Cooperative Programs--Cont.</u>			
Total suspended particles (DOE)	High-volume sampler	Continuous 1 filter wk <sup>-1</sup>	
Total suspended particles (EPA)	High-volume sampler	Every 12 days	24-h (0000-2400) sample
Ultraviolet radiation (Temple Univ.)	Ultraviolet radiometer (erythema)	Continuous	Radiation responsible for sunburning of skin
Ultraviolet radiation (Smithsonian)	7-wavelength UV radiometer	Continuous	295-325 nm, narrowband
Solar variability† (Univ. of Arizona)	Solar photometer	Discrete	Program began Sept.
Solar Aureole Intensity† (Colo. State Univ.)	Multi-aperture tracking photometer	Continuous	Program began Jan.
Precipitation collection (DOE)	Exposed collection pails	Continuous	
Precipitation collection (ISWS)	Aerochemetric automatic collector	Continuous	Analysis for <sup>7</sup> Be and <sup>10</sup> Be
Precipitation collection (Univ. of Virginia)	Aerochemetric automatic collector	Continuous	Organic acid analysis
Wet-dry deposition (ISWS)	Aerochemetric automatic collector	Continuous	NADP
Aerosol chemistry (Univ. of Washington)	Nuclepore filters	Continuous	Upslope-downslope discrimination
<sup>13</sup> C (USGS, Denver)	10-L stainless steel flasks	Biweekly	
Carbon monoxide (Max Planck Inst.)	Chemical reaction with HgO	Continuous	
Various trace gases (OGC)	Stainless steel flasks	1 set wk <sup>-1</sup> (3 flasks)	MLO and Kumukahi

\*Indicates program recorded by CAMS.

†Indicates new program initiated during 1985.

### Carbon Dioxide

Atmospheric CO<sub>2</sub> was monitored continuously using both the GMCC URAS-2T infrared analyzer and an automatic gas chromatograph with a flame ionization detector. The SIO Applied Physics infrared analyzer was also operated in parallel with the GMCC systems. Preliminary results from the GMCC URAS system indicate that the rate of CO<sub>2</sub> increase for 1985 was approximately 1.33 ppm yr<sup>-1</sup>.

The weekly CO<sub>2</sub> flask sampling programs at MLO and Cape Kumukahi, the easternmost point on the island, were continued during the year. It is usually expected that CO<sub>2</sub> concentrations at Kumukahi will be slightly higher than those at MLO. In the past 9 years, 1976 through 1984, Kumukahi values have averaged 0.3 ppm higher while the differences ranged from 0 to 0.8 ppm.

As in past years, outgassing from the volcanic caldera at the summit of Mauna Loa and from vents along the northeast rift caused disruptions of some of the CO<sub>2</sub> records in each month of the year. These events occurred mainly between 0000 and 0800 LST during the downslope wind regime. Since these disruptions are readily detectable in the instrument records, they can be excluded from the concentration data and do not influence the MLO CO<sub>2</sub> record. The frequency of the 1985 monthly occurrences is listed in table 2.

Table 2. Monthly occurrences of outgassing from the volcanic caldera on Mauna Loa during 1985

	Jan	Feb	Mar	Apr	May	Jun	Jul	Aug	Sep	Oct	Nov	Dec	Year
No. of days	10	20	13	11	19	20	15	21	9	17	12	9	176
Percent of days	32	71	42	37	61	67	48	68	30	55	40	29	48

The 1985 frequency of outgassing events, 48%, is a significant decrease from the 61% frequency that occurred in 1984 in the 8 months following the 1984 Mauna Loa eruption. Both values are significantly greater than the pre-eruption 5-yr average frequency of 27%. It should be noted that these frequencies relate to the number of occurrence days and not to the number of hours of data that are affected; most events last only about an hour or so.

#### Ozone

Ozone measurements were made using three separate procedures: total surface ozone using the Dasibi UV photometer; total ozone in the atmospheric column, and the tropospheric and stratospheric ozone profile using the Umkehr technique and automated Dobson instrument no. 76; and ozone profiles to about 40 km on a weekly basis using ECC ozonesonde systems. The automated Dobson instrument is set to take daily morning and afternoon Umkehr measurement sequences, although the afternoon observation is frequently affected by upslope stratus cloud formations. Total ozone Dobson measurements are initiated manually three times a day when sky conditions permit. The ECC ozonesonde flights are made on a weekly schedule from the NWS radiosonde facility at the Hilo airport and are supported by NOAA NESDIS. In 1985 52 flights were launched, of which 46 or 88% were successful in reaching the ozone layer. The maximum altitude attained by an ozonesonde was 42 km, and 70% of the successful flights reached 39 km or higher. When possible the ozonesonde flights were scheduled to coincide with overpasses of the NOAA-7 satellite, which carries ozone profiling instrumentation.

Surface ozone concentrations were obtained nearly continuously using the Dasibi UV photometric instrument. Calibrations were carried out on a regular weekly schedule.

#### Surface Aerosol Measurements

Three instruments were in use to characterize the surface aerosol particles: the G.E. CNC, the Pollak CNC, and the nephelometer.

The G.E. CNC operated continuously with only occasional maintenance or mechanical problems. The Pollak counter was operated in the normal manner during the year and served as a convenient calibration check on the performance of the continuous G.E. CNC system. The nephelometer was placed back into service in May after an extended period in GMCC Boulder laboratories for rebuilding and calibration.

## Stratospheric Aerosols-Lidar

Lidar observations were carried out, sky conditions permitting, on approximately a weekly schedule. When possible lidar observations were correlated with SAGE II satellite overpasses so that the lidar profiles could be coordinated with the SAGE aerosol experiments. A total of 52 observations were made during the year. The stratospheric aerosol loading from the spring 1982 El Chichon eruption continued the decreasing trend established in previous years and apparently approached a pre-El Chichon background in November 1985.

During 1985 work supported by an EPA grant to upgrade the MLO lidar system was continued. This upgrade will include new optical components, a redesigned mounting configuration, and improved data acquisition systems. Completion is expected in early 1987.

## Meteorology

Meteorological measurements were continued without major problems during 1985. The tipping-bucket rain collection system was installed in October to provide input signals to the CAMS and the daily weather report.

## Solar Radiation

No major changes were made in the MLO solar radiation program. There are several components in this system: continuous solar and total-sky measurements using both stationary and tracking instruments; discrete broadband and narrowband observations on a routine, weather-permitting basis; discrete manual, high-precision observations; and calibrations and intercomparisons of instruments using MLO facilities and instruments as working standards. All of these activities continued in 1985.

A normal incidence pyrhelimeter with Q filter, three global pyranometers with Q, OG1, and RG8 cutoff filters, and a diffuse Q pyranometer with shading disk were operated throughout the year to obtain continuous radiation measurements. A filter-wheel pyrhelimeter with Q, OG1, RG2, and RG8 cutoff filters was operated to obtain discrete broadband radiation measurements. Transmission generally increased slightly as the year progressed. Turbidity measurements were obtained with hand-held sunphotometers J202 (380 and 500 nm) and J314 (778 and 862 nm) throughout the year.

The active solar tracker and the 32-channel CAMS operated the whole year with only minor problems in the automated solar dome. The dome and shutter controllers operated reasonably well, although there were some problems with the dome positioning motor and controller. Instruments mounted in the solar dome included a normal incidence pyrhelimeter, an infrared water vapor meter, a three-wavelength PMOD sunphotometer, and an active cavity radiometer.

The MLO solar radiation program was augmented by a number of cooperative programs.

## Precipitation Chemistry

The GMCC precipitation chemistry program continued without difficulties at about the same level of activity as in prior years. The usual MLO program consists of the collection and analysis of precipitation collected at five local sites, although the coastal site at Cape Kumukahi was out of service for many months because of repeated vandalism. MLO also carries out the analysis of precipitation samples collected on the Island of Kauai and at the GMCC observatories at Barrow, Samoa, and South Pole. Weekly snow or rain samples are collected at these GMCC sites. Samples are analyzed in the MLO Hilo laboratory for pH and conductivity. Both anions and cations are determined in these samples using ion chromatography. Several cooperative programs in precipitation and deposition chemistry augment the GMCC program.

### COOPERATIVE PROGRAMS

The large number of cooperative programs at MLO continued in normal operation and with little change through 1985. These are listed in table 1, and a brief summary of some of these activities follows.

The program of high-precision UV radiation measurements at seven wavelengths (295-325 nm) was continued at MLO by the Smithsonian Institution Radiation Biology Laboratory as was the erythema (sunburn) radiation data gathered at MLO for a number of years by Temple University. These two sets of data are important in assessing the potential impact of changes in the ozone layer.

Precipitation collection for chemical analysis continued, and there were several cooperative investigator programs in this research area. Collections of precipitation for organic acid analysis for the University of Virginia and for beryllium 7 and 10 analyses for the ISWS continued, as did sample collections for DOE and NADP.

Aerosol particle samples were collected for the University of Washington on a weekly schedule using Nuclepore filters. This program used a sampler-controller discriminating on the basis of time of day, wind speed, wind direction, and Aitken nuclei count. The purpose of this controller is to separate sample collections according to upslope and downslope air trajectories and to exclude calm conditions. Downslope air should be representative of mid-tropospheric conditions whereas upslope air masses may contain various amounts of material with a recent origin at the earth's surface. Total particle filters were also collected for DOE. High-volume filter samples were collected for EPA using standard EPA methods with one 24-h filter sample being taken every 12 days. This EPA observational data series began in 1971, although there have been some significant breaks in the record. Annual geometric mean values for total suspended particles appear to range between 2 and 4  $\mu\text{g m}^{-3}$  with no evidence of a long-term trend for the period 1973 to 1984.

Total ozone and  $\text{SO}_2$  in the atmosphere were measured for AES, Canada, during the year with a Brewer spectrophotometer. The CO analyzer of the Max Planck Institut, Mainz, Germany, was operated during the year; however, there were a number of periods of downtime due to mechanical problems.

The SIO Applied Physics infrared CO<sub>2</sub> analyzer operated without major problems during 1985 in parallel with the GMCC CO<sub>2</sub> analyzer. Flask samples of air from MLO and Cape Kumukahi continued to be supplied to SIO on a weekly basis.

Flask sample collections were made both at MLO and at the seacoast at Cape Kumukahi for several investigators. Flask collections were made at MLO for the Australian CSIRO who are analyzing the samples for the <sup>13</sup>C/<sup>12</sup>C ratio as well as for CO, CO<sub>2</sub>, and CH<sub>4</sub>. Other flask sample programs include those of the OGC, NCAR, and SIO. Colorado College continued their periodic sampling at MLO for nitric acid and hydrochloric acid vapors over 2-wk periods every 3 months.

Two new cooperative solar radiation programs were begun, one by Colorado State University and one by the University of Arizona. The CSU program installed a five-element, multi-field-of-view tracking solar photometer system designed to monitor the solar aureole. The University of Arizona program, supported by a NOAA ARL grant, includes the installation of a multi-wavelength solar spectroradiometer and its long-term operation at MLO. The overall goal of the program is to determine the long-term variability of solar spectral irradiance, i.e., the "solar constant." Measurements over a solar cycle are contemplated.

#### REFERENCES

- Lockwood, J.P., and R. Romano, 1985. In Sicily: Lava diversion proved in 1983 tests at Etna. Geotimes 30(5):10-12.

## 2.2 Barrow

### FACILITIES

Ukpiagvik Inupiat Corporation completed the takeover of NARL. Power and third-party support that had been previously supplied by NARL is now being supplied by the DEW line site.

BRW can now order supplies through the GSA Alaska Customer Supply Center.

The station staff at BRW began an extensive program to utilize the IBM PC to the fullest extent. The PC is now being used for most of the word processing duties.

A water still was added to the station inventory, giving the station a good supply of distilled water for the G.E. CNC and the MLO precipitation program. Water was formerly supplied by NARL.

Because the cost of shipping tanks of gas by air increased this year, the barge was used to transport the tanks to BRW. This method worked without any major problems, so it will probably be continued in the future.

During the winter the largest herd of Caribou ever, 250,000 and growing by 10% per year, moved into the North Slope. A small number were as close as 50 ft to the station.

Acoustic tile was installed at the observatory bringing the sound level down from 85db.

The interior of GMCC housing unit B-5 was painted and carpeted.

### Vehicles

The 1982 Dodge truck, which has had a history of problems, threw a rod and had to have the engine replaced. The 1979 GMC had very few problems and is still the best vehicle. New tires were put on late in the year. The Sidewinder was excessed and is no more. Paperwork was also begun to excess the 1977 Chevy Suburban.

Procedures have been initiated to purchase a new snow machine early in 1986.

### PROGRAMS

Programs carried out in BRW are listed in table 3. Comments on some of the programs follow.

Table 3.--Summary of sampling programs at BRW in 1985

Program	Instrument	Sampling frequency
<u>Gases</u>		
CO <sub>2</sub>	URAS-2T infrared analyzer	Continuous
	0.5-L glass flasks, P <sup>3</sup>	1 pair wk <sup>-1</sup>
	0.5-L glass flasks, through analyzer	1 pair wk <sup>-1</sup>
	3-L glass flasks	1 pair wk <sup>-1</sup>
Surface ozone	Dasibi ozone meter	Continuous
Methane	0.5-L glass flasks	1 pair wk <sup>-1</sup>
	Carle GC with HP acquisition	Continuous
CFC-11, CFC-12, and N <sub>2</sub> O	300-mL stainless steel flasks	1 pair wk <sup>-1</sup>
Total ozone	Ozone balloons	1 wk <sup>-1</sup>
	Dobson ozone spectrophotometer	Discrete
<u>Aerosols</u>		
Condensation Nuclei	Pollak CNC	Discrete
	G.E. CNC	Continuous
Optical properties	Four-wavelength nephelometer	Continuous
<u>Solar Radiation</u>		
Albedo	Eppley pyranometer	Continuous
Global irradiance	Eppley pyranometers with Q and RG8 filters	Continuous
Direct irradiance	Tracking NIP	Continuous
Direct irradiance	Eppley pyrhelimeter with Q, OG1, RG2, and RG8 filters	Discrete
Terrestrial (IR) radiation	Eppley pyrgeometer	Continuous
Turbidity	Sunphotometers with 380-, 500-, 778-, and 862-nm narrowband filters	Discrete
<u>Meteorology</u>		
Air temperature	Thermistor	Continuous
	Max.-min. thermometers	1 day <sup>-1</sup>
Dewpoint temperature	Dewpoint hygrometer	Continuous
Pressure	Capacitance transducer	Continuous
	Microbarograph	Continuous
	Mercurial barometer	Discrete
Wind (speed and direction)	Bendix Aerovane	Continuous
<u>Precipitation Chemistry</u>		
pH	pH meter (samples analyzed at MLO)	Discrete
Conductivity	Conductivity bridge (samples analyzed at MLO)	2 mo <sup>-1</sup>
<u>Cooperative Programs</u>		
Total surface particulates (DOE)	High-volume sampler	Continuous (1 filter wk <sup>-1</sup> )
Aerosol chemistry (URI)	High-volume sampler	Continuous (2 filters wk <sup>-1</sup> )
Ultraviolet radiation (Temple Univ.)	Ultraviolet radiometer	Continuous
Precipitation gauge (ASCS)	Wyoming shielded precipitation gauge	2 mo <sup>-1</sup>
Various trace gases (OGC)	Stainless steel flasks	1 set wk <sup>-1</sup> (3 flasks set <sup>-1</sup> )
Magnetic fields (USGS)	Magnetometer	1 station check wk <sup>-1</sup> )
<sup>13</sup> C (USGS)	10-L stainless steel flasks	1 pair mo <sup>-1</sup>
Various trace gases (NCAR)	3-L stainless steel flasks	1 pair wk <sup>-1</sup>
<sup>13</sup> C/ <sup>12</sup> C (CSIRO)	5-L glass flasks	1 pair (2 wk) <sup>-1</sup>
CO <sub>2</sub> , <sup>13</sup> C, N <sub>2</sub> O (SIO)	5-L evacuated glass flasks	1 pair wk <sup>-1</sup>
<sup>12</sup> C/ <sup>13</sup> C (Univ. Washington)	35-L stainless steel flasks	1 (2 wk) <sup>-1</sup>
Halocarbon monitoring (Univ. of Calif., Irvine)	Various stainless steel flasks	1 set (3 mo) <sup>-1</sup>
Aerosol chemistry (Univ. of Alaska)	Hi-Vol filters	Continuous 3 filters wk <sup>-1</sup>
ULF waves (Univ. of Tokyo)	Cassette recorder	Continuous 1 tape wk <sup>-1</sup>
Earthquake detection (Univ. of Alaska)	Seismograph	Continuous Check site wk <sup>-1</sup> Change tape mo <sup>-1</sup>

## Carbon Dioxide

The only problem with the URAS/NDIR analyzer this year was a thermal cut-out switch that burned open and had to be replaced. CO<sub>2</sub> monitoring, including the flask samples, went smoothly all year.

## Surface Ozone

The Dasibi meter was sent to Boulder for repair early in the year. On the return trip it was apparently dropped during shipping and damaged; therefore, it was again returned to Boulder. It was back in operation in May.

## Total Ozone

A Dobson instrument is being considered for reinstallation in the near future.

## Aerosols

Aside from the usual maintenance, the G.E. CNC ran well all year. The Pollak counter (no. 16) malfunctioned late in the year and was replaced by no. 21. This did not solve the problem. A series of small leaks and new zero filters that were defective from the factory were found to be the problems and corrected.

## Solar Radiation

An albedo rack was installed to study the heat budget. The two hand-held sunphotometers were sent to MLO to be calibrated. A new solar tracker, with a built-in ephemeris, was installed and was found to be an excellent tracker.

## Meteorology

The dewpoint hygrometer had problems most of the year even after being sent to the factory for repair work. The BRW staff repaired the unit and returned it to operation late in the year.

## Cooperative Programs

In 1985 LBL shut down its filter sampling equipment. This consisted of a daily sampler, a weekly Hi-Vol sampler, and a weekly dichotomous sampler. All of the solar equipment including an albedo rack, from the University of Alaska was also returned this year. The University of Tokyo installed a set of three sensors to look at ULF waves. The data were logged on a Walkman-like cassette recorder.

## 2.3 Samoa

### FACILITIES

A complete changeover of personnel occurred in June and July at SMO with the appointment of a new technician and station chief. The departing staff, Don Nelson and Roger Williams, had served in Samoa for 10 and 8 years respectively.

The observatory building was upgraded and reorganized in August. The roof-top grating table was painted in August, and the roof was resurfaced with an epoxy paint in October. That same month the shingles were stained and the water catchment was drained and cleaned. GMCC instruments in the building were put on a UPS in 1985.

In April, three sections were added to the Matatula Point tower, bringing its total height to 15 m. The GMCC CO<sub>2</sub> sampling line and the SEASpan aerosol sampler were relocated to this new height.

The photovoltaic system operated well all year. A replacement CAMS box configured to control the system was tested from April to June but proved unsatisfactory. For the remainder of the year the system was operated under control of the original factory-installed circuits. The Samoa photovoltaic system provides uninterrupted, "clean" power to all three CAMS boxes, the CO<sub>2</sub> analyzer system, all meteorology instruments, and all solar radiation instruments.

On 31 March, a fire destroyed NOAA housing unit #T-6 in Tafuna, the station chief's quarters. Appliances, furniture, personal belongings, and most of the wooden structure of the house were substantially lost. The cause of the blaze is believed to be an electrical short that occurred somewhere in the vicinity of the master bedroom ceiling.

The station chief's quarters were relocated to unit #T-7, a vacant NOAA house next door. The new unit required a considerable amount of renovation including the installation of new screening, flooring, appliances, and sinks, along with a complete interior and exterior paint job and minor repair work. The other NOAA/GMCC housing unit also underwent improvements with the addition of new appliances, a new counter top and faucets, and the remodeling of the bathroom.

In March, the badly rusting Datsun pickup was replaced by a new Toyota four-wheel-drive pickup.

### PROGRAMS

Programs carried out in SMO are listed in table 4. Comments on some of the programs follow.

#### Carbon Dioxide

A URAS-2 infrared analyzer continuously monitored the concentration of CO<sub>2</sub> during 1985 with no appreciable downtime. Throughout the year, 5-L and 3-L flask pairs were exposed weekly.

Table 4.--Summary of sampling programs at SMO in 1985

Program	Instrument	Sampling Frequency
<u>Gases</u>		
CO <sub>2</sub>	URAS-2T infrared analyzer 0.5-L glass flasks P <sup>3</sup>	Continuous 1 pair wk <sup>-1</sup>
	0.5-L glass flasks, through analyzer	1 pair wk <sup>-1</sup>
	5-L evacuated glass flasks	1 pair wk <sup>-1</sup>
Surface ozone	Dasibi ozone meter	Continuous
Total ozone	Dobson spectrophotometer no. 42	3 day <sup>-1</sup>
Methane	0.5-L glass flasks	1 pair wk <sup>-1</sup>
CFC-11, CFC-12, and N <sub>2</sub> O	300-mL stainless steel flasks	1 pair wk <sup>-1</sup>
<u>Aerosols</u>		
Condensation nuclei	Pollak CNC	Discrete
	G.E. CNC	Continuous
Optical properties	Four-wavelength nephelometer	Continuous
<u>Solar Radiation</u>		
Global irradiance	Eppley pyranometers with Q and RG8 filters	Continuous
	Eppley pyranometers with Q filters on tilted mounts	Continuous
Direct irradiance	Eppley pyrhemometer with Q filter	Continuous
Direct irradiance	Eppley pyrhemometer with Q, OG1, RG2, and RG8 filters	Discrete
Turbidity	Sunphotometers with 380-, 500-, 778-, and 862-nm narrowband filters	Discrete
<u>Meteorology</u>		
Air Temperature	Thermistor	Continuous
	Max.-min. thermometers	1 day <sup>-1</sup>
	Hygrothermograph	Continuous
	Thermistor	1 day <sup>-1</sup>
Dewpoint temperature	Dewpoint hygrometer	Continuous
Relative humidity	Hygrothermograph	Continuous
	Sling psychrometer	Discrete
Pressure	Capacitance transducer	Continuous
	Microbarograph	Continuous
	Mercurial barometer	Discrete
Wind (speed and direction)	Bendix Aerovane	Continuous
Precipitation	Polyethylene funnel, bottle	1 day <sup>-1</sup>
<u>Precipitation Chemistry</u>		
pH	Corning model 125 meter with semimicro combination electrode	1 day <sup>-1</sup> (GMCC); 1 wk <sup>-1</sup> (NADP)
Conductivity	Beckman model RC-16C meter	1 day <sup>-1</sup> (GMCC); 1 wk <sup>-1</sup> (NADP)
<u>Cooperative Programs</u>		
CO <sub>2</sub> , <sup>13</sup> C, N <sub>2</sub> O (SIO)	5-L evacuated glass flasks	1 pair wk <sup>-1</sup>
ALE project: CFC-11, CFC-12, N <sub>2</sub> O, CH <sub>2</sub> CCl <sub>2</sub> , CCl <sub>4</sub> (OGC)	HP5840A gas chromatograph	1 h <sup>-1</sup>
ALE project: CH <sub>4</sub> , CO, CO <sub>2</sub> (OGC)	Carle gas chromatograph	3 h <sup>-1</sup>
Various trace gases (OGC)	Stainless steel flasks	1 set wk <sup>-1</sup> (3 flasks set <sup>-1</sup> )
<sup>13</sup> C, <sup>18</sup> O, CO <sub>2</sub> (CSIRO)	5-L glass flasks	1 set mo <sup>-1</sup>
<sup>13</sup> C (USGS)	10-L stainless steel flasks	2 pair mo <sup>-1</sup>
Wet-dry deposition (NADP)	HASL wet-dry collector (new Chemetrics, Dec 81)	1 wk <sup>-1</sup> , wet; 2 mo <sup>-1</sup> , dry
Bulk deposition (EML)	Plastic bucket	1 mo <sup>-1</sup>
Hi-Vol sampler (EML)	Hi-Vol pump and filter	1 wk <sup>-1</sup>
Hi-Vol sampler (SEASpan Project)	Hi-Vol pump and filter with clean	1 wk <sup>-1</sup>

### Surface Ozone

Surface ozone was measured continuously by a Dasibi UV ozone monitor and recorded on a strip chart. Beginning in June, long periods of digital data loss occurred when the CAMS box failed to read the digital data stream from the Dasibi. In an attempt to "unstick" the system, boards were replaced, connectors remade, and various keyboard inputs tried. The problem was eventually resolved by tying together the ground from the main observatory building with the ground from the aerosol-sampling building.

### Total Ozone

Dobson ozone spectrophotometer no. 42 provided discrete total atmospheric column ozone measurements throughout the year.

### Surface Aerosols

Condensation nuclei were measured by a G.E. CNC continuously in 1985 except for a period from June through August when the instrument was in Boulder for repairs. The four-wavelength nephelometer ran without interruption. An attempt to operate a Knollenberg Counter was thwarted because of tape drive problems.

### Solar Radiation

The complement of solar radiation instruments of SMO remained unchanged. In March, a preamp was added to the CAMS input to boost the millivolt signal levels and improve the signal-to-noise ratio.

### Meteorology

Meteorological instrumentation remained the same as in 1984. In September a dewpoint hygrometer was calibrated and put on line.

### Precipitation Chemistry

Both GMCC and NADP precipitation chemistry programs continued at SMO, providing on-site measurements of pH and conductivity in rainwater. NADP samples were collected weekly and GMCC samples were collected daily when precipitation was present. The observatory receives an annual average of 100 inches of precipitation.

### Cooperative Programs

OGC continued to monitor trace gases in 1985. At the start of the year a Carle and an HP5840 gas chromatograph were in operation. In July, OGC installed an HP5880 chromatograph and a UPS. After some months of side-by-side comparison, the Carle was removed during a subsequent visit by OGC staff in November.

## 2.4 South Pole

### FACILITIES

The National Science Foundation's CAF experienced few problems functionally or structurally during the 1984-1985 season. There were some modifications made to the floor plans of the CAF; fig. 1 illustrates the latest layout. Improvements or changes made inside the CAF areas follow: (1) GMCC's CAMS units were installed. (2) The ICDAS clock was wired to print each hour on the aerosol and the solar radiation chart recorders. (3) Antistatic matting was installed in the NOAA room. (4) A new flask sampling table was built and all flask pumps were mounted to it for air sampling through the new sampling pipe discussed below. (5) A new storage shelf was built above the CO<sub>2</sub> tanks in the NOAA room. (6) A new work table with a plexiglass top was built for the Pollak area. (7) An ink drawing of the CAF's floor and roof plan was produced on Mylar. (8) A new work table for the O<sub>2</sub>N<sub>2</sub> pump and flasks was built. (9) All excess wires in the overhead racks were cleaned out. (10) New stainless steel shelves were installed in the Co-op room. (11) A new plexiglass Dobson hatch was built and installed. (12) The instrument racks' front panels were painted. (13) All pump controls in the Co-op room were rewired. (14) All sampling stacks were heat traced and insulated. (15) The solar radiation heater/aspirator box was rebuilt and replumbed, and thermostatically controlled heat was added. (16) Fluorescent lighting was installed near the mercurial barometer. (17) The CAF's thermostats were relocated. (18) The pump cabinet in the Co-op room was reorganized and rewired--it is now used for only sampling pumps and not miscellaneous storage as before.

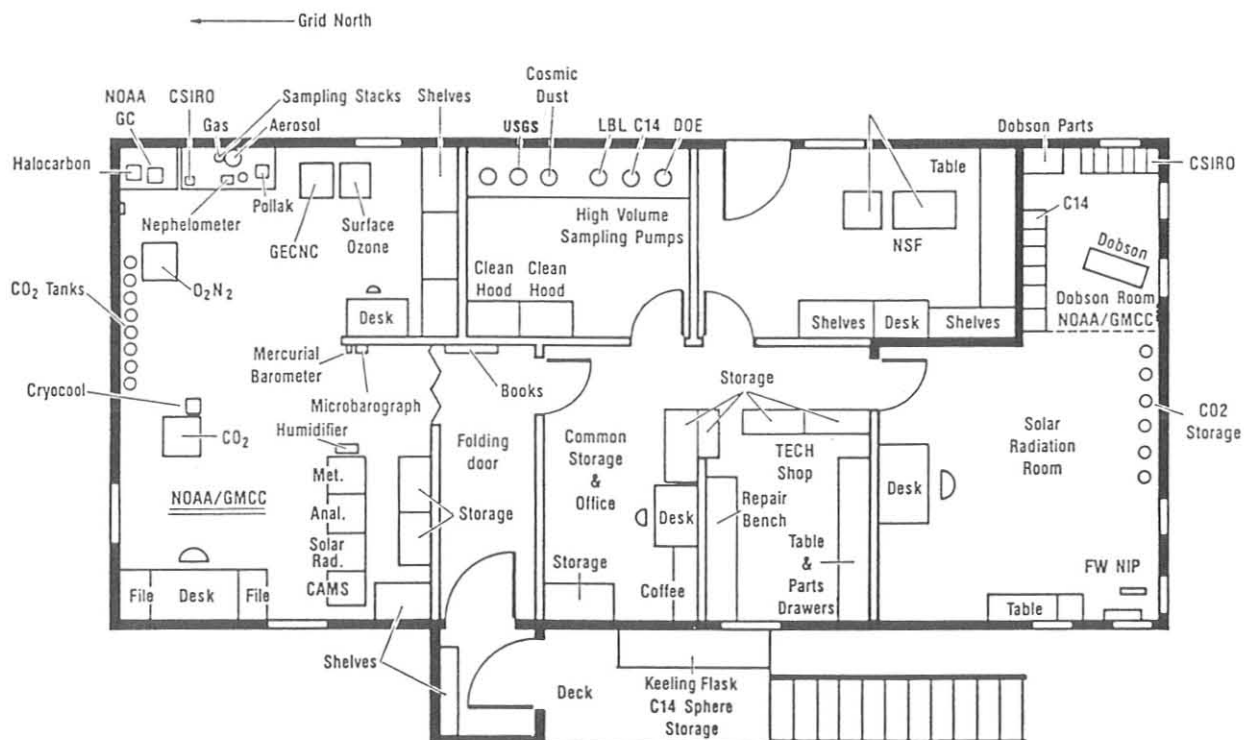


Figure 1.--Clean Air Facility SPO, 1985

The following synopsis describes those events affecting data acquisition. On 12 March 1985, the trace gas sampling stack was pressurized with CO<sub>2</sub> from the aerosol unit after both ends were sealed. Three pinpoint leaks, each located at the base of a sampling stem, were immediately apparent. An attempt was made to weld, solder, and braze these leaks closed, but the efforts were fruitless. The CO<sub>2</sub> intake line was moved to the aerosol stack, surface ozone's line was moved to its own sampling line outside, and halocarbon's and NCAR's intake remained on the trace gas sampling stack until the sampling pipe, mentioned below, was installed.

On 21 March 1985, a new sampling pipe was installed in the northeast corner of the CAF. Within the pipe are two 1/4-in copper tubes, one 1/4-in stainless steel tube, one 1/4-in Teflon tube, and one 3/8-in Teflon tube. The pipe stands approximately 15 ft above the CAF's roof and is heat traced with 4-W heat tape. Surface ozone, halocarbons, NCAR, O<sub>2</sub>N<sub>2</sub>, and a separate flask sampling line now utilize this pipe.

On 2 April 1985, the CAF had a power loss due to a break in one of three power phases somewhere between the CAF and the power plant. The location of this break was unknown until 29 August 1985. It is believed that this break resulted from ice shifting. Power was restored by means of an open-delta connection between the CAF and the power plant transformers on 4 April 1985.

On 24 May 1985, a D-6 Caterpillar cut through a powercable to the CAF while removing snow from the station's front entrance. The cable was spliced back together and power was restored 1 1/2 hours later. On 29 August 1985, two power phases to the CAF were cut by a D-6 Caterpillar while it was removing snow from the station's front entrance. By coincidence, the lost power phase of 2 April 1985 was found within 20 ft of the newly broken cables. All three were spliced to their appropriate halves giving the CAF three-phase power 5 1/2 hours later.

GMCC's CAMS units were installed to replace ICDAS, to control and monitor aerosols, carbon dioxide, meteorology, solar radiation, and surface ozone. Three CAMS units were installed during the 1984-1985 season. The ASR (aerosol and solar radiation) CAMS was initiated on 27 November 1984 at 0539 GMT, the CO<sub>2</sub> (carbon dioxide) CAMS on 14 November 1984 at 0022 GMT, and the MO3 (meteorology and surface ozone) CAMS on 19 November 1984 at 2310 GMT. All CAMS data are stored via cassette tape drives onto Digital DECTAPE II cassettes.

Heavy demands on the station's power plant resulted in 13 blackouts, 11 brownouts, and 3 power surges. Although no instrument damage resulted, all blackouts resulted in an "AUTORESTART" on each CAMS unit. Four "BRAM LOST" messages were recorded for the year, all of which resulted from power blackouts.

#### PROGRAMS

Table 5 lists the sampling programs carried out during the 1984-1985 seasons.

Table 5.--Summary of sampling programs at SPO in 1985

Program	Instrument	Sampling frequency
<u>Gases</u>		
CO <sub>2</sub>	URAS-2T infrared analyzer	Continuous
Surface ozone	0.5-L glass flasks P <sup>3</sup> 0.5-L glass flasks, through analyzer Dasibi ozone meter	1 pair (2 wk) <sup>-1</sup> 1 pair wk <sup>-1</sup> Continuous
Total ozone	Dobson spectrophotometer no. 80	3 day <sup>-1</sup>
CFC-11, CFC-12, and N <sub>2</sub> O	300-mL stainless steel flasks	1 pair wk <sup>-1</sup> 1 pair wk <sup>-1</sup> , summer; 1 pair mo <sup>-1</sup> , winter
O <sub>2</sub> N <sub>2</sub> (NOAA/ARL)	Gas chromatograph Flasks	1 pair week <sup>-1</sup> 2 analyses wk <sup>-1</sup> 1 flask mo <sup>-1</sup> present
<u>Aerosols</u>		
Condensation nuclei	Pollak CNC	Discrete
Optical properties	G.E. CNC Four-wavelength nephelometer	Continuous Continuous
<u>Solar Radiation</u>		
Global spectral irradiance	Eppley pyranometers with Q and RGB filters	Continuous
Turbidity	Eppley pyrhemliometer with Q, OG1, RG2, and RGB filters	Discrete
Albedo	Sunphotometers with 380-, 500-, 778-, and 862-nm narrowband filters	Discrete, summer
Terrestrial (IR) radiation	Eppley pyranometers with Q and RGB filters, downward-facing Eppley pyrgeometers, upward- and downward-facing	Continuous Continuous
<u>Meteorology</u>		
Air Temperature	Platinum resistor	Continuous
Snow temperature	Platinum resistor 0.5 cm	Continuous
Pressure	Capacitance transducer Mercurial barometer	Continuous 2 times day <sup>-1</sup>
Wind speed/direction	Bendix Aerovane recorder	Continuous
<u>Cooperative Programs</u>		
CO <sub>2</sub> , <sup>13</sup> C, N <sub>2</sub> O (SIO)	5-L evacuated glass flasks	2 mo <sup>-1</sup> (3 flasks sample <sup>-1</sup> )
Total surface particulates (DOE)	High-volume sampler	Continuous (1 filter wk <sup>-1</sup> )
Aerosol physical properties (SUNYA)	Pollak CNC with diffusion battery Nuclepore filters	Discrete Discrete
Carbon aerosol (LBL)	High-volume sampler	Continuous
Various trace gases (OGC)	Stainless steel flasks	Twice mo <sup>-1</sup> (3 flasks set <sup>-1</sup> )
<sup>13</sup> C/ <sup>12</sup> C, CH <sub>4</sub> (USGS)	10-L stainless steel cylinder	1 mo <sup>-1</sup> (2 cylinders sample <sup>-1</sup> )
<sup>14</sup> C (NOAA/ARL)	3,000 psi spheres	500 psi day <sup>-1</sup>
Snow acidity (NOAA/ARL)	125-mL Nalgene flasks	Weekly
CH <sub>4</sub> , CO (NCAR)	Baseline gas chromatograph Aluminum flasks	Daily Weekly
<sup>14</sup> C/ <sup>12</sup> C NaOH samples (USGS)	Gas bubbler	20 days mo <sup>-1</sup>
Atmospheric Tracer Exp. (Los Alamos Nat. Lab.)	CH <sub>4</sub> detector	3-60 day periods
Cosmic Dust Collection (Univ. of Pittsburgh)	Cosmic dust collector	Continuous
Interhemispheric <sup>13</sup> C/ <sup>14</sup> C (CSIRO)	Flasks	2 flasks mo <sup>-1</sup>

## Surface Aerosols

The Pollak CNC operated well all year. Both G.E. CNCs, nos. 7007 and 3264296, functioned well all year with very few complications. No. 7007 experienced two bad chips on the electronics board, three malfunctioned thermistors, and one system boil out. The thermistor problem was resolved by a new electronic water level sensing circuit. No. 3264296 required numerous high-voltage adjustments from 5-8 October 1985. This CNC was totally rebuilt.

No major problems were experienced with the nephelometer. CO<sub>2</sub> and relative calibrations, power blackouts, and power brownouts caused data on all four channels to be lost occasionally. These data were quickly restored by erasing the memory and then simultaneously using "hold ambient" and "mode A" for each filter. This procedure resulted in minimal data loss.

## Carbon Dioxide

On 15 December 1984, before realigning the URAS-2T, the optical quartz glass tube cracked while using Dust Off to remove particles from its surface. GMCC in Boulder was notified. A replacement tube was sent, and it was in place by 12 January 1985. The three pinpoint leaks found in the trace gas sampling stack on 12 March 1985 resulted in the CO<sub>2</sub> intake line being moved to the aerosol stack for the remainder of the year. Other problems included one faulty regulator, cracked Dyna pump diaphragms, and two burned-out fuses. The P<sup>3</sup> sampler functioned well throughout the year. After the 21 March 1985 sampling pipe installation, all P<sup>3</sup> flasks were exposed via the pipe's 3/8-in Teflon tube. P<sup>3</sup> flasks prior to this date were exposed on the roof.

The O<sub>2</sub>N<sub>2</sub> high-pressure flask sampler experienced a leak in the compressor's stage no. 1. New compressor rings were sent on the midwinter airdrop, though once installed the pump could only attain 30 psi and 60 rpm. This problem was alleviated by using a 10-in pulley and a 2-hp motor to achieve 750 rpm. This allowed us to take the required 1750-psi flask samples.

## Halocarbons

Halocarbon sampling proceeded with no problems.

## Meteorology

There were no problems with this program except that the Bendix Friez's wind direction accuracy was constantly off by several degrees and the switching mechanism would not function properly when the wind direction pen reached the 0° or 180° mark. These problems were corrected on 25 June 1985 after the anticipated replacement recorder did not arrive on the midwinter airdrop. New points were fabricated from relay contacts and the pen adjusted to track accurately with CAMS. The Bendix Friez tracked with 1° from then on.

## Ozone

Surface ozone and Dobson measurements continued with no difficulties.

## Solar Radiation

There were no major problems with this program. Solar irradiance was measured from 21 September 1984 to 22 March 1985. After the austral winter, these instruments were reinitiated on 25 September 1985 and have worked well. A new solar radiation preamp for CAMS was installed on 2 February 1985. Aside from general maintenance, it has functioned well throughout the year.

## COOPERATIVE PROGRAMS

All programs operated without incident with the following exceptions: The U.S. DOE's high-volume sampler's main motor and backup shorted out during November 1984. DOE was notified, but replacement motors did not arrive until the midwinter airdrop. This project ran well once reinitiated. After the power outage of 2 April 1985, the three-phase carbon-14 motor could no longer be used because of CAF's new two-phase power. On 21 April 1985, the first sample using a new two-phase pump built by the GMCC electronic technician, was taken. All samples before and after this down period went smoothly.

Many electronic and mechanical problems were experienced with NCAR's GC this year. An average of 6 to 8 of the required 12 runs per month were made between GC repairs. Early in the year the GC's hydrogen generator developed a hole in its ECC assembly. NCAR was informed of this, though no replacement came on the midwinter airdrop. This project was retrograded to NCAR in November 1985 at their request.

### 3. AEROSOLS AND RADIATION MONITORING GROUP

#### 3.1 Continuing Programs

##### SURFACE AEROSOLS

The GMCC baseline aerosol monitoring program continued operations during 1985 as in previous years. Condensation nucleus (CN) concentration and aerosol scattering extinction coefficient ( $\sigma_{sp}$ ) were measured continuously at BRW, MLO, SMO, and SPO. A G.E. automatic CN counter (CNC) operates continuously and a Pollak CNC provides daily calibration points at each station. A four-wavelength nephelometer at each station continuously measures  $\sigma_{sp}$  at 450-, 550-, 700-, and 850-nm wavelengths.

A renovated four-wavelength nephelometer was installed at MLO during the last week of May. The renovation involved use of the original optics with upgraded electronics so that the MLO instrument is now identical to the instruments at BRW, SMO, and SPO. The design of the original MLO nephelometer was described by Miller (1975), and the new design was described by Hanson (1977) and Bodhaine (1979). Although the optics are identical in both designs, the electronics in the old design performed an internal geometric mean, whereas the new design performs an arithmetic mean. This implies that during hours of significant signal variation, the new instrument may give slightly higher data values than those given by the old design. It is not possible to deduce one from the other without knowing the statistical distribution of the data during the hour.

Figure 1 shows daily geometric means of CN concentration and  $\sigma_{sp}$  at the GMCC stations for 1985. Angstrom exponents calculated from the four-wavelength light scattering data are shown in the upper portions of each graph. Monthly geometric means for each station are shown in fig. 2 for the entire data record and are listed in table 1 for 1985.

The BRW data in fig. 1 show elevated  $\sigma_{sp}$  values in excess of  $10^{-5} \text{ m}^{-1}$  in the springtime, typical of the well-known Arctic haze. The regular annual cycle is apparent in the BRW long-term record shown in fig. 2 in which monthly means exceed  $10^{-5} \text{ m}^{-1}$  in the spring and can be below  $10^{-6} \text{ m}^{-1}$  in the summer. The BRW CN long-term record shows a more variable semiannual cycle in which maxima usually occur in March and August, and minima usually occur in June and November.

The MLO CN data shown in fig. 1 are typical for the downslope conditions at Mauna Loa and are most likely representative of the background troposphere for this region of the atmosphere. The  $\sigma_{sp}$  record for MLO shown in fig. 1 was produced by the new MLO nephelometer and shows an annual trend similar to that of previous years. The long-term record of  $\sigma_{sp}$  in fig. 2 shows a repeatable annual cycle with a maximum in April-May that is caused by the long-range transport of Asian desert dust in the upper troposphere to the vicinity of Hawaii.

The SMO  $\sigma_{sp}$  and CN data continue as in previous years with no significant annual cycle or long-term trend. The SMO aerosol is representative of a background marine air mass. Bodhaine and DeLuise (1985) presented a detailed analysis of the entire SMO data record.

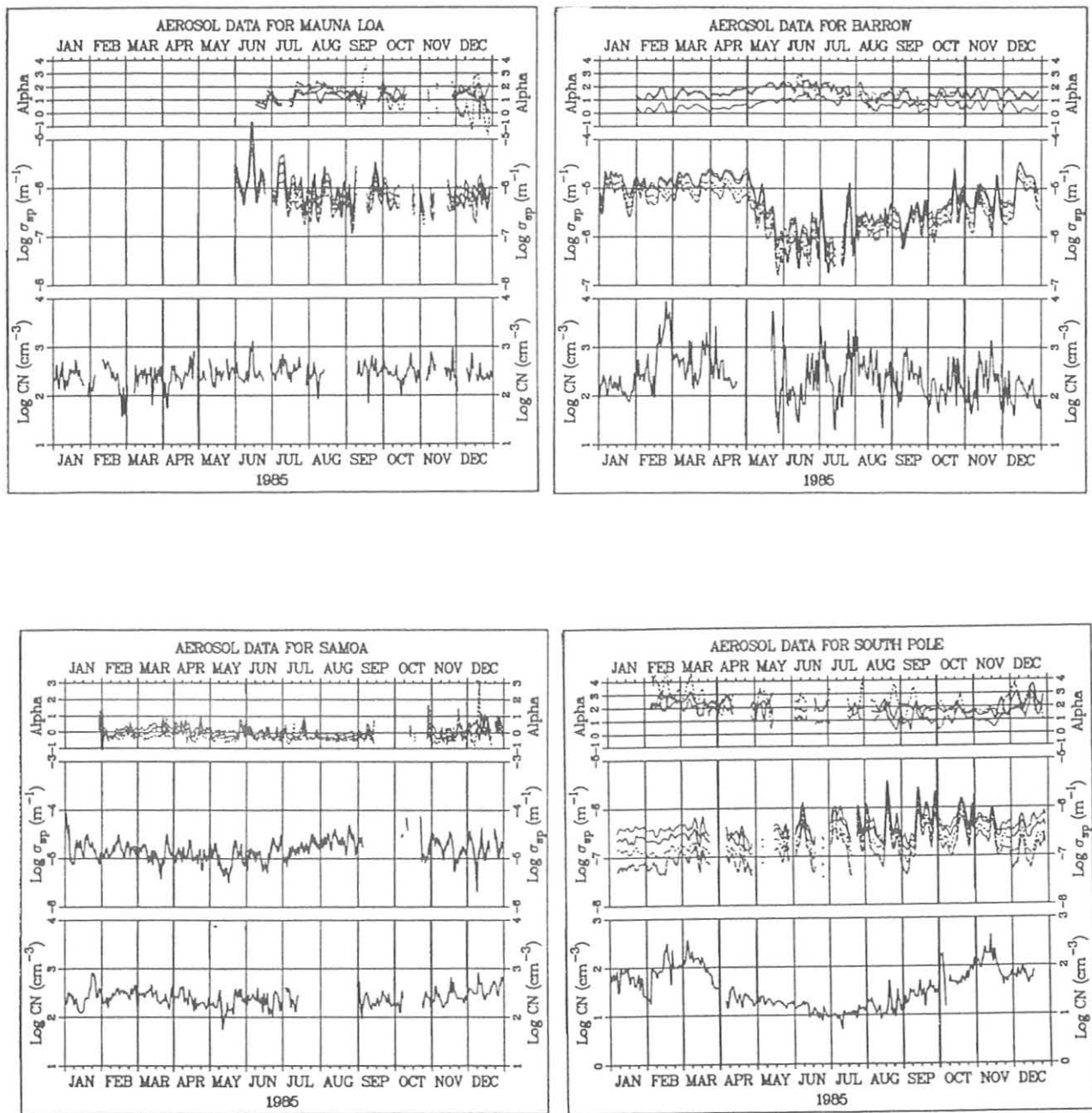


Figure 1.--Daily geometric means of  $\sigma_{sp}$  and CN data at BRW, MLO, SMO, and SPO for 1985. For each station, CN concentration (lower) is shown as a solid line.  $\sigma_{sp}$  data (middle) are shown for 450 (dotted), 550 (solid), 700 (dashed), and 850 nm (long-dashed). Angstrom exponents were calculated from 450- and 550-nm (dotted), 550- and 700-nm (solid), and 700- and 850-nm (dashed)  $\sigma_{sp}$  data.

Table 1.--Monthly geometric means of CN concentration ( $\text{cm}^{-3}$ ) and  $\sigma_{\text{sp}}$  ( $\text{m}^{-1}$ ) at 450, 550, 700, and 850 nm, for BRW, MLO, SMO, and SPO during 1985

	Jan	Feb	Mar	Apr	May	Jun	Jul	Aug	Sep	Oct	Nov	Dec
BRW												
CN	144	668	497	309	237	165	314	322	238	147	184	113
$\sigma_{\text{sp}}$ (450)	1.44-5	1.35-5	1.65-5	1.98-5	5.44-6	1.59-6	1.68-6	2.70-6	3.17-6	5.47-6	7.11-6	1.21-5
$\sigma_{\text{sp}}$ (550)	1.35-5	1.25-5	1.53-5	1.72-5	4.39-6	1.24-6	1.33-6	2.44-6	2.88-6	4.70-6	6.21-6	1.11-5
$\sigma_{\text{sp}}$ (700)	9.66-6	8.80-6	1.09-5	1.09-5	2.65-6	7.26-7	8.80-7	1.79-6	2.20-6	3.29-6	4.28-6	7.83-6
$\sigma_{\text{sp}}$ (850)	7.34-6	6.68-6	8.26-6	7.61-6	1.76-6	4.93-7	6.90-7	1.35-6	1.76-6	2.46-6	3.17-6	5.80-6
MLO												
CN	238	216	221	229	275	304	346	252	333	281	343	262
$\sigma_{\text{sp}}$ (450)	-	-	-	3.20-6	2.14-6	2.05-6	1.36-6	1.08-6	1.25-6	9.59-7	7.04-7	1.05-6
$\sigma_{\text{sp}}$ (550)	-	-	-	2.58-6	1.73-6	1.67-6	9.90-7	7.85-7	9.29-7	6.86-7	5.24-7	7.39-7
$\sigma_{\text{sp}}$ (700)	-	-	-	1.94-6	1.50-6	1.39-6	7.37-7	5.58-7	6.68-7	5.14-7	3.49-7	5.61-7
$\sigma_{\text{sp}}$ (850)	-	-	-	1.45-6	1.14-6	1.10-6	5.08-7	3.98-7	4.80-7	5.03-7	3.35-7	5.88-7
SMO												
CN	266	291	269	229	190	225	262	427	221	213	259	383
$\sigma_{\text{sp}}$ (450)	1.74-5	1.57-5	1.25-5	1.12-5	9.75-6	1.20-5	1.48-5	2.20-5	2.15-5	1.99-5	1.62-5	1.78-5
$\sigma_{\text{sp}}$ (550)	1.65-5	1.47-5	1.16-5	1.08-5	9.38-6	1.19-5	1.46-5	2.23-5	2.14-5	1.91-5	1.57-5	1.59-5
$\sigma_{\text{sp}}$ (700)	1.71-5	1.46-5	1.15-5	1.12-5	9.55-6	1.25-5	1.55-5	2.40-5	2.28-5	1.98-5	1.67-5	1.57-5
$\sigma_{\text{sp}}$ (850)	1.76-5	1.54-5	1.18-5	1.20-5	9.95-6	1.33-5	1.68-5	2.62-5	2.46-5	2.09-5	1.74-5	1.49-5
SPO												
CN	56	86	104	23	19	13	11	16	28	60	106	65
$\sigma_{\text{sp}}$ (450)	3.90-7	3.68-7	3.81-7	2.91-7	3.40-7	3.88-7	5.91-7	5.25-7	5.94-7	6.43-7	5.41-7	5.16-7
$\sigma_{\text{sp}}$ (550)	2.33-7	2.45-7	2.53-7	2.01-7	2.50-7	3.13-7	4.46-7	4.26-7	4.85-7	5.02-7	4.41-7	3.49-7
$\sigma_{\text{sp}}$ (700)	1.31-7	1.31-7	1.43-7	1.11-7	1.53-7	1.80-7	2.85-7	2.65-7	3.19-7	3.33-7	2.96-7	1.81-7
$\sigma_{\text{sp}}$ (850)	6.06-8	7.11-8	9.20-8	7.12-8	9.72-8	1.13-7	1.74-7	1.74-7	2.10-7	2.34-7	2.06-7	1.16-7

A compact exponential format is used for  $\sigma_{\text{sp}}$  such that  $1.44-5 = 1.44 \times 10^{-5}$ .

The SPO CN data show a strong annual cycle: a maximum greater than  $100 \text{ cm}^{-3}$  in the austral summer and a minimum of about  $10 \text{ cm}^{-3}$  in the winter. The  $\sigma_{\text{sp}}$  data show a cycle dominated by events in the austral winter. These events are caused by the transport of seasalt in the upper troposphere from stormy regions near the coast to the interior of the continent. An analysis of the SPO data set, case studies of the winter seasalt events, and a study of aerosol chemistry were presented by Bodhaine et al. (1986, 1987).

The least-squares trend lines shown in fig. 2 are not statistically significant, and the results are given in table 2. Trend lines have been calculated for these data in previous years and presented in previous GMCC Summary Reports. In general, as the data records have increased in length, the trend lines have been getting flatter, confirming previous suggestions that there is no significant long-term trend in the background aerosol measured at these four stations.

Nephelometer and CN data are available in NOAA data reports. Requests for specific data sets on electronic recording media should be made to GMCC personnel.

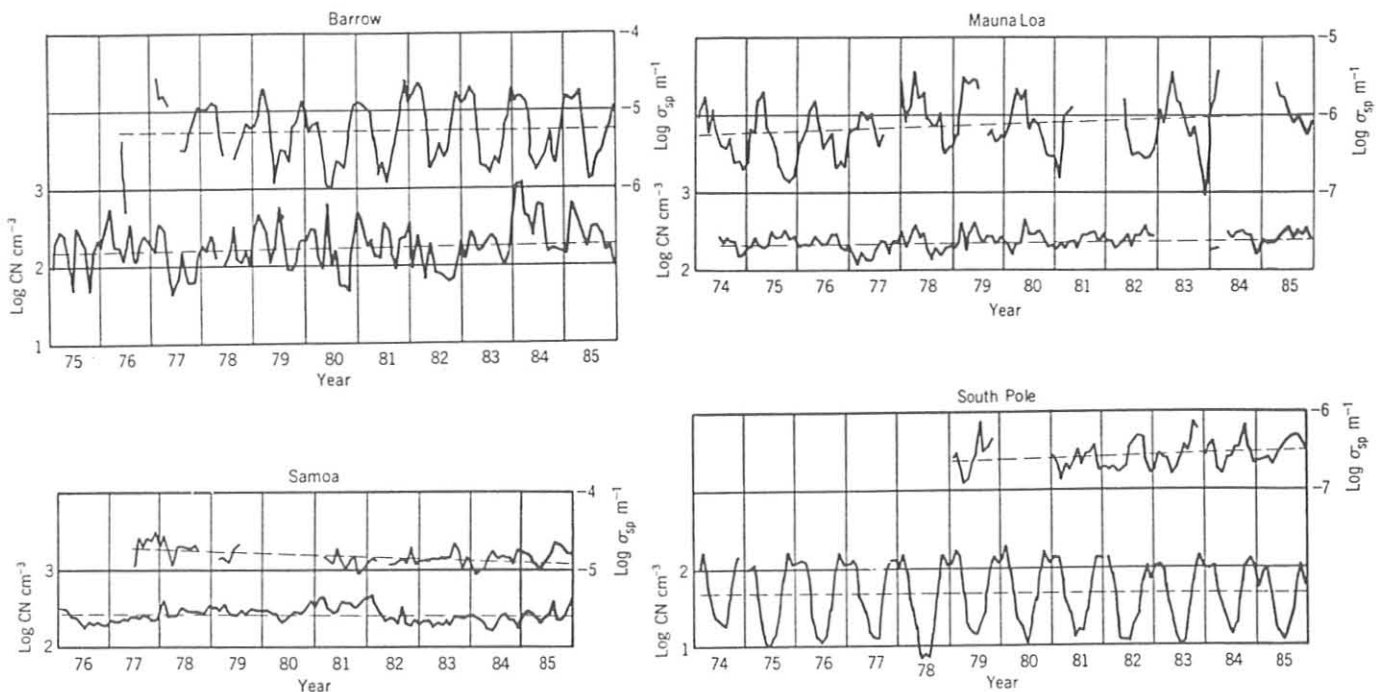


Figure 2.--Monthly geometric means of  $\sigma_{sp}$  and CN data for the entire data record. Details of the trend lines are given in table 2.

Table 2.--Least-squares trend analysis of the common logarithms of the data shown in fig. 2

Parameter	Slope	Intercept	S.E.	Trend (% yr <sup>-1</sup> )
BRW CN	0.0162	-29.8	0.284	3.8
BRW $\sigma_{sp}$	0.00345	-12.1	0.395	0.80
MLO CN	0.00713	-11.7	0.120	1.7
MLO $\sigma_{sp}$	0.0159	-35.7	0.348	3.5
SMO CN	-0.00357	9.5	0.102	-0.82
SMO $\sigma_{sp}$	-0.0288	52.3	0.106	-6.4
SPO CN	-0.00462	10.8	0.414	-1.1
SPO $\sigma_{sp}$	0.0242	-54.6	0.180	5.7

#### SOLAR AND THERMAL RADIATION

This section covers the solar and thermal radiation measurements at the four GMCC baseline observatories. Included are a summary of activities at the sites, a discussion of calibration intercomparisons between field and reference instruments over the past 10 years, and partial results from various monitoring projects.

## Barrow

A new automated solar tracker was installed in the fall of 1985. The tracker is the commercially available 20/20 Licor that continuously adjusts for solar declination as well as hour angle. The new tracker improves the tracking accuracy, especially during extended periods of cloudiness when the sun is only occasionally visible.

The blowers, which were installed to prevent condensation buildup on the pyranometer domes, were removed from service when it was determined that their useful life had been exceeded. A new blower system was developed and placed into operation in early 1986. The new blowers operate only on the quartz and RG8 upward-facing pyranometers and not on the downward-facing pyranometers. The instruments not served by the blowers rarely experience frost deposition.

An HP-71 calculator-based backup data acquisition system was tested throughout 1985. A few minor problems were encountered, the worst of which was the quality of the printing on the system's strip chart.

Complete radiation balance measurements were begun in June with the installation of a downward-facing pyranometer and pyrgeometer. The inverted instruments are suspended 2 m above the tundra at a distance of 300 m due east of the main building. These instruments measure upwelling solar shortwave and terrestrial longwave radiation. The downwelling flux is measured by two identical instruments mounted on the roof of the building. The instruments' signals are routed to the ASR CAMS in the main building.

## Mauna Loa

The Leeds and Northrup radiation strip chart recorder was replaced by an HP-71-based backup data system in May 1985.

The dependence upon the Mauna Loa facility and staff as a primary sunphotometer calibration facility increased during 1985. This is due to both the realization of the extent of problems with Boulder-based calibrations and the expanded awareness of the availability of the site to other government and nongovernment laboratories. The impact on the MLO staff's workload has been minimized by requiring the outside users to supply their own personnel to perform the required operations.

The automated solar observatory dome continues to operate, providing a sheltered platform for instruments requiring highly accurate solar tracking during early morning hours. The automated observatory's current principal function is to facilitate operation of the PMOD three-wavelength precision sunphotometer that serves as the primary calibration standard for the U.S. and GMCC sunphotometer networks.

## Samoa

Radiometer degradation is extreme at SMO. The RG8 domes show visible changes in color after less than a year in the field at SMO. Fortunately, these color changes do not significantly change the filter transmission characteristics. A more serious instrument deterioration is seen in the loss

of sensitivity in the quartz pyranometers. Sensitivity losses as great as 3% per year have been documented. However, the calibration drifts were well enough documented so that the data could be corrected to the  $\pm 1.0\%$  level over the long term.

### South Pole

In December 1985, an HP-71-based data system was installed at SPO. The major problem encountered was the quality of the printer operation. This problem was solved in part by increasing the humidity in the building.

The present mounting rack for the inverted radiometers is slowly being buried by snow. As of the end of 1985, the downward-facing instruments, quartz and RG8 pyranometers and a pyrgeometer, were suspended about 2.5 ft over the snow surface.

### Intercomparison With Traveling Reference Instruments

Each year a reference standard pyranometer and pyrheliumeter with a filter wheel are sent to each of the observatories for a period of comparison with the station instruments. The comparisons are accomplished during several days of side-by-side measurements. Although the comparisons can be examined for hourly and daily performance, the final result is the overall average of the ratio between the calibrated output of each instrument. The calibrations assigned to all the instruments for the purpose of the intercomparison have been held constant over the last 10 years so that the results of the comparison will show any relative change in sensitivity between the reference and station instrument. The reference instruments are calibrated in Boulder at the Solar Radiation Facility.

In general the pyrheliumeters stayed relatively steady whereas the pyranometers started out stable but have increasingly drifted in recent years. The drifts in the station pyranometers are less at the colder, drier locations.

The filter factors for the station filter wheels used with the hand-held pyrheliumeters are also determined each year. The procedure involves measuring the transmission of a reference filter in the laboratory and then using that filter in the field to verify the transmission of the station filter.

### Clear-Sky Normal Incident Irradiance

Measurements of the direct normal solar irradiance in four spectral bands have been made at the four GMCC observatories since 1977. The measurements are only recorded when an observer verifies that visible clouds are not influencing the measurement. Observations are taken nominally three times a day, near local noon and 2 hours before and after. Results from these measurements for 1977 through 1981 were presented by Bodhaine and Harris (1982). The previously reported results are up to 6% in error because an incorrect sun/earth distance correction form was applied. A reanalysis of the data for that time and subsequent years is given in tabular form in fig. 3. Also, corrected data for 1977 through 1981 are presented here in fig. 4, which replaces fig. 23 in Summary Report No. 10 (Bodhaine and Harris, 1982). These

SMAO FWNIP 1977-1986 AVERAGE OVER AIR MASS INTERVAL										SPO FWNIP 1977-1986 AVERAGE OVER AIR MASS INTERVAL											
YEAR	AM	QUARTZ	SD	OG1	SD	RG2	SD	RG8	SD	N	YEAR	AM	QUARTZ	SD	OG1	SD	RG2	SD	RG8	SD	N
1977-1981	1.1	92.19	2.89	69.48	2.35	54.53	1.95	45.34	1.73	252.	1977-1981	2.5	102.37	2.39	82.34	2.14	68.05	1.91	58.55	1.73	110.
1977-1981	2.1	77.44	3.74	60.98	3.01	48.18	2.47	39.97	2.25	60.	1977-1981	3.5	94.57	4.36	78.06	3.52	65.03	3.12	56.17	3.22	28.
1982	1.1	90.65	3.00	69.15	2.29	54.37	1.98	45.38	1.43	43.	1982	2.5	96.03	2.16	77.43	1.74	65.32	1.49	58.24	1.36	24.
1982	2.1	75.32	3.61	59.98	2.77	47.46	2.16	39.45	1.77	14.	1982	3.5	93.85	4.75	75.47	3.82	63.77	3.52	50.87	4.45	43.
1983	1.1	88.56	4.11	67.97	2.97	52.63	2.49	43.91	2.17	55.	1983	2.5	89.62	4.58	74.04	3.39	63.29	2.80	56.43	2.46	11.
1983	2.1	72.16	2.76	56.94	2.39	45.20	1.86	37.65	1.73	12.	1983	3.5	89.62	4.58	74.04	3.39	63.29	2.80	56.43	2.46	11.
1984	1.1	90.86	2.24	68.61	1.77	53.85	1.46	44.84	1.34	35.	1984	2.5	94.35	.22	75.68	.37	63.94	.15	55.58	.35	4.
1984	2.1	75.14	2.56	58.59	2.24	46.64	1.92	38.87	1.73	3.	1984	3.5	86.54	8.28	70.44	6.62	58.98	5.53	51.71	6.44	14.
1985	1.1	91.73	2.88	69.26	2.63	54.28	2.21	45.27	1.91	42.	1985	2.5	97.14	1.74	77.10	1.75	64.71	1.78	57.18	1.81	4.
											1985	3.5	92.05	4.45	75.00	3.47	63.53	3.18	56.28	2.98	5.

BRW FWNIP 1977-1986 AVERAGE OVER AIR MASS INTERVAL										MLO FWNIP 1977-1986 AVERAGE OVER AIR MASS INTERVAL											
YEAR	AM	QUARTZ	SD	OG1	SD	RG2	SD	RG8	SD	N	YEAR	AM	QUARTZ	SD	OG1	SD	RG2	SD	RG8	SD	N
1977-1981	1.5	91.03	4.11	72.83	3.05	58.14	2.50	51.09	2.26	73.	1977-1981	1.1	112.44	2.08	85.43	2.87	68.96	2.06	60.90	2.17	816.
1977-1981	2.5	77.57	5.59	65.60	3.93	55.32	3.12	49.56	3.03	48.	1977-1981	2.1	105.29	2.52	83.33	2.42	67.92	2.38	60.09	2.37	26.
1982	1.5	84.25	7.24	67.99	1.67	54.98	1.55	48.09	1.53	16.	1982	1.1	96.02	7.92	73.99	6.12	60.17	5.02	53.41	4.41	103.
1982	2.5	71.95	4.33	61.86	2.52	52.76	1.14	47.72	.96	3.	1982	2.1	89.24	12.26	71.10	9.56	58.14	7.68	51.74	6.83	6.
1983	1.5	77.15	2.78	62.44	2.03	50.75	1.71	44.90	1.58	14.	1983	1.1	108.47	1.94	83.46	1.73	67.75	1.88	60.14	1.58	223.
1983	2.5	58.66	5.60	50.10	4.07	42.88	3.09	38.83	2.66	8.	1983	2.1	97.48	2.73	77.80	2.24	63.89	2.16	56.88	2.15	16.
1984	1.5	86.08	6.54	68.97	5.85	54.71	3.08	49.75	7.71	17.	1984	1.1	111.88	2.30	86.22	2.04	70.05	1.78	61.99	1.82	210.
1984	2.5	72.85	11.64	60.79	7.29	50.83	4.46	45.65	3.33	6.	1984	2.1	103.73	3.60	83.04	3.27	68.29	3.14	60.97	3.25	4.
1985	1.5	89.99	4.37	71.34	2.77	57.28	1.99	50.72	1.65	7.	1985	1.1	111.76	2.61	85.74	2.44	69.68	2.36	61.61	2.36	90.
1985	2.5	53.03	9.04	45.27	7.77	38.23	6.35	34.68	6.03	4.											

Figure 3.--Mean direct beam solar flux ( $\text{mW cm}^{-2}$ ) and standard deviation (SD) for the 5-yr period of 1977-1981 and each individual subsequent year. Values are for two selected relative air mass values (AM). N is the number of observations. The spectral intervals Quartz, OG1, RG2, and RG8 are the same as described in fig. 4.

measurements establish an absolute level for confirmed clear-sky background solar measurements. The variability in the data indicates the degree of variability of radiation attenuators such as water vapor, ozone, and aerosols. The distinctly different results between the four sites are due to altitude and latitude differences, which cause different amounts of Rayleigh scattering and water vapor absorption. Two global extremes are represented by South Pole, at 2.8 km and very dry, and Samoa, at sea level in the tropics.

### BRW Radiation Budget

Figure 5 shows preliminary results of the radiation budget measurements at BRW. The three graphs show daily totals of the net longwave, net shortwave, and the net all-wave radiation flux, where downward flux is positive. Each of the four components of the radiation budget (up and down, longwave and shortwave) was individually measured with an Eppley thermocouple instrument. The instruments were periodically intercalibrated by turning the normally downward-facing instruments up for a few hours each week. The absolute calibration of the data is dependent on the manufacturer's calibration and on in-house calibration of the solar instruments. No intercalibration between the longwave and shortwave instruments was made. Also, pyrgeometer dome solar heating was not corrected for. The pyrgeometer output signal was taken directly from the battery-compensated circuit, and no temperature corrections were applied. Additional processing and calibration of these data are necessary to ensure the most accurate possible results.

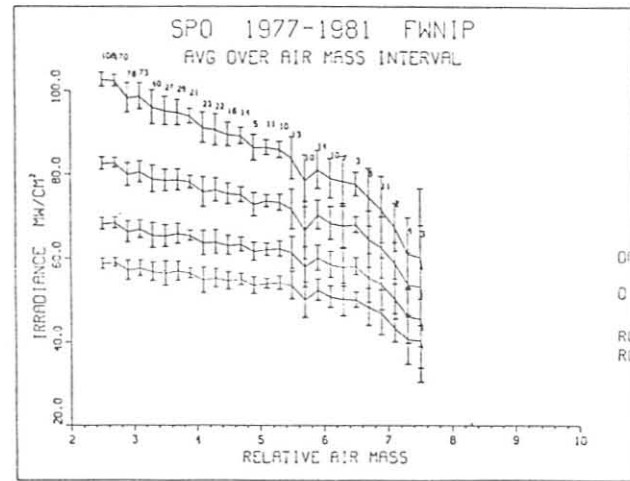
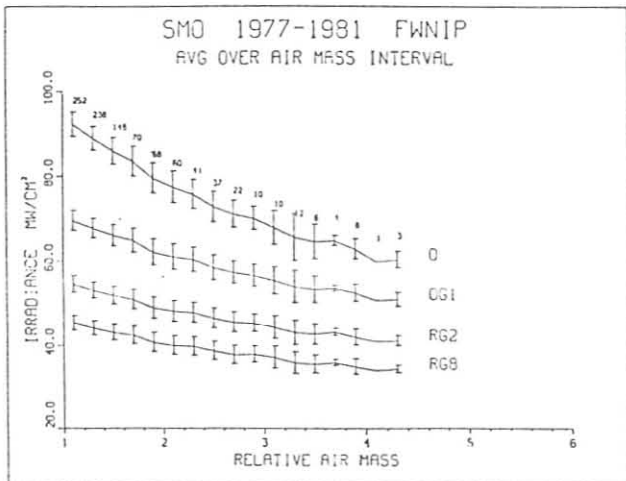
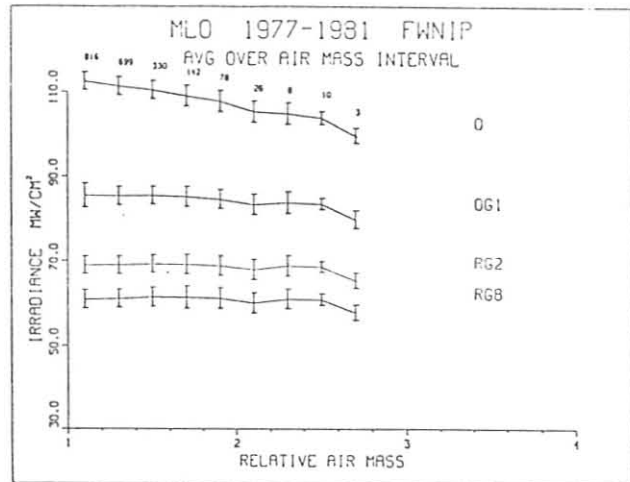
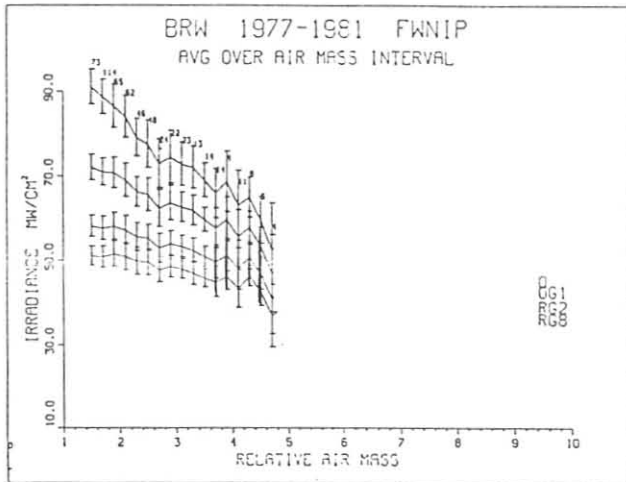


Figure 4.--Direct beam solar irradiance in four spectral bands, (Q) 0.28-3.0 $\mu$ m, (OG1) 0.53-3.0  $\mu$ m, (RG2) 0.63-3.0  $\mu$ m, and (RG8) 0.695-3.0  $\mu$ m for a 5-yr period from each observatory as indicated. Data are plotted and averaged at the midpoint of each 0.2 air mass interval.

The radiation budget at a given location such as BRW is determined by many variables: solar position, cloud cover, surface reflectivity, surface and air temperature, and atmospheric composition. By measuring each of the four budget components separately, it will be easier to determine which variables are responsible for any observed changes in the radiation budget. Identification of radiation budget perturbations and their causes is the goal of this measurement project. Currently the data record is too short to warrant perturbation analysis.

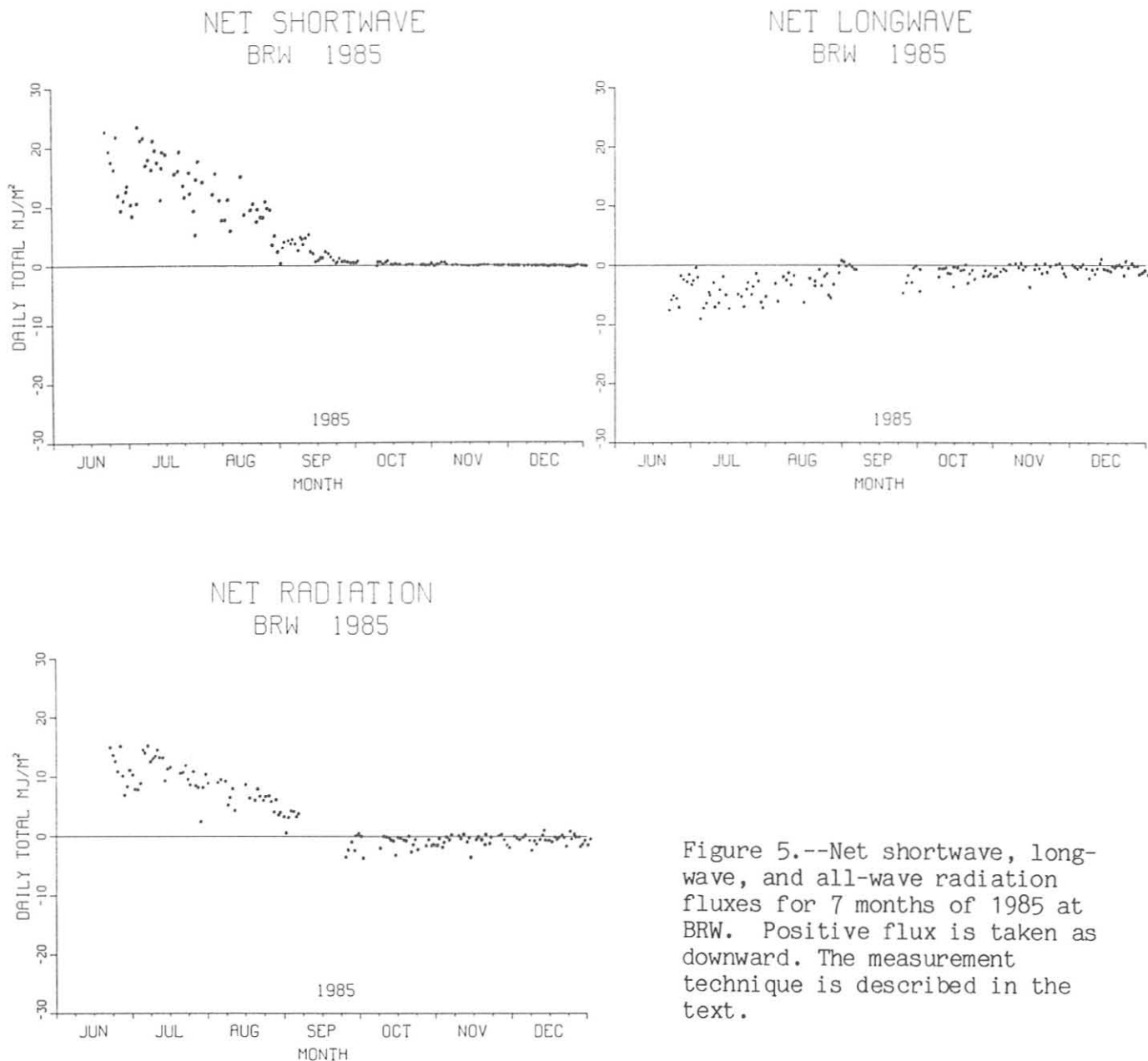


Figure 5.--Net shortwave, long-wave, and all-wave radiation fluxes for 7 months of 1985 at BRW. Positive flux is taken as downward. The measurement technique is described in the text.

#### MLO STRATOSPHERIC AEROSOL LIDAR OBSERVATIONS

Lidar observations continued at MLO at a rate of once per week. In late November a new stratospheric aerosol cloud appeared and continued to be quite evident into early 1986. This stratospheric cloud appeared first at around 27-km altitude and later between 20 and 23 km. It has tentatively been attributed to the 13 November 1985 eruption in Columbia of the volcano Nevada del Ruiz. Figure 6 shows the six lidar observations taken in November. The strong scattering layer above 25 km on 26 and 27 November is believed to be the Ruiz plume.

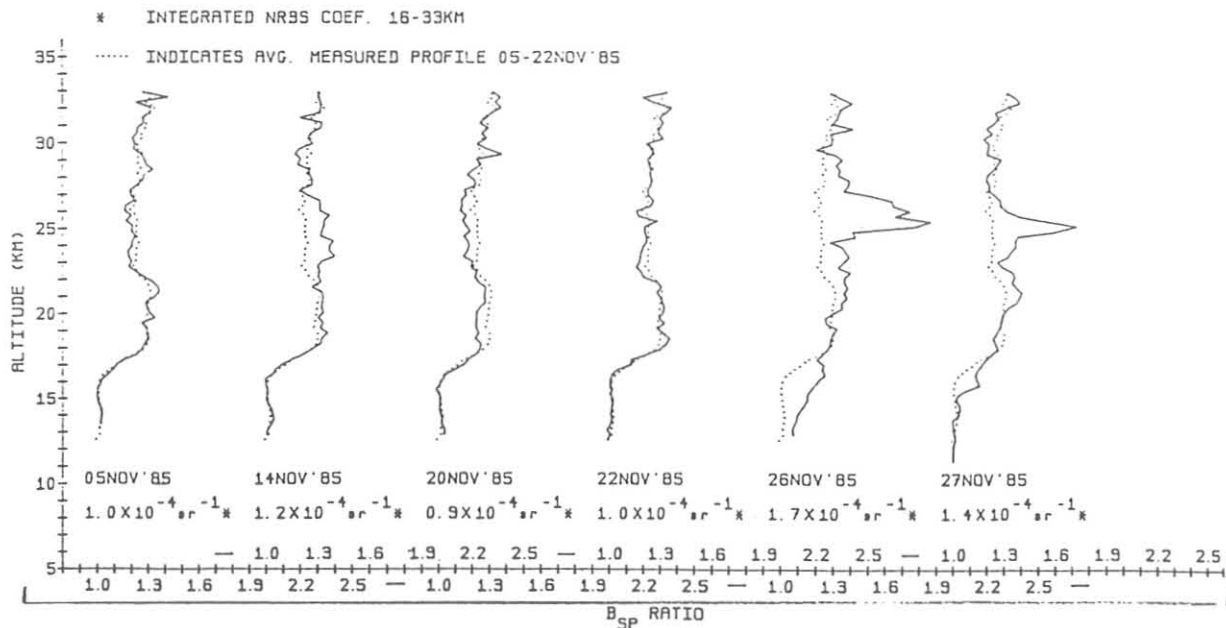


Figure 6.--Six lidar backscatter profiles taken at MLO in November 1985.

A total of 367 lidar measurements was acquired at MLO from 1974-1985. These measurements were summarized in terms of yearly averaged profiles of optical thickness per kilometer and the standard deviations that are mainly composed of the natural variability and the measurement uncertainty. The number of observations per year has varied considerably. For example, in 1974 the number was 4 (the lowest of all years) and in 1982 it was 67 (the highest of all years). Figure 7 displays average optical thickness profiles for 1974-1985. To facilitate plotting, the abscissa is scaled to accommodate the large changes that occur between quiescent and perturbed years. The years having the lowest optical thickness are 1976-1979. Only five profiles were obtained in 1979, so the result may be questioned somewhat for its representativeness.

DeLuisi et al. (1986) gave the numerical values and standard deviations in tabular form for the profiles displayed in fig. 6. These data should be quite useful for studies of stratospheric aerosol effects on climate and optical remote sensing. More details on summaries of lidar observations can be obtained from NOAA data reports issued earlier by GMCC.

#### GMCC SOLAR RADIATION FACILITY

During 1985, the NOAA SRF merged with the GMCC ARM group. Although the SRF has been located in Boulder since 1975, it operated independently when it was transferred from the NWS to ERL/ARL.

The primary purposes of the facility are maintenance of NOAA radiometric standards, calibration of NOAA pyranometers and pyrhemometers for the NOAA national network, and maintenance of traceability of the NOAA standards to the World Radiometric Reference in Davos, Switzerland.

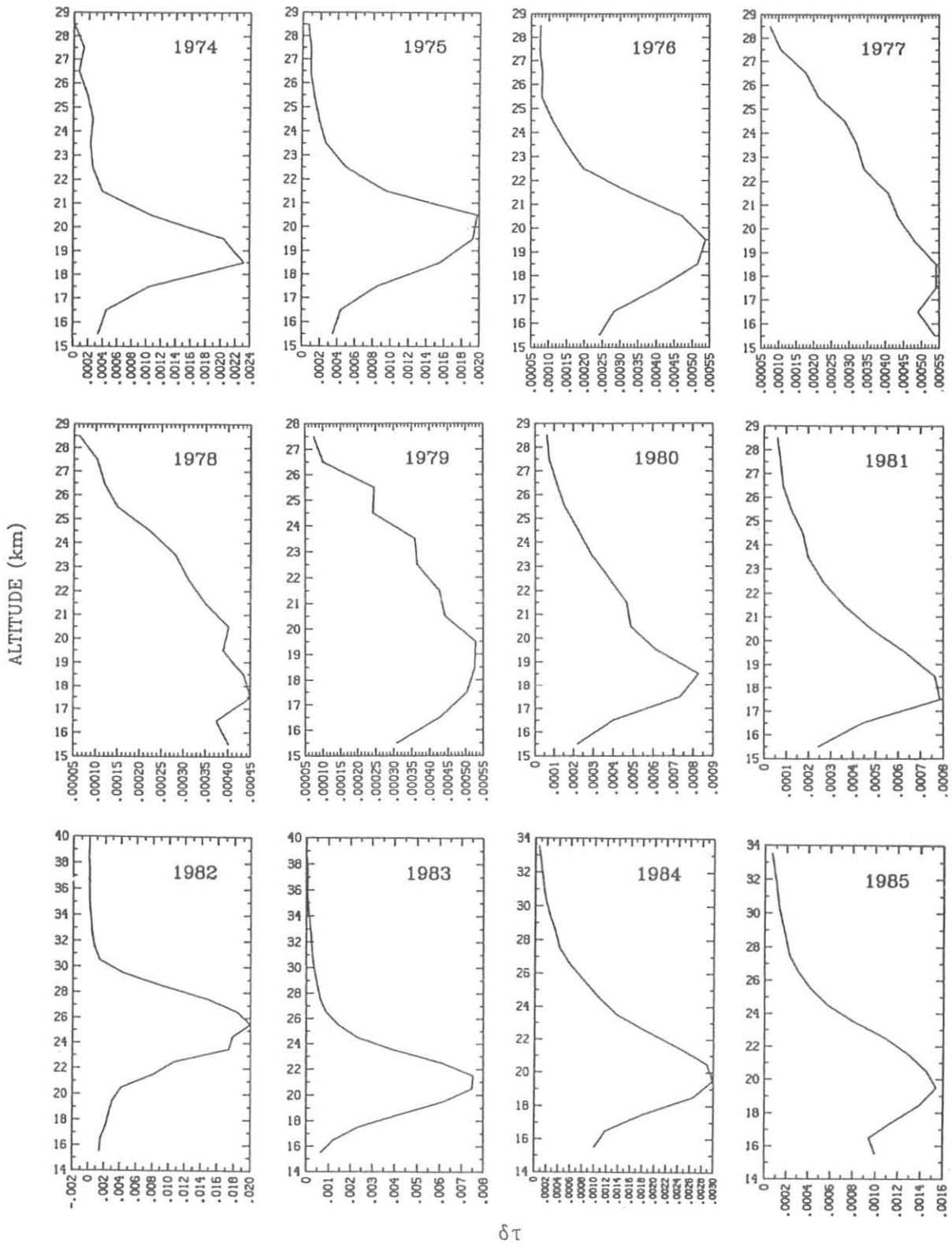


Figure 7.--Plots of annual average aerosol profiles: altitude vs. optical thickness per kilometer ( $\delta\tau$ ) for years 1974-1985. Note that the abscissa scale changes according to the magnitude of the aerosol cloud maximum.

Primary reference instruments of the facility are two absolute cavity radiometers, a TMI Mark VI (SN 67502), and an Eppley model HF (SN 15745). Traceability to the World Radiometric Reference Scale is by means of the TMI SN 67502 and its participation in the IPC held in Davos in 1975, 1980, and 1985. Both the TMI and the HF have also participated in seven NRIP events dating from 1978 held in New River, Arizona, at the DSET laboratory facility. Historically, the NRIP's have been scheduled approximately every 2 years during the month of November. Their purpose is to establish a check on performance of participating absolute cavity radiometers by comparison with a designated reference instrument (SN 67502). A second purpose has been to allow participating radiometers to compare with radiometers with IPC histories and establish unofficial traceability to the world reference. At present, no officially sanctioned mechanism exists for establishing such traceability.

Plans for 1986 include installation of replacement instrument tables on the roof and installation of a new data acquisition system and microcomputer for data collection and analysis.

Support activities for the NOAA national network during 1985 included drafting of the RFP for new "smart" solar trackers, scheduled to replace those currently in use, and the initial prototype testing of the new network IBM PC-based data acquisition system.

#### TURBIDITY

The 10 NOAA atmospheric turbidity stations within the contiguous United States were brought under the GMCC ARM Group at the beginning of 1985. Turbidity observations continued at these stations and at the four baseline stations during 1985. A list of the 14 stations and the wavelengths at which turbidity is measured is given in table 3.

The working instrument at most of the 14 stations is the NOAA J-series sunphotometer. A new calibration procedure initiated in late 1984 was refined and continued in 1985. In the previous calibration scheme, a designated standard J-series instrument was calibrated repeatedly by the Langley plot method in Boulder. The other J-series sunphotometers were calibrated in intercomparisons with this instrument. In the new scheme, a high-precision, automated, temperature-stabilized PMOD-type sunphotometer is calibrated daily at MLO where more accurate and consistent Langley plot calibrations are possible. The PMOD-type sunphotometer is returned to Boulder about every 4 months for intercomparisons with the J-series instruments. This procedure ensures greater accuracy in the calibrations assigned to field instruments. However, it delays the processing of field measurements because of the cycle time of the PMOD-type instruments between MLO and Boulder.

While this new procedure is superior to the previous procedure, there are still some problems associated with it and with the instruments themselves. Two of the filters in the PMOD-type sunphotometer failed in April 1985. It took until September to obtain replacement filters and get the instrument back in the system. This interrupted the scheduled cycles of intercomparisons for summer and fall 1985. Even after replacement of the bad filters, an unusually

Table 3.--GMCC turbidity monitoring sites and filter wavelengths for sunphotometers used at each site

Station	Sunphotometer wavelengths (nm)
Barrow, AK*	380, 500, 778, 862
Mauna Loa, HI*	380, 500, 778, 862
Samoa*	380, 500, 778, 862
South Pole*	380, 500, 778, 862
Alamosa, CO*	380, 500
Atlantic City, NJ	380, 500
Boulder, CO	380, 500, 778, 862
Bismarck, ND	380, 500
Caribou, ME*	380, 500
Huron, SD	380, 500
Meridian, MS*	380, 500
Salem, IL*	380, 500
Tallahassee, FL	380, 500
Victoria, TX*	380, 500

\*BAPMoN stations

high, but acceptable drift was observed in the replacement filters. In-house design and construction of two new precision sunphotometers continued in 1985. Once these are working, the calibration process should be less vulnerable to the breakdown of a standard instrument.

Apparent shifts in filter transmission also proved to be a problem with many of the J-series instruments. The result of these shifts is a substantial change in calibration constants over the period of a year. Fortunately, in many instances, the change is linear with time (see fig. 8). A partial solution to the data analysis problems associated with calibration changes is recycling and recalibrating instruments every 4 to 6 months. GMCC is seeking ways to reduce the filter decay rate so that calibrations can be done at longer time intervals.

The data analysis software for the turbidity project was completely revised in 1985. Data for 1983-1985 for Boulder, CO (see fig. 9), and 1983 through February 1985 for the nine remaining stations in the U.S. network have been processed.

Data for Boulder and other stations show a clear annual cycle with maxima in the spring or summer months and minima during November, December, or January. The impact of the eruption of El Chichon is visible at many stations and appears as a slow downward trend in optical depths since the beginning of the record in early 1983.

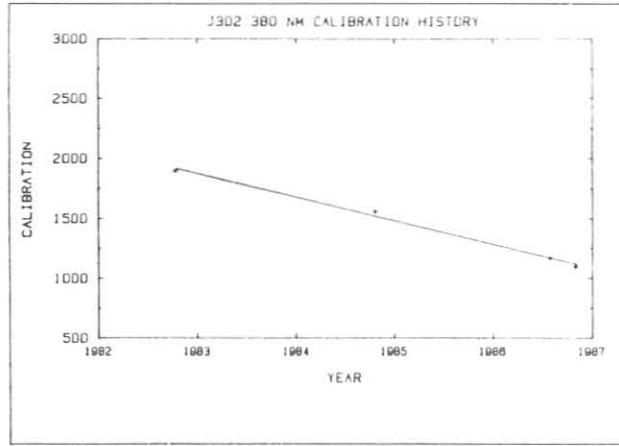


Figure 8.--Linear drift in J-Series sunphotometer calibrations.

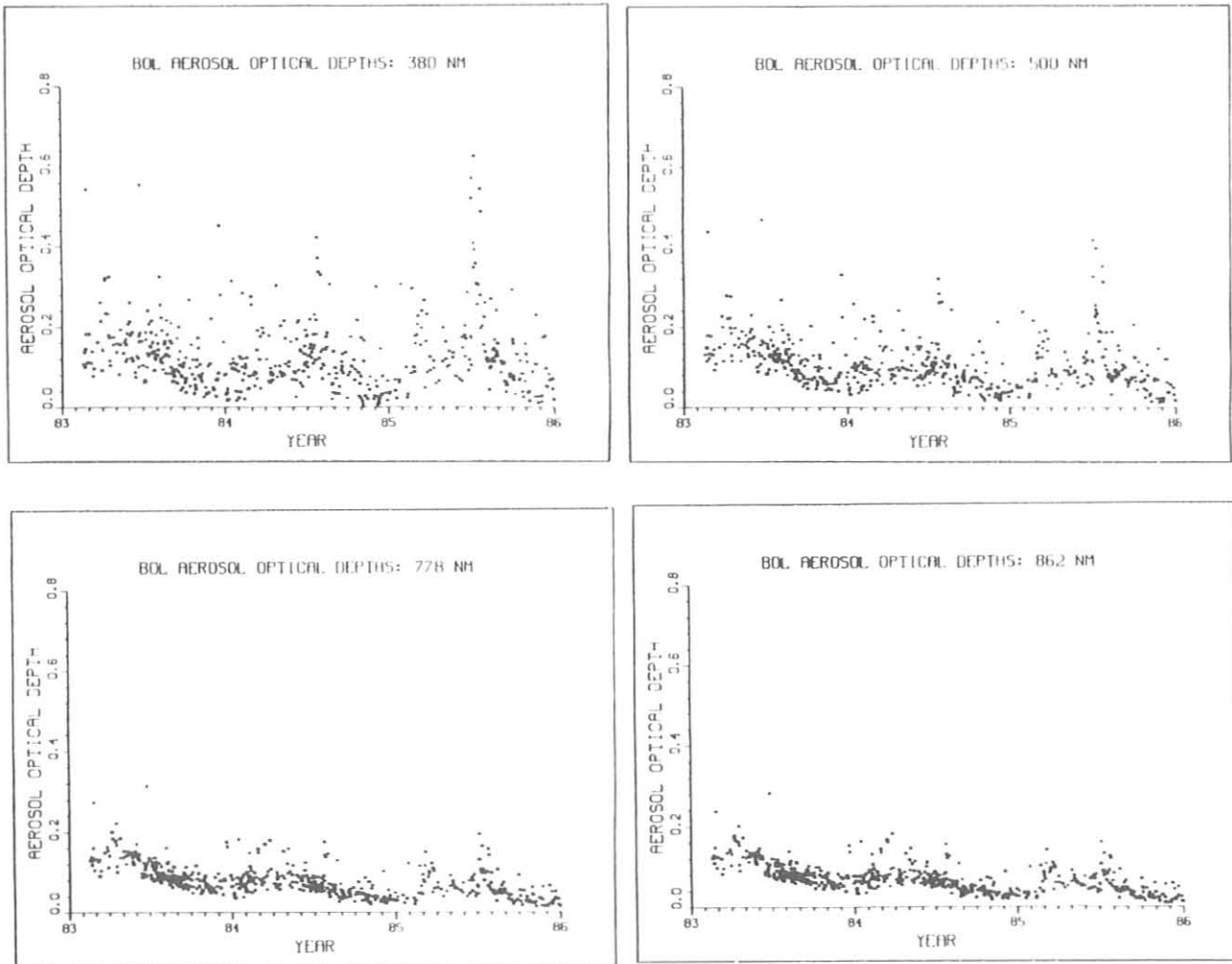


Figure 9.--Daily average aerosol optical depths at Boulder for 380, 500, 778, and 862 nm.

### 3.2 Special Projects

#### AEROSOL CORRECTION TO THE UMKHER OZONE PROFILE

AT MLO, a long-term series of concurrent Umkehr observations of stratospheric ozone and lidar observations of stratospheric aerosol from the El Chichon eruption of March-April 1982 permitted an empirical analysis of the error to the Umkehr ozone profile caused by a significant optical effect of the stratospheric aerosol. The effect is due to the separation of the effective primary scattering layers near twilight, where the short wavelength (311.4 nm) is near 40 km and the long wavelength (332.3 nm) is near 25 km, which is often directly located in the aerosol layer. The aerosol layer near 25 km attenuates the solar UV radiation at 332.3 nm, traveling a tangential path, and this is interpreted by the Umkehr inversion algorithm as less ozone above the ozone maximum. The error becomes increasingly worse with increasing altitude.

Theoretical calculations for all orders of scattering by Dave et al. (1980) modeled the physical processes of the error; some experimental verification was done by DeLuisi (1979) and Reinsel et al. (1984). However, the concurrent lidar and Umkehr data provided a unique data set for experimental investigation of the error. The error analysis is an iterative regression on the departure of the Umkehr stratospheric ozone from a normal condition that exists after the volcanic aerosol has diminished.

Figure 10 compares results from Dave et al. (1980), Reinsel et al. (1984), and the present study. The outcome is encouraging because the experimental results closely match the theoretical results, thus providing confidence in the methods used in the theoretical calculations for a spherical atmosphere. The great value of the present result is that it lends further credibility to the use of theoretical stratospheric aerosol corrections to long-term Umkehr measurements for detecting trends in stratospheric ozone.

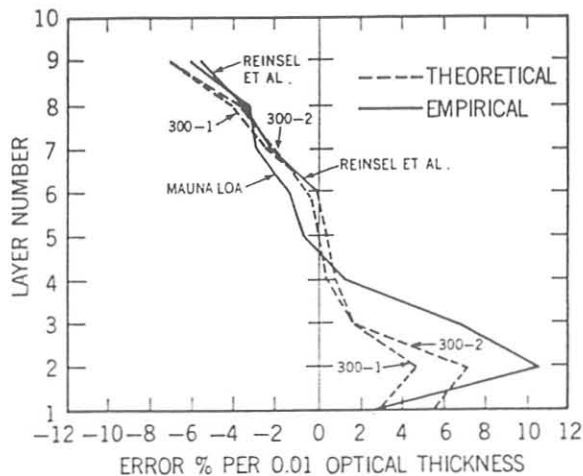


Figure 10.--Percent error to the Umkehr ozone profile per 0.01 optical thickness of stratospheric aerosol at 700 nm for layers 1-9: theoretical (Dave et al., 1980--dashed); experimental (Reinsel et al., 1984; Mauna Loa, this study--solid). Two different ozone profiles having total ozone amounts of 300 milli-atm-cm are given as 300-1 and 300-2.

### 3.3 References

- Bodhaine, B. A., 1979. Measurement of the Rayleigh scattering properties of some gases with a nephelometer. Applied Optics 18:121-125.
- Bodhaine, B. A., and J. J. DeLuisi, 1985. An aerosol climatology of Samoa. Journal of Atmospheric Chemistry 3:107-122.
- Bodhaine, B. A., and J. M. Harris (Eds.), 1982. Geophysical Monitoring for Climatic Change, No. 10: Summary Report 1981. NOAA Environmental Research Laboratories, Boulder, CO, 158 pp.
- Bodhaine, B. A., J. J. DeLuisi, J. M. Harris, P. Houmère, and S. Bauman, 1986. Aerosol measurements at the South Pole. Tellus, in press.
- Bodhaine, B. A., J. J. DeLuisi, J. M. Harris, P. Houmère, and S. Bauman, 1987. PIXE analysis of South Pole aerosol. Nuclear Instruments and Methods, in press.
- Dave, J. J., J. J. DeLuisi, and C. L. Mateer, 1980. Results of a comprehensive theoretical examination of the optical effects of aerosols on the Umkehr measurement. Papers presented at the WMO Technical Conference on Regional and Global Observation of Atmospheric Pollution Relative to Climate, Boulder, CO, 20-24 August 1979, WMO No. 549, Spec. Environ. Rep. No. 14, World Meteorological Organization, Geneva, Switzerland, 15-22.
- DeLuisi, J. J., 1979. Umkehr vertical ozone profile errors caused by the presence of stratospheric aerosols. Journal of Geophysical Research 84:1766-1770.
- DeLuisi, J., T. DeFoor, and D. Longenecker, 1986. Lidar observations of stratospheric aerosol over Mauna Loa Observatory: 1984-1985. NOAA Data Report, NOAA Environmental Research Laboratories, Boulder, CO, in press.
- Hanson, K. J. (Ed.), 1977. Geophysical Monitoring for Climatic Change, No. 5: Summary Report 1976. NOAA Environmental Research Laboratories, Boulder, CO, 110 pp.
- Miller, J. M. (Ed.), 1975. Geophysical Monitoring for Climatic Change, No. 3: Summary Report 1974. NOAA Environmental Research Laboratories, Boulder, CO, 107 pp.
- Reinsel, G. C., G. C. Tiao, J. J. DeLuisi, C. L. Mateer, A. J. Miller, and J. E. Frederick, 1984. Analysis of upper stratospheric Umkehr ozone profile data for trends and the effects of stratospheric aerosols. Journal of Geophysical Research 89:4833-4840.

## 4. CARBON DIOXIDE GROUP

### 4.1 Continuing Programs

#### CONTINUOUS ANALYZERS

The in situ NDIR CO<sub>2</sub> analyzers at the four GMCC observatories continued to operate in 1985. The preliminary monthly and annual means for each of the observatories for 1985 are shown in table 1. The complete record for each station is shown in fig. 1. Daily averages for 1985 are shown in fig. 2, showing the decreased amplitude of the seasonal cycle and decreased variability when moving from north to south.

Data acquisition procedures remained the same since the installation of the CAMS data acquisition units in 1984. The SPO analyzer system was refurbished in December.

The in-house calibration of CO<sub>2</sub>-in-air reference gases for GMCC continued in 1985; 170 calibrations were performed. The GMCC secondary standards were calibrated by SIO in 1985, and results were reported in the WMO X85 provisional scale. A new Ultramat 3 NDIR CO<sub>2</sub> analyzer, manufactured by Siemens Corporation of West Germany, was purchased. The Ultramat 3 will be used for the tank calibration program. This analyzer exhibits greater stability and precision than the URAS 2T analyzers currently being used.

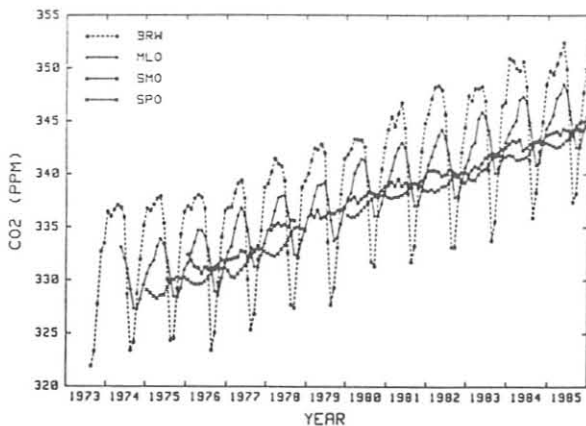


Figure 1.--Provisional selected monthly mean CO<sub>2</sub> concentrations from continuous measurements at BRW, MLO, SMO, and SPO. Values are in ppm with respect to dry air (1973-1984, X81 mole fraction scale; 1985, X85 mole fraction scale).

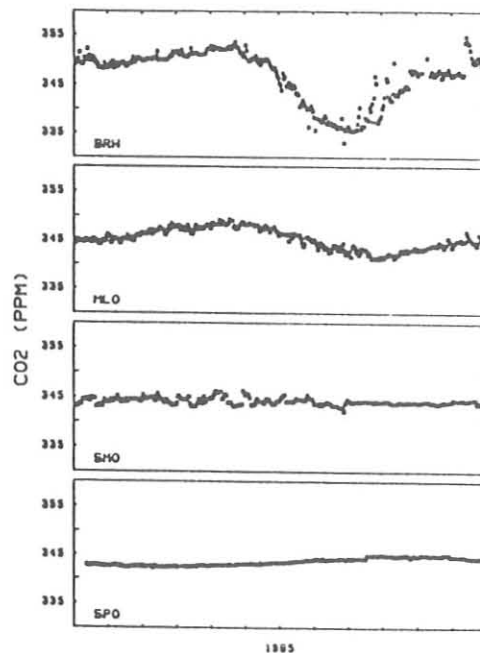


Figure 2.--Daily averages of provisionally selected continuous measurements at BRW, MLO, SMO, and SPO.

Table 1.--Provisional selected monthly and annual mean CO<sub>2</sub> concentrations for continuous measurements at BRW, MLO, SMO, and SPO

Year	Jan	Feb	Mar	Apr	May	Jun	Jul	Aug	Sep	Oct	Nov	Dec	Annual mean
BRW													
1973	--	--	--	--	--	--	--	322.0	323.4	327.8	332.7	333.5	--
1974	336.5	336.0	336.7	337.1	336.9	335.9	328.7	323.5	324.2	328.8	332.0	335.2	332.6
1975	336.8	336.6	337.1	337.7	337.9	335.4	330.1	324.4	324.6	329.2	334.3	336.5	333.4
1976	337.0	336.7	337.7	338.0	337.8	336.8	331.0	323.5	325.1	329.8	334.1	336.6	333.7
1977	336.8	336.9	338.2	339.2	339.4	337.7	330.1	325.4	326.8	332.0	334.7	338.8	334.7
1978	339.1	340.2	341.5	341.0	340.8	339.4	332.6	327.7	327.4	332.1	338.8	339.4	336.7
1979	340.1	341.3	342.5	342.4	342.9	342.0	333.6	327.7	329.3	333.1	338.1	341.5	337.9
1980	341.9	342.4	343.4	343.3	343.3	342.6	337.3	331.8	331.4	337.9	340.5	342.6	339.9
1981	344.3	345.5	344.6	345.8	346.8	344.4	338.2	331.8	333.3	338.8	342.2	344.9	341.7
1982	345.8	347.2	348.3	348.4	348.0	345.7	339.2	333.2	333.2	337.9	342.1	344.5	342.8
1983	347.5	347.0	348.1	348.1	348.3	347.0	340.4	333.8	335.5	340.6	346.5	346.8	344.1
1984	351.0	350.7	350.0	349.8	350.7	348.3	341.3	335.9	338.3	342.2	345.0	348.5	346.0
1985	349.8	349.5	350.5	351.4	352.5	349.9	343.4	337.4	338.2	344.3	347.7	349.7	347.0
MLO													
1973	--	--	--	--	--	--	--	--	--	--	--	--	--
1974	--	--	--	--	333.1	332.1	331.1	329.1	327.4	327.3	328.2	329.6	--
1975	330.6	331.4	331.9	333.2	333.9	333.4	331.9	330.0	328.5	328.4	329.2	331.0	331.1
1976	331.6	332.6	333.6	334.7	334.7	334.2	333.0	330.8	329.0	328.6	330.2	331.6	332.0
1977	332.7	333.2	334.9	336.1	336.8	336.1	334.8	332.6	331.3	331.2	332.4	333.5	333.8
1978	334.7	335.2	336.5	337.8	338.0	338.0	336.4	334.5	332.5	332.3	333.8	334.8	335.4
1979	336.0	336.6	337.9	339.0	339.1	339.3	337.6	335.7	333.8	334.1	335.3	336.8	336.8
1980	337.8	338.3	340.1	340.9	341.5	341.3	339.4	337.7	336.1	336.1	337.2	338.4	338.7
1981	339.3	340.4	341.7	342.5	343.0	342.5	340.9	338.7	337.1	337.1	338.5	339.9	340.1
1982	340.9	341.7	342.7	343.7	344.3	343.4	342.0	340.0	337.8	338.0	339.2	340.6	341.2
1983	341.4	342.7	343.0	345.3	345.9	345.4	344.2	342.1	340.1	340.2	341.4	343.0	342.9
1984	343.6	344.5	345.1	--	347.3	346.6	345.0	342.7	340.9	341.1	342.8	344.3	344.2
1985	344.9	345.6	347.2	347.6	348.5	347.9	346.0	343.9	342.6	342.6	344.1	345.5	345.5
SMO													
1973	--	--	--	--	--	--	--	--	--	--	--	--	--
1974	--	--	--	--	--	--	--	--	--	--	--	--	--
1975	--	--	--	--	--	--	--	--	--	--	--	--	--
1976	332.4	331.9	331.3	331.2	330.6	331.3	331.1	331.1	331.3	331.5	331.9	331.9	331.5
1977	331.9	332.0	332.1	332.2	332.8	332.7	332.2	333.1	332.9	333.3	--	--	--
1978	--	334.7	335.2	335.4	335.1	335.3	335.0	335.7	335.6	--	--	--	--
1979	--	336.2	336.0	336.6	335.9	336.0	336.4	336.3	336.3	336.6	336.6	336.9	--
1980	337.5	337.6	337.9	337.3	337.7	338.0	338.3	338.3	338.2	338.1	338.5	338.9	338.0
1981	339.0	339.3	338.9	339.6	338.9	339.2	339.0	339.2	339.2	338.9	339.5	339.8	339.2
1982	340.4	340.4	340.4	340.3	339.9	340.0	340.5	340.4	340.1	340.0	340.2	340.2	340.2
1983	340.0	340.5	340.8	340.6	341.1	341.6	341.9	341.9	341.9	342.1	342.4	342.6	341.4
1984	342.9	343.2	343.1	343.3	342.3	342.6	342.9	343.0	343.2	343.1	343.1	343.7	343.0
1985	343.8	344.0	344.1	343.8	344.3	344.2	344.1	343.7	344.3	344.2	344.2	344.5	344.1
SPO													
1973	--	--	--	--	--	--	--	--	--	--	--	--	--
1974	--	--	--	--	--	--	--	--	--	--	--	--	--
1975	329.1	328.8	328.5	328.3	328.6	328.6	329.4	329.8	330.1	330.3	330.2	330.2	329.3
1976	330.1	329.8	329.6	329.6	329.7	329.9	330.3	330.7	331.0	331.1	331.1	331.1	330.3
1977	330.9	330.3	330.3	330.6	331.0	331.4	331.8	332.2	332.7	333.0	333.0	332.7	331.7
1978	332.6	332.4	332.3	332.5	333.0	333.3	333.8	334.4	334.9	335.0	334.9	334.7	333.7
1979	--	--	--	--	--	--	--	--	--	--	--	--	--
1980	336.1	336.0	336.0	336.2	336.6	336.9	337.4	337.7	337.9	338.1	338.0	338.0	337.1
1981	337.8	337.8	337.9	337.9	338.1	338.3	338.7	339.0	339.2	339.1	338.9	338.5	338.4
1982	338.5	338.6	338.4	338.6	338.9	338.9	339.2	339.6	339.9	339.8	339.5	339.2	339.1
1983	339.7	339.5	339.5	340.0	340.4	340.5	341.0	341.6	341.7	341.8	341.8	341.7	340.8
1984	341.8	341.7	341.4	341.4	341.5	341.7	342.0	342.7	343.1	343.4	343.2	343.0	342.2
1985	342.9	342.7	342.6	342.7	342.9	343.3	343.7	344.2	344.7	345.0	345.0	344.5	343.7

Note: For 1973-1984 the values are in the X81 mole fraction scale, for 1985 in the X85 scale. The scale discontinuity is on the order of a few hundredths of a ppm.



Table 2.--GMCC flask network sampling sites during 1985

Code	Station	Latitude (deg)	Longitude (deg)	Elevation (m)
ALT	Alert, N.W.T., Canada	82.50N	62.33W	6
AMS	Amsterdam I.	37.95S	77.53E	150
ACS	Ascension I.	7.92S	14.42W	54
AVI	St. Croix, VI	17.75N	64.75W	3
AZR	Terceira I., Azores	38.75N	27.08W	30
BRW	Barrow, AK	71.32N	156.60W	11
CBA	Cold Bay, AK	55.20N	162.72W	25
CGO	Cape Grim, Tasmania	40.68S	144.73E	94
CHR	Christmas I.	2.00N	157.30W	3
CMO	Cape Meares, OR	45.00N	124.00W	30
COS	Cosmos, Peru	12.12S	75.33W	4600
GMI	Guam, Mariana I.	13.43N	144.78E	2
HBA	Halley Bay, Ant.	75.67S	25.50W	0
KEY	Key Biscayne, FL	25.67N	80.17W	3
KUM	Cape Kumukahi, HI	19.52N	154.82W	3
MBC	Mould Bay, Canada	76.23N	119.33W	15
MID	Midway I.	28.20N	177.38W	4
MLO	Mauna Loa, HI	19.53N	155.58W	3397
NWR	Niwot Ridge, CO	40.05N	105.63W	3749
PSA	Palmer Station, Ant.	64.92S	64.00W	10
SEY	Mahé I., Seychelles	4.67S	55.17E	3
SGI	South Georgia I.	54.00S	38.00W	?
SHM	Shemya I.	52.75N	174.08E	40
SMO	Cape Matatula, Am. Samoa	14.25S	170.57W	30
SPO	South Pole, Ant.	89.98S	24.80W	2810
STM	Station M	66.00N	2.00E	0

For comparison purposes, a small shipment of flasks was sent to Tohoku University, Japan, for collecting samples at Syowa Station, the Japanese Antarctic research site. The data from these flasks will be compared with the Japanese in situ continuous analyzer and flask measurements. Similarly, the GMCC CO<sub>2</sub> data for Amsterdam Island have been compared with in situ measurements made by the CFR. The results indicate good agreement between GMCC and CFR following the introduction of the GMCC battery-powered portable sampling unit in 1982. Prior to that time the GMCC data are ~1 ppm higher and are more scattered than the CFR data (Gaudry et al.; CFR, France, unpublished manuscript, 1985).

Provisional annual mean CO<sub>2</sub> concentrations for 1985 are given in table 3. Sites for which a full year is lacking (Alert, Midway, Shemya, and South Georgia) are not included. The 1985 Halley Bay samples had not been received in Boulder at the time this report was written. The annual means in table 3 are the result of preliminary data selection and curve fitting. The values are also subject to revision based on final analysis of the calibration gases used for flask sample analysis. The annual means for 1981-1984 in table 3 have been adjusted by -0.1-0.2 ppm on the basis of a reanalysis of the data Conway et al.; NOAA/GMCC, Boulder; unpublished manuscript, 1985).

Table 3.--Provisional annual mean atmospheric CO<sub>2</sub> concentrations (ppm relative to dry air--X83 mole fraction scale) for the flask network sites

Station	1968	1969	1970	1971	1972	1973	1974	1975	1976	1977	1978	1979	1980	1981	1982	1983	1984	1985
AMS	0	0	0	0	0	0	0	0	0	0	0	(335.9)	337.8	339.4	339.4	341.1	342.3	343.7
ASC	0	0	0	0	0	0	0	0	0	0	0	[337.3]	338.8	339.8	340.7	342.7	343.7	344.7
AVI	0	0	0	0	0	0	0	0	0	0	0	337.1	339.6	340.3	340.9	342.0	343.2	345.0
AZR	0	0	0	0	0	0	0	0	0	0	0	0	338.4	339.4	341.3	343.0	344.4	346.0
BRW	0	0	0	327.4	330.2	332.0	333.4	333.0	333.9	335.0	336.6	337.7	340.2	341.4	342.7	343.8	345.2	346.5
CBA	0	0	0	0	0	0	0	0	0	0	0	337.8	339.8	341.0	341.8	343.4	345.4	346.4
CGO	0	0	0	0	0	0	0	0	0	0	0	0	0	0	0	0	342.0	343.4
CHR	0	0	0	0	0	0	0	0	0	0	0	0	0	0	0	0	344.8	345.7
CMO	0	0	0	0	0	0	0	0	0	0	0	0	0	0	341.3	343.0	345.0	346.6
FLK	0	0	0	0	0	0	0	0	0	0	0	0	0	339.7	0	0	0	0
GMI	0	0	0	0	0	0	0	0	0	0	0	337.7	340.0	341.2	340.9	342.7	344.2	345.6
HBA	0	0	0	0	0	0	0	0	0	0	0	0	0	0	0	0	341.4	342.6
KEY	0	0	0	0	0	330.7	[333.4]	0	332.7	335.2	336.7	338.8	(340.2)	341.7	341.6	343.4	345.0	346.1
KUM	0	0	0	0	0	0	0	0	332.3	334.4	335.7	337.4	339.3	340.6	341.2	342.6	344.1	345.4
MBC	0	0	0	0	0	0	0	0	0	0	0	0	340.3	341.8	342.4	343.7	345.6	346.5
MKO	0	0	0	0	0	0	0	0	0	0	0	337.3	0	0	0	0	n	0
MLO	0	[322.8]	325.2	0	0	0	0	0	332.1	333.6	335.2	336.7	338.9	340.4	341.0	342.5	344.0	345.2
NWR	323.1	324.1	325.6	325.2	326.3	330.2	[334.0]	0	332.1	333.6	335.2	336.7	338.1	339.9	340.9	342.5	344.6	345.6
NZL	0	0	0	0	0	0	0	0	0	0	0	0	0	0	0	340.7	342.3	0
PSA	0	0	0	0	0	0	0	0	0	0	0	333.9	335.2	(337.5)	340.1	339.7	341.0	342.7
SEY	0	0	0	0	0	0	0	0	0	0	0	0	339.3	340.1	340.5	341.1	343.8	344.8
SMD	0	0	0	0	0	[330.2]	330.8	330.7	331.5	332.8	334.3	336.0	338.1	339.3	340.4	341.5	343.4	344.3
SPO	0	0	0	0	0	0	329.4	330.2	331.5	333.7	335.5	336.7	338.1	339.3	339.3	340.8	342.1	343.4
STC	0	324.0	326.4	326.9	327.6	0	0	0	0	0	0	0	0	0	0	0	0	0
STM	0	0	0	0	0	0	0	0	0	0	0	0	0	341.8	341.7	342.6	344.6	345.5

Note: ( ) = number of interpolated points  $\geq$  one-half of total number of points; [ ] = incomplete year.

Annual mean CO<sub>2</sub> concentration is plotted versus sin(latitude) in fig. 4 for 1981-1985. It is appropriate to plot against sin(latitude) since equal intervals of sin(latitude) correspond to equal areas on the surface of the earth. The curves in fig. 4 are cubic spline curves fit to the data using the smoothing spline of Reinsch (1967). In this method the stiffness of the spline is determined by the weights, Dy(i), assigned to the points. These weights should be the uncertainty associated with the annual mean value. For 1981-1984 the weights were taken to be 3 $\sigma$ , where  $\sigma$  is the statistical standard error of the annual mean determined by an objective statistical method (Conway et al.; NOAA/GMCC Boulder; unpublished manuscript, 1985). Although this weight, and thus the  $\pm 3\sigma$  error bars in fig. 4, overstates the uncertainty of the annual mean at a given site, the smooth curves thus obtained suggest that 3 $\sigma$  is a reasonable value for the variability due to longitudinal gradients and indicates how well a site represents a given zone.

The overall north-to-south gradient of -3 ppm is fairly consistent from 1981 through 1985. However, considerable variability is observed in the appearance of the equatorial hump in CO<sub>2</sub> concentration. This feature in the annual mean gradient has been ascribed to an equatorial ocean source of atmospheric CO<sub>2</sub> (Mook et al., 1983; Pearman et al., 1983). The near absence of this "hump" in 1982 has been attributed to the interruption of the normal upwelling of cold water with high CO<sub>2</sub> supersaturations during the 1982-1983 ENSO event (Keeling and Revelle, 1985; Feely et al., 1986). In 1983 a partial recovery is observed, and in 1984 the hump is well defined resulting in part from the addition of Christmas Island to the network in 1984. The latitude gradient for 1985 is interesting in that only a slight equatorial enhancement is observed. Since 1985 was not an ENSO year, these results suggest the possibility of significant variation in the equatorial source of atmospheric CO<sub>2</sub> not related to ENSO events.

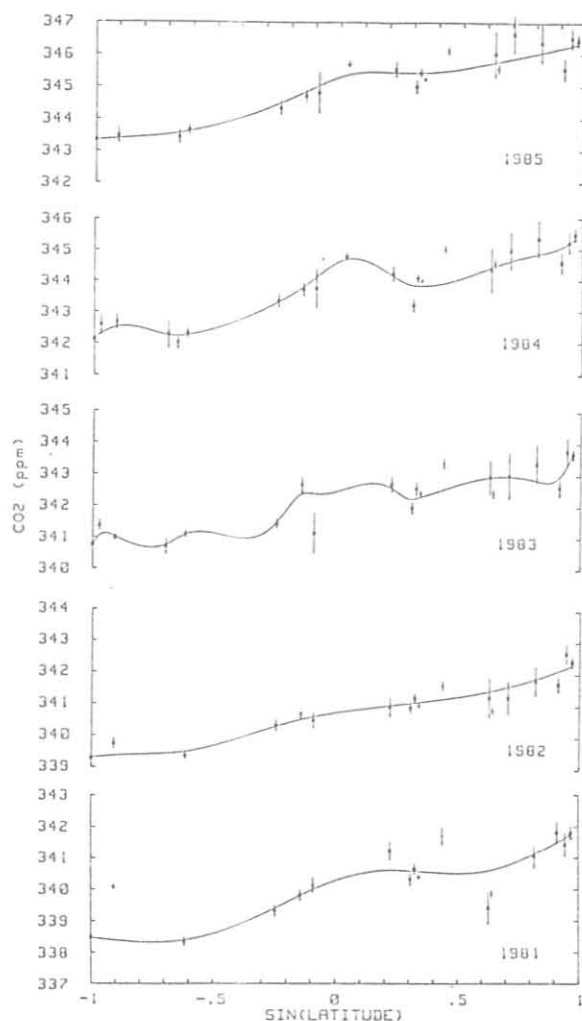


Figure 4.--Annual mean CO<sub>2</sub> concentrations vs. sin(latitude) for the GMCC flask sampling network. Data plotted with the symbol (+) have not been included in fitting the curves. The 1981 annual mean for AMS has been adjusted by -1 ppm on the basis of comparisons with CFR data.

The 1984-1985 global CO<sub>2</sub> growth rate was  $\sim 1.2 \text{ ppm yr}^{-1}$ . This rate is somewhat lower than the  $1.5 \text{ ppm yr}^{-1}$  average of the past decade, which may be related to a decrease in the equatorial source. The 1984-1985 growth rate is still 2 times higher than the low growth rate associated with the 1982-1983 ENSO event.

#### FLASK SAMPLE METHANE MEASUREMENTS

Measurement of methane in air samples from the NOAA/GMCC cooperative flask network continued through 1985. During this year, flask sampling was initiated at four additional sites (Shemya Island, AK; Alert, N.W.T., Canada; Midway Island; and South Georgia Island), and terminated at Kaitorete Spit, New Zealand. The active sites in the network during 1985 are shown in both fig. 3 and table 2.

Methane concentrations continued their long-term increase at all sampling sites. This is illustrated by monthly mean data from two sites (South Pole and Mould Bay) through January 1986 (fig. 5). The corresponding 12-mo running

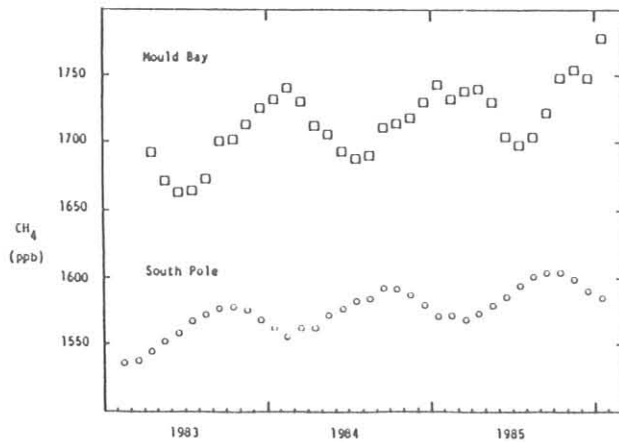


Figure 5.--Monthly mean background methane concentrations at SPO and Mould Bay, Canada.

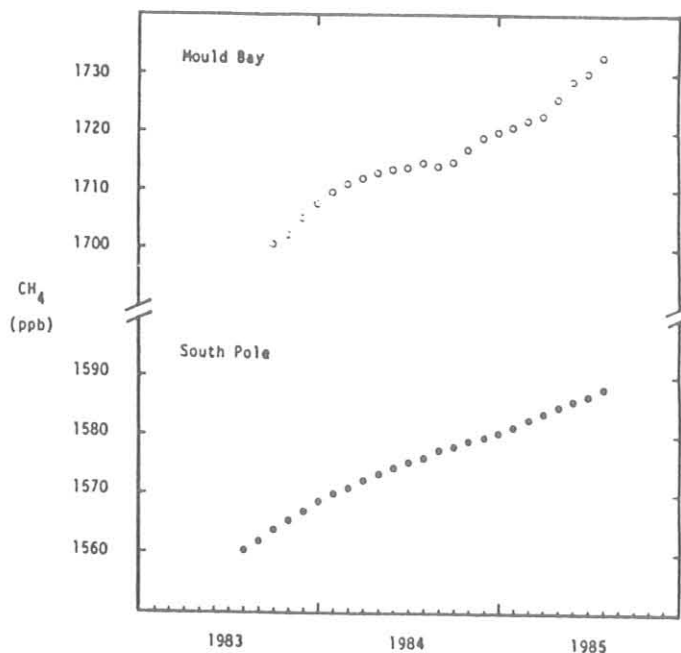


Figure 6.--Twelve-month running mean methane concentrations at SPO and Mould Bay, Canada. Values are plotted at the midpoint of the appropriate interval.

means (plotted at the midpoint of the appropriate interval) are shown in fig. 6. The seasonal variations and the significant latitudinal difference in concentrations are apparent in fig. 6, where the vertical axis is unbroken.

To emphasize features of the long-term increase, the vertical axis was broken in fig. 6. In particular, the 3-yr record of data at the South Pole shows clearly that the growth rate of methane has not been constant over this period. Twelve-month averages calculated directly from the background flask data are 1560 ppb (Feb 1983-Jan 1984 inclusive), 1576 ppb (Feb 1984-Jan 1985), and 1588 ppb (Feb 1985-Jan 1986), yielding respective 12-mo increases of 16 ppb and 12 ppb. The average annual growth rate is 0.88% when referenced to the concentration at the midpoint of this 3-yr period. This long-term slowing of the methane growth rate has also been seen at other sites from middle to high latitudes of the Southern Hemisphere, and is most obvious in the long record from Cape Grim, Tasmania (see Steele et al., 1986). The reason for this slowing of the methane growth rate is not yet understood.

If any slowing of the growth rate in methane is occurring at Mould Bay, it is not yet apparent from the data. However, any such change will be more difficult to detect at sites in the Northern Hemisphere, since the seasonal variations are not as well defined as in the Southern Hemisphere, and the magnitude of the seasonal variations may change from year to year. Thus, the 12-mo running means used in this analysis are not able to completely suppress the seasonal changes. Nevertheless, the overall increase seen in methane at Mould Bay is comparable to that at the South Pole.

## 4.2 Special Projects

### 1985 OCEANOGRAPHIC ACTIVITIES ABOARD NOAA SHIP DISCOVERER

The CO<sub>2</sub> Group participated in the EPOCS and CO<sub>2</sub> cruises aboard the NOAA Ship DISCOVERER during 1985. The cruise track is shown in fig. 7. A total of 1199 hours of atmospheric air and 1101 hours of air equilibrated with surface ocean water were sampled for CO<sub>2</sub> measurements between 24 May and 19 July.

The Weiss-design custom-built gas chromatograph was set up aboard the ship prior to the ship's departure on EPOCS leg 1 by GMCC personnel. The equipment was activated in San Diego prior to sailing on EPOCS leg 2. The monitoring program was operated on the CO<sub>2</sub> cruise in the North Pacific between Honolulu and Kodiak by PMEL personnel.

The 1985 monitoring program was identical in most respects to the 1984 mode of operation (see Nickerson, 1986, p. 41). Preliminary results are graphically depicted in figs. 8-10. The mean atmospheric CO<sub>2</sub> concentration is represented by a straight line and is intended to be a reference level for illustrating the CO<sub>2</sub> undersaturation and supersaturation in the ocean surface waters.

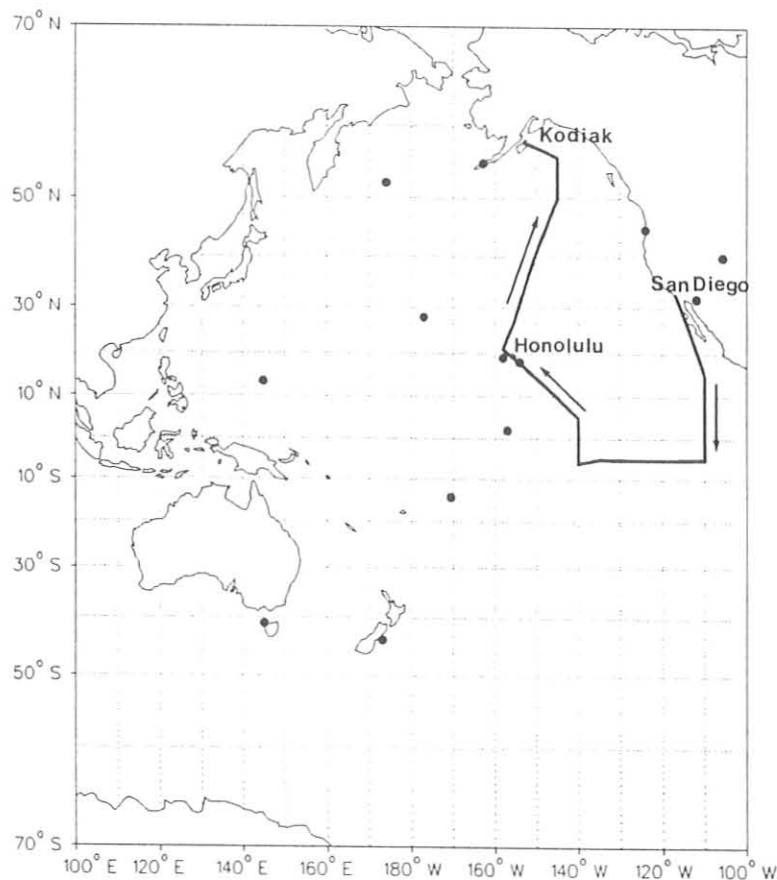


Figure 7.--1985 DISCOVERER cruise (.....). The solid circles show the locations of the GMCC flask network sites.

Figure 8 depicts the results from 24 May-5 June from San Diego to about 5°S, mostly along 110°W longitude. The equatorial partial pressure of dissolved CO<sub>2</sub> (pCO<sub>2</sub>) peak exceeds 490 ppm at -2°N and -500 ppm in the interval 4-5°S. Inasmuch as 5°S represents the southern turning point for the cruise track, the equatorial high pressure feature was not fully resolved. It appears that the supersaturation feature is split into two peaks at this longitude and is slightly skewed to the south with respect to the equator. These peaks represent the highest degree of equatorial supersaturation so far seen in our measurements in the Eastern Pacific. From this one track it is not clear whether the high peak represents the usual degree of supersaturation for this region, or whether this is an abnormal condition seen in 1985.

Figure 9 depicts the results for the westward run along 5°S between 110°W and 140°W longitude with an excursion to 6°S near 140°W to retrieve an instrumented buoy. It is clear that the unusual ΔpCO<sub>2</sub> values that were seen on the 110°W transect appear to be confined to the area east of ~113°W. West of this point the ΔpCO<sub>2</sub> ranges from 50 to 110 ppm with an average of about 70 ppm, typical of the usual differences observed on previous transects. The eastern limit of the 500-ppm area of high values is unknown, although pCO<sub>2</sub> values appear to be back in the 420-450 ppm range at 95°W (Weiss; SIO, La Jolla, CA; unpublished manuscript, 1984).

Figure 10 shows the equatorial transect at 140°W, the run into Honolulu, and the Hawaii to Alaska track. The north side of the equatorial transit is nearly identical to the two records obtained in 1984 (Nickerson, 1986, p. 41, figs. 11 and 12) between the equator and 7-8°N. From -10°N to -40°N, the mostly undersaturated region seen in 1984 during April-May has changed to an area where air and sea surface are in equilibrium or slightly supersaturated. The unresolved plunge to about 300 ppm at 40°N observed in 1984 can now be identified as the sub-Arctic front in the 1985 data.

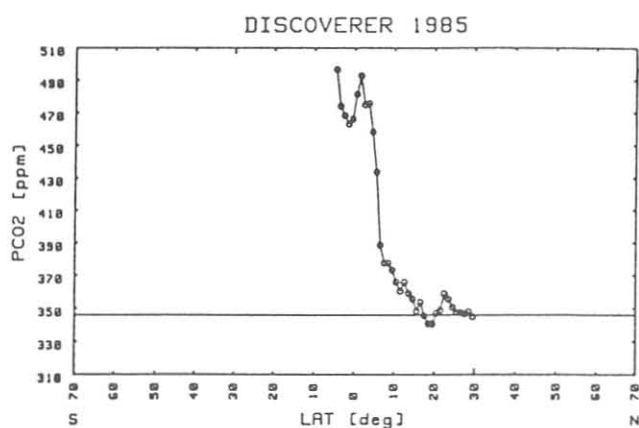


Figure 8.--pCO<sub>2</sub> the along N-to-S track at 110°W longitude.

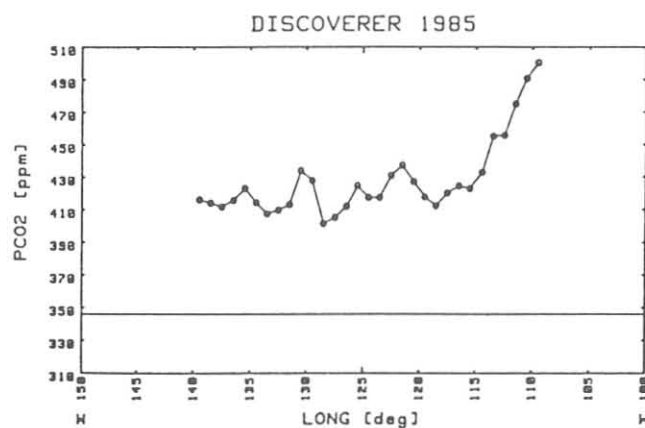


Figure 9.--pCO<sub>2</sub> along the E-to-W track from 5°S, 110°W to 6°S, 140°W.

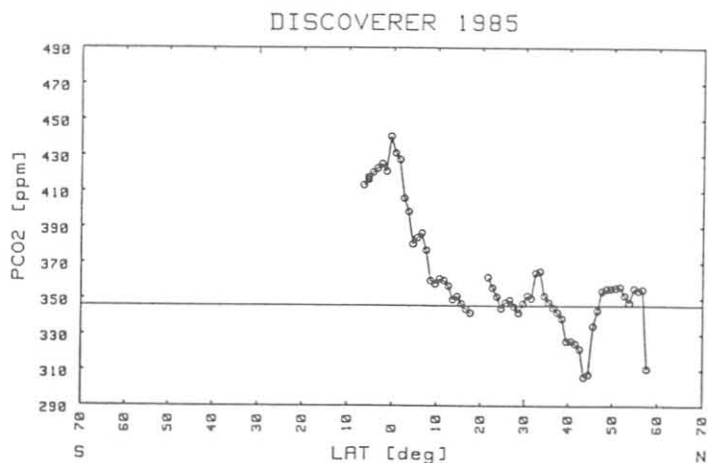


Figure 10.--pCO<sub>2</sub> along the S-to-N track at 140°W longitude, into Honolulu, then north to Kodiak Island, AK.

#### 4.3 References

- Feely, R. A., R. H. Gammon, B. A. Taft, P. E. Pullen, L. S. Waterman, T. J. Conway, and J. F. Gendron, 1986. Distribution of chemical tracers in the eastern equatorial Pacific during and after the 1982-83 El Nino/Southern Oscillation event. Journal of Geophysical Research (submitted).
- Keeling, C. D., and R. Revelle, 1985. Effects of El Nino/Southern Oscillation on the atmospheric content of carbon dioxide. Meteoritics 20(2):437-450.
- Komhyr, W. D., R. H. Gammon, T. B. Harris, L. S. Waterman, T. J. Conway, W. R. Taylor, and K. W. Thoning, 1985. Global atmospheric CO<sub>2</sub> distribution and variations from 1968-1982 NOAA/GMCC CO<sub>2</sub> flask sample data. Journal of Geophysical Research 90(D3):5567-5596.
- Mook, W. G., A., M. Koopmans, A. F. Carter, and C. D. Keeling, 1983. Seasonal, latitudinal, and secular variations in the abundance and isotopic ratios of atmospheric carbon dioxide: 1, Results from land stations. Journal of Geophysical Research 88(C15):10,915-10,933.
- Nickerson, E. C. (ed.) 1986. Geophysical Monitoring for Climatic Change, No. 13: Summary Report 1984. NOAA Environmental Research Laboratories, Boulder, CO, 111 pp.
- Pearman, G. I., P. Hyson, and P. J. Fraser, 1983. The global distribution of atmospheric carbon dioxide: 1. Aspects of observations and modeling. Journal of Geophysical Research 88(C6):3581-3590.
- Reinsch, C. H., 1967. Smoothing by spline functions. Numerische Mathematik 10:177-183.
- Steele, L. P., P. J. Fraser, R. A. Rasmussen, M. A. K. Khalil, T. J. Conway, A. J. Crawford, R. H. Gammon, K. A. Masarie, and K. W. Thoning, 1986. The global distribution of methane in the troposphere. Journal of Geophysical Research (in press).

## 5. TRACE GASES GROUP

### 5.1 Continuing Programs

#### TOTAL OZONE

Routine total ozone observations were made with Dobson spectrophotometers during 1985 at 14 stations that constitute the U.S. total ozone station network (table 1). Of the 14 stations, 4 are operated by GMCC personnel; 3 are foreign cooperative stations; 3 are domestic cooperative stations; and 4 are operated by the NWS.

Table 1.--U.S. Dobson ozone spectrophotometer station network for 1985

Station	Period of record	Inst. no.	Agency
Bismarck, ND	01 Jan 1963-present	33	NOAA
Caribou, ME	01 Jan 1963-present	34	NOAA
SMO	19 Dec 1975-present	42	NOAA
Tallahassee, FL	02 May 1964-present	58	NOAA; Fla. State Univ.
Nashville, TN	01 Jan 1963-present	79	NOAA
SPO	17 Nov 1961-present	80, 82	NOAA
Wallops I., VA	01 Jul 1967-present	38	NOAA; NASA
Huancayo, Peru	14 Feb 1964-present	91, 87	NOAA; Huancayo Obs.
Fresno, CA	22 Jun 1983-present	94	NOAA
Boulder, CO	01 Sep 1966-present	61	NOAA
Poker Flat, AK	06 Mar 1984-present	63	NOAA; Univ. of Alaska
MLO	02 Jan 1964-present	76	NOAA
Perth, Australia	30 Jul 1984-present	81	NOAA; Aust. Met. Dept.
Haute Provence, France	02 Sep 1983-present	85	NOAA; Obs. Haute Prov.

Daily 1985 total ozone amounts applicable to local apparent noon for stations in the U.S. Dobson instrument network have been archived by the World Ozone Data Centre, 4905 Dufferin Street, Downsview, Ontario M3H5T4, Canada, in Ozone Data for the World. Table 2 lists provisional monthly mean total ozone amounts for 1985 for the NOAA observatories and cooperative stations.

During 1985, GMCC personnel continued to participate in the WMO Global Ozone Research and Monitoring Project to upgrade the quality of Dobson ozone spectrophotometers throughout the world. Table 3 lists the instruments that were recalibrated relative to World Standard Dobson Instrument No. 83 maintained by GMCC in Boulder, CO.

In November 1985, Dobson instrument No. 82 was shipped to the South Pole so that instrument No. 80 could be returned to Boulder for recalibration. Dobson instrument No. 87, installed at Huancayo, Peru, is automated for Umkehr observations. It replaced instrument No. 91, which was in operation at Huancayo since September 1982.

Table 2.--Provisional 1985 mean total ozone amounts (milli-atm-cm)

	Jan	Feb	Mar	Apr	May	Jun	Jul	Aug	Sept	Oct	Nov	Dec
Bismarck, ND	325	360	361	349	327	339	311	335	299	297	336	345
Caribou, ME	402	414	385	405	387	370	341	331	309	309	327	371
SMO	264	264	257	262	263	245	254	263	270	275	274	268
Tallahassee, FL	274	278	285	320	333	316	321	-	304	293	294	287
Boulder, CO	329	338	322	339	328	315	297	298	295	278	314	301
Poker Flat, AK	-	446	435	473	392	352	325	313	304	352	-	-
MLO	231	232	250	272	282	280	281	266	264	254	260	251
Nashville, TN	325	324	312	340	358	328	331	311	296	282	287	315
SPO	288	278	-	245	213	236	234	207	-	161	238	314
Perth, Australia	283	267	272	276	276	263	286	296	304	310	292	278
Wallops I., VA	328	329	317	333	335	336	324	315	302	281	289	323
Haute Provence, (France)	353	336	367	363	370	332	325	326	304	289	312	314
Huancayo, Peru	252	253	250	-	258	-	-	-	262	257	260	256
Fresno, CA	305	324	333	333	334	321	308	306	305	289	297	310

Table 3.-- Dobson spectrophotometers calibrated in 1985

Country	Station	Instrument number
Peru	Huancayo	87
United Kingdom	Bracknell	41
United States	Boulder, CO	72
United States	South Pole, Antarctica	82
United States	Wallops Island, VA	38

A new round of spectrophotometer calibrations in the global Dobson instrument station network was undertaken in March 1985 by means of traveling standard lamps. Results from all stations are expected in 1987. A similar program was conducted in 1981 (Grass and Komhyr, 1985).

Plans were formulated for conducting an international comparison of Dobson spectrophotometers and Brewer ozone photometers in Arosa, Switzerland, during summer 1986.

#### TOTAL OZONE DECREASE AT SOUTH POLE

Analysis of South Pole total ozone data for the years 1964-1985 (Komhyr et al., 1986a) showed that ozone has decreased at South Pole by 25% since the mid-1960's (fig. 1). Largest ozone decreases occurred during the months of October and November; smaller decreases occurred in other months, except

February months when ozone slightly increased. A similar decrease in ozone at Halley Bay, Antarctica, was attributed to ozone destruction by gas phase (Farman et al., 1985) and heterogeneous (Solomon et al., 1985) reactions involving  $\text{ClO}_x$  and  $\text{NO}_x$  photochemistry, which no doubt occur. However, analysis of the South Pole data indicated that the decrease in ozone may be due predominantly to a change in atmospheric circulation and the transport of ozone into Antarctica. This change in ozone transport is manifested in a delay in recent compared with past years in the time of stratospheric warming in Antarctica (fig. 2), as well as in ozone decreases that have occurred periodically in Antarctica. These ozone decreases are probably related to the 4-yr oscillation (FYO) in ozone (Hasebe 1980, 1983), and are influenced by Hadley and Brewer-Dobson circulations. In past years, substantial ozone recovery occurred (fig. 1) within 1 to 2 years following onset of an FYO event, but such recovery did not occur following the FYO event of 1980.

Figure 3 presents additional evidence for a change in the transport of ozone to Antarctica. The latitudinal source regions of 10-day isobaric back trajectories of air parcels that arrived at McMurdo, Antarctica ( $78^\circ\text{S}$ ,  $166^\circ\text{E}$ ) at 50 mb in October and November 1978 and 1985 are plotted in the figure. The trajectories were computed using the ARL/GMCC Trajectory Program (Harris, 1982). The marked difference for the 2 years in the frequency of outbreaks of subtropical, ozone-rich, stratospheric air transported to McMurdo is readily apparent.

The slight increase in ozone at South Pole that has occurred in February months during 1964-1985 appears to be due to an increase with time in ozone transport to Antarctica from the subtropical, stratospheric ozone production region. Vertical distribution ozone measurements have indicated that the transport occurs at pressure altitudes of 30 mb and above. As shown in fig. 4, an episode of transport of an unusually large amount of ozone to South Pole occurred in early February 1984 (Komhyr et al., 1986). The increase in ozone measured at that time at South Pole was comparable in magnitude to ozone changes that occur during October and November months when large amounts of ozone are transported each year to Antarctica.

#### OZONE VERTICAL DISTRIBUTION

In late 1984, funding was obtained from NESDIS to conduct ozonesonde observations at three stations and Umkehr observations at five stations to obtain atmospheric ozone vertical distribution data for validation of SBUV ozone data obtained aboard the NOAA F satellite. The ozonesonde observations are made with balloonborne ECC ozonesondes (Komhyr, 1969), and the Umkehr observations are made with automated Dobson spectrophotometers (Komhyr et al., 1985). In addition, ECC ozonesonde observations were made as part of the SAGE II satellite ozone validation program from Boulder, CO; Laramie, WY; and Fairbanks, AK.

Weekly ECC ozonesonde flights began at Boulder, CO and Hilo, HI, in January 1985. The sounding program was expanded later in 1985 to include observations at Edmonton, Canada, in a cooperative endeavor with the AES.

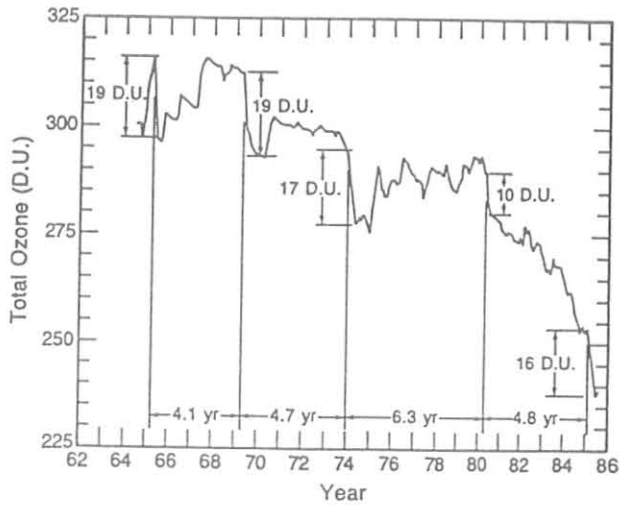


Figure 1.--South Pole 12-mo running plot of mean monthly total ozone data. Long vertical bars indicate times of abrupt downward shifts in ozone. Short vertical arrow denote magnitudes of the shifts.

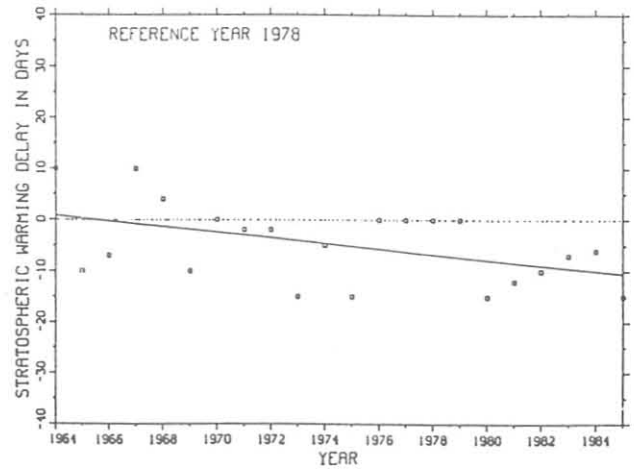


Figure 2.--Differences in times of onset of stratospheric warming at South Pole during 1964-1985 compared with the time of warming in 1978. The slope of the best fit line is  $0.53 \pm 0.48 \text{ day yr}^{-1}$ .

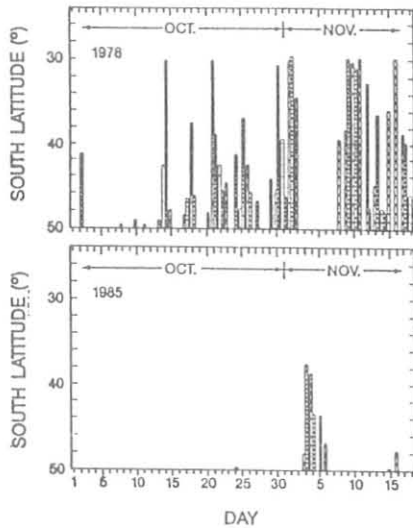


Figure 3.--Latitudinal origin and frequency of 50-mb, 10-day, isobaric back trajectories arriving at McMurdo, Antarctica ( $78^{\circ}\text{S}$ ,  $166^{\circ}\text{E}$ ) 1 October to 18 November 1978 and 1985. Hatched bars and crossed bars denote arrival times of 0000 and 0012 GMT, respectively.

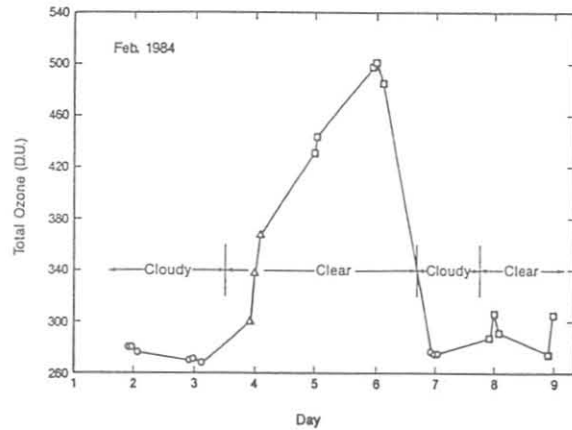


Figure 4.--Sudden total ozone increase at SPO during 3-6 February 1984. Total ozone observations were made with a Dobson spectrophotometer on cloudy sky and CC' wavelengths (o); direct sun and CD wavelengths ( $\Delta$ ); and focused image of the sun and CD wavelengths ( $\square$ ).

Mean Boulder and Hilo 1985 seasonal ECC sonde data, for mandatory atmospheric pressure levels, are presented in table 4. Plots of the data are shown in figs. 5 and 6. All data were normalized to Dobson spectrophotometer total ozone. Mean normalization factors were  $0.993 \pm 0.038$  for Boulder and  $1.003 \pm 0.059$  for Hilo, where the indicated variabilities (standard deviations) include effects caused by nonsimultaneity of the ECC sonde and Dobson spectrophotometer observations, and imprecision in total ozone measurements that occur when observations are made on cloudy sky.

Table 4.--Seasonal ozone partial pressure data\* for mandatory atmospheric pressure levels obtained from ECC ozonesonde soundings in Boulder and Hilo in 1985

Pressure (mb)	Boulder				Hilo			
	Winter	Spring	Summer	Autumn	Winter	Spring	Summer	Autumn
sfc	11 (37.7) 11.3	14 (39.5) 10.7	14 (37.8) 17.1	14 (26.6) 11.0	9 (27.3) 16.5	11 (23.9) 10.0	11 (15.1) 9.2	12 (16.7) 10.3
1000	--	--	--	--	9 (31.7) 13.5	11 (26.1) 10.0	11 (15.8) 8.5	12 (18.3) 10.2
700	11 (36.4) 4.8	14 (39.9) 6.8	14 (39.4) 12.2	14 (32.9) 3.8	9 (31.2) 12.0	11 (33.5) 9.6	11 (28.3) 13.0	12 (25.7) 9.8
500	11 (26.2) 1.8	14 (30.2) 6.6	14 (29.7) 5.7	14 (28.6) 10.1	9 (24.3) 8.2	11 (28.5) 8.8	11 (20.3) 6.4	12 (21.5) 7.8
300	11 (25.3) 17.4	14 (21.6) 9.4	14 (18.8) 8.0	14 (18.4) 12.2	9 (15.3) 4.7	11 (21.0) 5.6	11 (8.3) 2.2	12 (13.5) 9.9
200	11 (51.9) 31.8	14 (49.2) 36.0	14 (17.8) 11.3	14 (29.9) 21.5	9 (13.8) 5.8	11 (14.2) 7.6	11 (4.8) 1.5	12 (9.5) 6.7
150	11 (67.2) 52.9	14 (63.1) 34.4	14 (21.9) 15.2	14 (39.7) 23.9	9 (11.9) 4.9	11 (20.9) 14.5	11 (6.2) 2.1	12 (12.1) 9.3
100	11 (53.2) 36.5	14 (73.9) 33.1	14 (41.8) 15.1	14 (60.7) 28.6	9 (14.4) 7.4	11 (26.9) 8.4	11 (16.8) 3.7	12 (15.8) 11.0
70	11 (109.4) 41.1	14 (85.1) 24.2	14 (85.3) 12.3	14 (98.9) 24.4	9 (35.3) 12.1	11 (58.0) 21.8	11 (49.4) 6.1	12 (45.7) 9.3
50	11 (135.9) 22.6	14 (113.9) 12.6	14 (111.7) 9.2	14 (118.5) 14.2	9 (71.7) 16.3	11 (87.4) 11.0	11 (86.5) 6.7	12 (75.3) 7.2
30	11 (146.9) 12.4	14 (138.6) 8.6	14 (142.9) 9.8	14 (143.3) 10.3	8 (106.6) 12.6	11 (130.1) 7.3	11 (131.8) 5.9	12 (123.2) 10.4
20	11 (104.8) 8.6	14 (123.1) 10.5	14 (133.7) 7.6	14 (119.1) 15.2	8 (124.9) 11.3	11 (144.1) 6.1	11 (144.2) 5.5	12 (132.3) 9.3
10	11 (54.5) 5.0	14 (80.6) 3.9	14 (72.7) 8.7	14 (64.9) 8.8	8 (73.9) 5.4	11 (85.8) 5.4	11 (89.3) 3.8	12 (79.0) 9.6
7	11 (47.4) 4.6	14 (53.9) 3.9	14 (47.1) 9.7	14 (44.1) 4.1	8 (51.5) 6.4	11 (54.1) 4.5	11 (54.9) 2.8	12 (52.8) 6.2
5	11 (29.5) 4.2	14 (32.5) 3.1	14 (27.3) 7.0	14 (30.1) 1.9	8 (29.9) 9.8	10 (32.7) 6.0	9 (32.3) 4.3	12 (31.3) 5.5
3	4 (12.3) 2.2	3 (10.7) 3.1	--	6 (11.5) 3.1	1 (14.0) --	2 (11.0) 2.8	--	--

\*Values in brackets are ozone partial pressure in nanobars (nb). Values preceding and following each bracketed value are the number of observations per season and the standard deviation of the seasonal mean value, respectively.

Umkehr observations were made in 1985 at five stations: Boulder (BDR), Colorado, 40°N, 105°W; Mauna Loa Observatory (MLO), Hawaii, 20°N, 156°E; Observatory Haute Provence (OHP), France, 44°N, 6°E; Poker Flat (PKF), Alaska, 65°N, 148°W; and Perth (PTH), Australia, 32°S, 116°E. Table 5 shows the number of conventional and short Umkehr observations made at each of the stations.

Ozone vertical distribution at the five sites, derived from conventional Umkehr observations, are plotted in fig. 7. Mean annual ozone partial pressures for the various Umkehr layers are indicated on the plots, together with standard deviations of the layer annual mean values.

#### SURFACE OZONE

At least 10 years of continuous surface ozone measurements have now been obtained at all four GMCC observatories. The record of monthly mean surface ozone values through 1985 is shown in fig. 8. All measurements are referenced

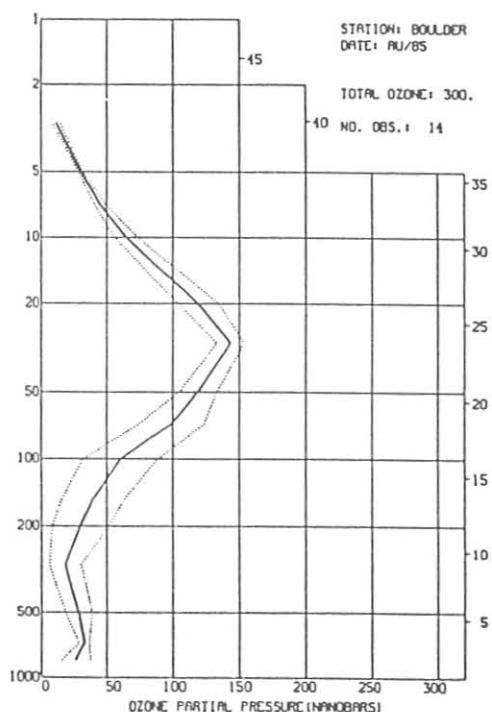
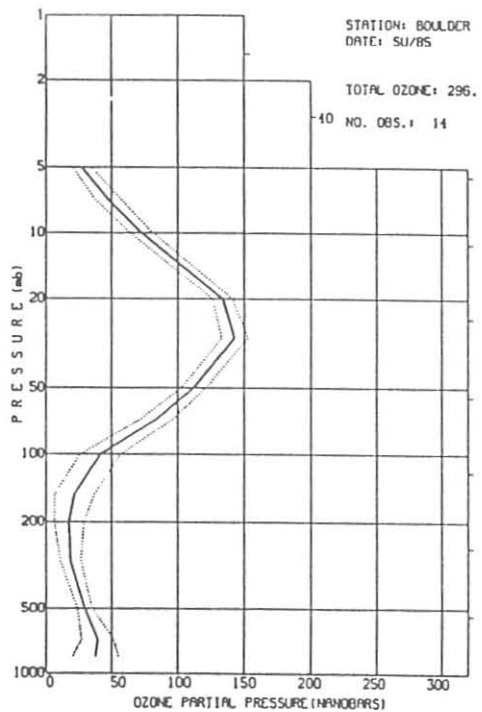
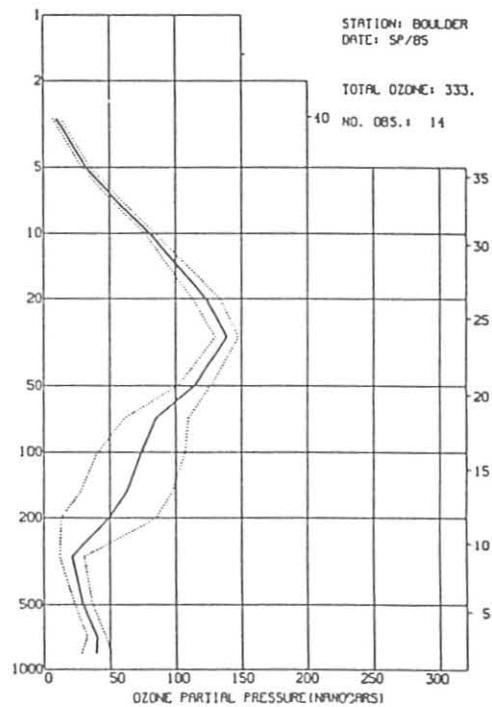
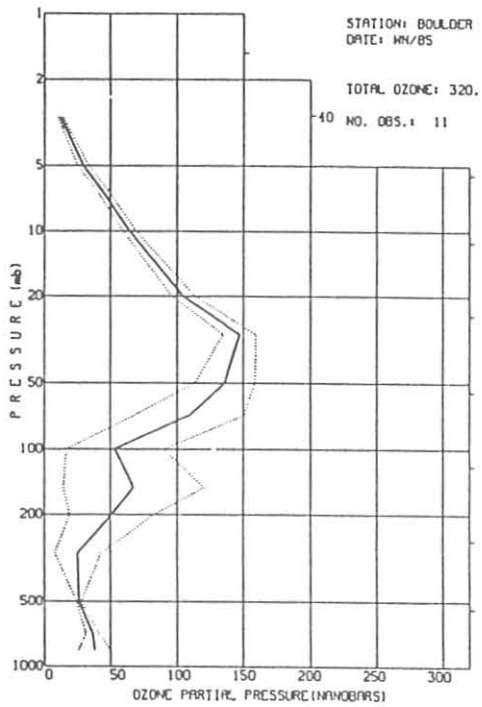


Figure 5.--Mean seasonal ECC-sonde ozone vertical distribution data for Boulder, 1985. Data are plotted for mandatory atmospheric pressure levels (table 4). Dotted lines denote variability ( $\pm 1$  standard deviation).

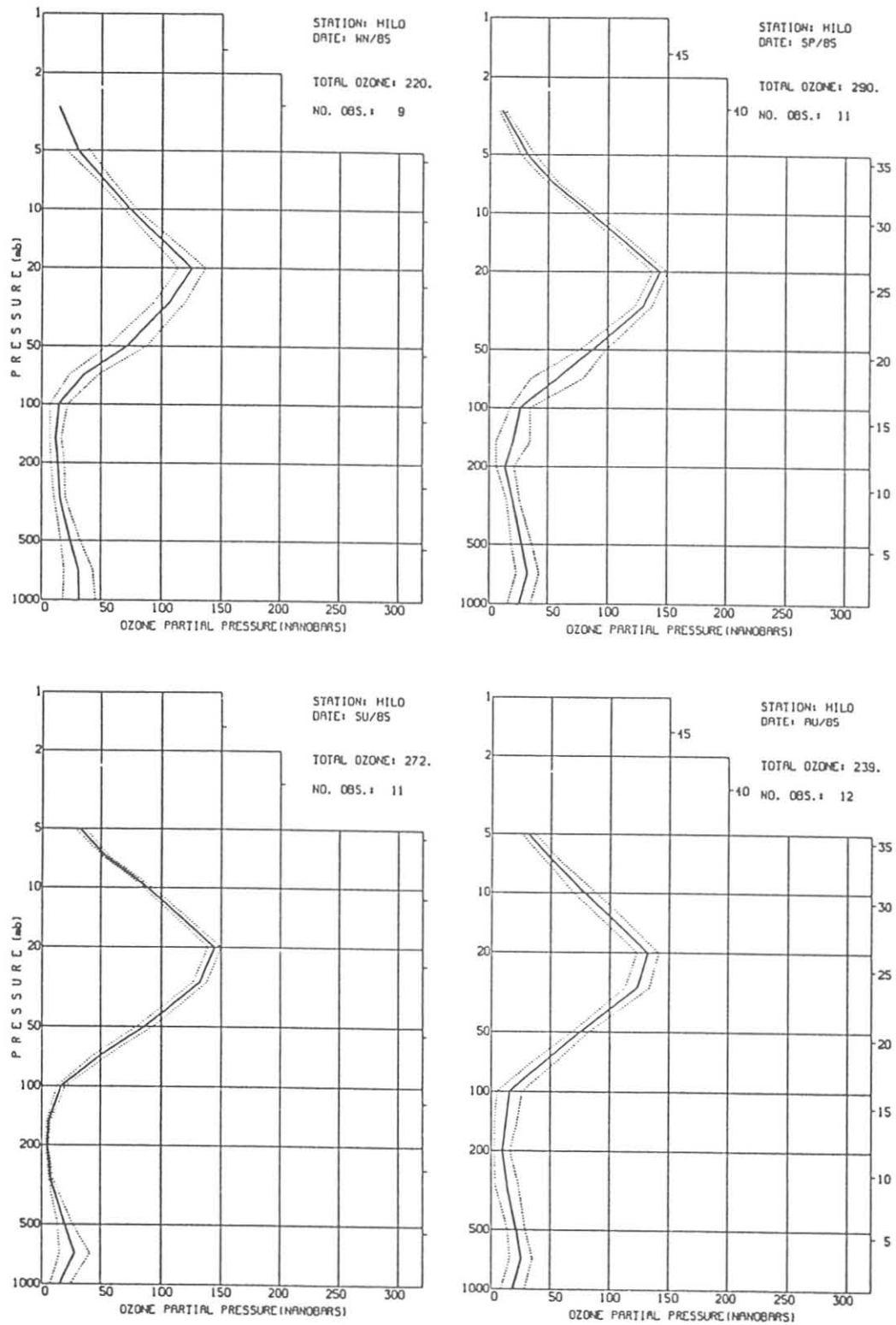


Figure 6.--Mean seasonal ECC-sonde ozone vertical distribution data for Hilo, 1985. Data are plotted for mandatory atmospheric pressure levels (table 4). Dotted lines denote data variability ( $\pm 1$  standard deviation).

Table 5.--Record of conventional and short Umkehr observations made at the automated Dobson spectrophotometer stations in 1985\*

Station	Jan	Feb	Mar	Apr	May	Jun	Jul	Aug	Sep	Oct	Nov	Dec
BDR	15/18	4/10	3/12	6/13	14/15	18/18	15/16	20/23	17/18	25/24	10/11	19/17
MLO	45/45	19/22	11/11	7/7	23/26	39/42	35/37	36/37	33/49	23/24	27/29	38/41
OHP	11/12	13/17	13/11	22/28	4/7	0/2	3/7	23/24	30/29	15/16	20/18	17/21
PKF	--	--	0/1	12/16	16/19	2/3	14/23	5/6	1/6	0/4	--	--
PTH	40/43	32/34	32/37	25/26	17/18	9/12	16/17	10/12	26/28	26/28	28/29	31/31

\*Number of Umkehr observations: conventional/short.

to a network standard Dasibi ozone monitor that is periodically calibrated against an NBS standard ozone photometer maintained at Gaithersburg, MD. Calibration of the network Dasibi in December 1985 showed its calibration to be unchanged from a previous calibration made October 1983.

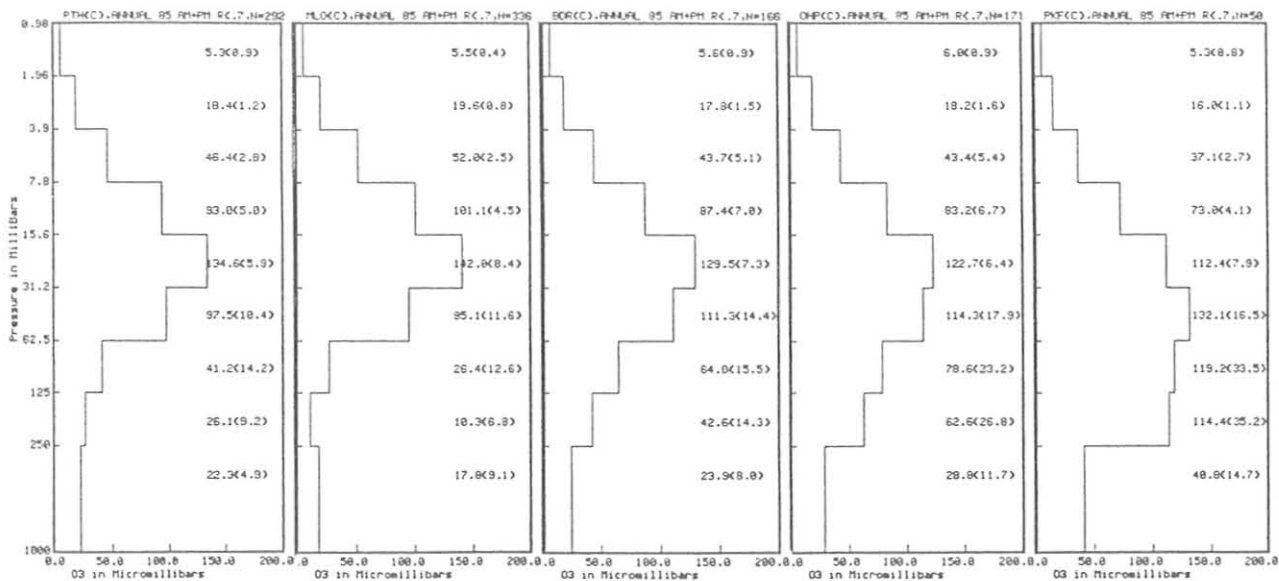


Figure 7.--Mean 1985 ozone vertical distribution profiles obtained from conventional Umkehr observations at the NOAA/GMCC automated Dobson spectro photometer station network.

Linear regression analyses applied to the data of fig. 8 indicate long-term increases in surface ozone at BRW and MLO (table 6). At SMO, there has been a statistically insignificant (at the 95% confidence interval level) ozone decrease with time, while at SPO essentially no trend in ozone is observed.

Trend estimates, including 95% confidence intervals, for the monthly anomalies are given in table 6 for the GMCC stations. Also given for BRW and MLO are trends for time periods ending in years other than 1985. The influence of large surface ozone values at these stations in late 1982 and early 1983 is reflected in the trend estimates. Lower surface ozone values at

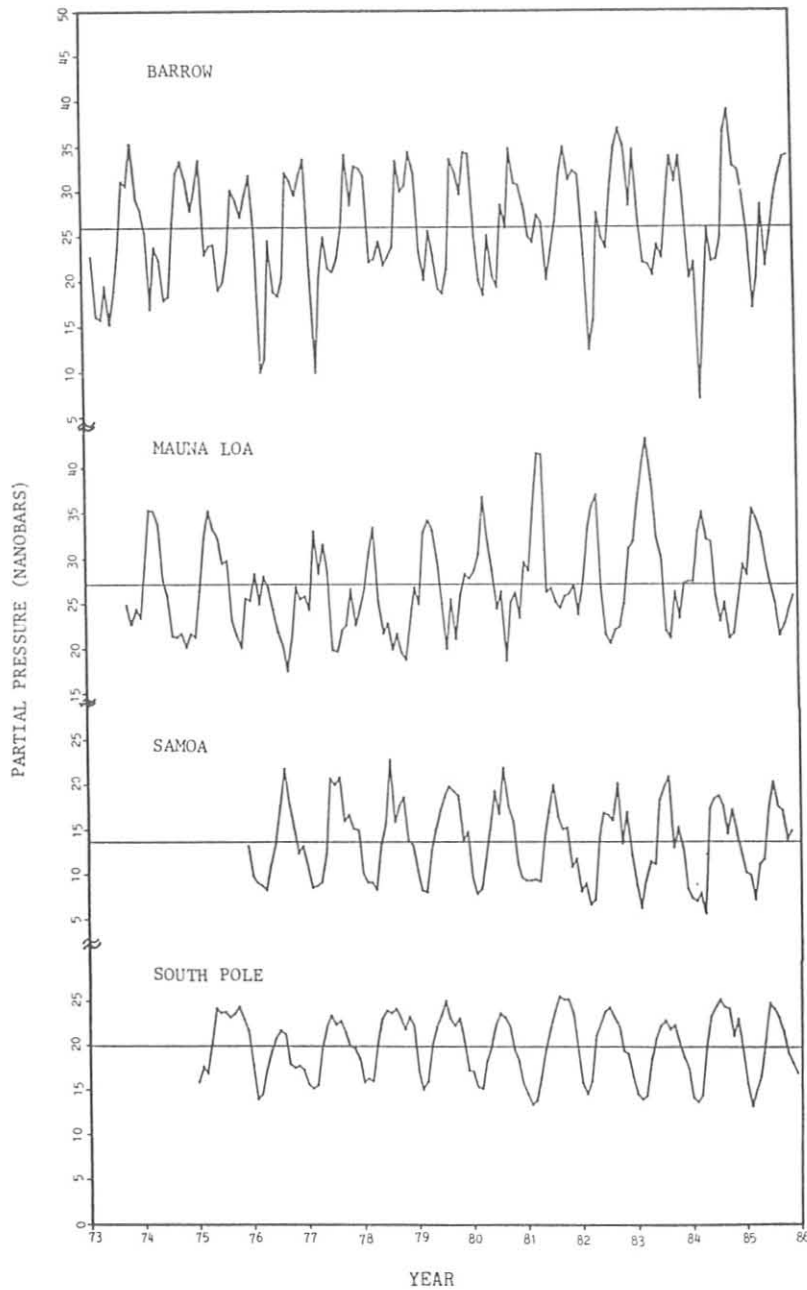


Figure 8.--Record of monthly mean surface ozone values at the NOAA/GMCC baseline stations for 1973-1985.

MLO during 1984 and 1985 have reduced the magnitude of the upward trend, compared with the magnitude of trend computed following 1983. The long-term surface ozone increase at MLO remains, however, highly significant.

Table 6.--Trends and 95% confidence intervals for surface ozone anomalies at the NOAA/GMCC observatories

Station	Years	Trends ( $\% \text{ yr}^{-1}$ )
BRW	1973-1983	$1.17 \pm 0.61$
	1973-1984	$0.76 \pm 0.61$
	1973-1985	$0.78 \pm 0.52$
MLO	1974-1982	$1.15 \pm 0.81$
	1974-1983	$1.74 \pm 0.71$
	1974-1984	$1.37 \pm 0.61$
	1974-1985	$1.20 \pm 0.52$
SMO	1976-1985	$-0.70 \pm 0.80$
SPO	1975-1985	$-0.05 \pm 0.32$

#### STRATOSPHERIC WATER VAPOR

Stratospheric water vapor profiles from balloonborne frost-point hygrometers were obtained during 1985 in Boulder, CO; Palestine, TX; and Fairbanks, AK. Plots of the water vapor mass mixing ratios of the stratospheric portions of the soundings are shown in fig. 9.

The six soundings made in Boulder were part of an ongoing program begun in 1981 to monitor the water vapor content of the stratosphere over Boulder. The two soundings made at Palestine concluded a series of correlative measurements begun in 1983 to test the concept of long-term, satellite-based monitoring of trace gases in the stratosphere using a multidetector infrared spectrometer and a solar occultation technique. The solar occultation experiment, involving balloonborne instrumentation, was designed by NOAA/NESDIS. The measurements at Fairbanks were part of a continuing series of soundings made to validate water vapor profiles obtained from the SAGE II instrumentation carried on board the Earth Radiation Budget satellite.

A NOAA Data Report (Oltmans, 1986) presents tabular and graphical stratospheric water vapor data from Washington, DC; Boulder, CO; Palestine, TX; Laramie, WY; and Fairbanks, AK. The data for Washington, DC from 1974-1980 represent the completion of the sounding program conducted by personnel of the Naval Research Laboratory, Washington, DC at that location. The data from Boulder for 1981-1985 are from the monthly sounding program that began in 1981. Profiles from Palestine, Laramie, and Fairbanks are from various intercomparison programs conducted during 1981-1985.

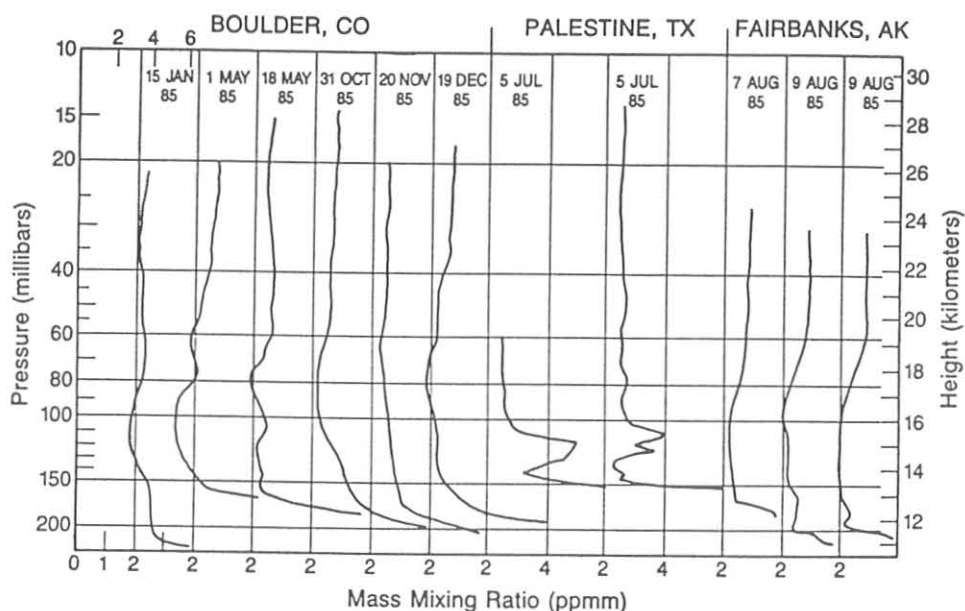


Figure 9.--Profiles of stratospheric water vapor mass mixing ratio (ppm) for 1985 at Boulder, CO; Palestine, TX; and Fairbanks, AK. Numbers along the top of the plot for the first water vapor profile are volume mixing ratios in ppm.

#### HALOCARBONS AND NITROUS OXIDE

Two new people were employed in 1985: A group leader, with specific expertise in calibration gas preparation, dissolved gas measurements, and infrared spectroscopy, who will arrive in 1986; and a CIRES employee, who began work in May as operations manager for field measurements.

Air samples continued to be collected weekly at BRW, NWR, MLO, and SMO, and weekly in January, November, and December only at SPO. These samples were returned to Boulder where  $\text{CCl}_3\text{F}$  (halocarbon F-11),  $\text{CCl}_2\text{F}_2$  (F-12), and  $\text{N}_2\text{O}$  concentrations were determined by an EC-GC.

Our calibration standards for F-11 and F-12 were tied to the OGC scale.  $\text{N}_2\text{O}$  calibration standards were made at GMCC in Boulder and based on diluting a precisely known mixture of  $\text{N}_2\text{O}$  in  $\text{CO}_2$  into a  $\text{CO}_2$ - and  $\text{N}_2\text{O}$ -free air mixture, measuring the  $\text{CO}_2$  concentration, and thereby yielding the  $\text{N}_2\text{O}$  concentration. Cylinder 3072, which has been used exclusively as the source of calibration gas for sample analyses since 1977 in Boulder, was replaced by cylinder 3088 on 20 September because of low pressure. The SPO gas chromatograph was operated twice a week, analyzing air for F-11, F-12, and  $\text{N}_2\text{O}$  concentrations. Calibration gas came from cylinder 3083. Calibration standards will be produced by gravimetric techniques in the future.

Work on the RITS Project began with the design of an automated gas chromatograph and data processing system to measure the in situ air concentrations of  $\text{N}_2\text{O}$ , F-12, F-11,  $\text{CH}_3\text{CCl}_3$ , and  $\text{CCl}_4$  at the baseline stations. Hardware and software were subsequently purchased, modified, and

tested. Installation of the system will begin in 1986 at SMO, BRW, and MLO. The system consists of a Hewlett-Packard Model 5890 EC-GC, a Nelson Analytical interface box, an HP9816 computer with Thinkjet printer, and an HP9133 hard disk and floppy drive.

Selected N<sub>2</sub>O, F-12, and F-11 data from BRW, NWR, MLO, SMO, and SPO are shown in figs. 10, 11, and 12 for the period 1977-1985. The data from September 1984 through February 1985 have been excluded from the record because of problems with the detector's response. Least-squares regressions using a quadratic model fit to the data are represented by the solid lines in the figures. Estimated growth rates and associated standard deviations are also shown.

N<sub>2</sub>O data have been corrected to account for the influence of CO<sub>2</sub> on the gas chromatographic analyses of air when it co-elutes with N<sub>2</sub>O. Increasing levels of CO<sub>2</sub> in the atmosphere have enhanced our EC-GC's response to N<sub>2</sub>O by approximately 0.2 ppb per ppm of CO<sub>2</sub> over the CO<sub>2</sub> range of 315-355 ppm.

Yearly means and standard deviations for the three constituents at the five stations are shown in Table 7. Years where data are missing have means estimated by the regression equation at midyear. The N<sub>2</sub>O data record shows no significant (95%) change in the average rate of increase (0.64 ppbv yr<sup>-1</sup>) for the 9 years for any of the stations. The rate of increase at SMO is increasing more rapidly than at other GMCC stations. The F-12 data likewise increase at a constant rate. However, in the Southern Hemisphere, F-12 concentrations are increasing 9% faster than in the Northern Hemisphere. All the stations except SPO show a significantly (99% confidence level) decreased rate of F-11 growth. The rate of growth of F-11 at SPO is also decreasing, but the large scatter in the data make it less significant (83% confidence level). Southern Hemispheric F-11 concentrations are growing 5% faster than at Northern Hemisphere sites. This is probably due to inter-hemispheric exchange rates being higher than Northern Hemisphere source rates.

Table 7.--Mean annual concentrations\* of N<sub>2</sub>O and halocarbons F-11 and F-12

	1977	1978	1979	1980	1981	1982	1983	1984	1985
<u>N<sub>2</sub>O (ppbv)</u>									
BRW	301.8	301.5±0.2	301.9±0.2	301.6±0.3	302.8±0.2	303.4±0.1	303.3±0.2	304.4	304.9
NWR	300.5	301.1±0.3	301.9±0.2	303.3±0.3	303.3±0.2	304.6±0.2	305.2±0.2	305.8	306.2
MLO	300.8	300.2±0.3	301.5±0.2	302.0±0.3	302.8±0.3	303.8±0.2	303.8±0.2	305.3	306.0
SMO	302.0	302.6±0.3	304.1±0.2	304.5±0.3	305.5±0.3	307.1±0.2	307.4±0.2	308.8	309.5
SPO	299.4	300.1	300.8	301.4	302.0	302.5	302.9	303.3	303.7
<u>F-12 (pptv)</u>									
BRW	263.7	281.1±1.5	295.3±0.9	310.8±1.2	329.9±1.5	345.2±1.0	360.2±1.2	375.5	390.7
NWR	263.3	284.7±2.6	295.5±1.0	306.0±1.0	322.1±1.1	339.6±1.0	357.1±1.1	369.4	384.5
MLO	261.9	278.4±1.1	293.1±1.4	305.9±1.2	324.8±1.4	336.4±0.8	350.6±1.3	367.0	381.7
SMO	239.3	259.6±0.8	273.8±0.6	286.6±0.7	308.0±1.1	325.3±0.6	343.8±1.2	358.0	374.3
SPO	230.3	250.1	269.1	287.2	304.6	321.3	337.1	352.1	366.4
<u>F-11 (pptv)</u>									
BRW	154.1	165.0±0.7	173.9±0.6	183.8±0.5	193.5±0.7	201.8±0.5	212.1±0.7	219.4	227.4
NWR	151.1	162.3±1.0	169.0±0.7	180.1±0.7	188.1±0.5	197.8±0.7	208.4±0.6	215.2	223.7
MLO	145.1	156.3±0.6	166.7±0.7	177.1±0.6	186.0±0.5	193.8±0.5	205.0±0.7	212.6	220.5
SMO	135.7	148.2±0.6	158.3±0.5	167.7±0.4	178.1±0.7	188.4±0.4	198.1±0.6	205.4	213.1
SPO	139.1	150.1	160.7	171.0	180.8	190.3	199.3	208.0	216.3

\*Values without standard deviations were calculated at midyear from the least-squares quadratic regression fits to the data.

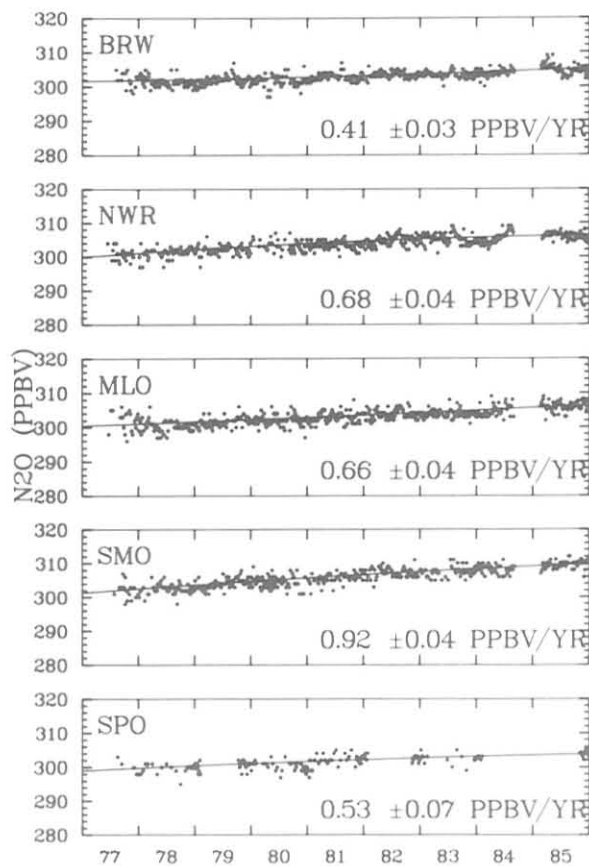


Figure 10.--Selected  $N_2O$  data record, and estimated growth rates and associated standard deviations.

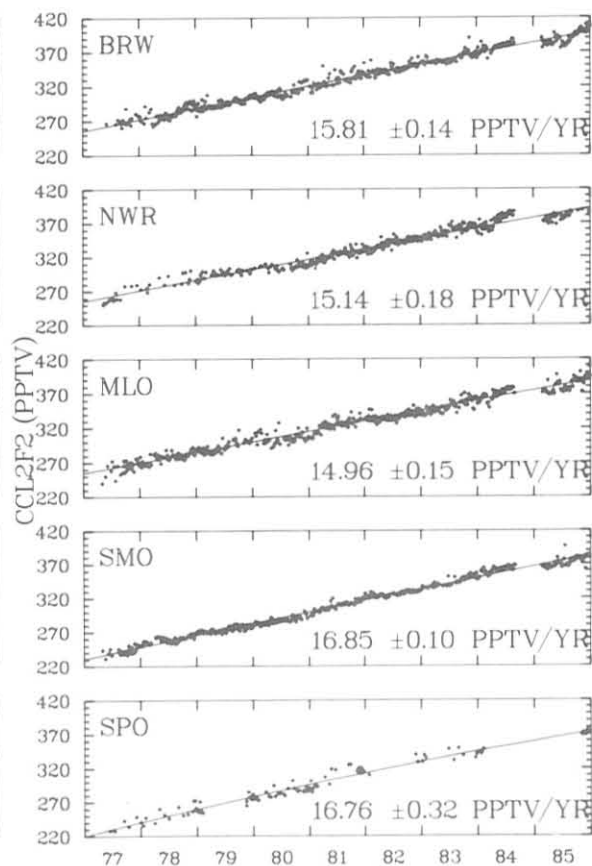


Figure 11.--Selected  $CCl_2F_2$  (halo-carbon F-12) data record, and estimated growth rates and associated standard deviations.

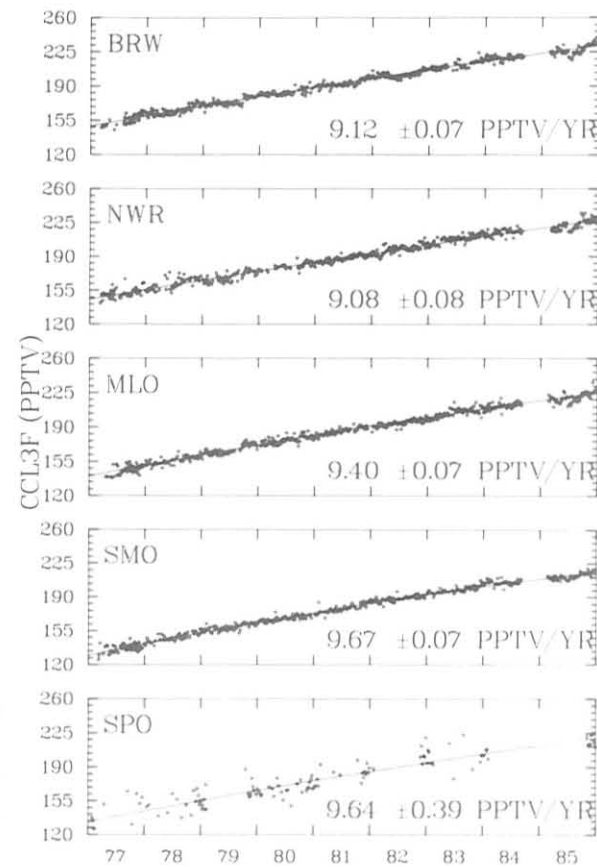


Figure 12.--Selected  $CCl_3F$  (halo-carbon F-11) data record, and estimated growth rates and associated standard deviations.

## 5.2 References

- Farman, J. C., B. G. Gardiner, and J. D. Shaklin, 1985. Large losses of total ozone in Antarctica reveal seasonal  $\text{ClO}_x/\text{NO}_x$  interaction. Nature 315:207-210.
- Grass, R. D., and W. D. Komhyr, 1985. Traveling standard lamp calibration checks on Dobson ozone spectrophotometers during 1981-83. In Atmospheric Ozone, Proceedings of the Quadriennial Ozone Symposium, Halkidiki, Greece, 3-7 September 1984, D. Reidel, Dordrecht, Holland, 376-380.
- Harris, J. M., 1982. The GMCC trajectory program. NOAA Tech. Memo ERL ARL-116, NOAA Environmental Research Laboratories, Boulder, CO, 30 pp.
- Hasebe, F., 1980. A global analysis of the fluctuation of total ozone: II, Non-stationary annual oscillation, quasi-biennial oscillation, and long-term variations in total ozone. Journal of the Meteorological Society of Japan 58:104-117.
- Hasebe, F., 1983. Interannual variations of global total ozone revealed from Nimbus 4 BUW and ground-based observations. Journal of Geophysical Research 88:6819-6834.
- Komhyr, W. D., 1969. Electrochemical concentration cells for gas analysis. Annales de Geophysique 25(1):203-219.
- Komhyr, W. D., R. D. Grass, R. D. Evans, R. K. Leonard, and G. H. Semeniuk, 1985. Umkehr observations with automated Dobson spectrophotometers. In Atmospheric Ozone, Proceedings of the Quadrennial Ozone Symposium held in Halkidiki, Greece, 3-7 September 1984. D. Reidel, Dordrecht, Holland, 371-375.
- Komhyr, W. D., R. D. Grass, and R. K. Leonard, 1986. Total ozone decrease at South Pole, Antarctica, 1964-1985. Geophysical Research Letters (in press).
- Komhyr, W. D., R. D. Grass, J. M. Harris, and R. K. Leonard, 1986b. A South Pole, Antarctica, ozone high. Geophysical Research Letters (in press).
- Oltmans, S. J., 1986. Water vapor profiles for Washington, DC; Palestine, TX; Laramie, WY; and Fairbanks, AK during the period 1974 to 1985. NOAA Data Report ERL ARL-7, NOAA Environmental Research Laboratories, Boulder, CO, 360 pp.
- Solomon, S., R. R. Garcia, F. S. Rowland, and D. J. Wuebbles, 1985. On the depletion of Antarctica ozone. Nature 321:755-758.

## 6. ACQUISITION AND DATA MANAGEMENT GROUP

### 6.1 Continuing Programs

#### STATION CLIMATOLOGY

##### Introduction

The interpretation of measured values of aerosols, trace gases, and turbidity requires the measurement of ancillary meteorological variables to assess the influence of local pollution sources. These variables include wind direction, wind speed, station pressure, air and dewpoint temperature, and a determination of boundary layer stability. The main criterion used in selecting the sensors was ruggedness, considering the stress of the polar environment at two of the stations. Where appropriate, commercially available instrumentation was chosen and WMO-recommended exposure standards were followed. A complete list of the sensors, model numbers, and the heights appear in Nickerson (1986).

With the installation of CAMS units at all stations during the latter half of 1984, downtime of the data acquisition activity was significantly reduced. As a result of the new daily routine of printing hourly averages and comparing them with observed conditions, the quality of the data improved as well. The printout known as the daily weather report was used for this purpose. It contains hourly average values for the wind measured at approximately 12 m height, air and dewpoint temperature measured at 2 m, air temperature measured at about 12 m, and station pressure. The reports are sent to Boulder, checked, and stored on microfiche for future reference. The numerical values, from which tables 1-4 are generated, are also stored on tape.

##### Barrow

A description of the Barrow site, its surroundings, and climate can be found in previous GMCC Summary Reports e.g., (DeLuisi, 1981). Wind roses of the hourly average resultant wind direction and speed are presented in 16 direction classes and 4 speed classes. The distribution of the wind by direction for 1985 is quite consistent with the average for the 1977 through 1984 period (fig. 1). The predominant wind direction is again from the "representative sampling sector," NE-SE, and all other directions are less than 5%. This was not the case in 1984 when an unusually large percentage of southwesterlies were observed (Nickerson, 1986). The 1985 wind rose contains 15.5% of the wind equal to or greater than  $10 \text{ m s}^{-1}$  as contrasted to 9% for the long-term average. New maximum wind speeds were observed for the months of March and July (table 1). The month-to-month changes in prevailing wind direction are significant. In 1985, easterlies (NE-SE), generally considered to be the preferred direction for baseline air sampling, occurred in excess of 92% of the time in January as contrasted to only 31% in February. These percentages are the monthly maximum and minimum for the year. The long-term average percentage of easterly winds is 61%; they occurred 59% of the time in 1985.

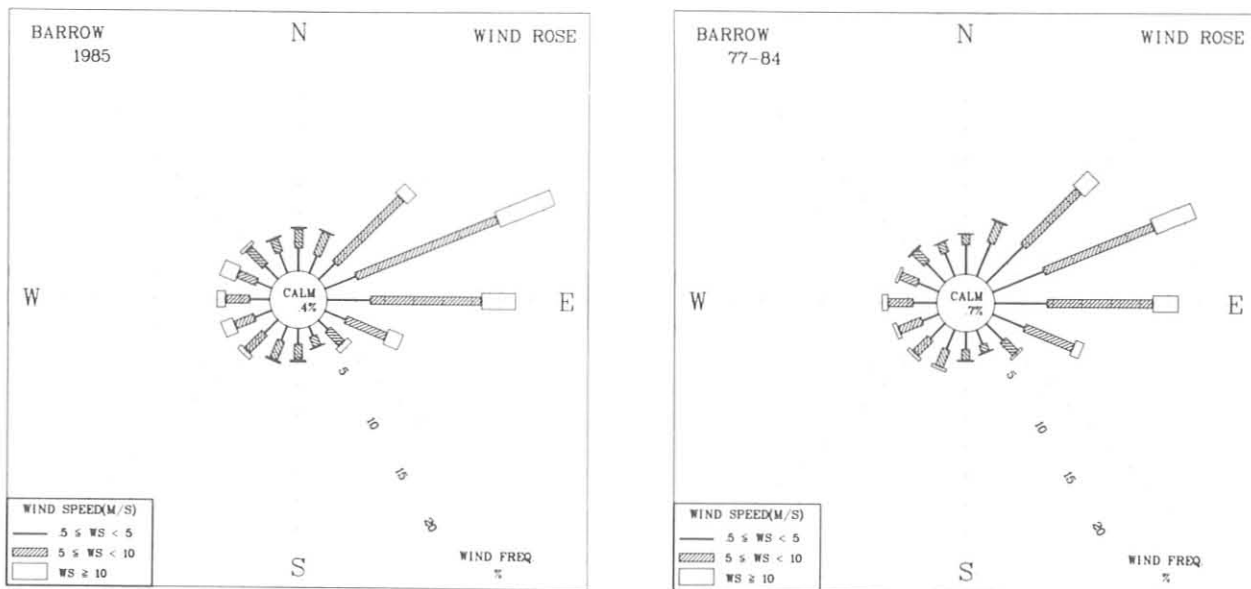


Figure 1.--Wind rose of surface winds for BRW for 1985 (left) and 1977-1984 (right). The distribution of the resultant wind direction and speed are in units of percent occurrence for the year and 8-yr period, respectively. Wind speed is displayed as a function of direction in three speed classes.

Table 1.--BRW 1985 monthly climate summary\*

	Jan	Feb	Mar	Apr	May	Jun	Jul	Aug	Sep	Oct	Nov	Dec	1985
Prevailing wind direction	ENE	WSW	ENE	NE	E	ENE	ENE	E	E	NW	ESE	ENE	ENE
Average wind speed (m s <sup>-1</sup> )	9.2	5.9	6.0	6.6	5.9	6.1	6.0	6.6	7.0	7.5	7.5	7.5	6.8
Maximum wind speed† (m s <sup>-1</sup> )	16	14	22	15	13	14	15	13	18	16	20	19	22
Direction of max. wind† (deg.)	55	280	105	75	115	260	250	105	285	265	115	65	105
Average station pressure (mb)	1017.2	1021.2	1009.4	1020.3	1011.7	1014.6	1016.2	1012.4	1008.5	1010.8	1020.7	1017.1	1014.9
Maximum pressure† (mb)	1031	1040	1028	1035	1030	1027	1029	1024	1031	1029	1037	1042	1042
Minimum pressure† (mb)	993	998	985	1003	995	997	996	998	994	984	982	994	982
Average air temperature (°C)	-22.2	-28.0	-26.0	-23.1	-6.8	-0.7	2.3	-2.9	-2.0	-12.4	-16.8	-22.3	-12.6
Maximum temperature† (°C)	-11	-7	-16	-12	-4	7	12	20	5	4	0	-6	20
Minimum temperature† (°C)	-35	-43	-36	-33	-24	-3	-2	-4	-17	-26	-32	-39	-43
Average dew point temperature (°C)	--	--	--	--	--	--	--	--	-5.5	-15.0	-19.7	-25.5	--
Maximum dew point† temperature (°C)	--	--	--	--	--	--	--	--	2	1	-4	-10	--
Minimum dew point† temperature (°C)	-35	--	--	--	--	--	--	--	-20	-29	-36	-44	--

\*Instrument heights: wind, 17 m; pressure, 9.5 m (MSL); air and dewpoint temperature, 3 m. Wind and temperature instruments are on a tower located 25 m northeast of the main building.

†Maximum and minimum values are hourly averages.

Following the unusually cold winter and spring of 1984, with monthly average temperatures as much as 11°C below normal, 1985 pressure and temperatures were generally close to normal. The average pressure for the year was 1.6 mb above the average for the previous 8 years. The average temperature was only 0.1°C cooler than normal. All frost-point measurements were converted to dewpoint. The hygrometer failed in mid-January and was not returned to service until mid-September.

### Mauna Loa

A description of the MLO site and its general climatology can be found in previous GMCC Summary Reports. The MLO 1985 monthly climate summary is shown in table 2. Keep in mind that for most variables, the average values are not representative of median values because of the bimodal distribution of the wind direction based on the time of day. The effect of the Mauna Loa volcano is to redirect stronger, predominantly easterly or westerly winds aloft, down the slope with a more southerly component. The winds were again predominantly from the south in 1985 as in earlier years (fig. 2). A typical number of spring storms was reported in February and March, but the number of storms and days with above-normal winds speeds in November was unusual. The maximum wind speed and the minimum pressure observed in November set new records for that month. The pressure is also a new low pressure for MLO for the period 1977 to present. The average pressure for 1985 was 1.3 mb below the 8-yr average for the period 1977-1984. Furthermore, the individual monthly averages were all below the comparable monthly averages for this period. Although there were a large number of storms at MLO in 1985 (precipitation amounts of 463 mm, i.e., 2.5 times that in 1984, were reported), it is difficult to believe this pattern would last

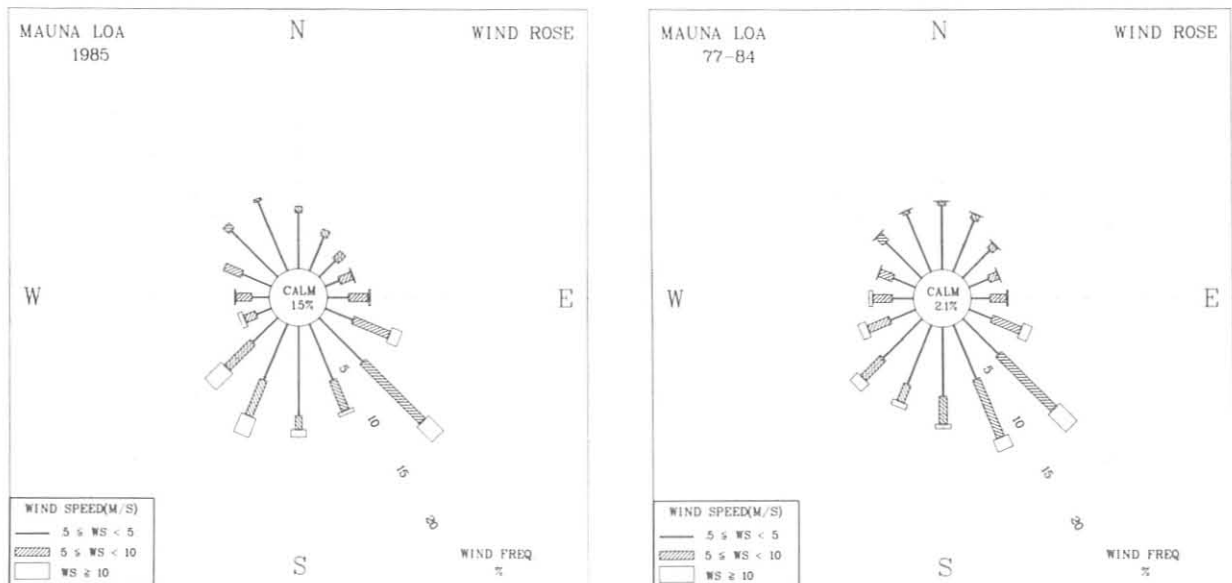


Figure 2.--Wind rose of surface winds for MLO for 1985 (left) and 1977-1984 (right). The distribution of the resultant wind direction and speed are in units of percent occurrence for the year and 8-yr period, respectively. Wind speed is displayed as a function of direction in three speed classes.

Table 2.--MLO 1985 monthly climate summary\*

	Jan	Feb	Mar	Apr	May	Jun	Jul	Aug	Sep	Oct	Nov	Dec	1985
Prevailing wind direction	SW	SE	SE	SW	SSW	SE	SE	SE	SE	SE	SSW	SW	SE
Average wind speed (m s <sup>-1</sup> )	5.6	5.5	5.9	4.8	5.1	3.9	4.6	4.6	5.1	3.8	5.5	5.1	5.0
Maximum wind speed† (m s <sup>-1</sup> )	21	17	16	14	15	12	13	12	13	13	20	14	21
Direction of max. wind† (deg.)	215	190	140	230	130	140	130	130	220	135	190	220	215
Average station pressure (mb)	679.1	678.1	678.6	679.0	679.7	680.6	680.9	681.0	680.0	680.3	678.2	679.6	679.6
Maximum pressure† (mb)	683	682	683	683	684	683	683	685	683	684	682	683	685
Minimum pressure† (mb)	671	674	674	674	674	678	679	679	676	675	668	673	668
Average air temperature (°C)	5.6	4.1	3.2	4.3	6.1	8.2	8.4	8.1	7.9	7.7	6.6	6.0	6.4
Maximum temperature† (°C)	14	16	14	12	15	16	19	18	16	14	14	13	19
Minimum temperature† (°C)	-3	-2	-3	-3	-1	0	2	1	1	1	-3	-3	-3
Average dewpoint temperature (°C)	-14.4	-8.1	-10.1	-6.5	-8.0	-8.6	-5.8	-4.6	-5.3	--	--	-11.2	-8.6
Maximum dewpoint† temperature (°C)	7	5	5	6	7	8	8	9	9	--	--	6	9
Minimum dewpoint† temperature (°C)	-29	-27	-37	-29	-31	-29	-24	-25	-26	--	--	-32	-37
Precipitation (mm)	14	125	140	15	32	2	20	39	3	22	46	5	463

\*Instrument heights: wind, 17 m; pressure, 3399 m (MSL); air and dewpoint temperature, 3 m. Wind and temperature instruments are on a tower located 25 m northeast of the main building.

†Maximum and minimum values are hourly averages.

for 12 months. The other explanation is a measurement error. The pressure sensor is checked against the mercurial barometer at the station twice weekly and the two are in good agreement. Thus, a recheck of the mercurial barometer is necessary before this difference can be resolved. Both air and dewpoint temperatures were within normal ranges for the year.

### Samoa

A comparison of the wind rose for 1985 to that for the preceding 8 years shows a very similar distribution except for the shift in the predominant wind direction to SSW and the higher percentage of wind equal to or greater than 10 m s<sup>-1</sup> (fig. 3). This is a marked change from 1984 when the distribution contained a higher percentage of winds from the northwest. Whereas the long-term average occurrence of wind speeds in the class greater than or equal to 10 m s<sup>-1</sup> is 3%, it was about 8% in 1985. The average wind speed for the year is 5.8 m s<sup>-1</sup>, which is 1.4 m s<sup>-1</sup> above the long-term average. Table 3 shows that new maximum wind speeds were observed for the months of January, May, and September. In January, wind speeds of 10 m s<sup>-1</sup> or greater were reported 12% of the time as compared with a normal of less than 1%. Early in the year, the stronger winds were northerly; later, southeasterly. In February the station staff reported the clearing of underbrush on the southeast slope of Lauagae Ridge, upwind of the sampling tower. This contributed to the increase in occurrence of stronger wind speeds in the trade wind direction. A discussion of the topography and climate of Cape Matatula, Samoa, can be found in previous GMCC Summary Reports. For example, the September occurrence of wind speeds in the ≥10 m s<sup>-1</sup> class was 17% compared with a normal occurrence of only 1%. The winds were from ESE-SSE 78% of the month.

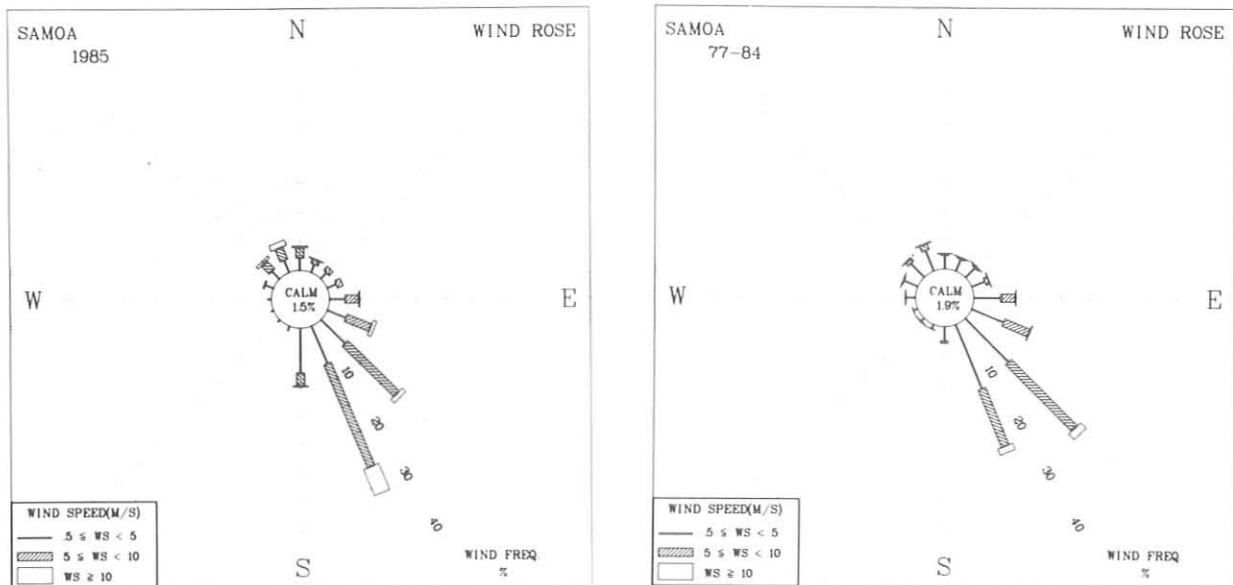


Figure 3.--Wind roses of surface wind for SMO for 1985 (left) and 1977-1984 (right). The distribution of the resultant wind direction and speed are in units of percent occurrence for the year and 8-yr period, respectively. Wind speed is displayed as a function of direction in three speed classes.

Table 3.--SMO 1985 monthly climate summary\*

	Jan	Feb	Mar	Apr	May	Jun	Jul	Aug	Sep	Oct	Nov	Dec	1985
Prevailing wind direction	NW	SE	N	SSE	SSE	SSE	SSE	SSE	SSE	SSE	SSE	NW	SSE
Average wind speed (m s <sup>-1</sup> )	4.9	5.2	5.3	4.9	5.7	5.9	7.0	8.3	7.6	6.1	5.4	3.5	5.8
Maximum wind speed† (m s <sup>-1</sup> )	16	12	13	13	16	13	13	18	13	12	10	9	18
Direction of max. wind† (deg.)	335	350	5	155	155	150	110	160	150	120	160	100	160
Average station pressure (mb)	998.9	999.5	999.0	1000.4	999.9	1001.6	1002.7	1003.0	1002.5	1001.4	999.4	998.9	1000.6
Maximum pressure† (mb)	004	1003	1004	1003	1005	1006	1006	1007	1006	1006	1004	1003	1007
Minimum pressure† (mb)	995	995	993	997	996	995	998	999	999	995	995	995	993
Average air temperature (°C)	27.0	27.2	28.0	27.2	26.8	26.4	26.1	26.2	25.9	26.6	26.6	27.8	26.8
Maximum temperature† (°C)	31	31	31	30	30	29	30	30	29	30	30	32	32
Minimum temperature† (°C)	23	23	25	24	23	23	24	23	23	24	23	23	23
Average dewpoint temperature (°C)	--	--	--	--	--	--	--	--	25.8	26.1	25.9	26.9	26.2
Maximum dewpoint† temperature (°C)	--	--	--	--	--	--	--	--	28	30	29	31	31
Minimum dewpoint† temperature (°C)	--	--	--	--	--	--	--	--	24	23	22	21	21
Precipitation (mm)	355	211	89	246	--	210	207	78	147	347	140	105	2135

\*Instrument heights: wind, 14 m; pressure, 30 m (MSL); air and dewpoint temperature, 9 m. Wind and temperature sensors located atop Lauagae Ridge, a distance 110 m northeast of the station. Pressure sensors are located in the station.  
 †Maximum and minimum values are hourly averages.

The remainder of the meteorological variables measured in 1985 were reasonably close to seasonal and annual norms (table 3). The station pressure of 1000.6 mb was only 0.3 mb above the long-term average. The average air temperature, measured at a height of 9 m above the level section on the east end of Lauagae Ridge, was 26.8°C, just 0.2°C below normal. In the case of both pressure and temperature, the extreme values are within normal limits. Early in 1985 the dewpoint hygrometer was returned to the manufacturer for repair and recalibration. It was returned and installed in September. The average monthly precipitation for the year of 194 mm is only 19 mm below normal.

### South Pole

The most distinguishing feature of the distribution of the surface wind directions at the South Pole station is the large percentage (80%) (wind flow from the NE quadrant (N-E). As shown in fig. 4, the distribution of surface wind with direction is very similar to the distribution for the preceding 8 years. The main difference in 1985 is that the predominant wind direction was grid northerly. For five of the months, the prevailing wind direction was also northerly (table 4). A second feature of the 1985 wind rose is the relatively large number of occurrences of wind speeds equal to or greater than  $10 \text{ m s}^{-1}$ : 8% as compared with 3% in the preceding 8 years. Nonetheless, the average wind speed for the year of  $5.9 \text{ m s}^{-1}$  was only  $0.6 \text{ m s}^{-1}$  greater than the long-term average. New maximum wind speeds were observed for the months of February, June, July, and August. The strongest winds were observed on 25 July at  $17.2 \text{ m s}^{-1}$  in association with a storm that established a new record low station pressure of 641 mb at the GMCC facility. The previous low pressure was 643 mb. Two hours earlier a new record high temperature for July

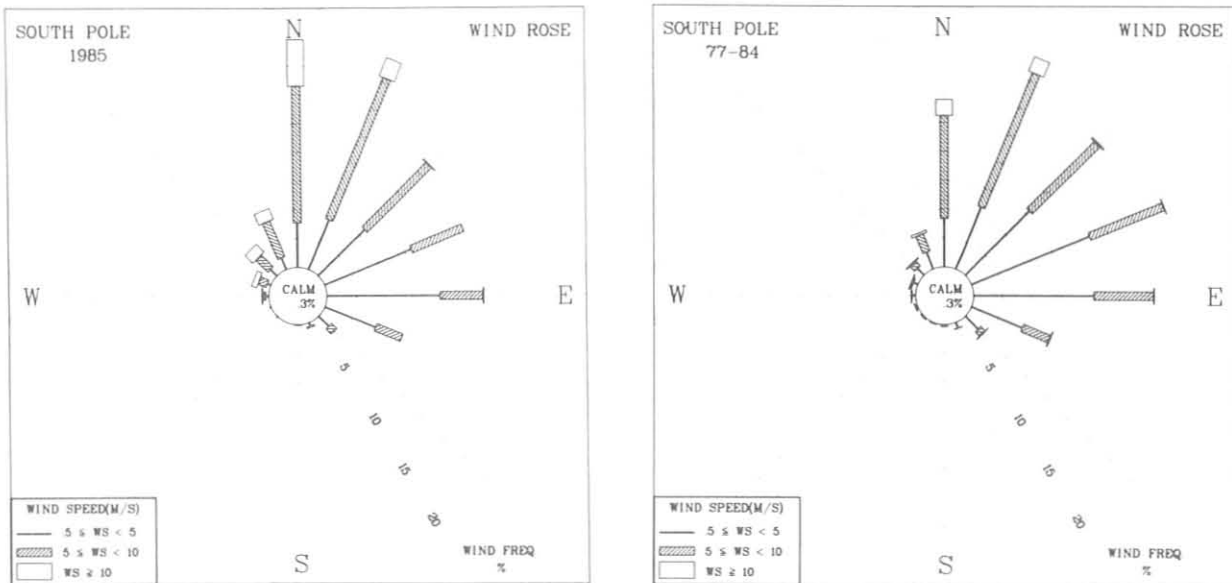


Figure 4.--Wind roses of the surface wind for SPO for 1985 (left) and 1974-1984 (right). The distribution of the resultant wind direction and speed are in units of percent occurrence for the year and 8-year period, respectively. Wind speed is displayed as a function of direction in three speed classes.

Table 4.--SPO 1985 monthly climate summary\*

	Jan	Feb	Mar	Apr	May	Jun	Jul	Aug	Sep	Oct	Nov	Dec	1985
Prevailing wind direction	NNE	N	E	NNE	E	N	NNE	N	NNE	N	E	N	N
Average wind speed (m s <sup>-1</sup> )	4.3	5.0	5.5	6.5	6.3	7.7	7.3	6.2	6.5	6.9	4.7	4.1	5.9
Maximum wind speed† (m s <sup>-1</sup> )	9	14	12	13	13	14	17	17	14	16	11	8	17
Direction of max. wind† (deg.)	20	15	5	15	10	350	5	300	360	15	285	360	5
Average station pressure (mb)	692.2	681.5	682.0	683.2	679.6	680.4	662.7	677.8	672.5	674.9	673.2	682.5	678.5
Maximum pressure† (mb)	699	694	693	699	691	696	674	694	689	692	683	694	699
Minimum pressure† (mb)	684	670	674	669	664	659	641	664	660	655	663	677	641
Average air temperature (°C)	-27.6	-43.2	-53.6	-55.8	-59.4	-53.0	-60.3	-57.8	-60.7	-50.5	-39.0	-29.3	-49.2
Maximum temperature† (°C)	-19	-28	-32	-36	-40	-35	-34	-35	-39	-33	-30	-22	-19
Minimum temperature† (°C)	-33	-52	-66	-72	-76	-70	-76	-75	-74	-67	-46	-36	-76

\*Instrument heights: wind, 12 m; pressure, 2841 m (MSL); air temperature, 2 m. The anemometer and thermometer are located on a tower 100 m grid ESE of CAF. Pressure measurements are made inside CAF.

†Maximum and minimum values are hourly averages.

was set at  $-34.1^{\circ}\text{C}$ . The average pressure for the year was 678.5 mb, which is 0.9 mb above the long-term average. The average temperature for the year was  $-49.2^{\circ}\text{C}$ , less than  $1^{\circ}\text{C}$  above the climatological average. The  $-53^{\circ}\text{C}$  average for June made it one of the warmest on record and a  $-35^{\circ}\text{C}$  maximum was  $3^{\circ}\text{C}$  above the previous maximum. Because of a series of equipment problems, no reliable frost-point measurements were made in 1985.

#### DATA MANAGEMENT

Between August and November 1984, CAMS units were installed at each of the GMCC stations, replacing the aging ICDAS. Details of this changeover can be found in Summary Report No. 13 (Nickerson, 1986). Most of the difficulties encountered with the hardware were resolved by the end of the year. The one persistent problem was the battery backup to the CAMS memory. As a rule, the charging circuit did not operate properly, causing the boards to fail. By the end of the year, the memory at two stations had been replaced with ZRAM, which does not use batteries. The remainder were changed early in 1986. This is the only significant hardware change that has been required to date. The CAMS that operates the  $\text{CO}_2$  analyzer is described in Herbert et al. (1986).

Table 5 gives the number of hours each CAMS was inoperative in 1985. A total of 926 hours of downtime was reported, slightly over 1% of the CPU hours in the year. By comparison, the four ICDAS units in continuous operation averaged 1556 hours of downtime per year between 1980 and 1984. Of significance is the very low number of hours of downtime at Samoa and the relatively

large number at the South Pole. This comparison points out the importance of having a reliable power system. The majority of downtime is caused by power outages or brownouts. The CAMS units in Samoa use power from the solar-powered uninterruptible power supply. At SPO, the number of power failures and brownouts has increased dramatically in the past few years. Although the average number of hours of downtime in the worst case was 83 hours at SPO, this is considerably less than the average reported for ICDAS for a comparable period.

Table 5.--GMCC CAMS downtime\* for 1985 (h)

Program	BRW	MLO	SMO	SPO	Total
ASR	145	112	21	101	379
CO2	34	65	6	131	236
MO3	25	83	65	138	311
Total	204	360	92	370	926

\*Downtime is the number of hours in the year for which the data tally indicates less than 80% of the expected number of data points for that hour.

## 6.2 Special Projects

### ATMOSPHERIC TRAJECTORIES

Descriptions of various atmospheric trajectory programs developed within GMCC have appeared in previous summary reports (Bodhaine and Harris, 1982, pp. 71-74; Harris and Bodhaine, 1983, pp. 67-75; Harris and Nickerson, 1984, pp. 73-80; Nickerson, 1986, pp. 71-75). This section describes new development of the trajectory programs that permitted trajectory computation over the southern polar regions and a case study of seasalt transport to SPO.

Table 6 lists most of the trajectories computed during 1985. These were provided for atmospheric researchers within GMCC and ARL as well as scientists at numerous universities and research institutes of foreign governments affiliated with GMCC.

Input data for the Northern Hemisphere model (65 x 65 grids) consist of E-W and N-S wind components from 1975 to the present. Data for the global model (2.5° grid) begin 2 years later in 1977 and extend until the present. Beginning in January 1986, access to the input data will be improved. Data will be available on a monthly rather than yearly basis so that trajectories can be produced in a more timely manner. Beginning March 1986, the 70- and 50-mb levels will be added to the input data set to make 12 mandatory levels of meteorological data (from 1000 to 50 mb) available for trajectory computation.

Table 6.--GMCC trajectories calculated in 1985

Destination	Date
Amsterdam Island	1984
Bermuda	1984
Western Mediterranean	1984
Katherine, Australia	1984
Palmer Station	Oct 1983
Arctic locations	Jan 1984, Jul 1985, Feb-Apr 1984, Jun-Jul 1984
SPO	Summer 1979, 1982
Antarctic locations	1984
Equatorial Pacific Cruise	1984
Poker Flat, AK	1984
Ascension Island	1983, 1984
SMO	1984
MLO	1984
BRW	1984
Miami	1984
McMurdo	1984
Charlottesville, VA	Jul, Dec 1977
Okushiri Island	Nov, Dec 1984
Urumqui, China	Aug 1980
Beijing, China	Apr 1980
Niigata, Japan	Apr 1980
Atlantic locations	1978-1979
Tallahassee, FL	Sep, Oct 1984
WATOX locations	Apr 1984
Korolev Cruise	1983
Whiteface Mountain, NY	Summer 1985

A new form was developed for plots of isentropic trajectories. Figure 5 shows tables beside the map with the isentropic trajectories. These tables give the time of arrival, 0000 or 1200 GMT, and the height, pressure, and temperature for each day back along the trajectories. The tables aid in the interpretation of isentropic trajectories, providing information about vertical motion.

The first GMCC trajectories for the southern polar region were produced this year after overcoming a computational problem. The problem relates to the method of converting the wind displacement from meters to degrees of latitude and longitude. In the tropics and midlatitudes, the displacement formulas used for the 2.5° global data are

$$\begin{aligned}
 DLAT &= -SV * 10800./111198.4 \\
 DLON &= -SU * 10800./((111198.4 * \cos(\text{ABS}(TSLATO * .017453))), \quad (1)
 \end{aligned}$$

where DLAT and DLON are the displacements in degrees of latitude and longitude respectively, SU and SV are the E-W and N-S components respectively of the wind displacement in meters, and TSLATO is the latitude of the start point of the trajectory segment.

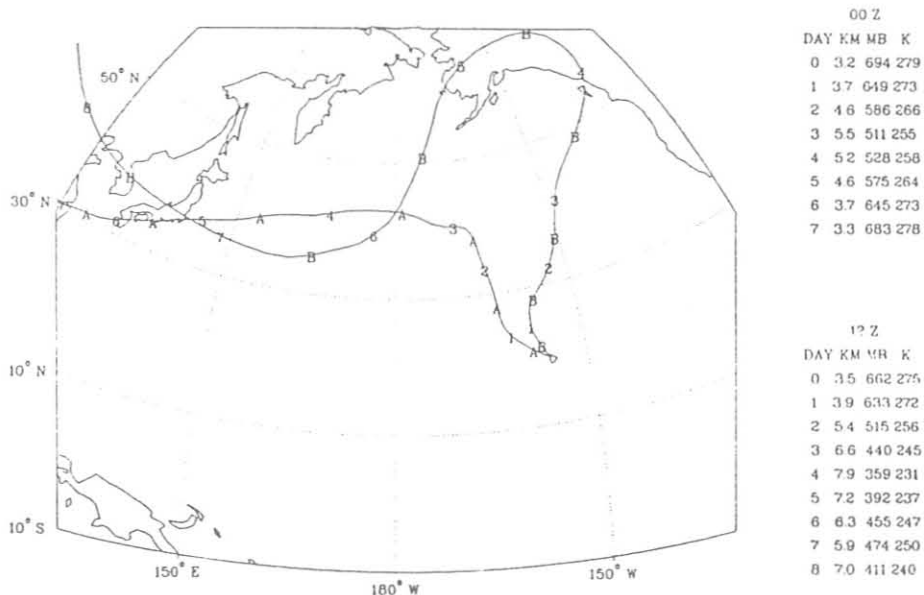


Figure 5.--MLO isentropic trajectories arriving 25 April 1979 on the 310-K surface at (A) 0000 GMT and (B) 1200 GMT.

In polar regions, the cosine of the latitude in the denominator in (1) can cause invalid results. For this reason we have reverted to the 65 x 65 stereographic x, y grid for Arctic trajectories, but data in this form are not provided for the Southern Hemisphere. The solution for the Southern Hemisphere polar regions is to transform each 3-h latitude and longitude along the trajectory to an x, y point on a similar 65 x 65 grid overlaying a stereographic projection of the Southern Hemisphere. The 3-h wind displacement is then converted from meters to x, y units and added to the start point to get an end point in x, y units. This end point is finally transformed to latitude and longitude.

Isentropic trajectories to SPO were produced for a study of seasalt events during the austral winter of 1982. Detailed results are reported in Bodhaine et al. (1986). These events are seen as peaks in the plot of hourly averages of aerosol scattering extinction at 550 nm (fig. 6, upper), which correspond to peaks in elemental Na (fig. 6, lower). The Na data were obtained by PIXE analysis of Nuclepore filter streakers with an 8-h time resolution. Figures 7 and 8 show trajectories arriving at SPO on 10 and 11 September 1982, during a strong seasalt event. The tracks indicate rapid transport (1-2 days) from the vicinity of the Ross Sea. The 500-mb heights (fig. 9) for 10 September 1982 at 1200 GMT, show a strong low to grid south of SPO. This well-developed storm produced winds as strong as 40 kt at 500 mb near SPO. The position of the low was fairly stationary throughout the seasalt event. It appears that it is strong winter storms such as this that provide the transport of Na from the coast to SPO. During austral summer these events are rare.

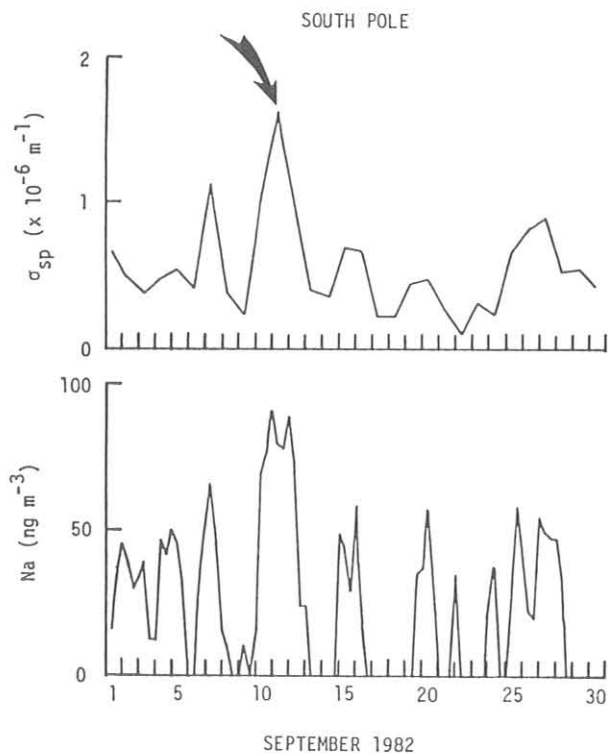


Figure 6.--(Upper) Hourly averages of aerosol scattering extinction at the 550-nm wavelength, September 1982, SPO. (Lower) Elemental Na, September 1982, SPO.

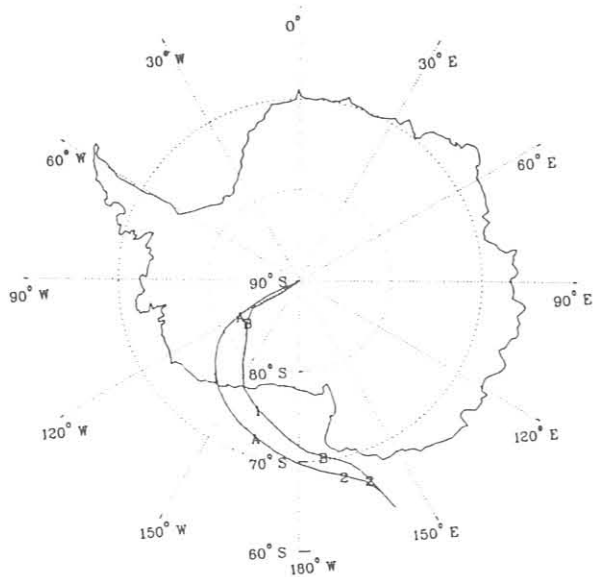


Figure 7.--SPO isentropic trajectories arriving 10 September 1982 on the 270-K surface at (A) 0000 GMT and (B) 1200 GMT.

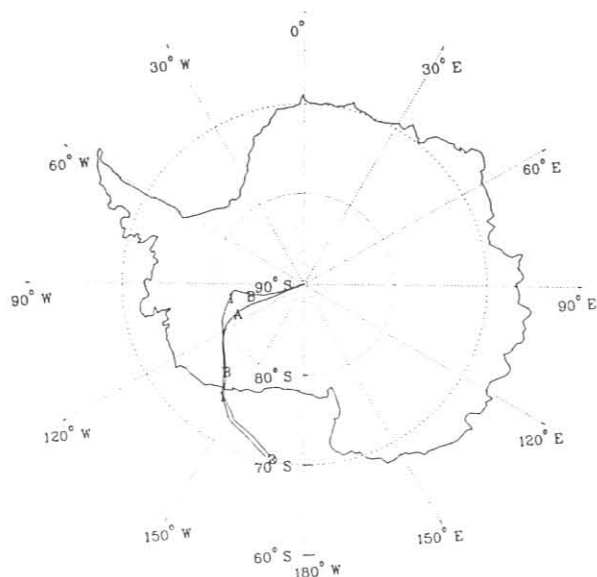


Figure 8.--SPO isentropic trajectories arriving 11 September 1982 on the 270-K surface at (A) 0000 GMT and (B) 1200 GMT.

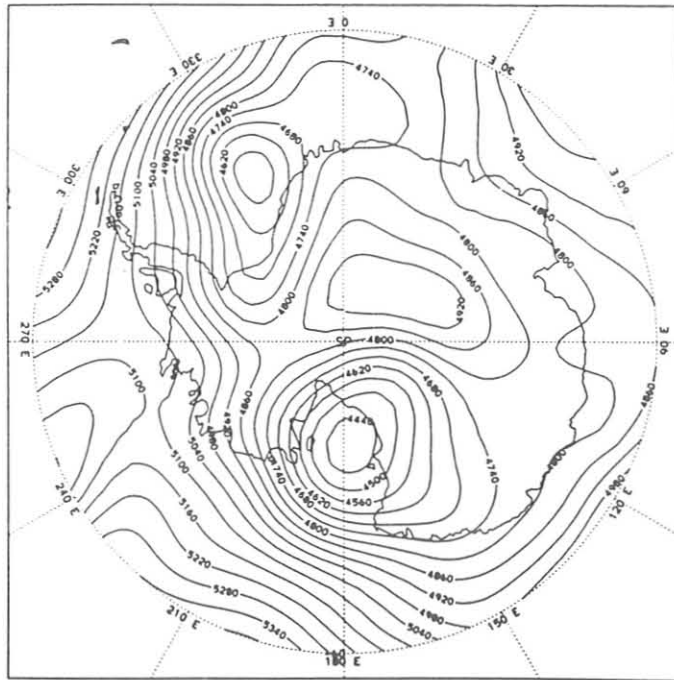


Figure 9.--Contours of 500-mb heights over Antarctica on 10 September 1982 at 1200 GMT.

### 6.3 References

- Bodhaine, B. A., and J. M. Harris (Eds.), 1982. Geophysical Monitoring for Climatic Change, No. 10: Summary Report 1981. NOAA Environmental Research Laboratories, Boulder, CO, 158 pp.
- Bodhaine, B. A., J. J. DeLuisi, J. M. Harris, P. Houmère, and S. Bauman, 1986. Aerosol measurements at the South Pole. Tellus (in press).
- DeLuisi, J. J. (Ed.), 1981. Geophysical Monitoring for Climatic Change, No. 9: Summary Report 1980. NOAA Environmental Research Laboratories, Boulder, CO, 163 pp.
- Harris, J. M., and B. A. Bodhaine (Eds.), 1983. Geophysical Monitoring for Climatic Change, No. 11: Summary Report 1982. NOAA Environmental Research Laboratories, Boulder, CO, 160 pp.
- Harris, J. M., and E. C. Nickerson (Eds.), 1984. Geophysical Monitoring for Climatic Change, No. 12: Summary Report 1983. NOAA Environmental Research Laboratories, Boulder, CO, 184 pp.
- Herbert, G. A., E. R. Green, J. M. Harris, G. L. Koenig, and K. W. Thaut, 1986. Control and monitoring instrumentation for the continuous measurement of atmospheric CO<sub>2</sub> and meteorological variables. Journal of Atmospheric and Oceanic Technology 3:414-421.
- Nickerson, E. C. (Ed.), 1986. Geophysical Monitoring for Climatic Change, No. 13: Summary Report 1984. NOAA Environmental Research Laboratories, Boulder, CO 111 pp.

## 7. AIR QUALITY GROUP

### 7.1 Continuing Programs

#### NATIONAL ACID PRECIPITATION ASSESSMENT PROGRAM

NAPAP is sponsored by the Interagency Task Force on Acid Precipitation. It was formed by Congress to address the complex issues associated with acid deposition in the United States. The Air Quality Group continued its participation in NAPAP during 1985.

This program was divided into task groups entitled (A) Natural Sources, (B) Man-Made Sources, (C) Atmospheric Processes, and (D) Deposition Monitoring. The Air Quality Group contributed to Task Groups A and C during 1985.

#### Contribution of Gulf Area Natural Sulfur to the North American Sulfur Budget

To assess the sulfur contribution of the Gulf of Mexico, possibly one of the major natural sources to the North American sulfur budget, a series of air sampling flights were conducted over the Gulf. The data, collected during late summer of 1984, revealed that, within the experimental uncertainty, the carbonyl sulfide (COS) concentration was nearly constant at  $440 \pm 35$  pptv. The dimethyl sulfide (DMS) level varied significantly, was not detected above the boundary layer, and had an average concentration of  $27 \pm 30$  pptv or  $7 \pm 3$  pptv during onshore or offshore flow, respectively.

As a result of its large atmospheric emission rate and its short atmospheric life time, DMS is one of the major sources for atmospheric sulfate aerosols and, therefore, for natural acidification of precipitation. On the basis of our data, the biogenic annual emission from the Gulf can be estimated to be about  $0.1 \text{ Tg (S) yr}^{-1}$ . The actual amount of sulfur from the Gulf area transported into North America is a function of two major parameters: the atmospheric lifetime of the sulfur compounds and the volume of the air mass entering through the corridor between Texas and Florida. The only removal mechanisms for  $\text{SO}_4^{2-}$  in the troposphere are wet and dry deposition. The rates of these processes can vary significantly according to the prevailing meteorological conditions, and therefore, only upper and lower limit estimates for these variables can be made. Table 1 summarizes the estimates made by the Air Quality Group.

The results of this study indicate that the potential contribution of biogenic sulfur to the overall North American sulfur budget is minimal (between 0.25% and 1.5%). Cloud water pH's evaluated from the lower limit estimate (3.7 to 5.1; see Luria et al., 1986) are identical with those calculated by Charlson and Rodhe (1982) from theoretical considerations. The upper limit estimate of natural sulfur transport into the continent may cause acidification of rainwater.

Table 1.--Upper and lower limit estimates of natural sulfur entering North America through the Texas-Florida corridor

Parameter	Upper limit estimate	Lower limit estimate
Boundary layer depth, m	1000	1000
Texas-Florida corridor width, m	$1.57 \times 10^6$	$1.57 \times 10^6$
Wind speed (IBL), $\text{m s}^{-1}$	5	5
Southerly airflow (IBL), $\% \text{ yr}^{-1}$	50	50
Annual volume of air mass, $\text{m}^3 \text{ yr}^{-1}$	$1.24 \times 10^{17}$	$1.24 \times 10^{17}$
$\text{SO}_4^{2-}$ atmospheric lifetime $(k_w+k_d), \text{h}^*$	530	530
Average $\{\text{SO}_4^{2-}\}$ , $\mu\text{g m}^{-3}$	6.1	1.0
Average $\text{SO}_4^{2-}$ flux, $\mu\text{g m}^{-2}\text{s}^{-1}$	30.5	5.0
Annual sulfur flux, Tg (S) $\text{yr}^{-1}$	0.251	0.041

\* $k_w$  and  $k_d$  represent wet and dry deposition in terms of first-order rate coefficients.

#### Computer Simulation of the Oxidation and Removal of Natural Sulfur Compounds in the Marine Atmosphere

To test our understanding of the natural sulfur cycle in the marine atmosphere, and its contribution to the atmospheric sulfur burden, a MPBL chemistry model was developed. The major focus of this study was a comparison between model predictions based on laboratory rate measurements and actual field data. Simulations were performed for clean-air conditions and for several polluted air scenarios. Figure 1 presents a schematic illustration of the chemistry model. A description of the model is given in Luria and Meagher (1986).

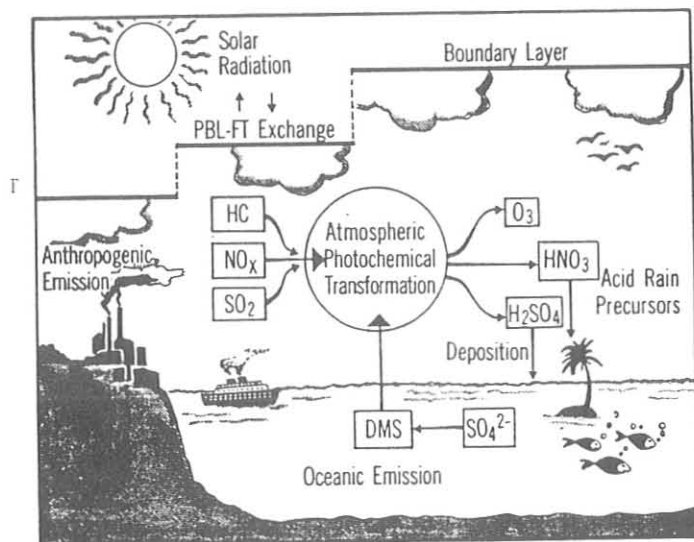


Figure 1.--A schematic representation of the MPBL chemistry model.

It is generally accepted that DMS is the most important reduced sulfur species in the marine atmosphere. Its concentration is determined by the balance of oceanic emission and atmospheric removal. Since DMS concentration data are available, the model was used to estimate the oceanic emission rate required to sustain the observed average level of 27 ppt. To support this average concentration an oceanic emission rate of  $60 \mu\text{g (S) m}^{-2} \text{ day}^{-1}$  was required. This emission estimate is lower than the value of  $290 \mu\text{g (S) m}^{-2} \text{ day}^{-1}$  reported by Andreae and Raemdonck (1983) but is in good agreement with the work of Gammon and Bates (1985) who reported an emission rate of  $80 \mu\text{g (S) m}^{-2} \text{ day}^{-1}$ . As expected, the model predicted a significant diurnal cycle for DMS, with levels varying by a factor of 4 from the daytime low to the nighttime high. Andreae and Raemdonck (1983) reported a similar diurnal variation, albeit with a lower amplitude (max./min. = 1.6). Plots of the model predictions for DMS and other sulfur species are presented in fig. 2.

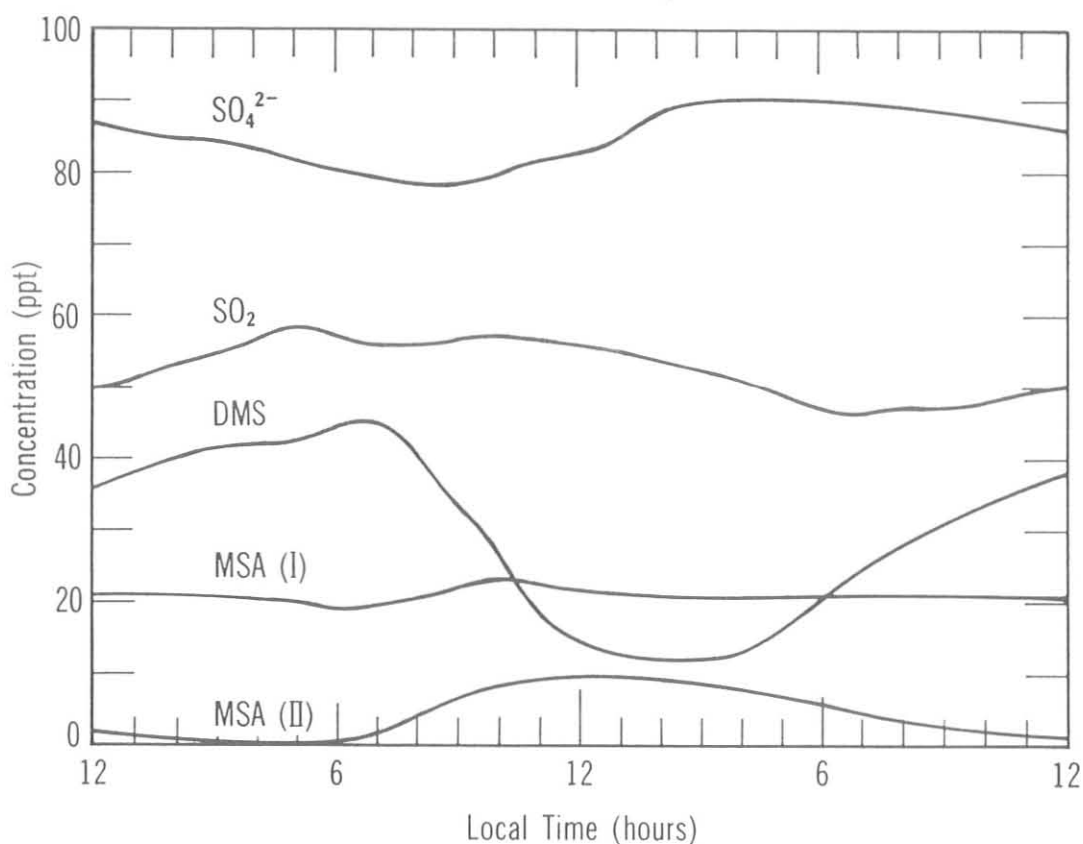


Figure 2.--The model-predicted concentrations of DMS and otherspecies as a function of time.

The photochemical model developed was found to reproduce accurately the major features that characterize the sulfur cycle in the marine atmosphere. In particular, the model predicted  $\text{O}_3$ ,  $\text{SO}_2$ ,  $\text{SO}_4^{2-}$ , and  $\text{NO}_3^-$  levels in good agreement with field observations. The DMS emission rate necessary to reproduce observed marine concentrations was found to be consistent with other estimates. The model was unable to reproduce reported methane sulfonic acid

(MSA) levels without the inclusion of an unreasonably high removal rate. The atmospheric fate of MSA requires additional research before this inconsistency can be resolved.

Diurnal fluctuation in DMS was predicted to be greater than that observed. The model assumes a constant DMS emission rate throughout the day, but changes in ocean surface temperature, wind speed, and atmospheric stability between day and night may serve to reduce the amplitude of the diurnal cycle. The model confirms the observation of relatively low levels of DMS in coastal areas influenced by anthropogenic emissions. However, under certain specific pollution conditions, the model predicted a short-term abatement of the DMS removal reactions.

#### Aerosol Enhancement by Cloud Evaporation

Clouds can dramatically alter the aerosol distribution in their environments. It is well known that nucleation- and accumulation-mode aerosols may be removed by cloud droplet nucleation and scavenging. As well, coarse-mode particles may be removed by precipitation scavenging. Researchers are only now beginning to explore how clouds may release aerosols as they evaporate. In this study the results of some preliminary measurements made atop Whiteface Mountain, NY, during two cloud evaporation events are presented.

An ASASP was used to sense aerosol particles in the diameter range 0.1 to 3  $\mu\text{m}$ . The ASASP probe consists of a laser imaging mechanism that examines a known sample area as particles pass through it. Its operational characteristics are described by Pinnick and Auvermann (1979) and Garvey et al. (1984). It was operated continuously during the sampling period, and complete spectra were recorded at 5-s intervals.

A stratiform cloud formed atop Whiteface Mountain during the night of 3 August 1983 (0200 GMT, 4 August 1983). It dissipated at about 0410 GMT only to reform at about 0515 GMT. The ASASP-derived particle spectrum concentration and mass prior to the onset of the cloud were  $3486 \text{ cm}^{-3}$  and  $31 \mu\text{g m}^{-3}$ , characteristic of a polluted air mass.

The 5-min-average particle spectra obtained using the ASASP before cloud formation and after cloud demise were compared. The differences between a particle spectrum measured between 0100 and 0105 GMT (before cloud formation) and particle spectra made during cloud evaporation are shown in fig. 3. They are plotted in a log difference vs. log diameter format. The ordinate is the decimal logarithm of the difference between the spectrum at the times indicated and the spectrum measured prior to cloud formation. The abscissa is the decimal logarithm of particle diameter.

The difference spectrum valid between 0345 and 0350 GMT was made prior to evaporation of the cloud. It shows that a marked depletion in the aerosol had taken place at diameters less than about 0.4  $\mu\text{m}$ . This effect can be qualitatively explained as a combination of initial nucleation and in-cloud scavenging.

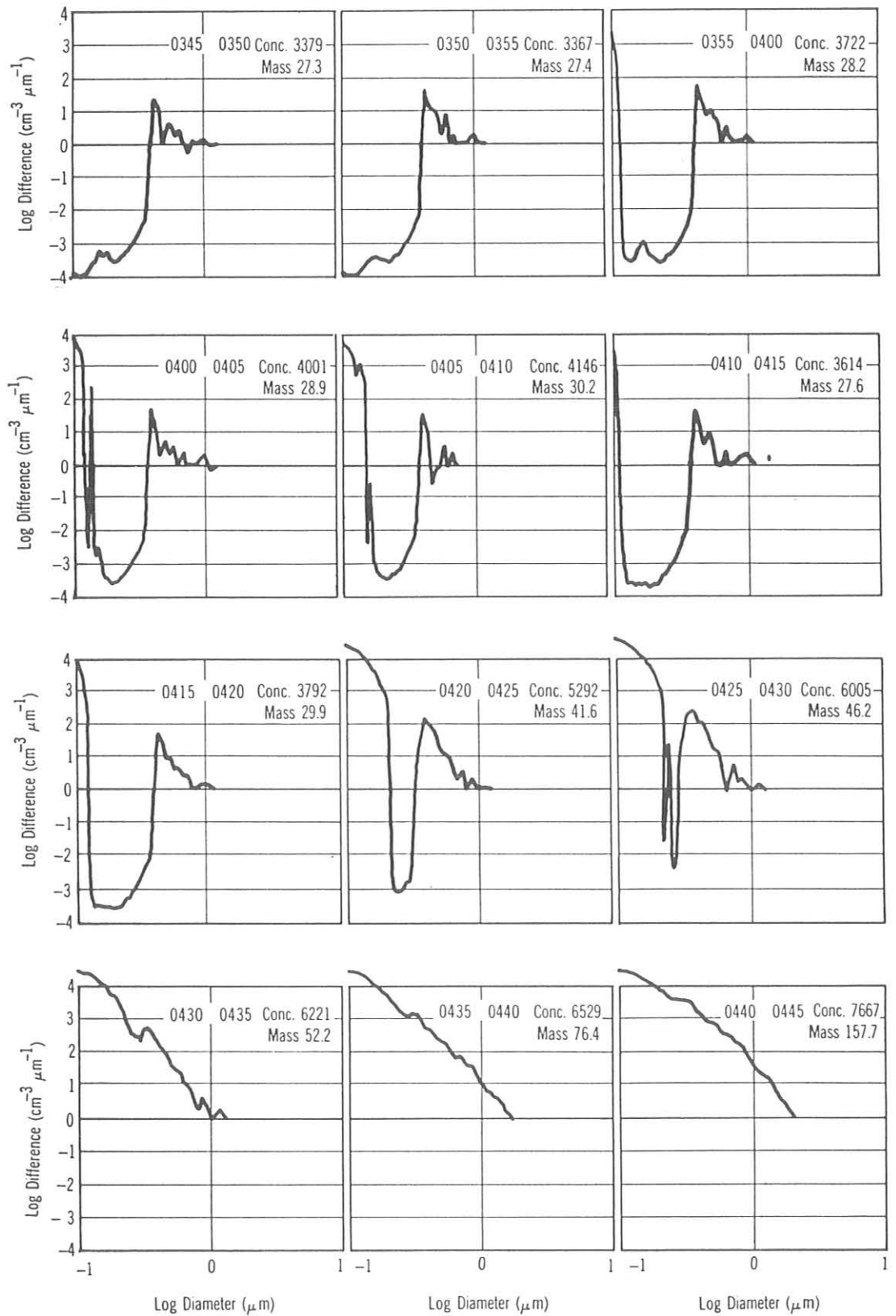


Figure 3.--The difference spectra between a particle spectrum measured before cloud formation and twelve 5-min mean spectra measured during cloud evaporation.

The difference spectrum valid between 0350 and 0355 GMT demonstrates the regularity of the depletion while the cloud was still present. Then, between 0355 and 0400 GMT, the cloud began to evaporate. Immediately, the difference spectrum shows that a significant excess of particles appeared at the smallest detectable sizes. Total particle concentration also increased, but total particle mass was relatively unaffected.

The difference spectrum valid between 0400 and 0405 GMT shows that significant numbers of new particles continued to be detected. The new particles also seemed to be creating excesses at diameters up to 0.4  $\mu\text{m}$ . The diameter range above 0.4  $\mu\text{m}$  remained relatively unaffected. The spectral differences remained relatively unchanged until 0420-0425 GMT. At that time, excess particles began to fill in the accumulation mode, which had been severely depleted during the life of the cloud. Significant numbers of new particles appeared at the larger sizes as well. The combination of new particles at small sizes and those at larger sizes were filling in the depleted accumulation mode completely. This filling-in process was complete by 0430-0435 GMT. Two 5-min averages after this demonstrate the stability of this new enhanced aerosol distribution.

We interpreted the facts presented in these distributions in the following way. Before the onset of evaporation, the nucleation-mode and accumulation-mode aerosol had been depleted by cloud droplet nucleation and in-cloud scavenging. As the cloud began to evaporate, a large number of new particles were created at sizes below our detection limits (0.1  $\mu\text{m}$  diameter). These particles grew rapidly by means of coagulation to fill in and later enhance the accumulation mode. Meanwhile, more new particles were continuously forming to replenish the supply lost through coagulation. As evaporation became complete, new larger particles began to appear as cloud droplets released the remaining particles contained within them. The final distribution was composed of the excess larger particles released by the droplets, and the new small particles created during the evaporation event.

#### Thunderstorms: An Important Mechanism in the Transport of Air Pollutants

Convection, as a means of vertical transport, is incompletely understood, although it is a key mechanism of circulation within the troposphere. The observations summarized here and presented by Dickerson et al. (1986) present the first unequivocal data in support of convective transport of photochemically active trace gases in a cumulonimbus cloud system.

Several research aircraft were outfitted with instruments to measure meteorological parameters and the trace gases CO, O<sub>3</sub>, NMHC, and reactive nitrogen compounds. For high-altitude work, a Sabreliner (twin-engine jet), operated by NCAR, was used. For the midtroposphere and PBL, two propeller-driven aircraft, the NOAA King Air and the Brookhaven Queen Air, were used. The flights were conducted in collaboration with the NOAA PRE-STORM project, which supplied radar, satellite, balloon soundings, and standard meteorological measurements. PRE-STORM was conducted in the Central Plains of the United States during May and June of 1985.

The gases CO and O<sub>3</sub> were selected as primary tracers of air motion through clouds because they are relatively insoluble in water, rapidly detected, and have atmospheric residence times that are much longer than the

detected, and have atmospheric residence times that are much longer than the lifetime of a thunderstorm. These gases generally demonstrate distinctive tropospheric altitude profiles. CO is produced primarily by ground sources and destroyed throughout the troposphere, and thus generally decreases with altitude. O<sub>3</sub> is produced primarily in the stratosphere and destroyed at the Earth's surface, and thus generally increases with altitude. Any deviation from environmental profiles of these gases within the cloud during the thunderstorm is presumed to be due to convection.

Late on the night of 14 June 1985, a large mass of cold, dry air moved south over warm, moist air from the Gulf of Mexico. The result was an intense band of thunderstorms stretching from Amarillo to Chicago. At dawn on 15 June the aircraft flew toward the expected inflow and outflow regions of the cumulonimbus.

As the Sabreliner climbed in clear air, the mixing ratio of CO fell smoothly (fig. 4) until the cumulonimbus anvil was penetrated at 10 km. Within seconds, the CO level rose sharply. Soon it more than doubled, reaching concentrations rarely observed at this altitude. The in-cloud CO concentration was higher than that of the air outside the cloud at all altitudes sampled. The maximum CO level and the core of the outflow appeared to be at about 10 km.

The downdraft of the thunderstorm can be clearly identified in fig. 4. There is a local minimum in CO at about 2 km. The vertical air motion in this region was about  $-1 \text{ m s}^{-1}$ . As we expect, the downdraft carries clean, dry air from aloft down to the lower troposphere.

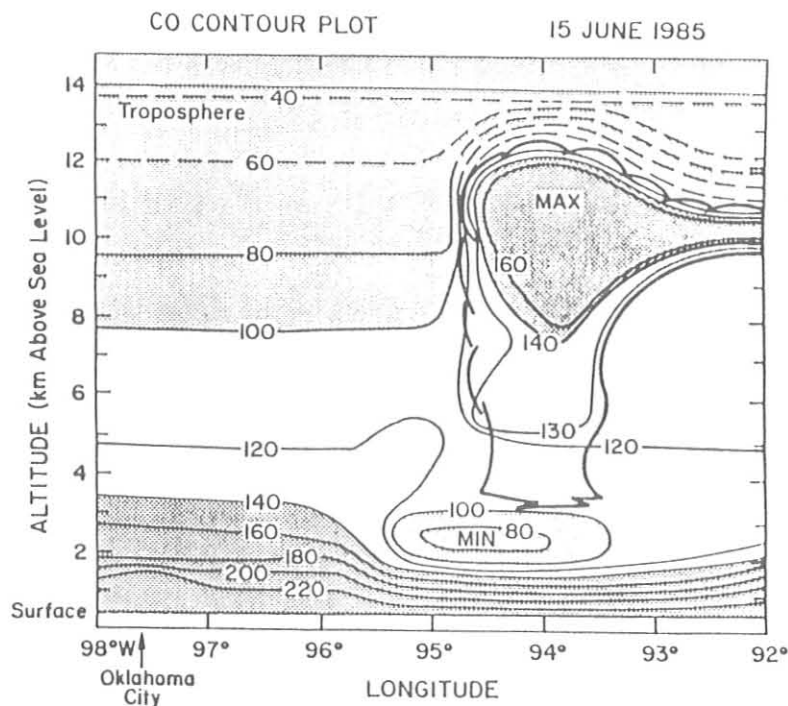


Figure 4.--The two-dimensional CO field (ppbv) measured using the research aircraft on 15 June 1985.

Dickerson et al. (1986) presented the first observations of trace gases measured in a thunderstorm. The results clearly indicate that convective processes such as occur during thunderstorms can be an important mechanism in the vertical transport of air pollutants.

Sulfur Dioxide Flux Measurement over the Western Atlantic Ocean

During the winter months of 1985, aircraft sampling flights were performed by the Air Quality Group over the Western Atlantic Ocean and in the vicinity of Bermuda. One purpose of these flights, which were carried out as part of WATOX, was to determine the eastbound flux of anthropogenic emissions from the North American continent to the Atlantic Ocean atmosphere. The results, summarized here and presented by Luria et al. (1987), represent our continuous measurements of gaseous sulfur and the evaluation of these data to estimate the eastbound sulfur dioxide flux. Sulfur dioxide was measured with a Meloy 285 sulfur analyzer with an FPD.

Galloway et al. (1984) estimated the flux of sulfur and nitrogen compounds eastward from North America using surface SO<sub>2</sub> measurements, climatologically derived wind speeds, and the coastal divisions established by Whelpdale et al. (1984). They estimated fluxes for eight coastal segments from the northern end of Newfoundland, Canada, to the southern tip of Florida. According to their estimates, the total annual SO<sub>2</sub> flux was 1.75 Tg (S) yr<sup>-1</sup>, of which 0.30, 0.82, and 0.37 Tg (S) yr<sup>-1</sup> were transported eastbound from coastal segments 4, 5, and 6. The availability, for the first time, of in situ SO<sub>2</sub> and wind speed data encouraged us to repeat these calculations. They are based on a limited data set and therefore must be considered as a preliminary estimate.

Since our study was performed within coastal segment 6, it was possible to compare our results with the estimates of Galloway et al. (1984). Our results are given in table 2. Our values and the estimates of Galloway et al. (1984) differ by a factor of 2.7. Nevertheless, the two estimates should be considered to be in good agreement, taking into account the different approaches.

Table 2.--Parameters used in estimation of the annual SO<sub>2</sub> flux eastward from the North American coastal segment 6

Parameter	Average	Maximum
time (1 year)	$3.15 \times 10^7$ s	$3.15 \times 10^7$ s
a*	82.0	161.0
b*	$1.44 \times 10^{-3}$	$1.48 \times 10^{-3}$
(r <sup>2</sup> )*	0.54	0.55
β†	0.69	0.69
Δx†	$8.4 \times 10^5$ m	$8.4 \times 10^5$ m
flux (SO <sub>2</sub> )	1.01 tg (S) yr <sup>-1</sup>	2.04 tg (S) yr <sup>-1</sup>

\*Regression and correlation coefficients for exponential fit.  
 †After Whelpdale et al. (1984).

It is obvious that more measurements, with improved analytical methods, which would be carried out throughout the year and at the different coastal segments, are needed for accurate flux estimations. However, this work has demonstrated that a rough agreement between climatological estimates and field observations can be obtained.

## AIRCRAFT INSTRUMENTS

### Aircraft Instruments and Their Capabilities

During 1983, the Air Quality Group acquired the use of a Beechcraft King Air aircraft from the National Park Service (NPS). Ownership of the aircraft has since transferred from the NPS to NOAA's Office of Aircraft Operations. The Air Quality Group has engaged in an ongoing effort to install and upgrade a scientific instrument package aboard the aircraft. The package consists of a suite of scientific instruments, a power distribution system to supply power to them, and a data acquisition system to digitize and record the incoming scientific data for later analysis.

Table 3 outlines the scientific instruments currently aboard the aircraft and gives their accuracies, response times, and precisions. In addition to the instruments outlined in table 3, several optical array probes are available for atmospheric aerosol measurements. They include an ASASP (0.1 to 3  $\mu\text{m}$ ), an FSSP (0.5 to 45  $\mu\text{m}$ ) and a two-dimensional probe (25 to 800  $\mu\text{m}$ ). These probes can provide aerosol particle size and shape information within their respective ranges.

Table 3.--Scientific instruments available aboard the King Air

Parameter	Units	Accuracy	Response	Precision	Description
Photometer	$\text{W m}^{-2}$	--	10 $\mu\text{s}$	--	Short wave sun photometer
TECO $\text{SO}_2$	ppbv	1 ppbv	60 s	0.1 ppbv	Pulsed fluorescence
Dynamic pressure	mb	0.1 mb	1 s	0.1 mb	Pitot tube
Temperature	$^{\circ}\text{C}$	0.1 $^{\circ}\text{C}$	1 s	0.1 $^{\circ}\text{C}$	Rosemount wire
Dew point	$^{\circ}\text{C}$	1.0 $^{\circ}\text{C}$	5 s	0.1 $^{\circ}\text{C}$	General Eastern cooled mirror
Air flow	lpm	0.1 lpm	1 s	0.1 lpm	Kurz meter (3)
Pressure	mb	0.5 mb	1 s	0.1 mb	Pitot tube
Meloy $\text{SO}_2$	ppbv	2 ppbv	10 s	0.1 ppbv	Photometric
TECO $\text{O}_3$	ppbv	0 ppbv	10 s	0.1 ppbv	Flame photometric
Position	degrees	$\pm 200$ m	1 s	--	Loran C
True air speed	$\text{m s}^{-1}$	$1 \text{ m s}^{-1}$	1 s	$0.1 \text{ m s}^{-1}$	Computed
Heading	degrees	1 deg	1 s	1 deg	Magnetic compass
Wind direction	degrees	1 deg	60 s	0.1 deg	Computed
Wind speed	$\text{m s}^{-1}$	$1 \text{ m s}^{-1}$	60 s	$0.1 \text{ m s}^{-1}$	Computed

## The Efficiency of an Airborne Cloud Water Separator

Numerous investigators have examined the chemistry and physics of dry atmospheric aerosol and water in clouds and precipitation. One problem to be addressed was the scavenging of atmospheric aerosol by cloud droplets. In order to examine both the cloud water and the interstitial aerosol, a combination cloud water separator and cloud water collector was developed.

To test the efficiency of the cloud water separator, we assembled a laboratory apparatus consisting of (1) a high-volume air blower ( $100,000 \text{ cm}^3 \text{ s}^{-1}$ ), (2) a hot-wire anemometer, (3) an ASASP aerosol sampler, and (4) an FSSP cloud droplet spectrometer.

The ambient aerosol distribution in the laboratory was measured to establish a control. Then, the ambient air was drawn through the separator at various airspeeds and the resultant aerosol distributions were measured. A comparison between these distributions and the control was made.

Figure 5 presents these comparisons. Each plot is the percent difference between the control distribution and the distribution sampled at a given airspeed after exiting the separator. The top left plot indicates that all particles up to  $3 \mu\text{m}$  in diameter passed through the cyclone at  $8 \text{ m s}^{-1}$ . The middle left plot shows that particles with diameters greater than  $1.2 \mu\text{m}$  were reduced in number by 20% or more after passing through the separator at  $13 \text{ m s}^{-1}$ . This effect progresses to smaller and smaller diameters at the faster airspeeds.

A more complete description of this work is given in Boatman and Wellman (1985). The primary results produced by the laboratory tests are the following:

- (1) Dry aerosols traveled through the cyclone, provided their diameters were smaller than about  $0.7 \mu\text{m}$  if the airspeed through the separator was less than  $24 \text{ m s}^{-1}$ .
- (2) All water drops larger than  $0.5 \mu\text{m}$  were removed from the airstream by the cyclone at airspeeds as small as  $12 \text{ m s}^{-1}$ .
- (3) A substantial portion of the water passing through the separator was collected at the bottom.

## Data Display Capabilities

The data collected using the King Air can be analyzed and displayed in a variety of ways. Tabulated values in engineering units for each variable measured are routinely produced. In addition, a variety of graphical presentations are available.

Figure 6 presents the flight track from a typical aircraft flight. The aircraft departed from Boston, MA, made a number of sampling runs about 100 km offshore, and returned to Boston. Figure 7 presents the outside air pressure (mb) versus time for the same flight. Such plots can be made for any scientific variable measured. Figure 8 presents the pressure (mb) versus temperature ( $^{\circ}\text{C}$ ) for this same flight. Any measured variable can be plotted against any other measured variable for comparison purposes.

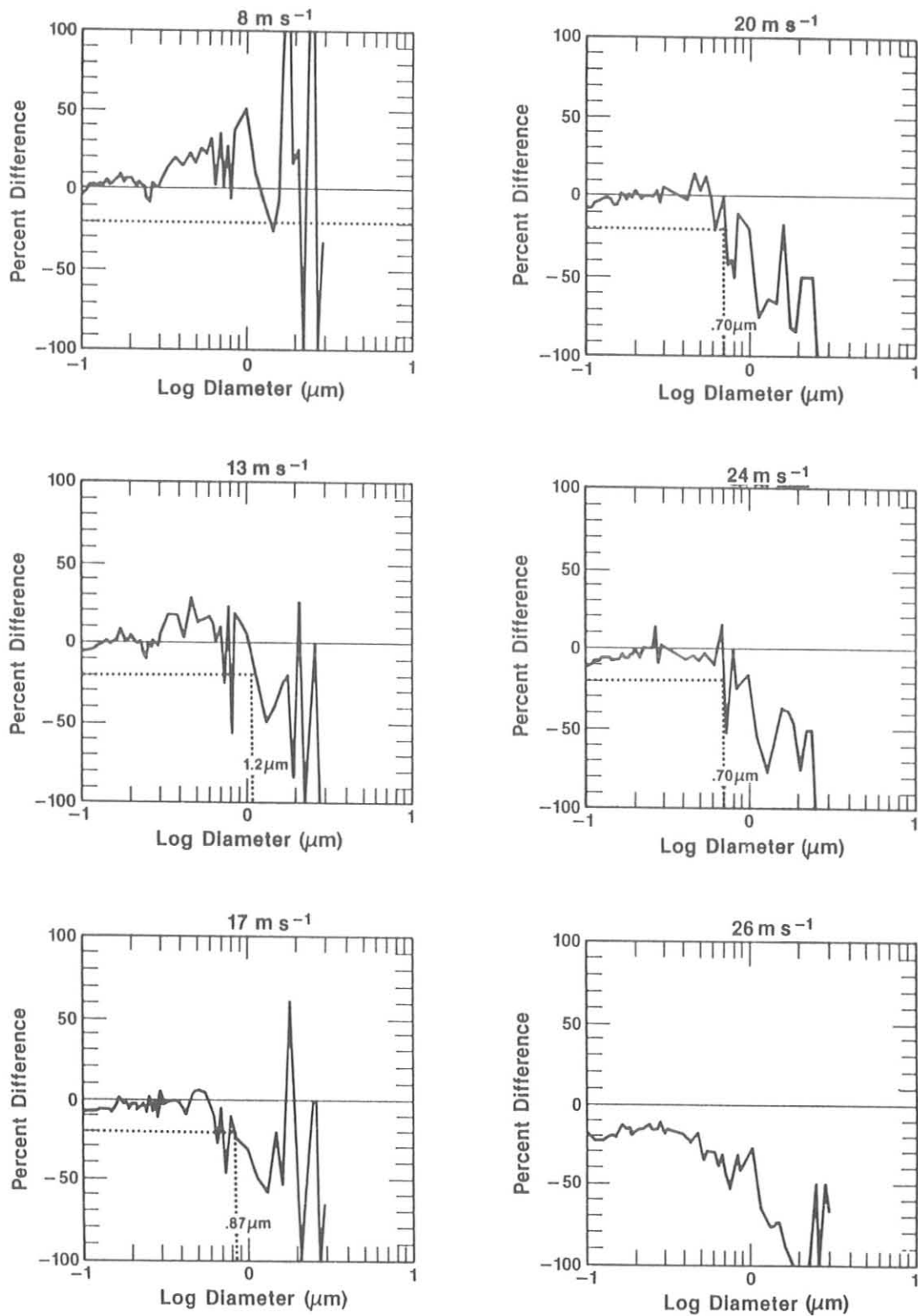


Figure 5.--Comparison plots between the control aerosol spectrum and aerosol distributions measured after passing air through the coud water separator at various speeds.

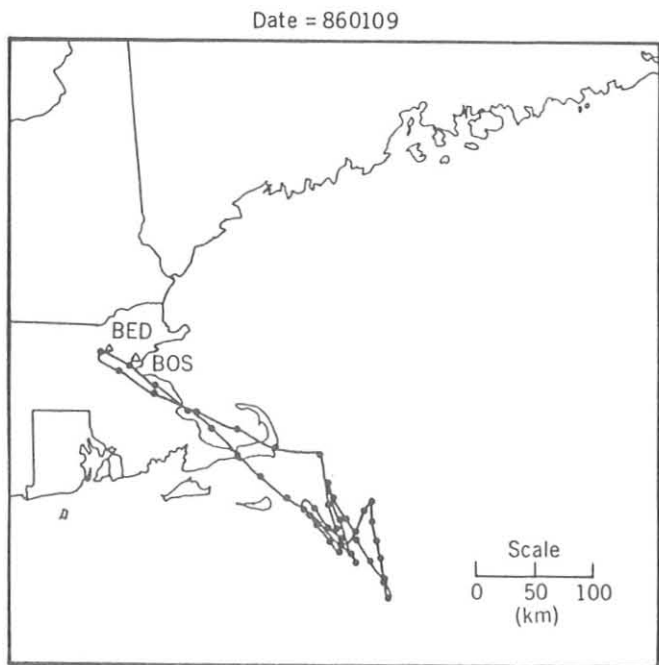


Figure 6.--The flight track from a typical research mission conducted near Boston, MA, as a part of WATOX.

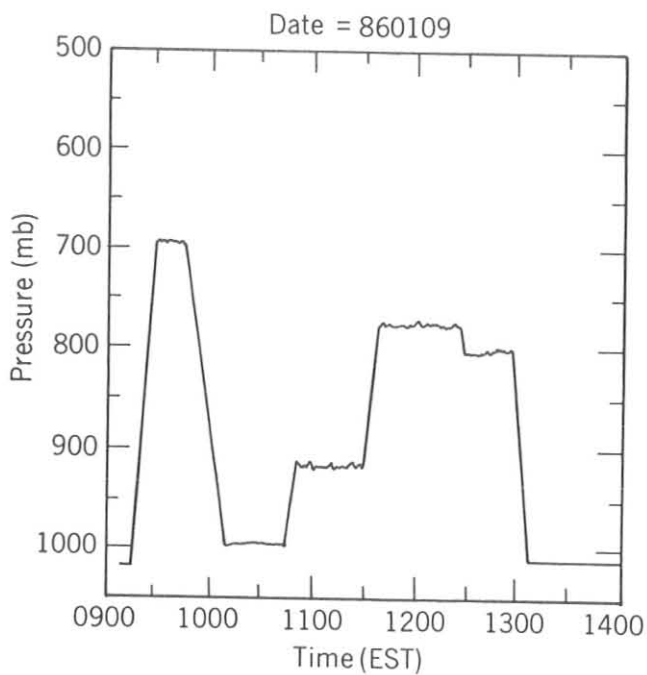


Figure 7.--The atmospheric pressure (mb) as a function of time during a portion of the research flight depicted in fig. 7.

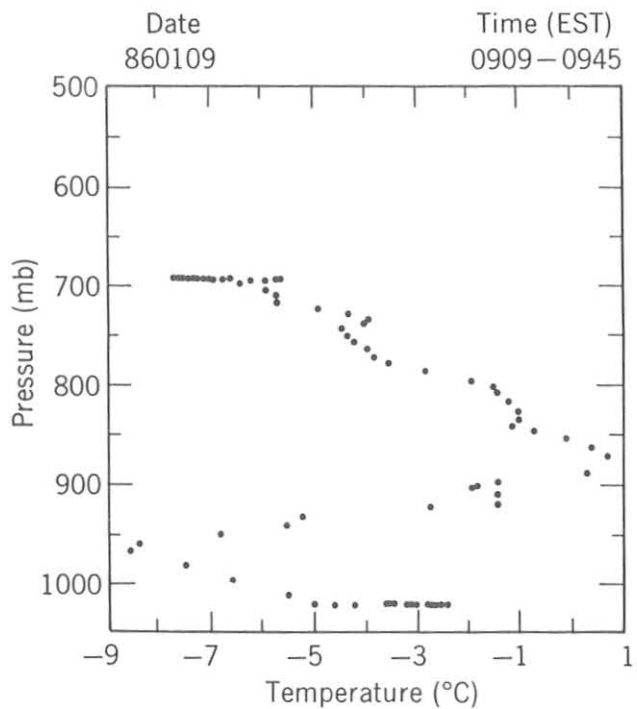


Figure 8.--The air temperature ( $^{\circ}\text{C}$ ) as a function of atmospheric pressure (mb) during a portion of the research flight depicted in fig. 7.

## 7.2 Special Projects

### SMALL-PARTICULAR DRY DEPOSITION

To predict possible environmental effects of air pollution, data are needed on natural removal rates as well as pollution emission rates from local and regional sources. The problem of acid deposition, for example, cannot be assessed unless both the dry and wet deposition values of strong acids can be determined reliably in remote as well as polluted environments. The removal rate of aerosol sulfur (S) from the atmosphere to an underlying surface is usually parameterized in terms of a deposition velocity,  $V_d$ --the ratio of particle S flux to its concentration at or near the surface of interest. Several measurements of particle S deposition have been reported (e.g., Droppo et al., 1983; Hicks et al., 1982; Sievering, 1982). These reported data do not include any high-wind-speed cases (i.e., speeds greater than  $6-7 \text{ m s}^{-1}$ ). The results summarized here and reported by Sievering (1986) are measurements of high-wind-speed S mass deposition (and also soil mass deposition as represented by Al, Ca, and Fe) over agricultural fields of moderate roughness. The measurements were taken during dry air (r.h. <40%) and relatively dry soil conditions, thereby avoiding the possibility of contamination by hygroscopic aerosol (especially sulfur-related) growth and decay, which has plagued some other aerosol deposition studies (Hicks et al., 1982; Sievering, 1982).

The measurements were made on 6 June 1982 at the BAO during a chinook wind. The westerly wind was quite steady ( $265^\circ$ - $290^\circ$  wind vector) and came from the clear-air Rocky Mountains source region located about 50 km west of the BAO. An undisturbed and adequate fetch has been observed for this wind sector (Schotz and Panofsky, 1980) to give logarithmic wind profiles up to 150 m with a well-specified roughness length,  $z_0$ , of  $4 \pm 2$  cm during low and moderate wind speeds. A detailed description of meteorological instrumentation and general BAO site characteristics for particle gradient measurement is found in Sievering (1982).

Sulfur- and soil-mass-gradient measurements over agricultural fields during clean-air and high-wind-speed conditions indicate very large deposition rates, even approaching momentum transfer. Mass deposition rates for soil-derived Al, Ca, and Fe were always greater than the rate of anthropogenic sulfur, as would be expected given the large MMD of soil particles relative to that of sulfur. These results, though somewhat preliminary owing to the small number of gradients observed, indicate substantially larger particle deposition velocities than predicted on theoretical grounds. For particle sulfur, no daytime surface resistance ( $r_s$ ) is calculated to have prevailed during the nearly  $9 \text{ m s}^{-1}$  wind speeds encountered, although some surface resistance is suggested for the nighttime  $6-7 \text{ m s}^{-1}$  wind speed data. This particular result is not in agreement with the  $r_s = 1-3 \text{ s cm}^{-1}$  obtained by others for small-particle, eddy flux measurements. Noting that the geometric mean (number) diameter for small-particle, eddy flux measurements has been several times smaller than the MMD for the particle S mass-flux gradient measurements here reported, the discrepancy in  $r_s$  is not unexpected. The S mass deposition rates of  $0.9$  and  $2.65 \text{ cm s}^{-1}$ , during stable and unstable periods, respectively, are applicable to anthropogenic sulfur deposition,

since its air concentration was 50-140 times that which could have been soil derived. The large deposition velocities for particle sulfur observed at this site may apply at other remote, overland sites under high-wind-speed conditions and over landforms of at least moderate roughness and having closely spaced surface roughness elements. Since essentially all the sulfur at the BAO (Ganor et al., 1983) is in the form of sulfate, these large deposition rates should apply equally well to sulfate.

## WINDS IN THE GRAND CANYON

The Air Quality Group has participated in a study, sponsored by the National Park Service, to better understand the wind patterns in the Grand Canyon. The terrain near both the south and north rims of the Canyon is heavily forested; therefore, controlled burning has become necessary along the rims to meet resource management objectives. This burning is done during the spring and fall of the year when the forest is dry and cool. A significant amount of smoke is produced, creating the potential for reduced visibility and a concomitant decrease in the Canyon's scenic splendor. Another problem is that the wood smoke, on occasion, could be transported from the burn site into the small town of Tusayan, south of the Canyon's rim, causing annoyance to residents and visitors alike.

In 1984 and 1985, three permanent ground stations were utilized to provide temperature, humidity, moisture, and wind data on the North and South Rims and on Tonto Plateau within the Grand Canyon. The distance between the North and South Rim Stations is about 34 km. The distance between the South Rim Station and Tonto Plateau is about 23 km. The purpose of the research was to determine wind patterns within and adjacent to the canyon.

Figure 9 illustrates the hourly wind vector averages for the month and the constancy of the winds in 1984 and 1985 in UT (GMT), where UT = MST + 7.

The South Rim Station data show an almost constant wind from the south to west quadrant. Winds with a northerly component occur mostly after 1800 UT except in January and February. The average wind is strongest in May and June and is also most constant in those months. This contrasts strongly with the North Rim Station where strong winds are more a function of time in April through November, but compares to the wind strength on the Tonto Plateau.

On the North Rim winds tend to be light at night and strong during the day. The winds are extremely constant during August, especially during 0000-1300 UT (1700 and 0600 MST). The very small vectors indicate that a light drainage wind from the north at speeds of  $0-1 \text{ m s}^{-1}$  is present. This conclusion is drawn from the average winds in the raw data.

On Tonto Plateau a downcanyon wind would be from the ESE. No such downcanyon winds are observed except in the winter months of December, January, and February. These winds are not confined to nighttime hours. Downslope winds at night, which might encourage downcanyon flow, would be expected around 0700-1200 UT, especially after hot days in the summer, and would be from the SSW. These are also not found in the canyon averages. The

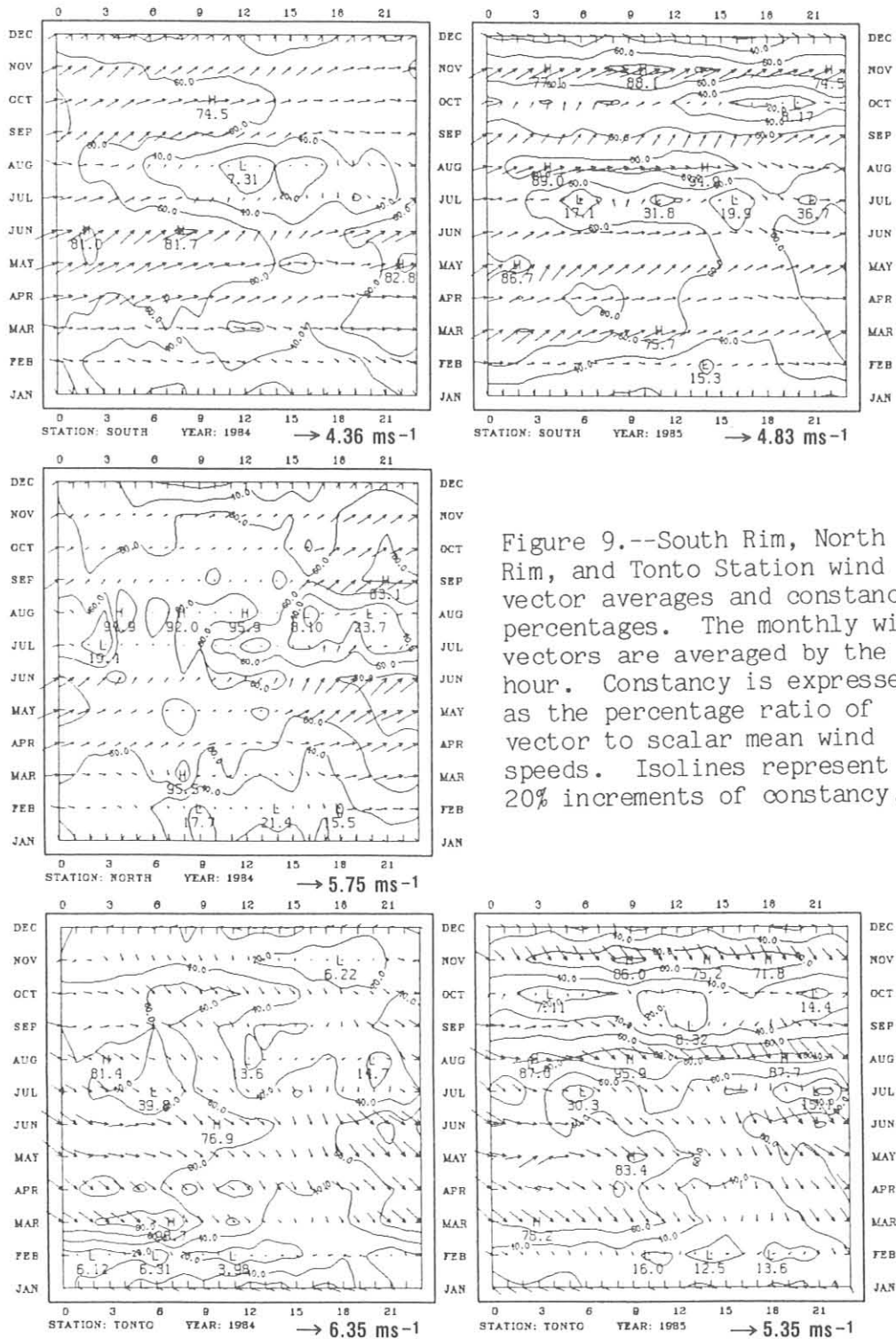


Figure 9.--South Rim, North Rim, and Tonto Station wind vector averages and constancy percentages. The monthly wind vectors are averaged by the hour. Constancy is expressed as the percentage ratio of vector to scalar mean wind speeds. Isolines represent 20% increments of constancy.

constancy of the wind is lowest at 1800 UT in November and all of January, and highest during nighttime hours in March-October. These combined facts reveal that the wind is primarily upcanyon throughout most of the year.

Meteorological measurements were also made from an instrumented aircraft and included studies of temperature, dewpoint, wall and interface temperatures, and horizontal and vertical wind speed and direction. The flight missions were made in the fall of 1984 and the spring of 1985 (April, May, June, September, and October). June and September data indicate that the canyon is capable of scouring or cleansing itself, whereas October data show that a strong new air mass is needed to remove pollutants from the canyon. This is so because of decreased solar heating of the walls and interface as a result of decreased sun angle and length of day in October.

To further understand the transport patterns under prevailing meteorological conditions, a conceptual model for the mean air motions in the Grand Canyon was developed using cavity flow. This model was enhanced after close examination of the Grand Canyon balloon-wind data available to us. Conversely, the wind data became more understandable and consistent when placed in this framework.

Consider first the case of coupled flow (where air from above and below the Canyon's rim is interacting) either during the day or at night. We propose that the mean winds in the Grand Canyon, under these conditions, are of the type shown in fig. 10. Figure 10 is a plan view of the wind pattern; fig. 10 is a cross-section view. Figure 10 suggests that air below the level of the Canyon rim moves predominantly parallel to the Canyon itself. The depiction indicates that the direction of this parallel motion is always along the direction of the airflow crossing above the Canyon. That is, air within the Canyon moves eastward (west wind) when the synoptic-scale winds are from the west. Figure 10 also indicates that the air below the Canyon rim is undergoing a spiral motion. This is due to the secondary cavity flow. Figure 9b depicts this flow in cross-section. The secondary cavity flow is proposed to produce updrafts along the upwind walls of the Canyon and downdrafts along the downwind walls. The air in the center of the Canyon is proposed to have no vertical motion. A secondary air current counter to the prevailing synoptic flow is proposed to occur at the bottom of the Canyon.

Consider second the case of decoupled flow (where air from above and below the Canyon's rim is not interacting), either during the day or at night. We propose that the mean winds in the Grand Canyon are of the type shown in fig. 11 under these conditions. Figure 11a is a plan view of the wind pattern; fig. 11b is a cross-section view. Figure 11a suggests that air below the level of the Canyon rim is undergoing drainage flow. Figure 11b suggests that no secondary cross-canyon flow is present under decoupled conditions. The potentially stable air below the Canyon rim is proposed to drain gently downriver (into the paper in fig. 11b).

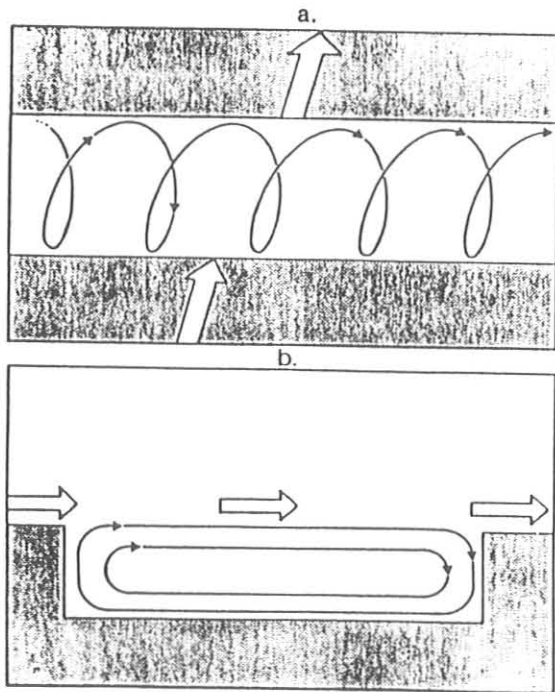


Figure 10.--A conceptual view of the wind pattern in the Grand Canyon under coupled conditions for (a) a plan view and (b) a cross-section view.

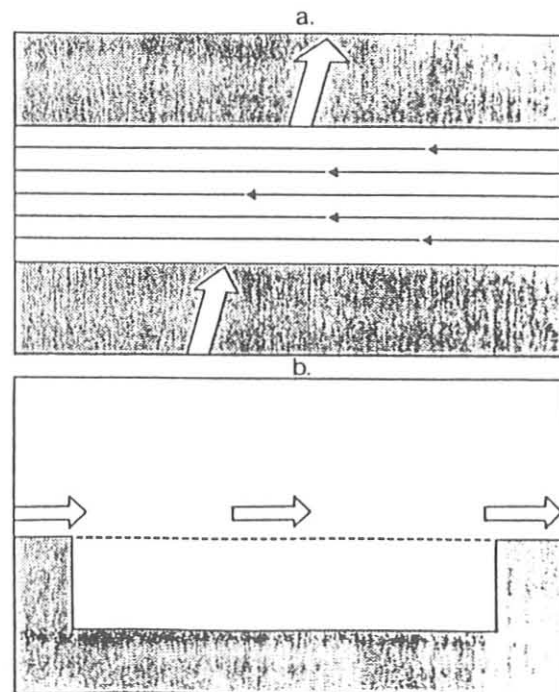


Figure 11.--A conceptual view of the wind pattern in the Grand Canyon under decoupled conditions for (a) a plan view and (b) a cross-section view.

The results, summarized here and given by Boatman and Henderson (1986) in support of this conceptualization, are as follows:

- (1) Airflow below the rim level moves predominantly parallel to the Canyon during coupled flow conditions that may occur during any month of the year.
- (2) The secondary cavity flow suggested in our conceptualization occurs predominantly during coupled conditions. These conditions are most often associated with periods of clear days and nights.
- (3) A strong shear layer was often present near the Canyon's rim level. Air below this layer appeared to be draining gently downriver. Above this layer, synoptic-scale forces predominated.
- (4) Winter months appeared more prone to decoupled (or drainage flow) behavior within the Canyon. It may be that potentially cold air from radiative cooling, frontal passages or snow at the rim is responsible for this.
- (5) Shear layers were present at lower levels within the Canyon. They may have been the product of a slow erosion process from above or the establishment of a radiation inversion. They appeared to act as an alternate bottom to the Canyon for airflow purposes.
- (6) At times, scouring occurred instead of secondary cavity flow. This may have been limited to very light wind cases or instances where shear layers established an alternate bottom to the Canyon.

### 7.3 References

- Andreae, M. O., and H. Raemdonck, 1983. Dimethyl sulfide in the surface ocean and the marine atmosphere: A global view. Science 221:744-747.
- Boatman, J. F., and D. Henderson, 1986. Grand Canyon wind study aids in smoke management. Park Science 6(4):18-19.
- Boatman, J. F., and D. Wellman, 1985. The efficiency of an airborne cloud water separator. Proceedings 1985 International Symposium on Moisture and Humidity, Washington, D.C., 15-18 April 1985. Instrument Society of America, Research Triangle Park, NC:143-146.
- Charlson, R. J., and H. Rodhe, 1982. Factors controlling the acidity of natural rainwater. Nature 295:83-684.
- Dickerson, R. R., G. J. Huffman, W. T. Luke, L. J. Nunnermacher, K. E. Pickering, A. C. D. Leslie, C. G. Lindsey, W. G. N. Slinn, T. J. Kelly, P. H. Daum, A. C. Delany, J. P. Greenberg, P. R. Zimmerman, J. F. Boatman, J. D. Ray, and D. H. Stedman, 1986. Thunderstorms: An important mechanism in the transport of air pollutants. Science (accepted for publication).
- Droppo, J. G., J. C. Doran, O. B. Abbey, and D. W. Glover, 1983. Dry deposition field studies. Electric Power Research Institute Document No. EA-3096, Westlake Village, CA.
- Galloway, J. N., D. M. Whelpdale, and G. T. Wolff, 1984. The flux of S and N eastward from North America. Atmospheric Environment 18:2595-2607.
- Gammon, R. H., and T. S. Bates, 1985. Marine source strength of reduced sulfur compounds. Paper presented at the NAPAP Conference, Boulder, CO, September, 1985.
- Ganor, E., R. F. Pueschel, and C. T. Nagamoto, 1983. Sulfates and nitrates: Concentration as a function of particle size in eastern Colorado. NOAA Air Resources Lab. Rep., Boulder, CO. (unpublished manuscript).
- Garvey, D. M., R. G. Pinnick, and G. Fernandez, 1984. Response characteristics of the Particle Measuring Systems active scattering aerosol spectrometer probe (ASASP-X). U.S. Army Electronic Research and Development Command Rep. ASL-TR-0156, Adelphi, MD, 24 pp.
- Hicks, B. B., M. L. Wesely, J. L. Durham, and M. A. Brown, 1982. Some direct measurements of atmospheric sulfur fluxes over a pine plantation. Atmospheric Environment 16:2899-2903.
- Luria, M. and J. F. Meagher, 1986. Computer simulation of the oxidation and removal of natural sulfur compounds in the marine atmosphere. Proceedings 6th International Clean Air Congress, Sidney, Australia, August, 1986.
- Luria, M., C. C. Van Valin, J. F. Boatman, D. L. Wellman, and R. F. Pueschel, 1987. Sulfur dioxide flux measurements over the western Atlantic Ocean, Atmospheric Environment (submitted).

- Luria, M., C. C. Van Valin, D. L. Wellman, and R. F. Pueschel, 1986. Contribution of Gulf area natural sulfur to the North American sulfur budget. Environmental Science and Technology 20:91-95.
- Pinnick, R. G., and H. S. Auvermann, 1979. Response characteristics of Knollenberg light-scattering aerosol counters. Journal of the Atmospheric Sciences 10:55-74.
- Reisinger, L. M., and T. L. Crawford, 1980. Sulfate flux through the Tennessee Valley region. Journal of the Air Pollution Control Association 30:1230-1231.
- Schotz, S., and H. A. Panofsky, 1980. Wind characteristics at the Boulder Atmospheric Observatory. Boundary-Layer Meteorology 19:155-164.
- Sievering, H., 1982. Profile measurements of particle dry deposition velocity at an air-land interface. Atmospheric Environment 16:301-306.
- Sievering, H., 1986. Gradient measurements of sulfur and soil mass dry deposition rates under clean air and high-wind-speed conditions. Atmospheric Environment 20:341-345.
- Whelpdale, D. M., T. B. Low, and R. G. Kolomeychuk, 1984. Advection climatology for the East Coast of North America. Atmospheric Environment 18:1311-1327.

## 8. DIRECTOR'S OFFICE

### 8.1 Alkaline Aerosols

#### IMPACT OF ALKALINE AEROSOL ON PRECIPITATION CHEMISTRY

It has been demonstrated that natural sources of alkaline material can have a significant effect on the chemistry of precipitation. Soil particles are often alkaline, particularly in the Western United States. These particles may act to neutralize the acidity of precipitation caused by pollutants such as the sulfur and nitrogen species produced by burning of fossil fuels in industrial plants and automobiles. The Alkaline Aerosol Project is concerned with estimating fluxes of alkaline aerosols and investigating their chemical properties.

A goal of the project is to estimate, by region and on a monthly basis, the total atmospheric input of suspended soluble alkaline aerosol that has neutralizing potential for precipitation. The importance of the 1-mon temporal scale and regional spatial scale is that alkaline source material is plentiful in some regions, particularly in the Western United States, during some months but is not plentiful in other regions or possibly during other months. Source mechanisms such as wind erosion, dust devils, and vehicles traveling on unpaved roads are quite different and lead to differing temporal and spatial aerosol input. The source mechanisms for alkaline aerosol production may have seasonal maxima that should be included in models that consider neutralizing effects of alkaline aerosols. Solubility and neutralizing potential must be known along with mass input of suspendable alkaline aerosol to calculate the effect on acid precipitation.

The Alkaline Aerosol Project is divided into efforts to assess the total input of aerosols from the various mechanisms of soil particle emissions and to analyze their chemical properties. Work on the input by wind erosion is taking place in GMCC under the direction of D.A. Gillette, work on the input by vehicles traveling on unpaved roads is taking place at the University of Illinois under the direction of G. Stensland, and work on dust devil emissions is taking place at Colorado State University by P. Sinclair. Stensland is also leading the effort to chemically characterize the soil particles emitted by the above source mechanisms.

Previous estimates of emissions of dust by wind erosion and by vehicles traveling on unpaved roads have been shown to be too large when compared with actual deposition of soluble alkaline particles. New methods are being developed in GMCC to estimate these inputs. For example, the National Resource Inventory (NRI) survey of U.S. farms and soils will be used along with 14 years of wind data recently compiled as the Wind Energy Resource Information System (WERIS). The fundamental approach of the dust emission studies will be to use an expectation integral

$$E = \int_{V_0}^{\infty} g(V)p(V) dV$$

UNITED STATES ANNUAL AVERAGE WIND POWER



Figure 1.--Wind energy in the United States. (Map courtesy of Battelle, Pacific Northwest Laboratories.) Darkest shading indicates greatest wind energy.

where  $g(V)$  is the dust flux for a given wind speed  $V$ ,  $p(V)$  is the probability density function of the wind speed, and  $V$  is the threshold value of the wind speed at which dust emissions begin. Since this approach has similarities with wind energy mapping, it is instructive to see that the areas of maximum wind energy correspond to historical areas of severe dust production.

Figure 1 shows that areas of maximum wind energy center on the Panhandle of Oklahoma. The areas of maximum land damage for 1935-1936 also center on the Panhandle of Oklahoma (see fig. 2.) The areas of maximum land damage for the drought of the 1950's occurred in the high plains too, but because of land use differences the location was slightly different from that of the 1930's drought.



Figure 2.--The general boundaries of the "Dust Bowl" from 1935-1936 (solid line). The region marked by slanting lines received the most severe wind erosion. (Information from Hurt, 1981.)

Chemically, some properties of the alkaline aerosols have been investigated by the University of Illinois team. They have shown that alkaline elements increase in solubility with time and dilution ratio (mass of water to mass of solids). Since they have shown that dilution ratio is typically on the order of 100,000 to 200,000, it follows that alkaline elements should be quite soluble in rainwater. That result was confirmed in samples of natural rainwater.

A schematic diagram of the approach that the Alkaline Aerosol Project team is taking to estimate the neutralizing effect of airborne alkaline aerosols is shown in Table 1. First, emission factors from the three major sources of alkaline aerosols are grouped into the top level. Second, the fraction of the total alkaline aerosol produced that is suspended for times long enough to interact with acid precipitation must be estimated from knowledge of settling rates and atmospheric turbulence. Third, the fraction of the aerosols that is alkaline must then be found from knowledge of fractionation of airborne material from parent material and composition of parent material. Fourth, the soluble fraction of the alkaline elements in the aerosols must be found. Finally, the neutralizing potential of the soluble suspended alkaline material must be found. Each of these individual components is being researched by the project.

Table 1. Alkaline aerosol flux estimations to be made by the Alkaline Aerosol Project and methods for the estimation of the neutralization of acid rain\*

Flux Estimate	Methods
Emission factor X source area	Expectation integrals, experimental threshold velocities; Road dust experimentation; dust-devil experimentation
Fraction suspended dust (for long time/distance)	Vertical turbulence model
Elemental fraction of suspended dust (fractionation X composition)	Fractionation experimentation; chemical survey of U.S. roads; USGS soil composition data
Soluble fraction of elemental suspended dust	Experimentation on solubility
Neutralization fraction	New experimentation

\* Each succeeding level is a fraction of the next higher level.

#### REFERENCES

Hurt, R. D., 1981. The Dust Bowl: An Agricultural and Social History. Nelson-Hall Inc., Chicago, 540 pp.

## PRECIPITATION CHEMISTRY

R. S. Artz  
Air Resources Laboratory, NOAA  
Silver Spring, MD 20910

### INTRODUCTION

Routine and special precipitation chemistry measurements continued at the four GMCC sites and at the regional sites. Special studies continued at MLO using the ion chromatograph for anion analysis for Samoa and the Hawaii network. A new Dionex ion chromatograph was purchased and shipped to the Mauna Loa Laboratory. Cation analysis should commence sometime during 1986. A cooperative project with the University of Virginia was instituted in order to measure organic acids in precipitation samples collected at Mauna Loa Observatory.

### BASELINE MEASUREMENTS

The five-site special network on the island of Hawaii and a sixth site on Kauai continued to operate on approximately a weekly schedule, with the exception of the Cape Kumukahi site. (Site locations are discussed in previous GMCC reports.) Problems with rust and corrosion of equipment coupled with relatively frequent power outages have resulted in the abandonment of the Kumukahi site.

As seen in Fig. 1, high sulfate and hydrogen ion concentrations existed during the months of June, September, and December at the Hawaiian sites. These observations can be explained by the very low precipitation received at the effected sites (Figure 2) and are probably not due to anthropogenic or volcanic activity. Typically, concentration increases sharply as precipitation amount approaches zero. Agreement for sulfate and hydrogen ion at Halai Hill and Kauai, sites with similar elevation and orientation to the trade winds, was very good throughout the year although Halai Hill values, as frequently observed in the past, tended to be 5 to 10 ueq/l higher.

In Fig. 3 monthly precipitation weighted  $\text{SO}_4^{=}$  and  $\text{H}^+$  means for the Hawaiian sites are presented. As usual, highest sulfate values usually occur at lowest elevations (Kauai and Halai Hill) due to the incorporation of sulfate laden sea spray. Sites at higher elevations are frequently decoupled from the marine boundary layer and therefore contain less sulfate. In addition, higher  $\text{H}^+$  concentration (lowest pH) are typically observed at the highest elevations.  $\text{H}^+$  concentrations near sea level are lower.

In Fig. 4 Samoa  $\text{H}^+$  and  $\text{SO}_4^{=}$  monthly precipitation weighted means are presented. With the exception of August, values are very constant. Missing data during May, June and July are due to a change in the staff at Samoa. It is not known whether the high concentration of  $\text{SO}_4^{=}$  in August is the result of problems associated with the program restart or if, in fact, the value is correct.

Snow sample data for BRW and SPO are shown in Fig. 5. SPO samples are exceptionally clean and constant, showing concentrations of less than 2 ueq/l of  $\text{SO}_4^{=}$  and approximately 8 ueq/l of  $\text{H}^+$ . Barrow values are somewhat more erratic but remain consistent with measurements from MLO and other background sites. Shipping problems resulted in the loss of measurements at BRW after August, 1985.

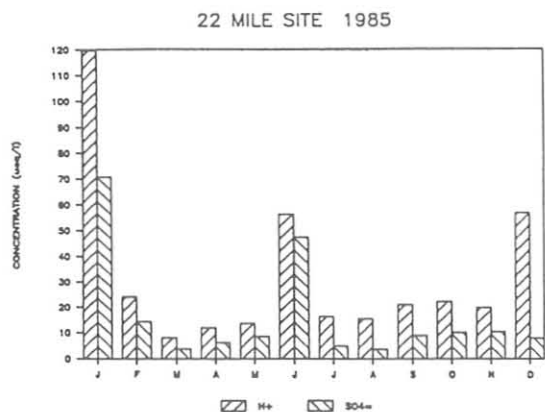
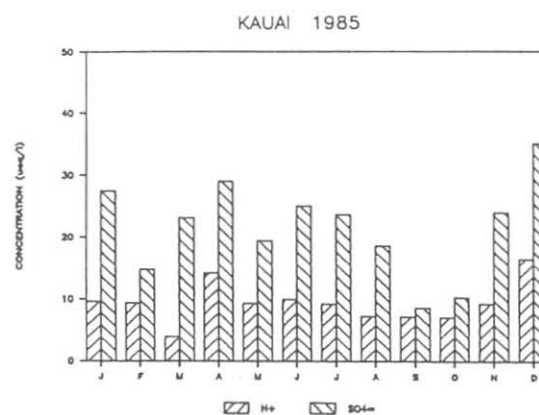
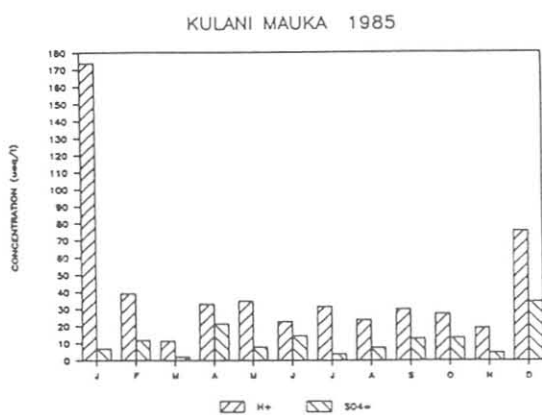
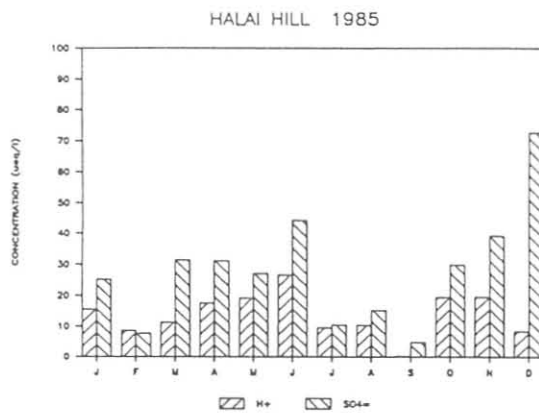
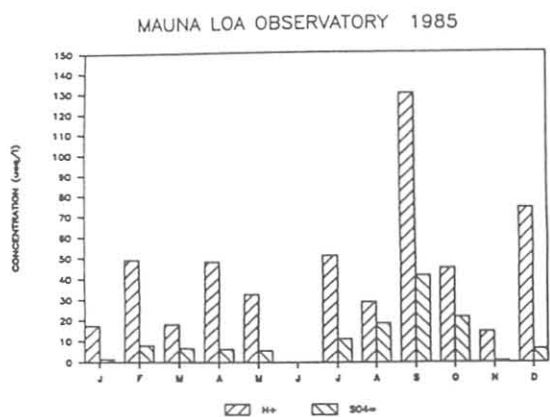


Figure 1.--Monthly precipitation weighted means for five sites on the islands of Hawaii and Kauai during 1985.

## REGIONAL MEASUREMENTS

All thirteen of the NOAA NADP/NTN regional precipitation sites remained in operation during 1985. No new sites were added to the network although tentative plans exist to establish a second site near Meridian, MS in an effort to quantify any effects a local pressed-wood facility may have on the existing site. Proposed site start-up time has been scheduled for sometime during 1986.

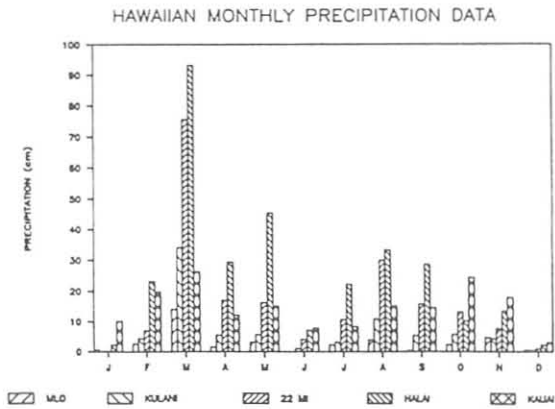


Figure 2.--Monthly precipitation at Hawaiian sites for 1985.

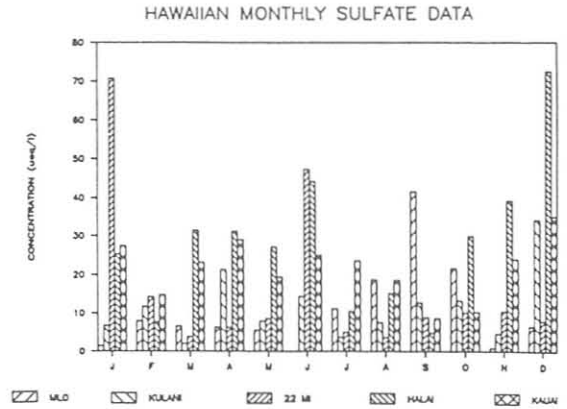


Figure 3a.--Monthly precipitation weighted sulfate means for the Hawaiian network.

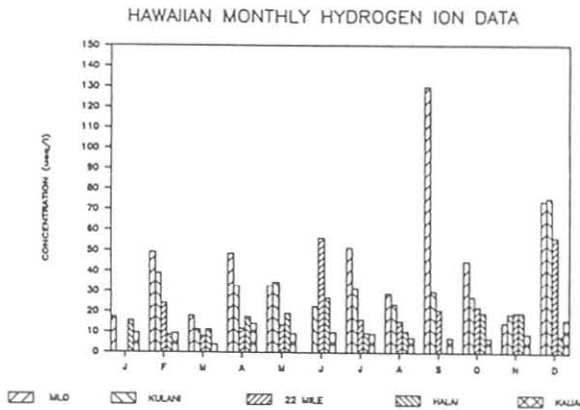


Figure 3b.--Monthly precipitation weighted hydrogen ion means for the Hawaiian network.

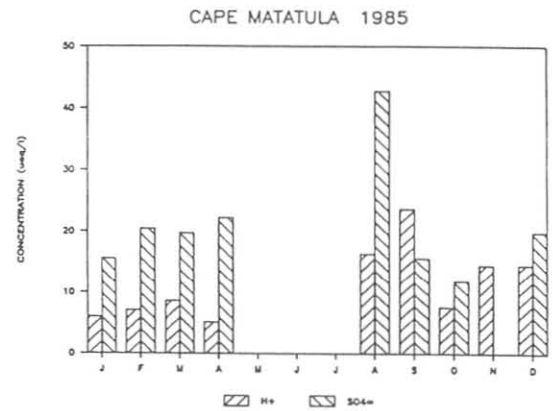


Figure 4.--Monthly precipitation weighted sulfate and hydrogen ion means for Samoa during 1985.

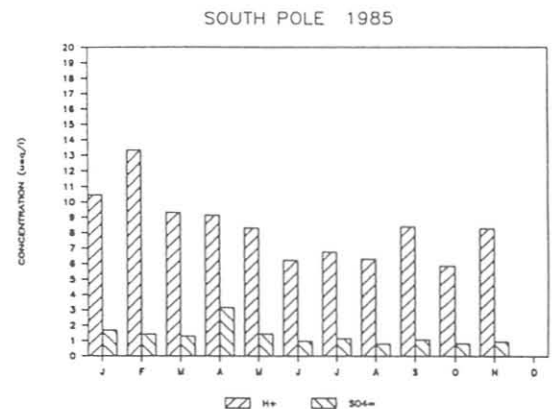
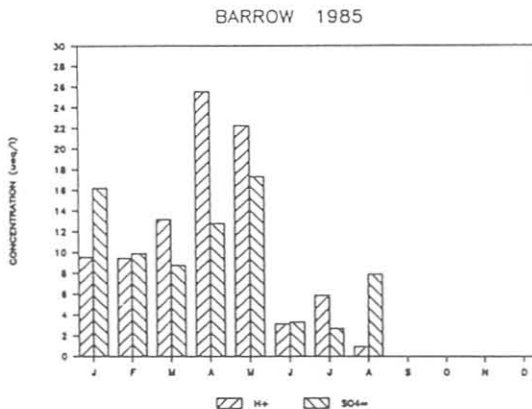


Figure 5.--Monthly average hydrogen ion and sulfate concentrations for snow samples collected in Barrow and at the South Pole for 1985.

## 8.2 Arctic Gas and Aerosol Sampling Program

### ARCTIC HAZE ABOVE THE BARROW BASELINE STATION

R.C. Schnell

Cooperative Institute for Research in Environmental Sciences  
University of Colorado, Boulder, CO 80309

#### INTRODUCTION

Analyses of data from the AGASP flights of March-April 1983 show that measurements of Arctic haze gas and aerosol concentrations at the surface are strongly influenced by the vertical temperature structure of the atmosphere. Under strong temperature inversion conditions, the stable Arctic boundary layer reduces mixing from aloft to the surface. Under these conditions, gas and aerosol concentrations measured aloft are higher than and peak-to-peak variations greater than those measured at the surface. Under stable atmospheric conditions, ozone is depleted within the boundary layer. A combined surface and airborne study for the Barrow station for 9-19 March 1983 is presented below.

#### BARROW SYNOPTIC CONDITIONS, 9-19 MARCH 1983

The surface pressure distribution over this region of the Arctic on 12 March 1983, 0000 GMT, was dominated by a large anticyclone (high-pressure area) located over the East Siberian Sea, a cyclone (low-pressure area) over the Canadian Archipelago, and a cyclone over the Gulf of Alaska. Organized air flow from Eurasia entered the Beaufort Sea area via the Canadian sector and crossed central Alaska on its way southward. Both the anticyclone and cyclone were developed as well at 500 mb. By 0000 GMT on 18 March 1983, the anticyclone had moved north and east of Barrow shielding Barrow from haze transport.

The occurrence of Arctic haze in the vicinity of Barrow during this period has been associated with well-organized transport of pollutants from Eurasia across the Pole into the Alaskan Arctic (Raatz, 1984). The pollutants from Eurasia were injected northward on 4-5 March (Raatz, 1984) reached Svalbard on 7-8 March (Ottar and Pacyna, 1984; Iversen, 1984), and according to air mass trajectories, arrived over the Alaskan Arctic on 11-12 March (Harris, 1984). By 17-18 March, haze was not observed either at the surface or above and upwind of Barrow.

#### AIR MASS TYPE AND SURFACE MEASUREMENTS

Cross sections of potential temperature and water vapor mixing ratio for 9-19 March are presented in fig. 1. The cross sections are based upon the 0000 GMT radiosonde data. The tropopause (as determined by the top of the isothermal temperature layer) and the top of the very stable surface boundary layer are indicated by dotted lines.

On the basis of temperature, pressure, moisture, and trajectory analyses, it has been determined that the air at Barrow was of marine Pacific cold (mPK) origins, 9-10 March; of continental Arctic cold (cAK) origins, 11-12 March; of continental Arctic warm (cAW) origins, 12-18 March; and of marine Pacific warm (mPW) origins 18-20 March. These air mass designations are shown in fig. 1.

A time series of surface measurements of ozone, CO<sub>2</sub>, aerosol scattering extinction coefficient  $\sigma_{sp}$ , aerosol concentration in the 0.24-0.84  $\mu\text{m}$  range, and CN concentration ( $\text{cm}^{-3}$ ) is presented in fig. 2. From these data it may be observed that there are distinct changes over time in both the gas and aerosol characteristics observed at the Barrow station in concert with the air mass changes.

On 13-14 March extensive aircraft measurements were conducted above and upwind of the Barrow station in order to determine the vertical and horizontal variability of the haze and to relate these measurements to the surface record. These measurements are presented in fig. 3 in latitude-altitude cross sections of aerosol backscatter, relative humidity (r.h.), CN concentrations, and ozone partial pressure as measured by the aircraft. Individual latitude-concentration series were obtained while the aircraft was flying at a constant pressure level.

As shown in fig. 3, at 1010 mb and 60 km upwind of Barrow (Barrow experienced a surface pressure of 1026 mb), a high  $\sigma_{sp}$  of  $60 \times 10^{-6} \text{ m}^{-1}$  was recorded. It decreased rapidly to  $25 \times 10^{-6} \text{ m}^{-1}$  north of this peak and then stabilized at  $30 \times 10^{-6} \text{ m}^{-1}$ , which is slightly greater than the average  $\sigma_{sp}$  values of  $27.8 \times 10^{-6}$  observed at Barrow during this day. At intermediate pressure levels (780 mb), the range of  $\sigma_{sp}$  values was  $(10 \text{ to } 30) \times 10^{-6} \text{ m}^{-1}$ , and  $\sigma_{sp}$  exhibited an abrupt decrease near 73°N. Above 705 mb,  $\sigma_{sp}$  values became lower with increasing altitude, as was observed in all the vertical profiles of  $\sigma_{sp}$  (Schnell and Raatz, 1984).

The cross section of r.h. suggests that within the surface boundary layer the variations in extinction were not related to variations in r.h., which was constant in the 65-75% range. This was also the case at the surface (Bodhaine et al., 1984). At the 780-mb level, however,  $\sigma_{sp}$  and r.h. appeared to correlate, with dry air having lower  $\sigma_{sp}$  values than moist air.

CN concentration varied between 70 and 1000  $\text{cm}^{-3}$ , with peak concentrations of 1000  $\text{cm}^{-3}$  observed at all but the highest (670-mb) flight level. Within the surface boundary layer, the peak in CN concentration occurring at 71.6°N correlated well with the increased  $\sigma_{sp}$  values. On the other hand, at the same level north of 73°N, a peak in CN concentration was associated with decreased  $\sigma_{sp}$ . The background average CN concentration in the 1010 mb flight leg (220  $\text{cm}^{-3}$ ) was lower than the Barrow background average CN values of 315  $\text{cm}^{-3}$  on this day, but is in excellent agreement with the Barrow background average CN value of 225  $\text{cm}^{-3}$  the following day. At the intermediate level (780 mb) north of 73°N, dry and less turbid air was associated with lower CN counts. At upper levels, changes in CN concentrations over space changed by large factors but in no discernible relationship to  $\sigma_{sp}$  and r.h. Ozone partial pressures were in the normal 20-35 nb background range observed at Barrow in the spring and exhibited little variation horizontally.

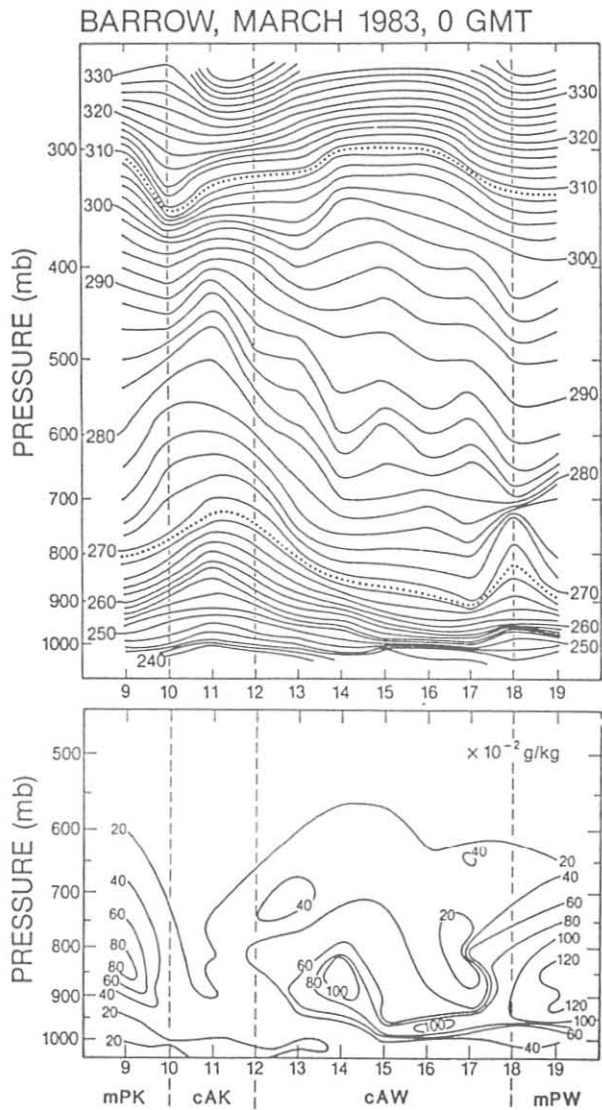


Figure 1.--Time-height cross section of potential temperature (K) (top) and water vapor mixing ratio ( $\times 10^{-2} \text{ g kg}^{-1}$ ) (bottom) at Barrow, 9-19 March 1983. The tropopause in the 300-350 mb level and the top of the stable surface boundary layer in the 725-900 mb level are indicated by dotted lines. The different air masses present over the time period are presented by marine Pacific cold (mPK), continental Arctic cold (cAK), continental Arctic warm (cAW), and marine Pacific warm (mPW).

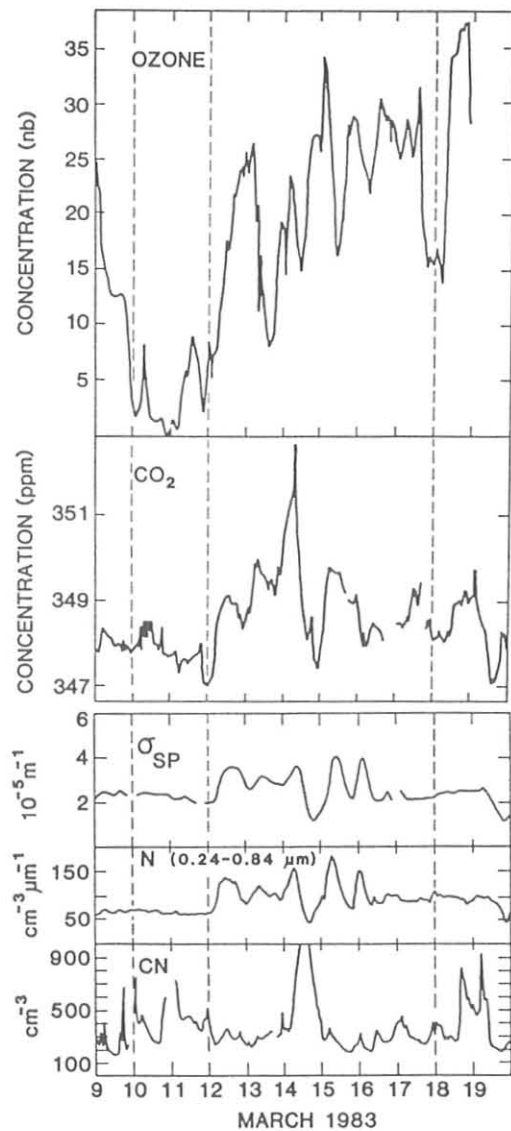


Figure 2.--Time series of ozone partial pressure, CO<sub>2</sub> concentration, aerosol scattering extinction coefficient, aerosol particle number, and CN concentration at Barrow, 9-19 March 1983.

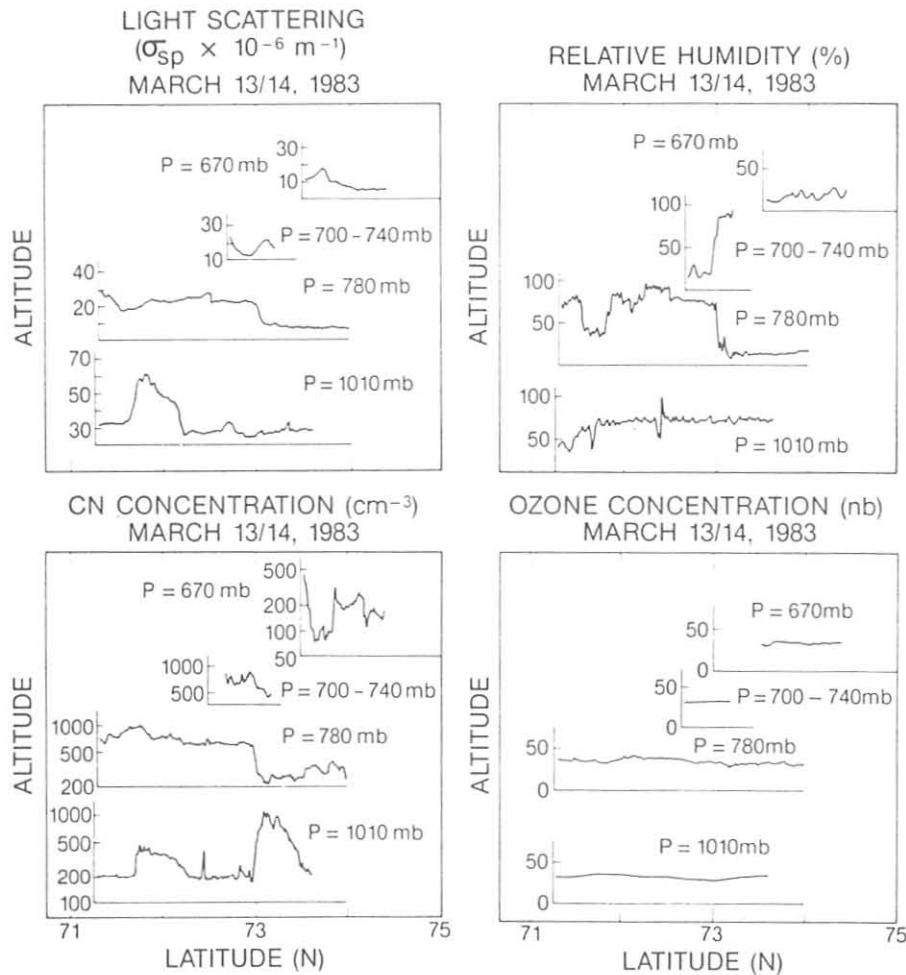


Figure 3.--Latitude-altitude cross sections of (a) aerosol scattering extinction coefficient ( $10^{-6} \text{ m}^{-1}$ ), (b) relative humidity (%), (c) CN concentration ( $\text{cm}^{-3}$ ), and (d) ozone concentration (nb), 13-14 March 1983.

The examples presented in fig. 3 are typical of the results from two other flight days (11-12 March and 15-16 March) when the aircraft flew similar patterns upwind and above the Barrow station.

As noted earlier, Barrow was under the influence of four different air masses (mPK, cAK, cAW and mPW) over the 9-19 March period (fig. 1). These changes in meteorological air mass characteristics were reflected in the surface measurements of CN, aerosol size and number distributions,  $\sigma_{\text{sp}}$  values, and  $\text{CO}_2$  concentrations and ozone partial pressures logged by 6-24 hours. Each air mass contained distinct characteristics in the concentrations and ratios of all the constituent parameters.

Comparison of the surface and aircraft aerosol and  $\text{CO}_2$  data, shows that in the free atmosphere the data spans a broader range; i.e., the minima aloft are lower and the maxima are higher than the corresponding surface measurements.

For 13-14 March, airborne ozone measurements show that the atmosphere above the surface contained an even and constant ozone distribution, whereas the surface records on this and other days exhibited fluctuating ozone concentrations. During this time of year the ozone chemistry in the free air is apparently unimportant (Levy et al., 1985), but ozone will be removed from the air by destruction at the surface of the ground (Galbally and Roy, 1980). Thus, the short-term fluctuations in the surface measurements probably reflect changes in the ability of ozone-rich air from above to penetrate to the surface.

## CONCLUSIONS

It is concluded that (1) tropospheric air mass changes above the Barrow GMCC site are detected at the surface within a day; (2) the absolute concentrations of gas and aerosols in the midtroposphere during strong temperature inversion situations are generally greater than those measured at the surface; and (3) the magnitude of the peak-to-peak variations in concentrations of gases and aerosols measured aloft tends to be greater than at the surface, thereby suggesting that the boundary layer may be producing a damping effect on aerosol perturbations measured at the surface. Thus, some caution is advised in extrapolating that surface Arctic haze measurements are being representative of the total tropospheric column.

## REFERENCES

- Bodhaine, B. A., E. G. Dutton, and J. J. DeLuisi, 1984. Surface aerosol measurements at Barrow during AGASP. Geophysical Research Letters 11:377-380.
- Galbally, I. E., and C. R. Roy, 1980. Destruction of ozone at the earth's surface. Quarterly Journal of the Royal Meteorological Society 106:599-620.
- Harris, J. M., 1984. Trajectories during AGASP. Geophysical Research Letters 11:457-460.
- Iversen, T., 1984. On the atmospheric transport of pollution to the Arctic. Geophysical Research Letters 11:457-460.
- Levy, H., Jr., J. D. Mahlmen, W. J. Moxim, and S. C. Liu, 1985. Tropospheric ozone: The role of transport. Journal of Geophysical Research 90(D2):3753-3772.
- Ottar, B., and J. M. Pacyna, 1984. Sources of Ni, Pb and Zn during the Arctic episode in March 1983. Geophysical Research Letters 11:441-444.
- Raatz, W. E., 1984. Tropospheric circulation patterns during the Arctic Gas and Aerosol Sampling Program (AGASP), March/April 1983. Geophysical Research Letters 11:449-452.
- Schnell, R. C., and W. E. Raatz, 1984. Vertical and horizontal characteristics of Arctic Haze during AGASP: Alaskan Arctic. Geophysical Research Letters 11:369-372.

### 8.3 Cooperative Programs

#### MONITORING FOR SULFUR DIOXIDE AND TOTAL SUSPENDED PARTICULATE AT MAUNA LOA OBSERVATORY

Henry Yee, Wilfred Ching, and Richard Sasaki  
Hawaii State Department of Health  
Honolulu, HI 96813

#### INTRODUCTION

Sulfur dioxide ( $\text{SO}_2$ ) and total suspended particulate (TSP) monitoring were reinstated as a long-term study at MLO by the state of Hawaii at the request of E.P.A. Region IX. The long-term trends in sulfur dioxide and particulate ( $10 \mu\text{m}$  diameter and smaller) concentrations will be studied to determine the factors contributing to increases observed in the past. Also, the study will work towards determining the atmospheric lifetime of the particular gases and particulates, and the chemical composition of the other particulates collected at the elevation of MLO.

Table 1 and fig. 1 show the integrated concentrations of 24-hr TSP and  $\text{SO}_2$  for samples collected at MLO in 1985.

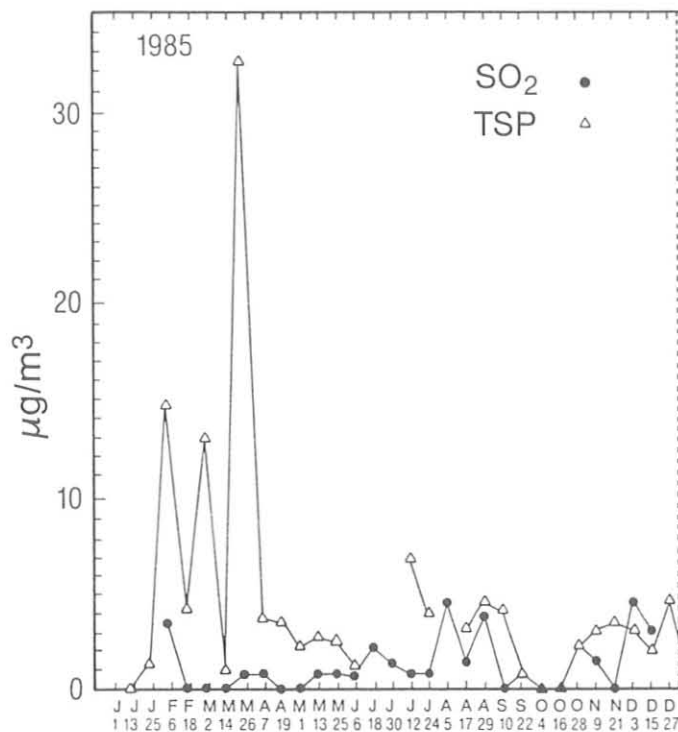


Figure 1.--Twenty-four-hour integrated concentrations of TSP and  $\text{SO}_2$  samples collected at MLO for 1985.

Table 1.--Twenty-four-hour concentrations  
of TSP (hi-vol, gravimetric) and SO<sub>2</sub>  
(pararosaniline method) at MLO (µg/m<sup>3</sup>)

	TSP	SO <sub>2</sub>
Jan 01	-	-
13	0	0
25	1.4	-
Feb 06	14.9	3.4
18	4.3	0
Mar 02	13.3	0
14	1.0	0
26	32.8	0.7
Apr 07	3.7	0.8
19	3.5	0
May 01	2.3	0
13	2.6	0.7
25	2.5	0.8
Jun 06	1.2	0.8
18	-	2.2
30	-	1.4
Jul 12	6.9	0.8
24	4.0	0.8
Aug 05	-	4.5
17	3.2	1.4
29	4.6	3.1
Sep 10	4.1	0
22	0.8	0.8
Oct 04	0	0
16	0	0
28	2.3	2.3
Nov 09	3.1	1.5
21	3.5	0
Dec 03	3.1	4.5
15	2.0	3.0
27	4.7	-

## THE GLOBAL PRECIPITATION CHEMISTRY PROJECT

W. C. Keene  
J. N. Galloway  
Department of Environmental Sciences  
University of Virginia, Charlottesville, VA 22903

G. E. Likens  
Institute of Ecosystems Studies  
Cary Arboretum, Millbrook, NY 12545

J. M. Miller  
Air Resources Laboratory  
NOAA, Silver Spring, MD 20910

### INTRODUCTION

Anthropogenic emissions of  $\text{SO}_2$  and  $\text{NO}_x$  have resulted in widespread acidification of precipitation and subsequent environmental damage in Eastern North America and Northern Europe. Of numerous research questions posed by this phenomenon, two are of special interest: (1) What was the composition of precipitation prior to the advent of fossil-fuel combustion; and (2) To what degree does the long-distance transport of sulfur and nitrogen species influence the composition of precipitation in remote regions of the world? The Global Precipitation Chemistry Project (GPCP) was initiated in 1979 to address these questions. Principal objectives are to measure the chemical composition of precipitation in remote areas of the world and to determine major processes controlling measured composition. Earlier reports of the GPCP include a preliminary assessment of the composition of precipitation in remote areas of the world (Galloway et al., 1982), an evaluation of the long distance transport of anthropogenic pollutants from North America to Bermuda (Jickells et al., 1982; Church et al., 1982), quantification of the importance of organic acidity in precipitation (Keene et al., 1983; Keene and Galloway 1984 a,b; 1985) an analysis of the influence of air mass source region on the composition of precipitation at remote locations (Galloway and Gaudry, 1984; Dayan et al., 1985) and a comparison between natural and anthropogenic components in precipitation (Galloway et al., 1984). In this report we will summarize current research and review more recent contributions of the project.

### MATERIALS AND METHODS

Samples of precipitation are collected by event in scrupulously washed polyethylene containers. Immediately after collection, pH is measured, samples are treated  $\text{CHCl}_3$  to prevent biological activity and aliquots are subsequently sent to the University of Virginia for analyses for major organic and inorganic chemical constituents. To-date we have analyzed approximately 1700 samples of precipitation collected at 12 land-based sites and during 4 oceanic cruises.

### RESULTS AND DISCUSSION

#### Seasalt Corrections in Marine Precipitation

Differentiation of seasalt and non-seasalt (or excess) components is essential for many studies of marine aerosol and precipitation chemistry.

Uncertainties in such calculations arise from (1) uncertainties in the composition of seawater, (2) analytical uncertainties, (3) the amount of dry deposited seasalt in samples, (4) the validity of assuming a purely marine source for the seasalt reference species, and (5) the validity of assuming no fractionation during or after production of seasalt aerosols. Keene et al. (1986) assessed these uncertainties and, using the reduced major axis regression technique, evaluated these assumptions by analyzing the composition of precipitation at Amsterdam Island (38°S, 78°E) and at Bermuda (32°N, 65°W). Precipitation on Amsterdam Island contained significant excess concentrations of Na<sup>+</sup> (2%) and Cl<sup>-</sup> (5%) relative to Mg<sup>2+</sup>. Indirect evidence indicates that these departures from seawater ratios are probably not due to the influence of terrestrial material. The excess Cl<sup>-</sup> was sufficient to account for approximately 20% of free acidity, suggesting that scavenging of vapor phase HCl may affect the acid-base chemistry of precipitation at the site. Volume-weighted excess SO<sub>4</sub><sup>2-</sup> based on Na<sup>+</sup> and Mg<sup>2+</sup> differed by 11%, a nonnegligible source of bias in estimating the wet deposition of non-seasalt sulfur. Precipitation on Bermuda contained significant concentrations of locally derived alkali and alkaline earth metals. The influence of continental and non-seasalt marine sources on concentrations of excess SO<sub>4</sub><sup>2-</sup> was also evident. These observations suggest that assumptions involved in seasalt corrections are not always satisfied and that it is therefore necessary to evaluate individual data sets, using objective criteria, to select the appropriate reference species.

#### Sources for Organic Acids in the Atmosphere

HCOOH (formic acid) and CH<sub>3</sub>COOH (acetic acid) are important chemical constituents of cloudwater and precipitation, but sources for these compounds in the atmosphere are at present unknown. The question of source of identification was addressed through the analysis of 465 samples of precipitation collected at 14 continental and marine locations around the world (Keene and Galloway, 1986). Continental precipitation during growing seasons contained, relative to marine precipitation and to continental precipitation during non-growing seasons, higher absolute concentrations of organic acids and higher ratios of HCOO<sub>T</sub> (HCOOH<sub>aq</sub> + HCOO<sup>-</sup>) to CH<sub>3</sub>COO<sub>T</sub> (CH<sub>3</sub>COOH<sub>aq</sub> + CH<sub>3</sub>COO<sup>-</sup>). The concentrations of HCOO<sub>T</sub> and CH<sub>3</sub>COO<sub>T</sub> in precipitation at most locations were also highly correlated. These results support the hypothesis that organic acidity in precipitation may originate with two major sources, volatile vegetative constituents over continents and a second weaker source in both continental and marine regions. Henry's Law constants for HCOOH (5.6 x 10<sup>3</sup> M/atm) and CH<sub>3</sub>COOH (8.8 x 10<sup>3</sup> M/atm) were derived from thermodynamic data and equilibrium vapor phase concentrations calculated from the aqueous phase measurements. Relative to the similar ratios of HCOO<sub>T</sub> to CH<sub>3</sub>COO<sub>T</sub> in the aqueous phase, differences in precipitation pH resulted in large regional differences in predicted equilibrium vapor phase concentrations. The mechanism by which proportionate concentrations of HCOO<sub>T</sub> and CH<sub>3</sub>COO<sub>T</sub> are maintained in the aqueous phase remains an open question. Comparisons between precipitation in impacted and remote regions indicate that, although possibly important near large population and industrial centers, anthropogenic emissions are probably not major sources for organic acids in precipitation over broad geographic regions.

#### ONGOING RESEARCH

Research efforts which are currently underway within the GPCP include:

- o A reevaluation of processes controlling precipitation chemistry on Bermuda.

- o Analysis of process controlling precipitation chemistry at Katherine, Australia and Amsterdam Island, Indian Ocean.
- o Comparison between the composition of precipitation in China, the United States, and remote regions.
- o An intercomparison of measurement systems for gaseous and particulate organic acids.

#### Reference List

- Church, T. M., J. N. Galloway, T. D. Jickells, and A. H. Knap, 1982. The chemistry of western Atlantic precipitation at the mid-Atlantic coast and on Bermuda. Journal of Geophysical Research 87: 11013-11018.
- Dayan, U., J. M. Miller, W. C. Keene, and J. N. Galloway, 1985. A meteorological analysis of precipitation chemistry from Alaska. Atmospheric Environment 19: 651-657.
- Galloway, J. N. and A. Gaudry, 1984. The chemistry of precipitation on Amsterdam Island, Indian Ocean. Atmospheric Environment 18: 2649-2656.
- Galloway, J. N., G. E. Likens, W. C. Keene, and J. M. Miller, 1982. The composition of precipitation in remote areas of the world. Journal of Geophysical Research 87: 8771-8786.
- Galloway, J. N., G. E. Likens, and M. E. Hawley, 1984. Acid precipitation: Natural versus anthropogenic components. Science 226: 829-830.
- Jickells, T. C., A. H. Knap, T. M. Church, J. N. Galloway, and J. M. Miller, 1982. Acid precipitation on Bermuda. Nature 297: 55-56.
- Keene, W. C., J. N. Galloway and D. H. Holden, Jr., 1983. Measurement of weak organic acidity in precipitation from remote areas of the world. Journal of Geophysical Research 88: 5122-5130.
- Keene, W. C., and J. N. Galloway, 1984a. A note on acid rain in an Amazon rainforest. Tellus 36: 137-138.
- Keene, W. C. and J. N. Galloway, 1984b. Organic acidity in precipitation of North America. Atmospheric Environment 18: 2491-2497.
- Keene, W. C., and J. N. Galloway, 1985. Gran's titrations: Inherent errors in measuring the acidity of precipitation. Atmospheric Environment 19: 199-202.
- Keene, W. C. and J. N. Galloway, 1986. Considerations regarding sources for formic and acetic acids in the troposphere. Journal of Geophysical Research (under review).
- Keene, W. C., A. A. P. Pszenny, J. N. Galloway and M. E. Hawley, 1986. Sea-salt corrections and interpretation of constituent ratios in marine precipitation. Journal of Geophysical Research 91: 6647-6658.

## $\delta C^{13}$ IN ATMOSPHERIC CARBON DIOXIDE

Irving Friedman, Jim Gleason, Augusta Warden  
U.S. Geological Survey  
Denver, CO 80225

### INTRODUCTION

We have continued monitoring of the  $\delta C^{13}$  of atmospheric  $CO_2$ . Samples were collected bi-weekly at South Pole, Mauna Loa, Samoa, and Point Barrow.

### EXPERIMENTAL

The only change to the experimental procedure described in the previous Summary Report (No. 13) has been the periodic analysis of the  $CO_2$  extracted from 10 L flasks filled from a high pressure tank containing Niwot Ridge air. The analysis of these samples assures that the  $CO_2$  extraction procedure, as well as the mass spectrometric analysis, does not change with time.

### RESULTS

The data for 1981 through August 1986 for Mauna Loa, Samoa and Point Barrow are shown in figs. 1, 2, and 3. The data for the South Pole is given from 1981 through December 1985 in fig. 4.

The line in figs. 1, 2, and 3 is the least square average of the data through 1984.

The data for Mauna Loa and Samoa in 1984 to the present shows less seasonal variation in  $\delta C$  than for the previous 3 years, in contrast to Point Barrow where the seasonality appears unchanged for the entire 6 years.

One explanation for the difference between the oceanic stations, Mauna Loa, Samoa, and Point Barrow, is the result of the 1983 El Nino, which would have influenced the ocean atmosphere  $\delta C^{13}$  exchange.

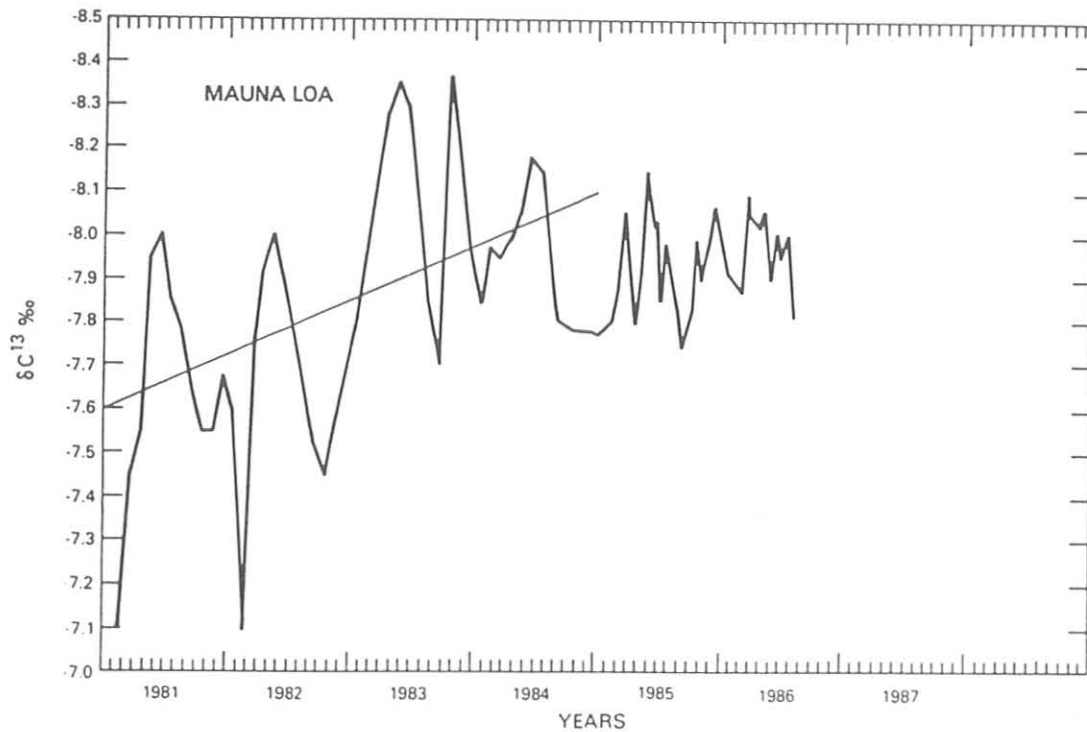


Figure 1.--Record of  $\delta C^{13}$  in atmospheric  $CO_2$  at Mauna Loa.

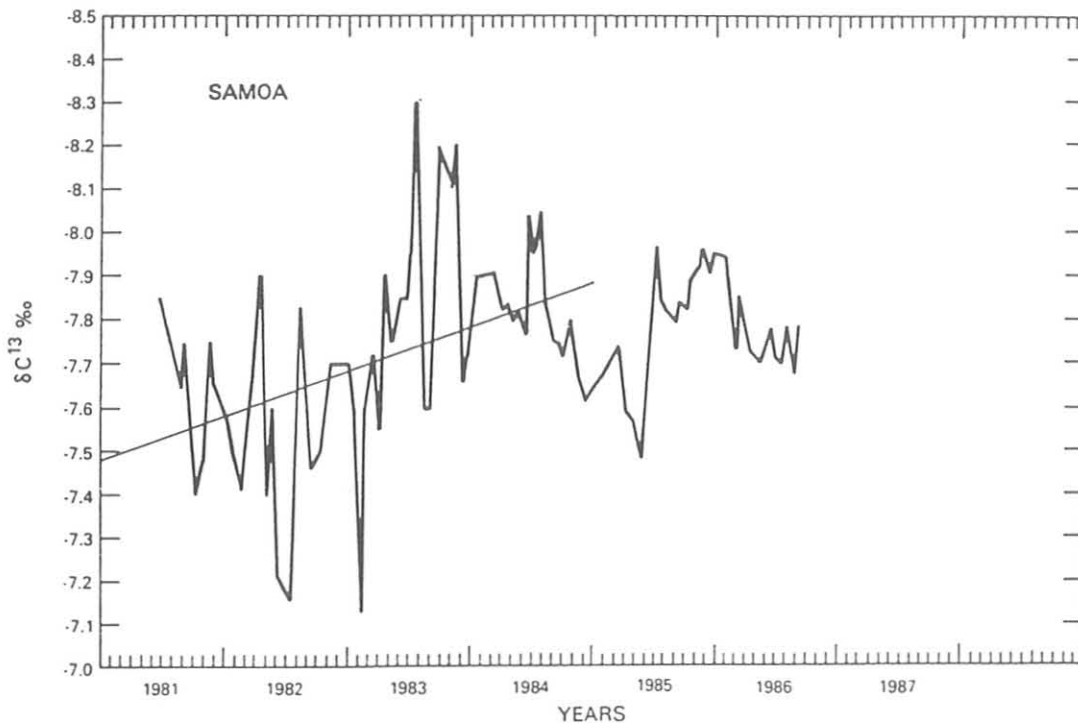


Figure 2.--Record of  $\delta C^{13}$  in atmospheric  $CO_2$  at Samoa.

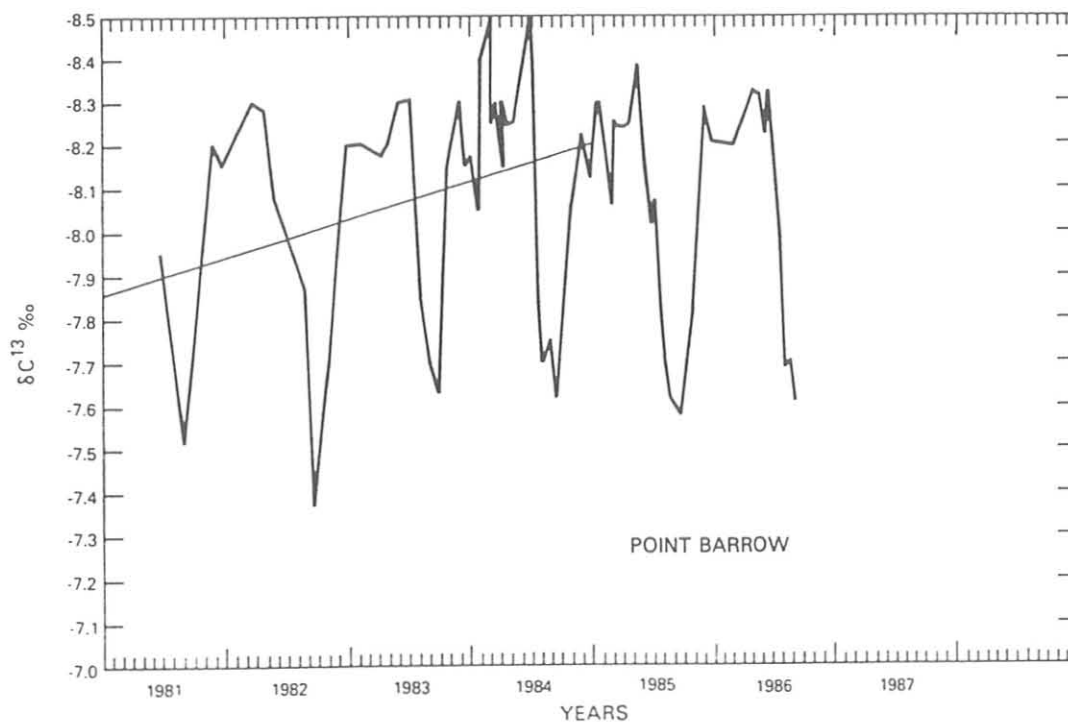


Figure 3.--Record of  $\delta C^{13}$  in atmospheric  $CO_2$  at Point Barrow.

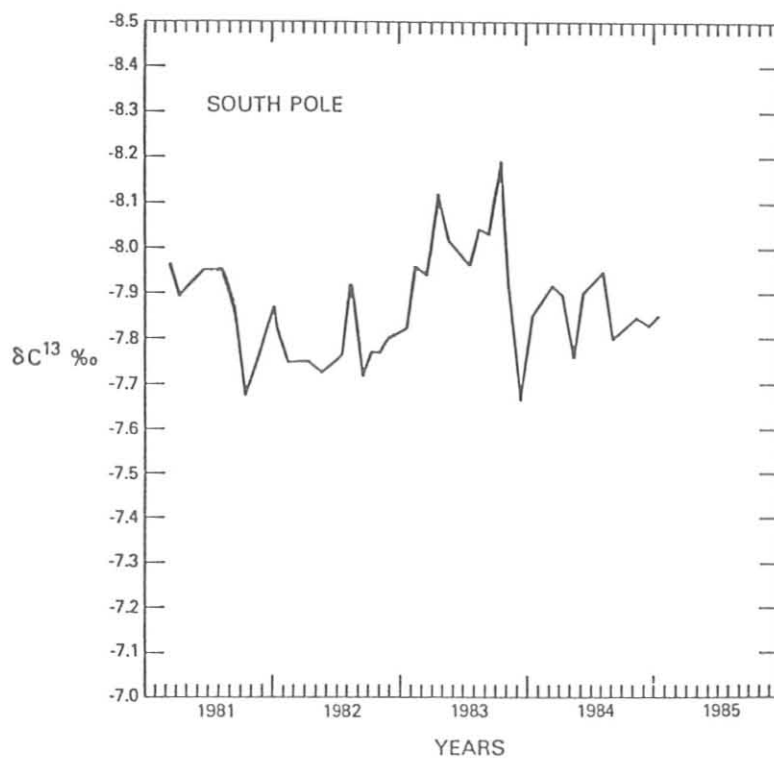


Figure 4.--Record of  $\delta C^{13}$  in atmospheric  $CO_2$  at South Pole.

## FOLLOWING THE TRAIL OF ANTARCTIC WINDS

Eugene J. Mroz, Mohammed Alei, John H. Cappis, Paul R. Guthals,  
Allen S. Mason, and Donald J. Rokop  
Los Alamos National Laboratory  
Los Alamos, NM 87545

The transport of tropospheric air masses from the north to the south (longitudinal transport) is responsible for bringing aerosols and trace gases to Antarctica from the lower latitudes. The atmospheric materials and pollutants from both natural and anthropogenic sources may then become part of the geological climatic record if they are trapped in the southern polar ice cap. If we are to use this record to evaluate the potential greenhouse and albedo effects of air pollutants on global climate, we need to understand the transport mechanisms involved. The Antarctic Tracer Experiment was designed to improve our scientific comprehension of these north-south transport processes by the use of unique atmospheric tracers.

“Heavy” methanes were chosen to track the antarctic winds. These are the heavy isotopic analogues of methane—so named because they are composed of the heavy isotopes of carbon and hydrogen. We released specific amounts of  $^{13}\text{CD}_4$  and  $^{12}\text{CD}_4$  gas into the Antarctic atmosphere and subsequently conducted air and surface sampling in search of the tracer gas. Figure 1 shows the experimental concept and the location of the sampling stations.

Sampling and mass spectrometric analysis techniques developed at Los Alamos can detect these tracers in quantities as small as a few parts in  $10^{17}$  in air. Because of their extremely low natural abundance, their long atmospheric lifetime, and the high sensitivity for their detection, these isotopically unique methanes are ideal for experimentally tracking air masses in Antarctica over long periods of time and more than 4000 km from the release point.

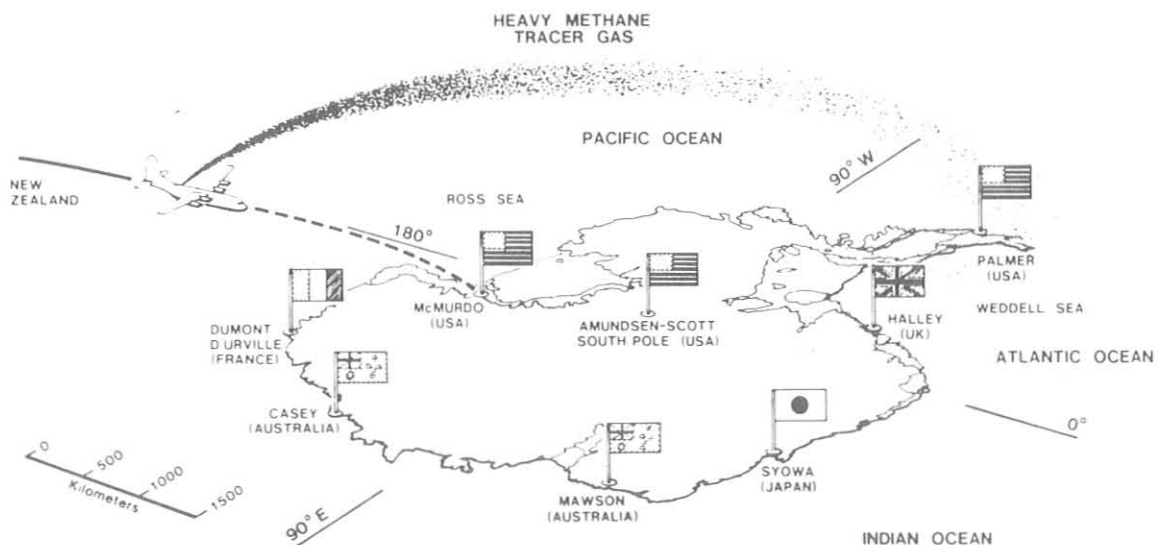


Figure 1.—Schematic showing the location of stations used for ground-based sampling of heavy methane tracers during the Antarctic Tracer Experiment.

Tracers were released between New Zealand and Antarctica in January, June, and October 1984. In January and June, 1 kg of  $^{13}\text{CD}_4$  was released by aircraft 18 000 ft above sea level. In October, 20 kg of  $^{12}\text{CD}_4$  was discharged into the antarctic atmosphere 18 000 ft above sea level and was followed by 1 kg of  $^{13}\text{CD}_4$  at 5000 ft. Following each release, the network of ground-based sampling stations (shown in Fig. 1) was activated and air samples were collected for a period of 60 days. Although no above-ground air sampling was possible during the austral winter, we did collect samples by aircraft after the January and October releases.

#### Detection of Heavy Methane Tracers in Antarctica

By August 1985, all the samples collected in Antarctica were returned to Los Alamos for analysis. Before any samples were analyzed for the heavy methane tracers, we determined normal methane concentrations by gas chromatography with flame ionization detection. This step is necessary because the mass spectrometric analysis of the heavy methanes is normalized to methane in the sample to increase the precision of the procedure. For a number of the samples, we have observed higher than anticipated levels of normal methane. We expected the concentration of methane in antarctic air to be  $\sim 1.65$  ppm with little variability; however, a number of analyses have given values exceeding 2 ppm. This poses no problem for the heavy methane tracer measurements, but it raises some interesting questions about our understanding of atmospheric methane sources and sinks in the southern hemisphere. We are evaluating these observations more carefully to determine whether the samples reflect local contamination, sampling, and/or storage artifacts.

In the aircraft-collected samples, the tracer was first observed over the Ross Ice Shelf  $\sim 26$  h after the release. For the first week following the release, the tracer was observed in nearly every sample collected by aircraft over western Antarctica. However, the heavy methane tracer was not detected in the McMurdo surface samples, indicating that the tagged air parcel had not yet mixed down to the surface as the air passed over the edge of the continent. The tracer's very rapid transport to the continent from the point of release was unexpected. Meteorological trajectory analyses did not predict that this would occur. During the second and third weeks following the release, the frequency of positive samples declined, which suggests that the tracer was being transported out of the region.

The first detection of tracer at the surface of the South Pole occurred 6 to 9 days after the release. During this 3-day period, the surface winds were blowing from the Weddell Sea sector. When this meteorological condition prevails, warm, moist, particle-laden air from the open ocean in the Ross and/or Weddell Sea areas is blown over the polar plateau. These conditions frequently coincide with the breakdown of the inversion over the South Pole and the enhanced downward mixing from above the inversion layer to the surface. We believe that the tracer was carried down to the polar surface in this manner. After a travel time of about 10 days, tracer was detected at Halley Bay (UK), which is located on the coast of the Weddell Sea. Analysis of several samples from the Palmer, Casey, Mawson, and Dumont D'Urville stations (collected after the last detection of tracer at Halley) have all been negative.

## Atmospheric Dispersion of the Tracer

One exciting outcome of this experiment has been the confirmation of a theoretically predicted atmospheric dispersion process. For years, a number of atmospheric researchers throughout the world have been searching for evidence of a transition between the regime in which the dominant atmospheric dispersive process is three-dimensional turbulence and a regime dominated by quasi-two-dimensional circulation systems. These meteorological systems cause extensive distortion by stretching, contorting, and breaking the tracer puff into a “lumpy” tracer plume. This distortion process effectively accelerates the rate at which atmospheric dispersion takes place because each “lump” then behaves as an independently dispersing puff of tracer.

We expected that the transition between these two regimes of atmospheric dispersion would occur at travel times of  $\sim 100$  to  $200$  h. Because the heavy methane tracers have a very high sensitivity for detection, we were able to follow the tagged air masses in the Antarctic Tracer Experiment over this time scale and thus were able to compare experimental data with theory. Figure 2 is a plot of the tracer concentrations as a function of transport time. The data clearly indicate that there is an apparent increase in the tracer’s rate of dilution at times of 100 to 200 h (that is, increased slope). This, to the best of our knowledge, represents the first direct experimental confirmation of the transition between the three- and quasi-two-dimensional dispersion domains.

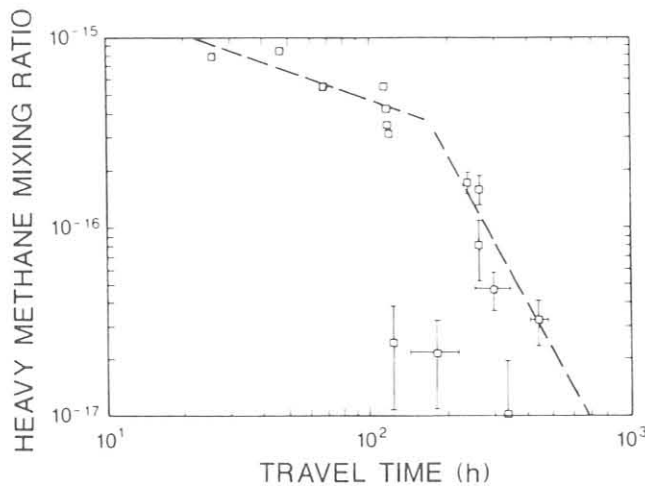


Figure 2.—Heavy methane concentrations as a function of air mass travel times are graphically represented. The change in slope after 100- to 200-h travel time is the first direct experimental indication of two dispersive regimes in the global troposphere.

## SOME RESULTS FROM UVB MEASUREMENTS AT MAUNA LOA AND ROCKVILLE, MD.

Bernard Goldberg  
Smithsonian Institution  
12441 Parklawn Dr.  
Rockville, MD 20852

### INTRODUCTION

The measurement of the UVB region of daylight (285nm-325nm) has been going on for some years at various sites around the world. One of the longest continuous records, other than the Berger-Robertson meters, has been that collected by the solar radiation group at the Smithsonian Institution. This record contains data from Rockville, MD., Wallops Island, VA., Panama Canal, Tallahassee, FL., Barrow, AK., Mauna Loa in Hawaii. The longest record is that from Rockville, MD.. The data are in five nanometer bands centered around 290, 295, 300, 305, 310, 315, 320 and 325 nanometers. These are nominal points that vary by + or - 1nm. The band widths can also vary by the same amount.

### DATA COLLECTION

The data are collected and recorded at one minute intervals from sunrise to sunset every day. Each of the one minute readings is the sum of seventy-two readings over the interval. The calibration of the instrument allows us to give the spectral band values in joules/square meter/nanometer. To make comparisons of the data over the year and from year to year a fixed solar secant value is used. This immediately detrends the variations due to geometry and time of day as well as the geographical location of the instrument. Because of the Rockville location we usually use a solar secant of 2.5 to accommodate all of the seasons. Ozone calculations are done at mid-day between 10 and 14 hrs. This allows us to use at least sixty values to determine a mean ozone value. A comparison with Dobson readings were made to check the data (fig.1).

Satellite data are from the ERB experiment on Nimbus 7 and are taken from nine track tapes. Two of the channels are UV sensors. These are channels 8 and 9 with channel 8 covering from 300-410nm and 9 from 275-360nm. Every fourth day is missing because of the manner in which data are gathered. The daily value is derived from the average of about fourteen measurements. The data are received in engineering units (counts) and then converted into irradiance values.

### RESULTS

The data from 1986 at Mauna Loa and Rockville, the only two sites now operational, had shown a major anomaly in February. There was a tremendous drop in the UVB irradiance. Because of the large amount of cloud cover at Rockville, the drop was noticed first in the Mauna Loa data (fig.2). Using only the clear days at Rockville it was found that the drop there was the same as at Mauna Loa (fig.3). Because the UVB is modulated by the ozone, a concomitant change in

ozone should have occurred. The expected change was found (fig.4). However, when looking for the reason for these sudden changes it was found that the ERB channels 8 and 9 showed the same drop in energy. The drop shown by the ERB channels was not the same order of magnitude. A spectral study showed that the change was greater at wavelengths more affected by ozone than those that are not absorbed by the ozone.

VARIABILITY IN ERB CHANNEL 8

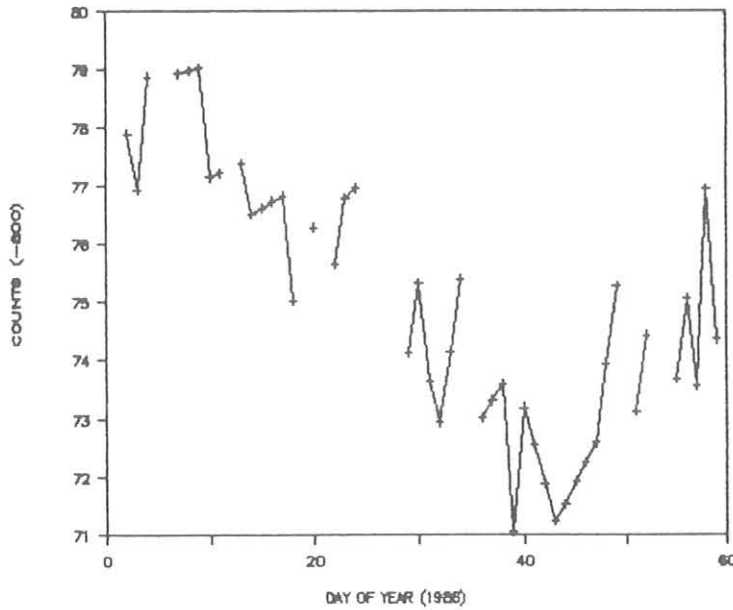


Fig.1. ERB data for the first 60 days in 1986. The drop in UV is very pronounced around day 40 which is in February.

1986 TREND AT 305 NM AT MAUNA LOA

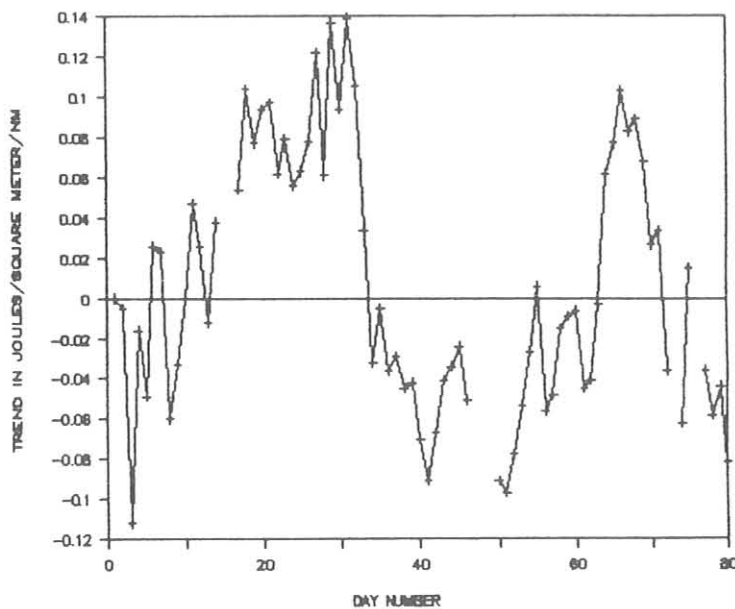


Fig.2. The 305nm band was used to illustrate the drop in irradiance because it clearly shows the large percentage change due to the ozone change. The trend units are data at a solar secant 2.5 and are one minute readings.

### 305NM TREND AT ROCKVILLE (1986)

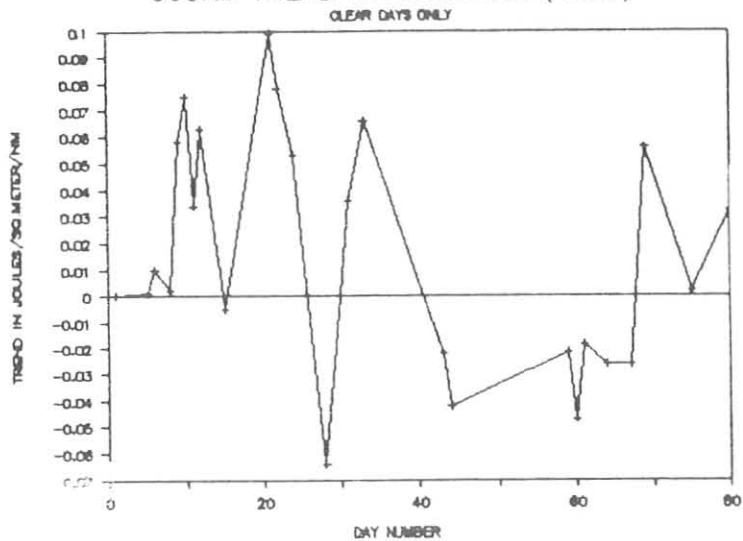
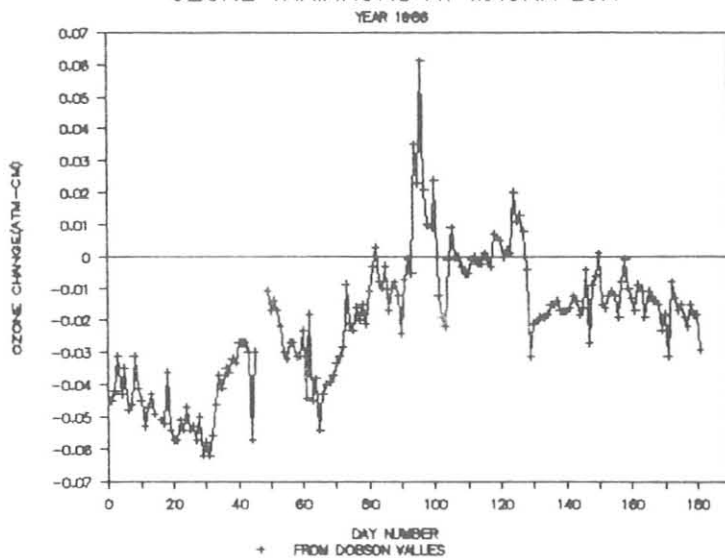


Fig.3. 305nm band trend at Rockville for clear days only. Values are the means of three one minute values around secant 2.5.

### OZONE VARIATIONS AT MAUNA LOA



### OZONE VARIATIONS AT MAUNA LOA

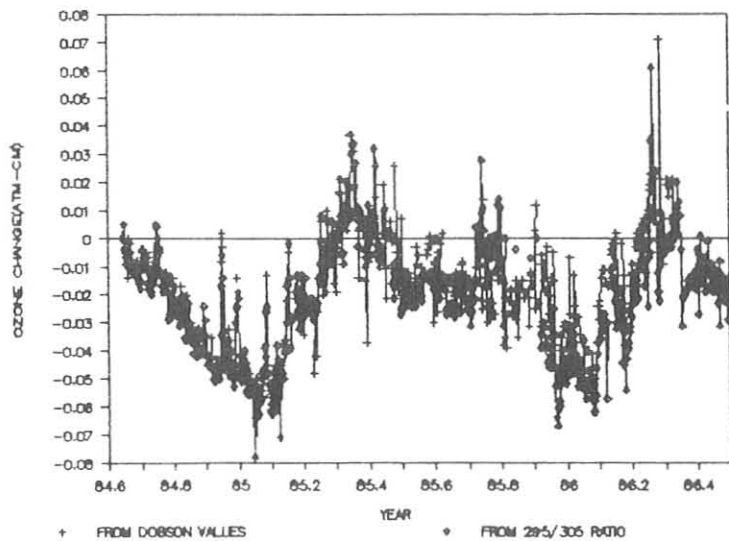


Fig.4. This two part figure shows the ozone trends at Mauna Loa for 1986 and since late 1984 when the UVB instrument was put into place. The upper graph shows the increase during the month of February 1986 while the bottom graph shows the comparison with the Dobson readings over a long period of time.

LOGISTIC AND OTHER MODELS FOR THE TRENDS OF NITROUS OXIDE

M.A.K. Khalil and R.A. Rasmussen  
 Institute of Atmospheric Sciences  
 Oregon Graduate Center  
 Beaverton, Oregon 97006

Nitrous oxide ( $N_2O$ ) and other trace gases have been measured for more than a decade in both hemispheres. This record consists of average concentrations during every January at the South Pole. For comparison, similar measurements have been taken in the Pacific Northwest around  $45^\circ$  north latitude. The results for several trace gases, including  $CCl_3F$ ,  $CCl_2F_2$ ,  $CH_4$ , and  $N_2O$ , were reported recently by Rasmussen and Khalil (1986). These trace gases are all increasing in the earth's atmosphere, probably because of increasing emissions from industrial and agricultural processes, and all have the potential for changing the earth's climate by adding to the greenhouse effect (Ramanathan et al., 1985). The effects of these trace gases on the environment are directly related to the concentrations expected in the future. In this paper we discuss the consequences of various assumptions for extrapolating the trends into the future and apply the methods to nitrous oxide.

The basic equations governing the behavior of a trace gas in the atmosphere are:

$$dC/dt = S - \eta C \quad (1)$$

$$dS/dt = f(S) \quad (2)$$

$$S = S_a + S_n \quad (3)$$

where  $C$  is the average global concentration (here in ppbv),  $S$  is the source (ppb/yr), and  $\eta$  is the inverse of the lifetime ( $\tau$ ).  $S_a$  and  $S_n$  are the anthropogenic and natural components of the global emissions. For  $N_2O$ , as for many other gases, the observed increase is probably related to increasing emissions from anthropogenic sources ( $S_a$ ). How these sources will increase in the future will determine the concentrations of  $N_2O$  and hence its importance in changing the climate. We have compared four possibilities assuming that the natural sources  $S_n$  are constant. The first is simply to extrapolate the present rate of increase into the future, which does not require eqns. (1)-(3). The remaining possibilities are described in eqns. (4)-(6):

$$f(S_a) = \alpha \quad (4)$$

$$f(S_a) = \alpha S_a \quad (5)$$

$$f(S_a) = BS_a(A - S_a) \quad (6)$$

where  $\alpha$ ,  $A$ , and  $B$  are constants and  $BA = \alpha$ . The first two models are simple linear and exponential extrapolations of the present rates of increase of the sources. While these may be adequate for projecting changes over a few years, they have no limits to their increase. The model of eqn. (6) is perhaps the simplest limited growth model, and eqns. (3) and (6) form the logistic equation for the growth of sources (Khalil and Rasmussen, 1982a, 1982b, 1983). In the logistic model the ultimate anthropogenic source is limited to be  $A$  as  $t \rightarrow \infty$ .

The solutions for the four cases mentioned above are:

$$C = C_0 + b t \quad \text{Linear C (7)}$$

$$C = S_n \tau + C_1 e^{-\eta t} + S_0 \tau (1 - e^{-\eta t}) + \alpha \tau^2 (\eta t - 1) e^{-\eta t} \quad \text{Linear S (8)}$$

$$C = S_n \tau + C_1 e^{-\eta t} + [S_0 \tau / (1 + \alpha \tau)] (e^{\alpha t} - e^{-\eta t})$$

Exponential S (9)

$$C = S_n \tau + C_1 e^{-\eta t} + [A S_0 e^{-\eta t} / (A - S_0)] \int_0^t \frac{e^{(\alpha + \eta)v} dv}{1 + [S_0 / (A - S_0)] e^{\alpha v}}$$

Logistic S(10)

where  $C_1$  is the present level of  $N_2O$  contributed by human activities,  $S_0$  is the present anthropogenic source, and  $\tau$  is the lifetime. The values of these parameters are given in Table 1.

Table 1.--Concentrations of  $N_2O$  between 1975 and 1985 and parameters for sources and sinks

Year	PNW (ppbv)	SP (ppbv)	Year	PNW (ppbv)	SP (ppbv)
1975	297	297	1981	304.3	305.0
1976	299	298	1982	306.8	305.4
1977	300.3	300.3	1983	306.7	306.5
1978	302.1	301.2	1984	306.2	306.5
1979	302.0	301.8	1985	307.3	307.5
1980	303.4	303.8			

Parameters for sources and sinks

$S_n$	$S(0)$ (ppbv/yr)	A	$\alpha$ ( $yr^{-1}$ )	$\tau$ (yrs)	$C_1$ (ppbv)
2.78	0.9	3	0.05	100	15

Notes: Contents of the table are based on Rasmussen & Khalil (1986) and Khalil & Rasmussen (1983). PNW denotes the Pacific Northwest representing the clean air of the mid-northern latitudes, and SP denotes the south pole.

For some trace gases, such as  $N_2O$ ,  $CH_4$ , and  $CO_2$ , the anthropogenic sources are related to production of food and energy, which are in turn related to the world population. Therefore, the rates of increase and the upper limits of the logistic equation may be set by the expected growths of population. We have used the estimates of world population from Erlich et al. (1977) to establish the limits of growth for the trace gases. These types of models and estimates have also been discussed earlier by Khalil and Rasmussen (1982a, 1982b, 1983) and applied to  $N_2O$  and  $CH_4$ .

The results are shown in Figure 1. Fig. 1a shows the long-term behavior of the solutions. For shorter lived trace gases the features shown in this panel appear much sooner than for  $N_2O$ . The figure illustrates the speed with which different models allow for large buildups of trace gases. The limited growth in a logistic model is evident in the figure. For instance, the expected doubling time of concentrations for the models discussed is about 65 years for the exponentially increasing sources, about 120 years for linearly increasing sources, and some 300 years for extrapolating the concentrations at present rates of growth. Since the logistic model has built-in limitations to growth, it does not predict a doubling of  $N_2O$  ever. This is perhaps the most significant feature of logistic models in that they provide some assessment

## Nitrous Oxide Trends

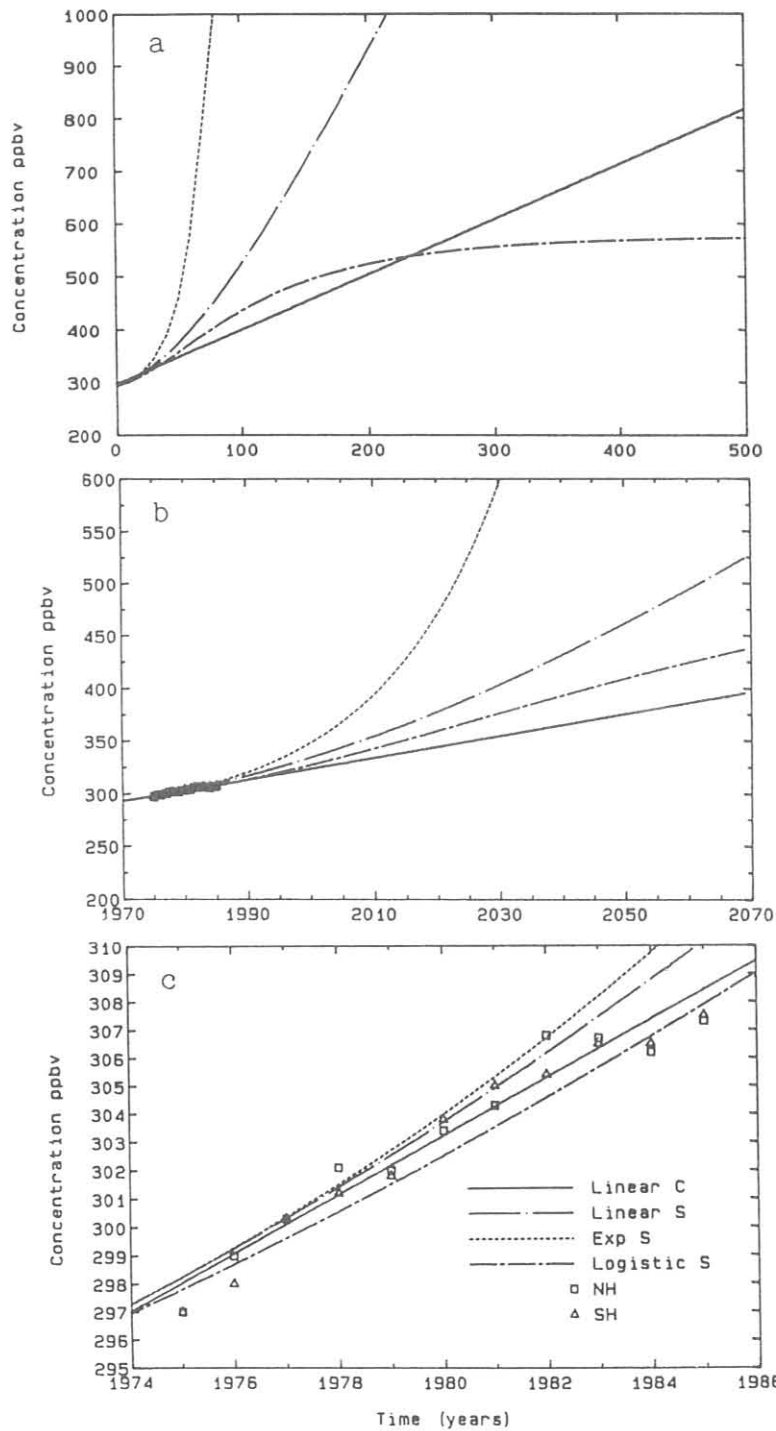


Figure 1.--Trends of N<sub>2</sub>O based on various models for extrapolating present concentrations and emissions. The methods considered are a linear extrapolation of present rates of growth of concentrations, linear and exponential increases of present anthropogenic emissions, and a logistic model for the growth of emissions. Figure 1a shows the overall behavior of the governing mass balance equations; Figure 1b is an expanded view over a century; Figure 1c is a view of N<sub>2</sub>O over the last decade.

of whether large atmospheric concentrations of trace gases are feasible. In other types of extrapolations any concentration can be achieved if sufficient time is allowed, even if these concentrations are unrealistic because they require anthropogenic emissions beyond our present expectations for the growth of population and industry.

Fig. 1b shows extrapolations of the concentration of  $N_2O$  over 100 years for the four cases mentioned above. Fig. 1c is a blowup of the first decade showing more clearly the relationships between the data and the models. The results show that all the models can properly describe the available data from 1975 to 1985. In the longer term the exponential solution (eqn. (5)) quickly becomes unrealistically large. Of the other three methods, the simple extrapolation of the present rate of increase provides the lowest estimated concentrations in the future. This result is perhaps not expected for most other trace gases. It comes about because the rate of growth of  $N_2O$  is relatively slow, at about 0.3% per year, compared to other trace gases that are increasing at much faster rates.

How the concentration of radiatively important trace gases is projected into the future has a substantial effect on the expected concentrations, which in turn determine whether the trace gas is likely to contribute significantly to global warming and climate change. Our results emphasize that physical models should be used to evaluate the expected increases of anthropogenic sources and the limits to their growth.

#### REFERENCES

- Ehrlich, P. R., A. H. Ehrlich, and J. P. Holdren, 1977. Ecoscience. W. H. Freeman, San Francisco.
- Khalil, M. A. K., and R. A. Rasmussen, 1982a. Secular trends of atmospheric methane. Chemosphere 11:877-883.
- Khalil, M. A. K., and R. A. Rasmussen, 1982b. Atmospheric methane ( $CH_4$ ): a review of current research. Proceedings, Second Symposium on the Composition of the Nonurban Troposphere, Boston, Massachusetts, May 25-28, 1982, American Meteorological Society, 120-122.
- Khalil, M. A. K., and R. A. Rasmussen, 1983. Increase and seasonal cycles of nitrous oxide in the earth's atmosphere. Tellus 35B:161-169.
- Ramanathan, V., R. J. Cicerone, H. B. Singh, and J. T. Kiehl, 1985. Trace gas trends and their potential role in climate change. Journal of Geophysical Research 90:5547-5566.
- Rasmussen, R. A., and M. A. K. Khalil, 1986. Atmospheric trace gases: trends and distributions over the last decade. Science 232:1623-1624.

## ATMOSPHERIC SUBMICRON PARTICLE COLLECTION AT THE SPO

R. E. Witkowski and W. A. Cassidy  
University of Pittsburgh  
Pittsburgh, PA 15260

G. W. Penney  
Carnegie-Mellon University  
Pittsburgh, PA 15213

### INTRODUCTION

The electrostatic-type particle collector that was installed at the SPO CAF during the month of December, 1983, for the purpose of collecting atmospheric submicron size particles, some of which may be of extraterrestrial origin, continues to operate successfully (Witkowski, et al., 1986). For the most part, only planned shutdowns of the device have occurred for routine specimen plate changes and, in one instance, for the replacement of the tungsten ionizer wire in the particle ionization chamber during October, 1985. In November, 1986, at the end of this current period of operation, more than 20,000 hours of collection time will have been logged with a total of 45 specimen plates being exposed.

During this present season (January through November, 1986) an experimental set of nine specimen plates, fabricated from high density graphite, are being evaluated. This material, an alternate to stainless steel, was chosen in an effort to reduce fabrication time and costs, while at the same time reducing the total collector inventory of structural metals that offer sources of sample contamination.

Single-particle characterization continues via scanning transmission electron microscopy (STEM) coupled with energy dispersive spectrometry (EDS) and selected area diffraction (SAD) measurements. At the present time, an automated STEM system is being evaluated for the purpose of providing a rapid method to survey scan the large number of specimen plates that have now been returned to the laboratory for study.

### RESULTS AND DISCUSSION

Because this electrostatic particle collection technique employs a low air sampling velocity ( $300 \text{ ft min}^{-1}$ ) coupled with long sampling times (to 4000 hours) and simple charged-particle attachment to a carbon-coated copper grid, the structure of very fine, delicate, submicron-size particles is preserved. It is felt that the delicate shapes of many of the collected particles may give clues as to their origin. Unlike impact-type collectors, no matting or fracturing of the collected material occurs, and no water soluble material is lost as is the case with ice-core-type sampling.

In this search for particles of cosmic origin, the large contribution of sulfuric acid (or sulfate) droplets to the background, as shown in Figure 1, continues to hinder STEM characterization of individual particles. These

droplets effloresce and immediately evaporate when the STEM electron beam impinges upon them. A number of rare particles that cannot be identified either as being of cosmic or terrestrial origin, which exhibit single element composition as measured by EDS, have been collected; some of these are illustrated in Figure 2. The source of these particles remains to be identified; they may be of artificial origin. Possible suggested sources may be from diesel heavy equipment or aircraft engine exhaust or even from earth-orbiting satellites (e.g. paint fragments) that have broken up or were destroyed in space (Marshall, 1985). Such a conclusion has obvious implications concerning contamination at the present site of the CAF.

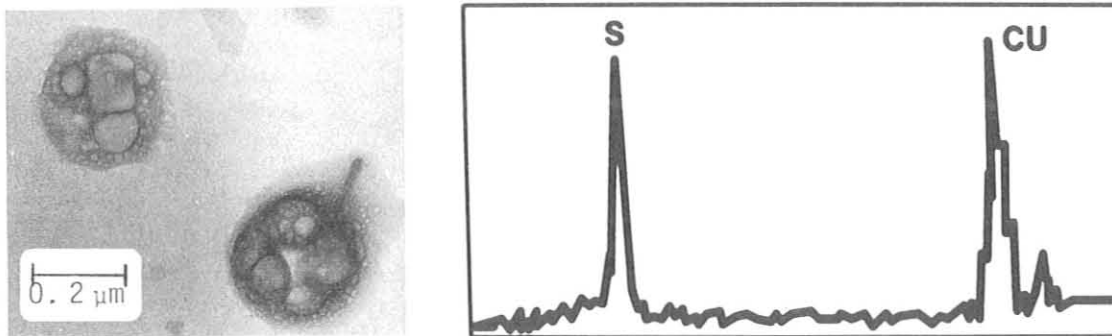


Figure 1.--STEM image and EDS spectrum generated from sulfur-rich droplets collected on specimen plate #8 after 168 hours of exposure. The Cu peaks noted in the EDS spectrum result from the copper grid material of the sampling system.

#### FUTURE PROGRAM

The major effort will be concentrated in the characterization of the particles collected on the returned specimen plates; the automated STEM specimen plate scanning system may prove to be very valuable for the routine survey and identification of the many particles collected. Initially, the survey will concentrate on the search for particles containing the elements Mg, Si, Fe and Ni. In addition, the use of backscattered electron detection, as opposed to the collection of X-ray signals (EDS process) from individual particles, offers some hope in relieving the sulfuric acid (sulfate) background problem while enhancing the ability to quickly identify particles or grains of interest.

#### ACKNOWLEDGMENTS

This continuing effort is part of the University of Pittsburgh Antarctic Search for Meteorites Project and is made possible through NSF Grant DPP 83 14496. We gratefully acknowledge the assistance of Mr. James Waddell, SPO CAF Station Chief, who maintained this experiment throughout the 1985 winter season.

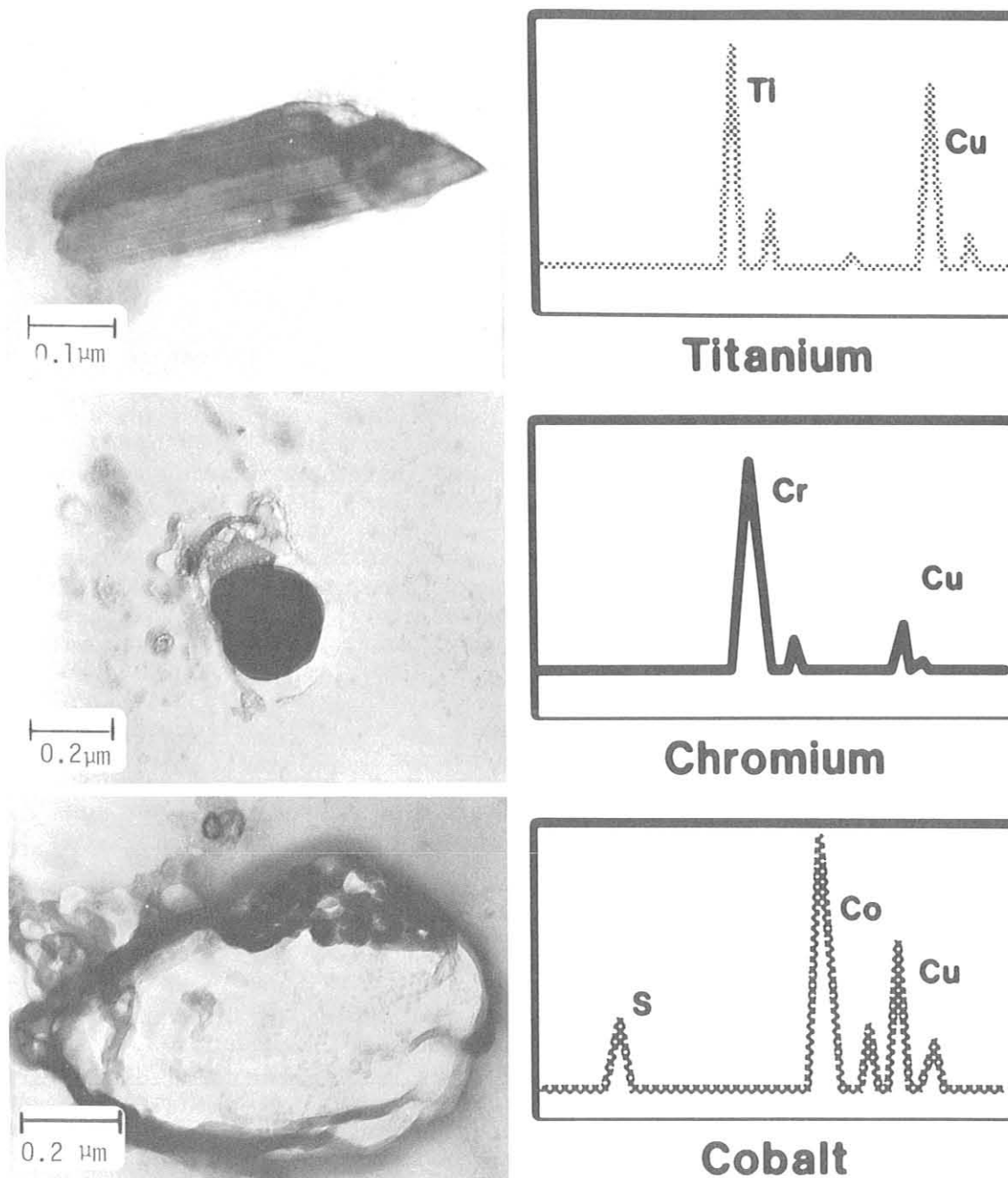


Figure 2.--STEM images and EDS spectra generated from rare particles collected on specimen plate #14 after 1032 hours of exposure. (Cu and S peaks from background.)

#### REFERENCES

Marshall, E., 1985. Space Junk Grows with Weapons Tests, Science, 230:424-425.

Witkowski, R. E., W. A. Cassidy and G. W. Penney, 1986. Atmospheric Submicron Particle Collection at the South Pole Observatory. GMCC Summary Report No. 13, February 1986, Everett C. Nickerson (Ed.) NOAA Environmental Research Laboratories, Boulder, CO, 102-103.

WASHOUT RATIOS OF NITRATE, NON-SEA-SALT SULFATE, AND SEASALT ON  
VIRGINIA KEY, FLORIDA, AND ON AMERICAN SAMOA

Dennis L. Savoie, Joseph M. Prospero, and Ruby T. Nees  
Rosenstiel School of Marine and Atmospheric Science  
University of Miami, Miami, FL 33149-1098

## INTRODUCTION

More precise estimates of the fluxes of nitrate and non-seasalt (NSS) sulfate to the ocean are required for a better understanding of the global atmospheric cycles of sulfur and nitrogen oxides. Estimates of deposition rates suggest that the washout of atmospheric aerosols by precipitation accounts for major portions of these fluxes. Because rainwater concentration data is sparse for marine areas, direct estimates of the wet flux are very uncertain. With precise estimates of the washout ratios, better estimates of the wet flux may be obtained from the relatively large data base which exists for the particulate concentrations of many constituents.

Here, the washout ratios are defined as the ratio of the volume-weighted mean (VWM) concentration in rainwater ( $\mu\text{g}/\text{kg}$  rain) divided by the arithmetic mean concentration in the particulate phase ( $\mu\text{g}/\text{kg}$  air); to obtain dimensionless washout ratios based on concentrations per unit volume, multiply our values by 833. We use the VWM rather than any other parameter because it is the VWM which, when multiplied by the total rainfall, yields a direct estimate of the total wet deposition. Estimates of the washout ratios of nitrate, non-seasalt (NSS) sulfate, and sodium (seasalt) are presented for three marine locations: Virginia Key, Miami, Florida; American Samoa ( $14^{\circ}\text{S}$ ,  $171^{\circ}\text{W}$ ); Bermuda ( $32^{\circ}\text{N}$ ,  $65^{\circ}\text{W}$ ).

## MATERIALS AND METHODS

High volume bulk aerosol samples were collected by drawing air through 20x25 cm Whatman-41 filters at volume flow rates of about  $1.2 \text{ m}^3/\text{min}$ . To minimize contamination from local sources, the pumps (automatically controlled by wind sensors) were in operation only when the winds blew from the ocean at speeds of greater than  $1 \text{ m}/\text{sec}$ . Quarter sections of each filter were extracted with 20-ml of Milli-Q water (Savoie and Prospero, 1982).

Rainwater samples were collected in using automatic wet-dry collectors similar to those used in the National Atmospheric Deposition Program (NADP). The rain was filtered, transferred to polyethylene bottles, and stored at  $5^{\circ}\text{C}$ .

Sulfate and nitrate concentrations in the rainwater and filter extraction solutions were determined to  $\pm 5\%$  by ion chromatography. Sodium was determined to within  $\pm 2\%$  by atomic absorption spectroscopy (Savoie and Prospero, 1982). NSS sulfate concentrations were estimated by subtracting the seasalt contribution ( $0.2517 \times \text{sodium}$ ) from the total sulfate concentrations.

## RESULTS

To determine the washout ratios on Virginia Key, we have used the results from all of the 78 rainwater and 171 aerosol samples collected during calendar year 1984. The results are summarized in Table 1. The 1984 rainwater data is

consistent with the means based on all of the available data (257 samples) from May 1982 through April 1985. The overall averages for that period are 0.51 ug/ml for nitrate, 0.74 for NSS sulfate, and 1.93 for sodium. The annual mean washout ratios for nitrate and NSS sulfate are similar to one another. The washout ratio for sodium is nearly a factor of two higher.

Table 1.--Mean concentrations and washout ratios of sodium, nitrate, and NSS sulfate at Virginia Key, Miami; American Samoa; and Bermuda

		SODIUM	NITRATE	NSS SULFATE
<u>VIRGINIA KEY</u>	Aerosol,ug/m <sup>3</sup>	3.7	1.9	2.8
	Rain,ug/ml	1.7	0.53	0.69
	Washout ratio	550	320	290
<u>AMERICAN SAMOA</u>	Aerosol,ug/m <sup>3</sup>	6.5	0.12	0.41
	Rain,ug/ml	2.83	0.022-0.033	0.136-0.153
	Washout ratio	520	220-330	400-450
<u>Geometric mean washout ratio</u>		540	300	350
<u>BERMUDA</u>	Aerosol,ug/m <sup>3</sup>	2.4	0.61	0.91
	Rain,ug/ml	3.9	0.25	0.64
	Washout ratio	1900	490	840

For American Samoa, the average particulate concentrations were determined by us from 89 weekly samples collected from March 1983 through April 1985 as part of the SEAREX South Pacific Aerosol Network (SEASpan). The weekly rainwater concentrations for the period spanning the SEASpan study were obtained from the NADP NTN database at Colorado State University. A range of values is given for the VWM's of both nitrate and NSS sulfate because most of the nitrate concentrations and a few of the sulfate concentrations were below the detection limit.

For comparative purposes, we have also estimated the washout ratios at Bermuda. However, these estimates must be used with caution. The aerosol and rainwater samples were collected during different periods and, thus, may not be directly comparable. Secondly, the particulate nitrate data at Bermuda was collected during a very small portion of a year. The annual VWM concentrations in rainwater at Bermuda have been reported by Keene et al. (1986). The results cover a period of almost two full years, 21 August 1982 to 18 May 1984, at the High Point site. This is the same site used by Chen and Duce (1983) for the collection of aerosol samples from April to October 1974; the mean NSS sulfate and sodium concentrations from that study are used for the current washout estimates. The particulate nitrate concentrations are based on samples which we collected during August 1982 and February 1983.

## DISCUSSION

For the two locations with long-term concurrent rainwater and aerosol data, Virginia Key and American Samoa, the mean washout ratios are very nearly equivalent to one another: about 300 to 400 for both nitrate and NSS sulfate and about 500 for sodium. In comparison, those estimated for Bermuda are markedly higher: by about 50% for nitrate, about a factor of two for NSS sulfate, and nearly a factor of four for sodium. It is still unclear how much of these differences are real and how much are actually related to the uncertainties in the washout ratios at Bermuda. A substantially different mean meteorology during rain events at Bermuda may well account for a major portion; however, what those difference(s) might be is not at all clear. Until further investigations are conducted to resolve the question, we consider the washout ratios at American Samoa and Virginia Key to be most representative of maritime areas.

On the basis of the variation in the above results and given sufficient aerosol data, we should be able to estimate the wet deposition flux of nitrate and NSS sulfate to the ocean with an accuracy of well within a factor of two using the geometric mean of the washout ratios from Virginia Key and American Samoa. Considering these results, the flux of NSS sulfate to the ocean is probably considerably less than that estimated by Varhelyi and Gravenhorst (1983). To estimate the total sulfate concentrations in rainwater, they used a washout ratio of  $1800 \pm 600$ . This ratio appears to be about a factor of 3 too high even for sea-salt sulfate, and it appears to be a factor of 4 to 6 too high for NSS sulfate. A factor of four correction to their deposition rates would have some major implications with regard to the inputs required to balance the sulfur budget of the marine atmosphere.

Acknowledgments- We wish to thank Tom Snowdon, Nancy Douglas, R. Williams, D. Nelson, and the NOAA GMCC program. The work was supported by National Science Foundation grants OCE-84-5609 and ATM-83-11335.

## REFERENCES

- Chen, L., and R. A. Duce, 1983. The sources of sulfate, vanadium and mineral matter in aerosol particles over Bermuda. Atmospheric Environment 17:2055-2064.
- Keene, W. C., A. A. P. Pszenny, J. N. Galloway, and M. E. Hawley, 1986. Sea-salt corrections and interpretation of constituent ratios in marine precipitation. Journal of Geophysical Research 91:6647-6658.
- Savoie, D. L., and J. M. Prospero, 1982. Particle size distribution of nitrate and sulfate in the marine atmosphere. Geophysical Research Letters 9:1207-1210.
- Varhelyi, G., and G. Gravenhorst, 1983. Production rate of airborne sea-salt sulfur deduced from chemical analysis of marine aerosols and precipitation. Journal of Geophysical Research 88:6737-6751.

## SEASONAL VARIATION OF $^{210}\text{Pb}$ AND $^7\text{Be}$ AT MAUNA LOA AND BARROW

Richard Larsen and Herbert Feely  
USDOE Environmental Measurements Laboratory  
New York, New York 10014

### INTRODUCTION

Air filter samples are routinely collected by GMCC personnel at BRW, MLO, SMO and SPO for the USDOE Surface Air Sampling Program. The primary objective of this program is to study the temporal and spatial distribution of specific natural and man-made radionuclides in the surface air. The concentrations of  $^{210}\text{Pb}$  at MLO show a seasonal cycle and wide variations on a weekly time scale. At BRW the concentrations of both  $^{210}\text{Pb}$  and  $^7\text{Be}$  display seasonal cycles, and week to week variability.

### MATERIALS AND METHODS

Hi-volume air filter samples are collected on a weekly basis using Microsorban filter material. The air samplers at MLO and BRW move about 1.0 and 2.0 thousand cubic meters of air per day, respectively, through a 20 cm diameter filter. A section of each filter is compressed into a 1 to 2  $\text{cm}^3$  cylinder, and is analyzed by gamma-ray spectrometry using a high purity germanium (HPGe) detector with a 1.5 cm diameter well. A second section of each filter is composited on a monthly basis. The monthly composite is compressed into a 45  $\text{cm}^3$  plastic planchet, and is analyzed for gamma-ray emitting nuclides using high resolution germanium detectors of either an n-type low energy coaxial or a Ge(Li) or HPGe p-type coaxial. Concentrations of the gamma-ray emitting nuclides are determined by computer resolution of the spectral data.

### RESULTS

Figures 1 and 2 show the long term seasonal cycle and the weekly surface air concentrations, respectively, of  $^{210}\text{Pb}$  at MLO. For BRW, analogous data for  $^{210}\text{Pb}$  are shown in Figures 3 and 4, and for  $^7\text{Be}$  in Figures 5 and 6.

The cumulative mean monthly surface air concentrations with one sigma errors are plotted in Figures 1, 3 and 5. The  $^{210}\text{Pb}$  monthly means represent about six years of measurements, while the  $^7\text{Be}$  monthly means represent about 10 years. The weekly surface air concentrations of  $^{210}\text{Pb}$  and  $^7\text{Be}$  are reported for 1985 samples. There are gaps in the curves in Figures 2, 4 and 6 because of missing data.

### DISCUSSION

The surface air concentrations of  $^{210}\text{Pb}$  at MLO show a seasonal cycle, with the highest concentrations observed in April and May. The weekly concentrations of  $^{210}\text{Pb}$  show a pronounced episodic behavior throughout the year. Parrington et al. (1983) reported that there is a spring peak in

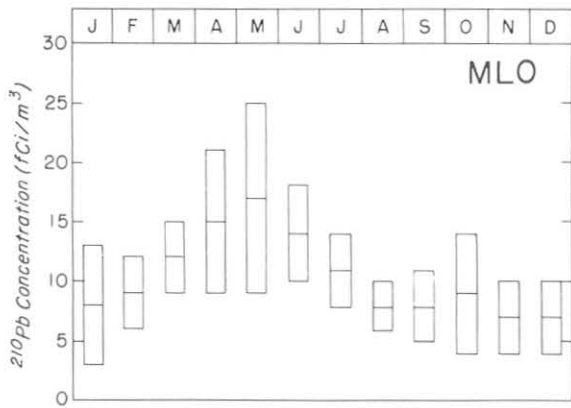


Figure 1.--Monthly  $^{210}\text{Pb}$  at MLO.

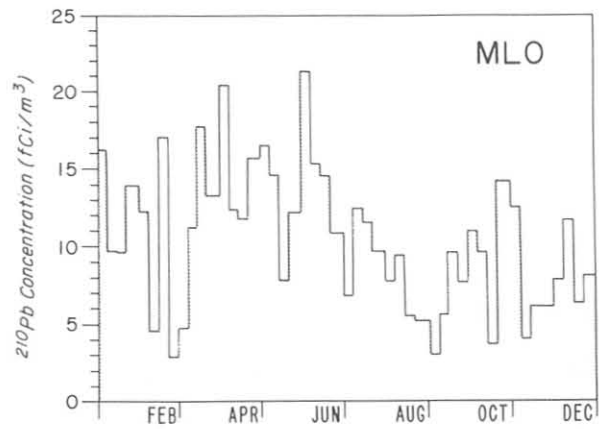


Figure 2.--Weekly  $^{210}\text{Pb}$  at MLO during 1985.

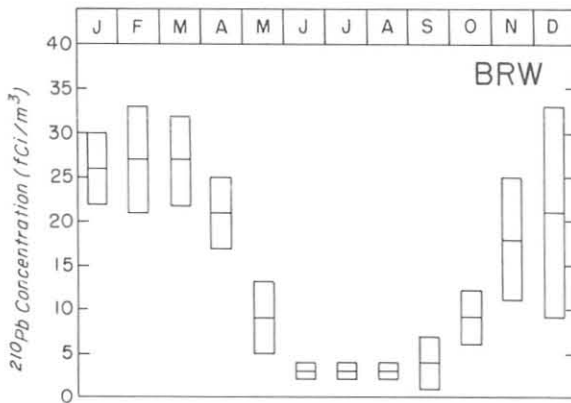


Figure 3.--Monthly  $^{210}\text{Pb}$  at BRW.

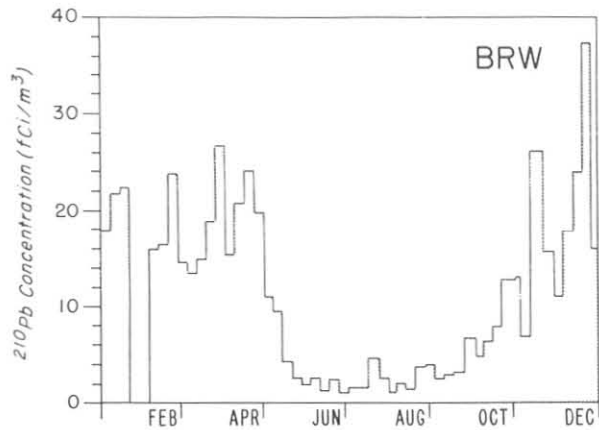


Figure 4.--Weekly  $^{210}\text{Pb}$  at BRW during 1985.

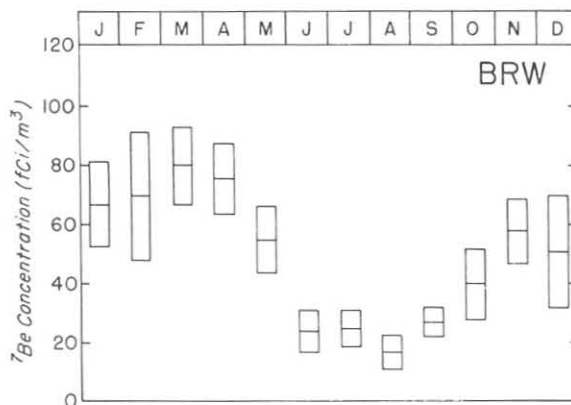


Figure 5.--Monthly  $^7\text{Be}$  at BRW.

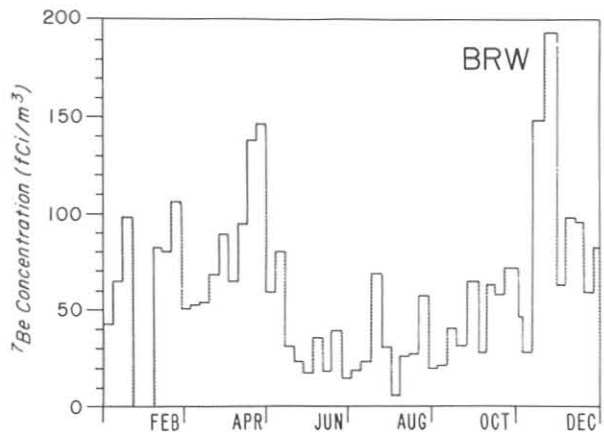


Figure 6.--Weekly  $^7\text{Be}$  at BRW during 1985.

aluminum concentrations in the aerosol at MLO, and attributed it to the influx of dust from the Asian continent. The  $^{210}\text{Pb}$  spring peak appears to be derived from the same source.

The concentrations of  $^7\text{Be}$  and  $^{210}\text{Pb}$  at BRW reach a maximum during the late winter and early spring. At that time of year the tropospheric circulation transports pollutants from mid-latitude continental regions into the polar regions, producing the Arctic haze layer (Lowenthal and Rahn, 1985; Barrie, 1986). Figures 4 and 6 show the episodic nature of the surface air concentrations of  $^7\text{Be}$  and  $^{210}\text{Pb}$  within the seasonal cycle. Iversen and Joranger (1985), among others, observed similar episodic behavior of anthropogenic materials in the Norwegian Arctic. Summertime episodes of elevated concentrations of  $^7\text{Be}$  and  $^{210}\text{Pb}$  can be observed in Figures 4 and 6. Summertime episodes of  $^{210}\text{Pb}$  in the Arctic were also described by Samuelsson et al. (1986), while Pacyna and Ottar (1985) described episodes of transport of crustal and anthropogenic materials into the Norwegian Arctic during the summer.

The rate of emission of  $^{222}\text{Rn}$ , from which  $^{210}\text{Pb}$  is derived, should be greater from the dry soils of the interior Asian continent than from the moist soils of Europe. Thus  $^{210}\text{Pb}$  may be useful, in conjunction with other elements and compounds, as a tracer for air masses that enter the Arctic from off the central regions of the Asian continent.

#### REFERENCES

- Barrie, L., 1986. Arctic air pollution: An overview of current knowledge. Atmospheric Environment 20: 643-663.
- Iversen, T. and E. Joranger, 1985. Arctic air pollution and large scale atmospheric flows. Atmospheric Environment 19: 2099-2108.
- Lowenthal, D. and K. Rahn, 1985. Regional sources of pollution aerosol at Barrow, Alaska during winter 1979-80 as deduced from elemental tracers. Atmospheric Environment 19: 2011-2024.
- Pacyna, J. and B. Ottar, 1985. Transport and chemical composition of the summer aerosol in the Norwegian Arctic. Atmospheric Environment 19: 2109-2120.
- Parrington, J., W. Zollner and N. Aras, 1983. Asian dust: Seasonal transport to the Hawaiian Islands. Science 220: 195-197.
- Samuelsson, C., L. Hallstadius, B. Persson, R. Hedvall and E. Holm, 1986.  $^{222}\text{Rn}$  and  $^{210}\text{Pb}$  in the Arctic summer air. Journal of Environmental Radioactivity 3: 35-54.

## RADIOACTIVITY AT BARROW AND MAUNA LOA FOLLOWING THE CHERNOBYL ACCIDENT

Richard Larsen and Z. Russell Juzdan  
USDOE Environmental Measurements Laboratory  
New York, New York 10014

### INTRODUCTION

With the support of NOAA/GMCC daily air filter and bulk deposition samples were collected at BRW and MLO following the Chernobyl accident. Bulk deposition samples were also collected at the GMCC office located in Hilo, Hawaii. These samples were analyzed by gamma-ray spectrometry to measure their content of fission products, such as  $^{131}\text{I}$  and  $^{137}\text{Cs}$ , that are present in the Chernobyl debris. The debris sampled at these sites exhibited large differences in composition, and at BRW there were significant day to day variations.

### MATERIALS AND METHODS

Hi-volume air filter samples were collected during May on a daily basis, whenever possible, at BRW and MLO using Microsorban filter material. Daily bulk deposition samples were collected at BRW and MLO using plastic bag inserts in a 3 1/2 gallon plastic container having a 28.5 cm diameter. At Hilo, plastic buckets were used to collect bulk samples. After every precipitation event the bucket was sealed and sent to EML, and a new bucket was exposed. Some of these deposition samples were composited for analysis. The air filters were placed into 45 cm<sup>3</sup> plastic planchets and were analyzed for gamma-ray emitting radioisotopes using high resolution germanium detectors. The wet bulk samples were placed in 90 cm<sup>3</sup> aluminum cans for gamma-ray counting. Samples that had large volumes and had specific activities that were too low to count were evaporated to 90 cm<sup>3</sup>. When the bulk sample contained no water, the plastic inserts were placed in Marinelli beakers and counted. None of the deposition samples contained  $^{131}\text{I}$  concentrations that were measurable without evaporation, and  $^{131}\text{I}$  can be lost during evaporation. Thus no  $^{131}\text{I}$  deposition data are reported.

### RESULTS

The surface air concentrations of  $^7\text{Be}$ ,  $^{131}\text{I}$ ,  $^{134}\text{Cs}$ ,  $^{137}\text{Cs}$  and  $^{103}\text{Ru}$  at BRW and MLO are presented in Tables 1 and 2, respectively. The deposition of  $^{134}\text{Cs}$ ,  $^{137}\text{Cs}$  and  $^{103}\text{Ru}$  at MLO and Hilo are given in Tables 3 and 4, respectively. For all samples the radionuclides are corrected for decay to the mid-point of the collection period.

### DISCUSSION

The data for the air filter samples in Tables 1 and 2 reveal that the Chernobyl debris intercepted at Barrow had a higher  $^{131}\text{I}/^{137}\text{Cs}$  ratio, and a lower  $^{103}\text{Ru}/^{137}\text{Cs}$  ratio than the debris intercepted at Mauna Loa.

**Table 1.--Surface air concentrations at BRW**

Collection Period	(Femtocuries/Cubic Meter)				
	<sup>7</sup> Be	<sup>131</sup> I	<sup>134</sup> Cs	<sup>137</sup> Cs	<sup>106</sup> Ru
5/05 - 5/06	34.6 ± 10.9	< 19.0	< 1.5	< 1.9	< 2.8
5/06 - 5/07	57.9 ± 8.0	23.2 ± 10.5	< 0.8	< 1.1	< 1.9
5/07 - 5/08	55.2 ± 9.1	17.5 ± 6.9	2.3 ± 0.8	1.6 ± 0.7	
5/08 - 5/09	104.1 ± 17.4	63.8 ± 13.8	2.9 ± 0.8	5.6 ± 1.4	4.6 ± 1.8
5/09 - 5/11	94.2 ± 0.1	46.2 ± 2.5	18.0 ± 1.4	27.6 ± 1.5	
5/11 - 5/12	52.4 ± 9.5	32.6 ± 2.2	18.6 ± 1.3	25.4 ± 1.3	
5/12 - 5/13	38.1 ± 11.7	42.9 ± 2.4	9.5 ± 0.7	19.4 ± 1.2	
5/13 - 5/14	61.7 ± 7.5	23.6 ± 1.6	11.0 ± 0.9	14.2 ± 0.9	
5/14 - 5/15	< 29.8	42.7 ± 3.1	< 1.8	< 2.3	
5/15 - 5/16	37.5 ± 4.9	34.5 ± 1.2	4.0 ± 0.3	8.2 ± 0.5	
5/16 - 5/17	29.8 ± 7.9	36.7 ± 1.6	2.6 ± 0.6	6.6 ± 0.8	
5/17 - 5/18	50.3 ± 12.0	178.6 ± 5.9	4.2 ± 1.1	6.3 ± 1.3	
5/18 - 5/19	40.4 ± 5.7	89.3 ± 5.7	3.6 ± 0.8	7.0 ± 0.8	2.8 ± 0.6
5/19 - 5/20	50.2 ± 5.7	66.1 ± 4.0	6.7 ± 0.7	13.3 ± 0.9	3.9 ± 0.6
5/20 - 5/21	57.6 ± 6.7	57.5 ± 4.0	8.1 ± 0.8	15.5 ± 1.0	5.6 ± 0.7
5/21 - 5/22	55.2 ± 5.6	218.7 ± 6.6	7.8 ± 0.8	15.5 ± 1.0	8.1 ± 0.8
5/22 - 5/23	46.3 ± 5.0	54.7 ± 3.0	6.0 ± 0.8	13.2 ± 0.8	8.3 ± 0.7
5/23 - 5/24	27.8 ± 2.7	57.3 ± 2.7	3.8 ± 0.4	7.3 ± 0.6	4.6 ± 0.5
5/24 - 5/25	33.8 ± 3.3	39.8 ± 2.0	4.3 ± 0.4	8.8 ± 0.5	4.9 ± 0.4
5/25 - 5/26	41.9 ± 3.5	33.7 ± 1.4	5.4 ± 0.4	11.0 ± 0.5	9.3 ± 0.5
5/26 - 5/27	47.3 ± 2.7	25.6 ± 1.0	8.2 ± 0.4	16.8 ± 0.5	15.3 ± 0.5

\* Air filter sample collected using a Brooks/Roots system (SASP pump)  
 < Less than reported value  
 Errors reported represent two standard deviations of the counting error  
 Blank spaces represent data calculations in progress

**Table 2.--Surface air concentrations at MLO**

Collection Period	(Femtocurie/Cubic Meter)				
	<sup>7</sup> Be	<sup>131</sup> I	<sup>134</sup> Cs	<sup>137</sup> Cs	<sup>106</sup> Ru
5/01 - 5/02	246.0 ± 16.1	< 5.3	< 1.5	< 1.7	
5/02 - 5/05	119.6 ± 8.3	< 1.7	< 0.6	< 0.7	
5/08 - 5/09	146.9 ± 24.1	< 5.4	< 2.5	< 3.2	
5/09 - 5/12	165.6 ± 6.2	1.1 ± 0.4	< 0.5	< 0.6	
5/12 - 5/13	283.1 ± 18.1	< 4.0	4.9 ± 1.7	< 2.5	
5/13 - 5/14	308.8 ± 25.4	< 14.9	< 2.2	3.5 ± 1.3	
5/14 - 5/15	304.2 ± 16.7	< 12.1	< 1.1	2.3 ± 0.7	
5/15 - 5/16	313.2 ± 2.7	< 12.6	< 1.0	1.8 ± 1.4	
5/16 - 5/19	35.7 ± 2.0	12.3 ± 4.8	< 1.6	< 1.3	
5/21 - 5/22	26.6 ± 2.2	< 10.5	< 2.9	< 2.3	
5/22 - 5/23	235.5 ± 9.7	2.6 ± 1.9	< 0.7	0.9 ± 0.5	1.3 ± 0.6
5/23 - 5/27	187.4 ± 3.5	3.4 ± 0.4	1.1 ± 0.2	2.2 ± 0.2	4.3 ± 0.2
5/27 - 5/28	186.5 ± 14.0	19.1 ± 3.3	5.8 ± 1.0	9.9 ± 1.3	24.9 ± 1.8
5/28 - 5/29	360.8 ± 16.3	28.5 ± 3.3	11.2 ± 1.6	22.9 ± 1.5	46.9 ± 2.0
5/29 - 5/30	125.4 ± 5.4	4.8 ± 1.3	2.6 ± 0.4	5.2 ± 0.5	10.8 ± 0.6
5/30 - 6/02	179.4 ± 2.6	7.1 ± 0.4	2.9 ± 0.2	6.3 ± 0.2	15.2 ± 0.3

\* Air filter sample collected using a Brooks/Roots System (SASP pump)  
 < Less than reported value  
 Errors reported represent two standard deviations of the counting error  
 Blank spaces represent data calculations in progress

Table 3.--Total deposition at MLO

Collection Period	Precipitation cm	<sup>134</sup> Cs mCi/km <sup>2</sup>	<sup>137</sup> Cs mCi/km <sup>2</sup>	<sup>106</sup> Ru mCi/km <sup>2</sup>
5/09 - 5/12	3.0	< 0.05	< 0.07	< 0.29
5/12 - 5/20	0.0	< 0.01	< 0.02	----
5/20 - 5/27	0.0	----	< 0.02	----
5/27 - 5/29	~0.2	< 0.05	0.09 ± 0.04	< 0.16
5/30 - 6/02	~0.4	< 0.02	0.03 ± 0.01	< 0.06

Table 4.--Total deposition at Hilo

Collection Period	Precipitation cm	<sup>134</sup> Cs mCi/km <sup>2</sup>	<sup>137</sup> Cs mCi/km <sup>2</sup>	<sup>106</sup> Ru mCi/km <sup>2</sup>
5/02 - 5/09	9.1	< 0.02	< 0.03	< 0.09
5/11 - 5/16	2.4	0.17 ± 0.01	0.34 ± 0.03	0.27 ± 0.08
5/18 - 5/27	1.3	0.05 ± 0.01	0.09 ± 0.02	0.14 ± 0.07
5/28 - 5/30	5.1	0.05 ± 0.02	0.09 ± 0.03	< 0.18

A similar pattern was observed by Uematsu (University of Rhode Island; personal communication, 1986) in surface air at Gambell, St. Lawrence Island and at Midway Island. At Barrow the <sup>131</sup>I concentrations and the <sup>131</sup>I/<sup>137</sup>Cs ratios were especially high during May 17-18 and May 21-22. Uematsu observed periods of high <sup>131</sup>I at Gambell during May 5-14 and May 20-22. We have not observed this pattern at any of our other North American sites (Larsen et al., 1986). Evidently the portions of the cloud of debris from Chernobyl that reached these Arctic sites were quite heterogeneous.

At MLO the concentrations of <sup>131</sup>I were below or near our limits of detection during the first half of May. On the other hand, beginning by May 10, Uematsu detected significant concentrations of <sup>131</sup>I and <sup>137</sup>Cs at Oahu. Our deposition data for MLO are consistent with our air filter measurements at that site, while our deposition data for Hilo are consistent with Uematsu's observations on Oahu. Evidently substantial portions of the Chernobyl cloud reached the Hawaiian Islands below the marine boundary layer by May 10, but only traces reached MLO, above the marine boundary layer before, May 16.

#### REFERENCE

Larsen, R. J., C. G. Sanderson, W. Rivera and M. Zamichieli, 1986. The characterization of radionuclides in North American and Hawaiian surface air and deposition following the Chernobyl accident. (Unpublished manuscript), 100 pp.

## EXPERIMENTAL SAMPLING OF ATMOSPHERIC METHANE

Lester Machta, Kirby Hanson, Monte Poindexter  
Air Resources Laboratory, NOAA  
Silver Spring, MD 20910

An experimental program of continuous air sampling for atmospheric methane was begun at Virginia Key, FL in August 1985, and at McMurdo Sound, Antarctica in November 1985. The air samplers are located at the AOML/ERL/NOAA Building on Virginia Key (4301 Rickenbacker Causeway, Miami) and in the Cosray Building at McMurdo Sound. During 1985 the equipment recovered discrete air samples over 24-hr periods. The feasibility of using cryogenic methods for extracting methane are being studied. Laboratory analysis of the samples for methane are planned.

## 9. INTERNATIONAL ACTIVITIES

During October 1985, the NOAA SRF absolute cavity radiometers were taken to Davos, Switzerland, for participation in the WMO-sponsored Sixth International Pyrheliometer Comparison (IPC VI). These comparisons are held every 5 years and enable participants to compare directly with the world standard group of radiometers. The WSG sensors are used to maintain the WRR scale, and participation by NOAA establishes a check of the performance of the SRF standards and maintains traceability to the WRR.

GMCC personnel continued to participate in the WMO Global Ozone Research and Monitoring Project to upgrade the quality of Dobson ozone spectrophotometers throughout the world. Instruments calibrated in 1985 were nos. 87 (Peru) and 41 (United Kingdom).

A new round of spectrophotometer calibrations in the global Dobson instrument station network was undertaken in March 1985 by means of traveling standard lamps.

Plans were formulated to conduct an international comparison of Dobson ozone spectrophotometers at Arosa, Switzerland in 1986. At least 12 countries are expected to participate.

Cooperative Umkehr observation programs with automated Dobson ozone spectrophotometers continued in 1985 at Observatory Haute Provence, France, and Perth, Australia.

R. Grass and R. Evans visited Huancayo, Peru, during September and October 1985 to install automated Dobson ozone spectrophotometer no. 87 for operation at the Huancayo Observatory. The Huancayo station is the sixth automated Dobson station to be installed by the NOAA GMCC group and is one of seven global sites where Umkehr observations will be made on a long-term basis to monitor possible future stratospheric ozone depletion.

E. Nickerson served on a thesis examining committee at the Université de Clermont II, Clermont-Ferrand, France. Also while in France, he assisted in completing revisions to a joint numerical modeling paper that was subsequently published in the Monthly Weather Review. During the course of this visit (19-26 March) discussions were held on the proposed use of the NOAA/LAMP mesoscale air-quality model in a field experiment in Germany.

R. Schnell was an invited speaker at the week-long Arctic Haze Policy and Research Planning Meeting, Cambridge, UK, 2-6 September 1985. At the meeting, plans for the Second Arctic Gas and Aerosol Sampling Program (AGASP II) were discussed with participants and European collaborators. Following the meeting, Schnell spent 2 days in France discussing a possible satellite-tracked balloon Arctic haze tracer program with French scientists from a variety of government and university groups.

During 26-28 August, J. DeLuisi visited G. Fiocco at the University of Rome to discuss the role of the Frascati lidar in a world network. Data from the world lidar network will be used to correct Umkehr observations of stratospheric ozone. Possible cooperative research projects were discussed in

the context of the U.S.-Italy bilateral agreement, which was scheduled for renewal in the fall of 1985. The possibility of Italy placing a lidar in Antarctica was brought up because Italy plans to establish a research site on that continent. F. Congeduti, lidar expert from Frascati, visited GMCC to become familiar with our lidar program and work with the improvement of the analysis of raw lidar data. His visit was supported mainly by the Italian ministry of research.

During 10-12 December, J. DeLuisi participated in a special WMO-sponsored workshop to organize a global lidar network intended to encourage research with modern lidar technology. Research areas in which modern lidar technology can make notable contributions in a networked system were suggested. Among these are aerosol vertical structure, ozone ground truth and relationships between ozone and atmospheric dynamics, atmospheric temperature structure up to the stratopause, aerosol corrections to satellite remote sensors, and cloud structure and dynamics. WMO will issue a special report on the workshop.

In September, C. Mateer from the Canadian AES at Toronto was a scientific visitor at GMCC in Boulder. He worked on new ozone absorption coefficients for the Dobson instrument, and also worked on the aerosol correction to the Umkehr measurement.

J. Peterson and T. Conway participated in the conference Atmospheric Carbon Dioxide: Its Sources, Sinks, and Global Transport at Kandersteg, Switzerland, 2-6 September 1985. The papers "CO<sub>2</sub> Variability Between High Northern Latitude Sites," and "Recent Results from the NOAA/GMCC CO<sub>2</sub> Flask Sampling Network" were presented by Peterson and Conway, respectively.

In October 1985, 24 glass flasks and a portable air-sampling unit were sent to T. Nakazawa of the Upper Atmosphere Research Laboratory, Tohoku University, Sendai, Japan. Air samples will be collected at Syowa Station (69.0°S, 39.6°E), the Japanese Antarctic Research Program site. The GMCC flask sample CO<sub>2</sub> measurements will be compared to in situ and flask CO<sub>2</sub> measurements made by the Japanese at Syowa during 1986. The flasks should arrive in Boulder in early 1987.

J. Peterson, P. Tans, and T. Conway attended the 2nd WMO Expert Meeting on Atmospheric Carbon Dioxide Measurement Techniques held at Lake Arrowhead, CA, 4-8 November 1985. The meeting was attended by representatives from Australia, Canada, Federal Republic of Germany, France, Italy, New Zealand, People's Republic of China, Peru, Republic of Korea, Spain, the United States, and WMO. Discussion topics were CO<sub>2</sub> standards and calibration techniques, field measurements and analytical techniques, reporting and publication of data, and recommendations. A summary of the discussions will be published as a WMO report.

Collection of flask samples for CO<sub>2</sub> and CH<sub>4</sub> analyses was begun in June 1985 at Alert, N.W.T., Canada (82.5°N, 62.3°W), in cooperation with N. Trivett, AES, Canada. Alert is now the northernmost sampling site in the GMCC flask sampling network. When AES begins in situ CO<sub>2</sub> and CH<sub>4</sub> measurements at Alert, the GMCC flask data will provide an intercomparison of the GMCC and AES measurement and calibration systems.

J. Peterson attended the conference International Assessment of the Role of Carbon Dioxide and of other Greenhouse Gases in Climate Variations and Associated Impacts, held at Villach, Austria, 1-15 October 1985. The conference was sponsored by UNEP, WMO, and ICSU. The conference findings called on international governments to take into account the likely climate changes expected from increasing amounts of greenhouse gases when they develop policies on social and economic development, environmental programs, and control of emissions of radiatively active gases.

An International Workshop on Sand Transport and Desertification in Arid Lands was held in Khartoum, Sudan, during the period 17-26 November 1985. It was attended by GMCC scientist D. Gillette along with 81 scientists from Sudan and 61 scientists from 29 other countries. The workshop was sponsored by the International Centre for Theoretical Physics and several other international agencies. The purpose of the workshop was to examine, through detailed case studies, the flow of sand in arid regions of the earth. The program of the first 5 days consisted of 12 scientific sessions during which several case studies, review papers, and contributed papers were presented. Gillette presented the paper "A Physically Based Wind Erosion Estimation Method." Following the scientific sessions, Gillette participated in two working groups concerned with developing wind erosion and desertification studies. A field excursion was organized during the period 23-25 November to central Sudan to observe regional problems caused by wind erosion and wind-driven sand.

At the invitation of the Soviet Union, B.G. Mendonca presented a paper on "Measurements in the Geophysical Monitoring for Climatic Change Division of NOAA, U.S.A.: A First Step in an Integrated Global Monitoring Effort" at the Third International Symposium on Integrated Global Monitoring of the State of the Biosphere. The conference was held in Tashkent, USSR, 13-20 October 1985 and was sponsored by the USSR State Committee for Hydrometeorology and Control of the Natural Environment, the USSR Academy of Sciences, the Uzbek SSR Council of Ministers with the support of the United Nations Educational, Scientific, and Cultural Organization. This well-attended conference was the third in a series held every 4 years to discuss world problems in the area of pollution and the Earth's biosphere.

10. PUBLICATIONS AND PRESENTATIONS BY GMCC STAFF, 1985

- Boatman, J. F., and D. L. Wellman. The efficiency of an airborne cloud water separator. Proceedings, International Symposium on Moisture and Humidity, April 15-19, 1985, Washington, DC.
- Bodhaine, B. A., and J. J. DeLuisi, 1985. An aerosol climatology of Samoa. J. Atmos. Chem. 3:107-122.
- Brainard, R. E. Geophysical Monitoring for Climatic Change, Amundsen-Scott South Pole Station, 1983-1984. Ant. J. U. S. XIX(5):202-203.
- Castillo, R., E. Patterson, and J. DeLuisi. Organic and elemental carbon loading in interstitial aerosol and hydrometeors, and its relationship to acidity of hydrometeors at a rural northeast site, Whiteface Mt., NY. Paper presented at the IAMAP/IAPSO Joint Assembly, Honolulu, HI, 5-16 August 1985,
- Conway, T. J., W. E. Raatz, and R. H. Gammon. Airborne CO<sub>2</sub> measurements in the Arctic during spring 1983. Atmos. Environ. 19(12):2195-2201.
- Conway, T. J., L. S. Waterman, R. H. Gammon, and R. F. Weiss. Measurements of Atmospheric CO<sub>2</sub> from the AKADEMIK KOROLEV cruise, October-December 1983. Paper presented at the AGU Fall Meeting, San Francisco, CA, 8-13 December 1985.
- Conway, T. J., L. S. Waterman, K. W. Thoning, and K. A. Masarie. Recent results from the NOAA/GMCC CO<sub>2</sub> flask sampling network. Paper presented at the conference Atmospheric Carbon Dioxide: Its Sources, Sinks, and Global Transport, Kandersteg, Switzerland, 2-6 September 1985.
- Dayan, U., J. M. Miller, A. M. Yoshinaga, and D. W. Nelson. An assessment of precipitation chemistry measurements from the Global Trends Network and its predecessors (1972-1982). NOAA Tech. Memo. ERL ARL-136, Boulder, CO, 61 pp.
- DeLuisi, J., T. DeFoor, K. Coulson, and F. Fernald. Lidar observations of stratospheric aerosol over Mauna Loa Observatory: 1982-83. NOAA Data Report ERL ARL-5, Boulder, CO, 78 pp.
- DeLuisi, J. J., E. G. Dutton, E. Flowers, and J. Peterson. Recent developments in atmospheric turbidity measurements in NOAA Geophysical Monitoring for Climatic Change. Lectures presented at the WMO Technical Conference on Observation of Atmospheric Contaminants, TECOMAC, Vienna, Austria, 17-21 October 1983. WMO No. 64, Spec. Environ. Rept. No. 16, World Meteorological Organization, Geneva, Switzerland, 381-386.
- DeLuisi, J. J., E. G. Dutton, and B. G. Mendonca. Physical features of the El Chichon stratospheric aerosol cloud over Mauna Loa. Paper presented at the IAMAP/IAPSO Joint Assembly, Honolulu, HI, 5-16 August 1985.

- DeLuisi, J. J., C. L. Mateer, and P. K. Bhartia. On the correspondence between standard Umkehr, short Umkehr, and solar backscattered ultraviolet vertical ozone profiles. J. Geophys. Res. 90(D2):3845-3849.
- DeLuisi, J. J., C. L. Mateer, and W. D. Komhyr. Effects of the El Chichon stratospheric aerosol cloud on Umkehr measurements at Mauna Loa, Hawaii. In Atmospheric Ozone. C. S. Zerefos and A. Ghazi (Eds.), D. Reidel Publ. Co., Boston, MA, 316-320.
- Dutton, E. G., J. J. DeLuisi, and A. P. Austing. Interpretation of Mauna Loa Atmospheric transmission relative to aerosols, using photometric precipitable water amounts. J. Atmos. Chem. 3:53-68.
- Dutton, E. G., J. J. DeLuisi, and D. J. Endres. Solar radiation at the Barrow, AK, GMCC baseline observatory 1976-1983. NOAA DR ERL ARL-6, Boulder, CO, 112 pp.
- Fraser, P. J., N. Derek, R. O'Brien, R. Shepherd, R. A. Rasmussen, A. J. Crawford, and L. P. Steele. Intercomparison of halocarbon and nitrous oxide measurements, 1976-1984. In Baseline Atmospheric Program (Australia) 1983-1984. R. J. Francey and B. W. Forgan (Eds.), Dept. of Science/Bureau of Meteorology, Aspendale, Australia, 17-26.
- Galloway, J., R. Pueschel, and R. Artz. Determination of the impact of North American emissions on the atmosphere of the Western Atlantic Ocean. Paper presented at the AGU Fall Meeting, San Francisco, CA, 8-13 December 1985.
- Gendron, J. F., R. A. Feely, R. H. Gammon, B. A. Taft, P. E. Pullen, L. S. Waterman, and T. J. Conway. Distributions of chemical tracers in the eastern equatorial Pacific during and after the El Niño-Southern Oscillation event. Paper presented at the AGU Fall Meeting, San Francisco, CA, 8-13 December 1985.
- Grass, R. D., and W. D. Komhyr. Traveling standard lamp calibration checks on Dobson ozone spectrophotometers during 1981-83. In Atmospheric Ozone. C. S. Zerefos and A. Ghazi (Eds.), D. Reidel Publ. Co., Boston, MA, 376-380.
- Halter, B. C., J. M. Harris, and K. A. Rahn. A study of winter variability in carbon dioxide and Arctic haze aerosols at Barrow, AK. Atmos. Environ., 19(12):2033-2037.
- Hoecker, W. H., E. C. Flowers, and G. F. Cotton. Variation of direct beam solar radiation in the United States due to the El Chichon debris cloud. Bull. Am. Meteorol. Soc. 66(1):14-19.
- Komhyr, W. D., R. H. Gammon, T. B. Harris, L. S. Waterman, T. J. Conway, W. R. Taylor, and K. W. Thoning. Global atmospheric CO<sub>2</sub> distribution and variations from 1968-1982 NOAA/GMCC CO<sub>2</sub> flask sample data. J. Geophys. Res. 90(D3):5567-5596.
- Komhyr, W. D., R. D. Grass, R. D. Evans, R. K. Leonard, and G. M. Semeniuk. Umkehr observations with automated Dobson spectrophotometers. In Atmospheric Ozone. C. S. Zerefos, and A. Ghazi (Eds.), D. Reidel Publ. Co., Boston, MA, 371-375.

- Oltmans, S. J. Tropospheric ozone at four remote observatories. In Atmospheric Ozone. C. S. Zerefos and A. Ghazi (Eds.), D. Reidel Publ. Co., Boston, MA, 796-802.
- Patterson, E. M., R. A. Castillo, and J. J. DeLuisi. Cloud washout ratios for graphitic carbon at Whiteface Mt., NY. Paper presented at the IAMAP/IAPSO Joint Assembly, Honolulu, HI, 5-16 August 1985.
- Peterson, J. T. Summary comments on the scientific highlights of the conference. Lectures presented at the WMO Technical Conference on Observation of Atmospheric Contaminants, TECOMAC, Vienna, Austria, 17-21 October 1983. WMO No. 64, Spec. Environ. Rept. No. 16, World Meteorological Organization, Geneva, Switzerland, xx-xxv.
- Peterson, J. T., and W. D. Komhyr. Atmospheric CO<sub>2</sub> measurements at Barrow, Alaska. Lectures presented at the WMO Technical Conference on Observation of Atmospheric Contaminants, TECOMAC, Vienna, Austria, 17-21 October 1983. WMO No. 64, Spec. Environ. Rept. No. 16, World Meteorological Organization, Geneva, Switzerland, 76-80.
- Peterson, J. T., T. J. Conway, and D. A. Gillette. CO<sub>2</sub> variability between high northern latitude sites. Paper presented at the conference Atmospheric Carbon Dioxide: Its Sources, Sinks, and Global Transport, Kandersteg, Switzerland, 2-6 September 1985.
- Pollack, J. B., M. P. McCormick, E. G. Dutton, and J. J. DeLuisi. A climatology of the El Chichon volcanic cloud for use in climate models. Paper presented at the IAMAP/IAPSO Joint Assembly, Honolulu, HI, 5-16 August 1985.
- Pueschel, R. F., D. L. Wellman, and J. F. Boatman. Tropospheric aerosols over the Western Atlantic: Scale height and concentrations. Paper presented at the AGU Fall Meeting, San Francisco, CA, 8-13 December 1985.
- Raatz, W. E. Meteorological conditions over Eurasia and the Arctic contributing to the March 1983 Arctic haze episode. Atmos. Environ. 19(12):2121-2126.
- Raatz, W. E., R. C. Schnell, and B. A. Bodhaine. Atmospheric cross sections for the Arctic Gas and Aerosol Sampling Program, March-April 1983. NOAA Tech. Memo. ERL ARL-134, Boulder, CO, 50 pp.
- Raatz, W. E., R. C. Schnell, and B. A. Bodhaine. The distribution and transport of pollution aerosols over the Norwegian Arctic on 31 March and 4 April 1983. Atmos. Environ. 19(12):2135-2142.
- Raatz, W. E., R. C. Schnell, B. A. Bodhaine, and S. J. Oltmans. Observations of Arctic Haze during polar flights from Alaska to Norway. Atmos. Environ. 19(12):2143-2151.
- Raatz, W. E., R. C. Schnell, B. A. Bodhaine, S. J. Oltmans, and R. H. Gammon. Air mass characteristics in the vicinity of Barrow, Alaska, 9-19 March 1983. Atmos. Environ. 19(12):2127:2134.

- Komhyr, W. D., T. B. Harris, and L. S. Waterman. Calibration of nondispersive infrared CO<sub>2</sub> analyzers with CO<sub>2</sub>-in-air reference gases. J. Atmos. Ocean. Technol. 2(1):82-88.
- Komhyr, W. D., S. J. Oltmans, A. N. Chopra, and P. R. Franchois. Performance characteristics of high-altitude ECC ozonesondes. In Atmospheric Ozone. C. S. Zerefos and A. Ghazi (Eds.), D. Reidel Publ. Co., Boston, MA, 499-503.
- Komhyr, W. D., S. J. Oltmans, A. N. Chopra, R. K. Leonard, T. E. Garcia, and C. M. McFee. Results of Umkehr, ozonesonde, total ozone, and sulfur dioxide observations in Hawaii following the eruption of El Chichon volcano in 1982. In Atmospheric Ozone. C. S. Zerefos and A. Ghazi (Eds.), D. Reidel Publ. Co., Boston, MA, 305-310.
- Luria, M., and G. Sharf. The influence of light intensity, SO<sub>2</sub>, NO<sub>x</sub> and C<sub>3</sub>H<sub>6</sub> on sulfate aerosol formation. J. Atmos. Chem. 2:321-329.
- Luria, M., U. Armit, and M. Peleg. Comparison of air quality data obtained from rooftop, sidewalk and suburban areas. Environ. Monitor. Assess. 5:249-254.
- Luria, M., T. David, and M. Peleg. Five year air quality trends in Jerusalem, Israel. Atmos. Environ. 19:715-726.
- Luria, M., C. C. Van Valin, J. F. Boatman, D. L. Wellman, D. Hastie, and R. F. Pueschel. SO<sub>2</sub> flux measurements over the Western Atlantic Ocean. Paper presented at the AGU Fall Meeting, San Francisco, CA, 8-13 December 1985.
- Mateer, C. L. and J. J. DeLuisi. A comparison of ozone profiles derived from standard Umkehr and short Umkehr measurements from fifteen stations. In Atmospheric Ozone. C. S. Zerefos and A. Ghazi (Eds.), D. Reidel Publ. Co., Boston, MA, 290-294.
- Mendonca, B. G. Measurements in the Geophysical Monitoring for Climatic Change Division of NOAA, U.S.A: A first step in an integrated global monitoring effort. Paper presented at the Third International Symposium of Integrated Global Monitoring of the state of the biosphere, Tashkent, U.S.S.R., 13-20 October 1985.
- Mendonca, B. G., J. J. DeLuisi, and E. G. Dutton. Twenty-six years of long-range transport of atmospheric aerosols over Mauna Loa. Paper presented at the IAMAP/IAPSO Joint Assembly, Honolulu, HI, 5-16 August 1985.
- Miller, J. M., and J. M. Harris. The flow climatology to Bermuda and its implications for long-range transport. Atmos. Environ. 19(3):409-414.
- Oltmans, S. J. Measurements of water vapor in the stratosphere with a frost-point hygrometer. Proceedings, International Symposium on Moisture and Humidity, April 15-19, 1985, Washington, D.C. Instrument Society of America, Research Triangle Park, NC, 251-258.

- Oltmans, S. J. Tropospheric ozone at four remote observatories. In Atmospheric Ozone. C. S. Zerefos and A. Ghazi (Eds.), D. Reidel Publ. Co., Boston, MA, 796-802.
- Patterson, E. M., R. A. Castillo, and J. J. DeLuisi. Cloud washout ratios for graphitic carbon at Whiteface Mt., NY. Paper presented at the IAMAP/IAPSO Joint Assembly, Honolulu, HI, 5-16 August 1985.
- Peterson, J. T. Summary comments on the scientific highlights of the conference. Lectures presented at the WMO Technical Conference on Observation of Atmospheric Contaminants, TECOMAC, Vienna, Austria, 17-21 October 1983. WMO No. 64, Spec. Environ. Rept. No. 16, World Meteorological Organization, Geneva, Switzerland, xx-xxv.
- Peterson, J. T., and W. D. Komhyr. Atmospheric CO<sub>2</sub> measurements at Barrow, Alaska. Lectures presented at the WMO Technical Conference on Observation of Atmospheric Contaminants, TECOMAC, Vienna, Austria, 17-21 October 1983. WMO No. 64, Spec. Environ. Rept. No. 16, World Meteorological Organization, Geneva, Switzerland, 76-80.
- Peterson, J. T., T. J. Conway, and D. A. Gillette. CO<sub>2</sub> variability between high northern latitude sites. Paper presented at the conference Atmospheric Carbon Dioxide: Its Sources, Sinks, and Global Transport, Kandersteg, Switzerland, 2-6 September 1985.
- Pollack, J. B., M. P. McCormick, E. G. Dutton, and J. J. DeLuisi. A climatology of the El Chichon volcanic cloud for use in climate models. Paper presented at the IAMAP/IAPSO Joint Assembly, Honolulu, HI, 5-16 August 1985.
- Pueschel, R. F., D. L. Wellman, and J. F. Boatman. Tropospheric aerosols over the Western Atlantic: Scale height and concentrations. Paper presented at the AGU Fall Meeting, San Francisco, CA, 8-13 December 1985.
- Raatz, W. E. Meteorological conditions over Eurasia and the Arctic contributing to the March 1983 Arctic haze episode. Atmos. Environ. 19(12):2121-2126.
- Raatz, W. E., R. C. Schnell, and B. A. Bodhaine. Atmospheric cross sections for the Arctic Gas and Aerosol Sampling Program, March-April 1983. NOAA Tech. Memo. ERL ARL-134, Boulder, CO, 50 pp.
- Raatz, W. E., R. C. Schnell, and B. A. Bodhaine. The distribution and transport of pollution aerosols over the Norwegian Arctic on 31 March and 4 April 1983. Atmos. Environ. 19(12):2135-2142.
- Raatz, W. E., R. C. Schnell, B. A. Bodhaine, and S. J. Oltmans. Observations of Arctic Haze during polar flights from Alaska to Norway. Atmos. Environ. 19(12):2143-2151.
- Raatz, W. E., R. C. Schnell, B. A. Bodhaine, S. J. Oltmans, and R. H. Gammon. Air mass characteristics in the vicinity of Barrow, Alaska, 9-19 March 1983. Atmos. Environ. 19(12):2127:2134.

- Raatz, W. E., R. C. Schnell, M. A. Shapiro, S. J. Oltmans, and B. A. Bodhaine. Intrusions of stratospheric air into Alaska's troposphere, March 1983. Atmos. Environ. 19(12):2153-2158.
- Robinson, E. Book review, "The Major Biogeochemical Cycles and Their Interactions," B. Bolin and R. B. Cook (Eds.). In Water, Air, Soil Pollut., 24(2):228-229.
- Robinson, E. Book review, "Air Pollution Modeling and Its Application III," C. DeWispelaere (Ed.). Water, Air, Soil Pollut., 25(2):233-234.
- Schnell, R. C. Arctic Gas and Aerosol Sampling Program. Paper presented at the Inter-Agency Workshop on Sensing from Aircraft, NCAR, Boulder, CO, 19-22 August 1985.
- Schnell, R. C. The international Arctic Gas and Aerosol Sampling Program. In Arctic Atmospheric Pollution, Abstracts of papers, International Conference, Scott Polar Research Institute, University of Cambridge, England, 2-5 September 1985. Sponsored by the State of Alaska, 6-7.
- Schnell, R. C., and W. E. Raatz. Rapid long-range transport of air pollutants across the Arctic: The March 1983 Arctic haze episode. Paper presented at the IAMAP/IAPSO Joint Assembly, Honolulu, HI, 5-16 August 1985.
- Schnell, R. C., W. E. Raatz, and J. T. Peterson. Arctic Gas and Aerosol Sampling Program. Lectures presented at the WMO Technical Conference on Observation of Atmospheric Contaminants, TECOMAC, Vienna, Austria, 17-21 October 1983. WMO No. 64, Spec. Environ. Rept. No. 16, World Meteorological Organization, Geneva, Switzerland, 324-333.
- Sievering, H. Gradient measurements of sulfur and soil mass dry deposition rates under clean air and high-wind-speed conditions. Atmos. Environ. 20(2):341-345.
- Stearns, L. P., and R. F. Pueschel. Particle distribution of clouds on Whiteface Mountain. Paper presented at the AGU Fall Meeting, San Francisco, CA, 8-13 December 1985.
- Steele, L. P., T. J. Conway, L. S. Waterman, R. H. Gammon, P. J. Fraser, R. F. Weiss, and R. A. Rasmussen. Measurements of atmospheric methane from the AKADEMIK KOROLEV cruise, October-December 1983. Paper presented at the AGU Fall meeting, San Francisco, CA, 8-13 December 1985.
- Steele, L. P., P. J. Fraser, R. A. Rasmussen, M. A. K. Khalil, A. J. Crawford, T. J. Conway, R. H. Gammon, K. A. Masarie, and K. W. Thoning. The global distribution of methane in the troposphere. Paper presented at the AGU Fall Meeting, San Francisco, CA, 8-13 December 1985.
- Thompson, T. M., W. D. Komhyr, and E. G. Dutton. Chlorofluorocarbon-11, -12, and nitrous oxide measurements at the NOAA/GMCC baseline stations (16 September 1973 to 31 December 1979). NOAA Tech. Rep. ERL-428-ARL-8, Boulder, CO, 124 pp.

- Van Valin, C. C., and M. Luria. O<sub>3</sub>, CO, hydrocarbons and dimethyl sulfide over the Western Atlantic Ocean. Paper presented at AGU Fall Meeting, San Francisco, CA, 8-13 December 1985.
- Waterman, L. W., T. J. Conway, R. H. Gammon, and R. F. Weiss. pCO<sub>2</sub> measurements in the equatorial Pacific Ocean. Paper presented at the AGU Fall Meeting, San Francisco, CA, 8-13 December 1985.
- Winchester, J. W., R. C. Schnell, S. F. Fan, S. Li, B. A. Bodhaine, P. S. Naegele, A. D. A. Hansen, and H. Rosen. Particulate sulfur and chlorine in Arctic aerosols, spring 1983. Atmos. Environ. 19:2167-2173.

## 11. ACRONYMS AND ABBREVIATIONS

AES	Atmospheric Environment Service, Canada
AGASP	Arctic Gas and Aerosol Sampling Program
ALE	Atmospheric Lifetime Experiment
ARL	Air Resources Laboratory, Silver Spring, MD (ERL)
ARM	Aerosols and Radiation Monitoring
ASASP	Active-scattering aerosol spectrometer probe
ASCS	Alaska Soil Conservation Service
ASR	Aerosols and Solar Radiation, referring to CAMS
BAO	Boulder Atmospheric Observatory
BAPMoN	Background Air Pollution Monitoring Network
BRW	Barrow Observatory, Barrow, Alaska (GMCC)
BUV	Biologically-active ultraviolet
CAF	Clean Air Facility
CAMS	Control and Monitoring System
CIRES	Cooperative Institute for Research in Environmental Sciences, University of Colorado, Boulder, CO
CFR	Centre des Faibles Radioactivites, Gif-sur-Yvette, France
CN	Condensation nuclei
CNC	Condensation nucleus counter
CO2	Carbon dioxide, referring to CAMS
CSIRO	Commonwealth Scientific and Industrial Research Organization, Australia
CPU	Central processing unit
DAS	Data acquisition system
DEW	Distant Early Warning
DOE	Department of Energy
DSET	Desert Solar Environment Testing
D.U.	Dobson unit
DOY	Day of year, Julian
EC-GC	Electron capture gas chromatograph
ECC	Electrochemical concentration cell
EDS	Energy dispersive spectrometry
EML	Environmental Measurements Laboratory (DOE)
ENSO	El Niño-Southern Oscillation
EPA	Environmental Protection Agency
EPOCS	Equatorial Pacific Ocean Climate Studies
ERL	Environmental Research Laboratories, Boulder, CO (NOAA)
FTS	Federal Telecommunication System
FPD	Flame photometric detector
FSSP	Forward-scattering spectrometer probe
FWNIP	Four-wavelength manual incidence pyrhelimeter
FYO	Four-year oscillation
GC	Gas chromatograph
G.E.	General Electric
GMCC	Geophysical Monitoring for Climatic Change, Boulder, CO (ARL)
GPCP	Global Precipitation Chemistry Project
GMT	Greenwich mean time
GSA	General Services Administration
HASL	Health and Safety Laboratory (EPA)
HAO	High Altitude Observatory
HP	Hewlett-Packard
IAMAP	International Association of Meteorology and Atmospheric Physics

IAPSO	International Association for the Physical Sciences of the Ocean
IBM	International Business Machines
ICDAS	Instrumentation Control and Data Acquisition System
ICSU	International Council of Scientific Unions
IPC	International Pyrheliometer Comparison
IR	Infrared
ISWS	Illinois State Water Survey
ITT	International Telephone and Telegraph
LAMP	Laboratoire Associe de Meteorologie, France
LBL	Lawrence Berkeley Laboratory (DOE)
LST	Local standard time
MLO	Mauna Loa Observatory, Hawaii (GMCC)
MMD	Mass mean diameter
MO3	Meteorology and ozone, referring to CAMS
MPBL	Marine planetary boundary layer
MSL	Mean sea level
NADP	National Atmospheric Deposition Program
NAPAP	National Acid Precipitation Assessment Program
NARL	Naval Arctic Research Laboratory, Barrow, AK
NASA	National Aeronautics and Space Administration
NBS	National Bureau of Standards
NCAR	National Center for Atmospheric Research, Boulder, CO
NESDIS	National Environmental Satellite, Data, and Information Service
NDIR	Nondispersive infrared
NH	Northern Hemisphere
NIP	Normal incidence pyrheliometer
NOAA	National Oceanic and Atmospheric Administration
NRI	National Resource Inventory
NRIP	New River Intercomparison of Pyrheliometers
NWR	Niwot Ridge, CO
NWS	National Weather Service
NWT	Northwest Territories, Canada
OGC	Oregon Graduate Center, Beaverton, OR
P <sup>3</sup>	Portable pressurizer pack air sampler
PBL	Planetary boundary layer
PC	Personal computer
PIXE	Proton-induced X-ray emission
PMEL	Pacific Marine Environmental Laboratory, Seattle, WA
PMOD	Physikalisch-Meteorologisches Observatorium Davos
PRE-STORM	Preliminary Regional Experiment for Storm Central
QBO	Quasi-biennial oscillation
RITS	Radiatively Important Trace Species
RFP	Request for proposal
SAD	Selected Area Diffraction
SAGE	Stratospheric Aerosol and Gas Experiment
SBUV	Solar backscattered ultraviolet
SEASPAN	SEAREX South Pacific Aerosol Network
SEAREX	Sea-Air Exchange Program
SH	Southern Hemisphere
SIO	Scripps Institution of Oceanography, La Jolla, CA
SMO	Samoa Observatory, American Samoa (GMCC)
SN	Serial number
STEM	Scanning Transmission Electron Microscopy
SUNYA	State University of New York at Albany

SPO	South Pole Observatory, Antarctica (GMCC)
SRF	Solar Radiation Facility
SRL	Smithsonian Radiation Laboratory
SRBL	Smithsonian Radiation and Biological Laboratory
SST	Sea surface temperature
TMI	Technical Measurements, Inc.
TTO	Transient Tracers in the Ocean
ULF	Ultralow frequency
UNEP	United Nations Environmental Program
UPS	Uninterruptible power supply
URAS	Ultra Rot Absorptions Schreiber (Hartmann-Braun infrared analyzer)
URI	University of Rhode Island, Kingston, RI
USGS	United States Geological Survey
UV	Ultraviolet
WATOX	Western Atlantic Ocean Experiment
WERIS	Wind Energy Resource Information System
WMO	World Meteorological Organization, Geneva, Switzerland
WRR	World Radiometric Reference
WSG	World Standard Group
ZRAM	"Z" random access memory